

NAS Technical Summaries

March 1993 –
February 1994

NASA Ames Research Center

On the Cover: The cover images are from three NAS Technical Summaries: Forrester T. Johnson's summary, "Multipoint Aerodynamic Design," is on page 10; John Rakiewicz's summary, "Titan Entry Flow Field of the Cassini-Huygens Probe," is on page 27; and Richard E. Young's summary, "Simulation of Volcanic Aerosol Clouds," is on page 99.

The use of color graphics is a powerful and flexible visualization tool for the science of computational fluid dynamics. Without color graphics, the millions of numbers that form the supercomputer solutions to the studies contained in this report and on the cover would be virtually incomprehensible.

NAS Technical Summaries

March 1993–
February 1994

NASA Ames Research Center

Preface


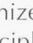
NASA created the Numerical Aerodynamic Simulation (NAS) Program in 1987 to focus resources on solving critical problems in aerospace and related disciplines by utilizing the power of the most advanced supercomputers available. The NAS Program provides scientists with computing resources to solve the most demanding computational fluid dynamics problems and serves as a pathfinder in integrating leading-edge supercomputing technologies. The benefits of numerical simulation of aerospace problems are tremendous savings in both time and money—savings that are critical to the viability and competitive edge of the American aircraft industry.

During the 1993–94 Operational Year, NAS high-speed processor resources included a Cray Y-MP and a Cray C-90. The Cray Y-MP had eight processors, 256 megawords of central memory, a peak speed of 4 billion floating point operations per second (GFLOPS) and a sustained speed of 1 GFLOPS. The Cray C-90 had 16 processors, 1,024 megawords of main memory, a peak speed of 16 GFLOPS and a sustained speed of 6 GFLOPS.

NAS Parallel resources included an Intel iPSC/860, an Intel Paragon, and a Thinking Machine CM-5. The Intel iPSC/860 had 128 nodes with 8 megabytes of memory per node and a peak speed of 5 GFLOPS. The Intel Paragon had 208 nodes with 32 megabytes of memory per node, a peak speed of 15 GFLOPS,

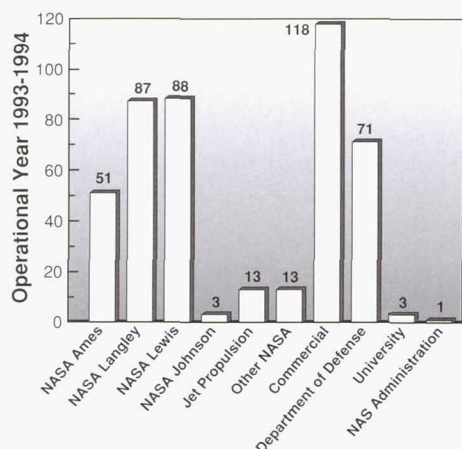
and a sustained speed of 1.2 GFLOPS. The Thinking Machine CM-5 had 128 nodes with 32 megabytes of memory per node, a peak speed of 16 GFLOPS and a sustained speed of 1.4 GFLOPS.

The 1993–94 Operational Year concluded with 448 high-speed processor projects and 95 parallel projects representing NASA, the Department of Defense, other Government agencies, private industry, and universities. This document provides a glimpse at some of the significant scientific results for the year.

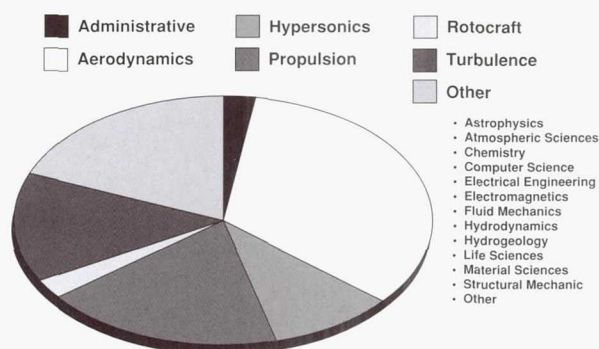
The content of the NAS Technical Summaries for the 1993–94 Operational Year contains selected scientific results computed using NAS high-speed processor (HSP) and parallel (PAR) resources. An icon at the top of each technical summary page indicates the resource used— represents HSP, and  represents PAR. This edition is organized by research disciplines and alphabetically within each discipline.

An online Mosaic version of this book is accessible from the NAS home page at URL <http://www.nas.nasa.gov/home.html>. Additional copies of the NAS Technical Summaries Report for this year and for previous years are available on request. Contact the NAS Documentation Center at NASA Ames Research Center, MS 258-6, Moffett Field, CA 94035-1000, or via email addressed to doc-center@nas.nasa.gov or telephone (415) 604-4632.

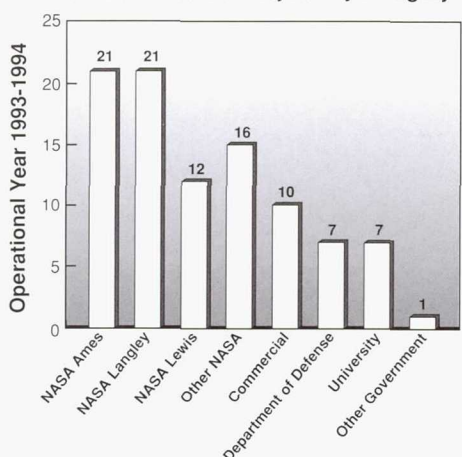
Number of Cray Projects by Category



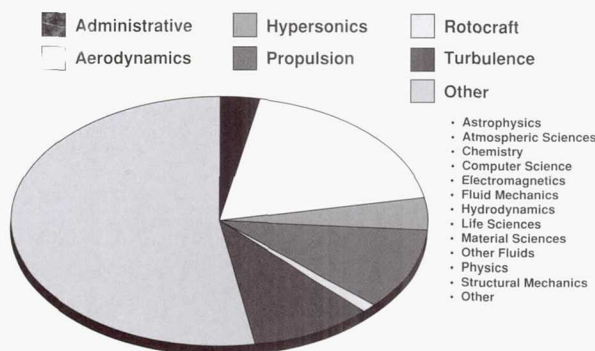
Number of Cray Projects by Discipline



Number of Parallel Projects by Category



Number of Parallel Projects by Discipline



Page intentionally left blank

Table of Contents

Principal Investigator	NAS Summary	Page
Aeronautics: Basic Research		
Ramesh K. Agarwal	<i>Unstructured Grid Finite-Element Solutions</i> Co-investigators: David W. Halt and David L. Marcum McDonnell Douglas Corporation/Mississippi State University	3
Timothy J. Barth	<i>Parallel Implementation of an Unstructured Mesh Navier-Stokes Solver</i> Co-investigator: Samuel W. Linton NASA Ames Research Center/Sterling Software Systems	4
Farhad Ghaffari	<i>Applied Computational Fluid Dynamics</i> Co-investigators: Brent L. Bates and James M. Luckring NASA Langley Research Center/ViGYAN, Inc.	5
Philip B. Gingrich	<i>Design-by-Optimization Method</i> Rockwell International, North American Aircraft Division	6
Fernando F. Grinstein	<i>Simulation of Spatially Evolving Jets</i> Naval Research Laboratory	7
Guru P. Guruswamy	<i>Aeroelasticity of Wing-Body-Control Configurations</i> Co-investigators: Chansup Byun, Eugene Tu, and Shigeru Obayashi NASA Ames Research Center/MCAT Institute	8
Guru P. Guruswamy	<i>Wing-Body Aeroelasticity</i> Co-investigator: Chansup Byun NASA Ames Research Center/MCAT Institute	9
Forrester T. Johnson	<i>Multipoint Aerodynamic Design</i> Co-investigators: Michael B. Bieterman, Craig L. Hilmes, William P. Huffman, Robin G. Melvin, and David P. Young The Boeing Company	10
Steven B. Kern	<i>Vortex-Flow Control</i> Naval Air Warfare Center	11
Sanjiva K. Lele	<i>Skewed Compressible Mixing Layers</i> Co-investigator: Ganyu Lu Stanford University	12
Frank Marconi	<i>Comparison of TLNS3D Computations with Test Data</i> Co-investigator: M. Siclari Grumman Corporate Research Center	13
Dimitri J. Mavriplis	<i>Navier-Stokes Computations on Unstructured Grids</i> ICASE	14
Pradeep Raj	<i>CFL3D Code Evaluation</i> Co-investigators: Tom Kinard and Richard Semmes Lockheed Aeronautical Systems Company	15

Principal Investigator	NAS Summary	Page
Yehia Rizk	<i>Prediction of the Unsteady F-18 Flow Field</i> Co-investigator: Scott Murman NASA Ames Research Center	16
David M. Schuster	<i>Analysis of High-Speed Civil Transport Transient Response</i> Lockheed Engineering and Sciences Company	17
James L. Thomas	<i>Complete F-18 Hybrid Solution</i> Co-investigators: Robert T. Biedron, Christopher L. Rumsey, W. Kyle Anderson, and Daryl L. Bonhaus NASA Langley Research Center	18
Chung-Jin Woan	<i>Flow Simulation about Attack Aircraft</i> Co-investigator: John D. Duino Rockwell International, North American Aircraft Division	19
David T. Yeh	<i>Multiple-Body Aerodynamics</i> Rockwell International, North American Aircraft Division	20

Aeronautics: Hypersonics, Subsonics, Supersonics, Transonics

Hypersonics

Andrew Anagnost	<i>Time-Accurate Simulation of Hypervelocity Wakes</i> Stanford University	23
Neal M. Chaderjian	<i>Effects of Roll Angle on Vortex Breakdown</i> Co-investigators: Lewis B. Schiff, John A. Ekaterinaris, and Yuval Levy NASA Ames Research Center/Naval Post Graduate School/Stanford University	24
Robert R. Chamberlain	<i>Jet Interaction Effects on Aerodynamic Control of Missiles</i> Co-investigators: Anthony Dang and Ken Xiques Adaptive Research Corporation	25
Hassan A. Hassan	<i>Transition Model for High-Speed Flow</i> Co-investigator: Eric S. Warren North Carolina State University	26
John Rakiewicz	<i>Titan Entry Flow Field of the Cassini-Huygens Probe</i> Co-investigators: Scott Ward, Darren Fricker, and David Wyn-Roberts Jet Propulsion Laboratory/McDonnell Douglas Aerospace/European Space Agency	27
S. H. Konrad Zhu	<i>Simulation of Rarefied Jet Interaction</i> Co-investigator: Leonardo Dagum Rockwell International, Rocketdyne Division/NASA Ames Research Center	28

Principal Investigator	NAS Summary	Page
Subsonics		
Kenneth M. Jones	<i>Subsonic High-Lift Analysis</i> Co-investigators: Victor Lessard, Simha Dodbele, Kevin Kjerstad, Steve Yaros, and Mamad Takallu NASA Langley Research Center/ViGYAN, Inc./Lockheed Engineering and Sciences Company	29
Lewis B. Schiff	<i>Investigation of Forebody Flow Control</i> Co-investigators: Ken Gee and Roxana Agosta NASA Ames Research Center/MCAT Institute	30
N. J. Yu	<i>Evaluation of Navier–Stokes Codes for Transport Configuration Analysis</i> Co-investigators: H. V. Cao and S. R. Allmaras Boeing Commercial Airplane Group	31
Supersonics		
Michael C. Fischer	<i>Supersonic Laminar Flow Control Experiment</i> Co-investigator: Chandra S. Vemuru NASA Lewis Research Center/AS&M, Inc.	32
Steve L. Karman, Jr.	<i>Unstructured Grid/Flow Solver Calibration</i> Co-investigators: Tracy J. Welterlen, Elizabeth A. Fuchs, and Doug Howlett Lockheed Engineering and Sciences Company	33
E. Tu	<i>Laminar Flow Supersonic Wind Tunnel</i> Co-investigator: G. H. Klopfer NASA Ames Research Center/MCAT Institute	34
Transonics		
Jassim A. Al-Saadi	<i>Transonic Flows Around Complex Geometries</i> Co-investigators: Peter A. Cavallo and William D. Smith NASA Langley Research Center/George Washington University	35
Christopher A. Atwood	<i>Simulation of Coupled Fluid and Flightdynamic Systems</i> Overset Methods, Inc.	36
Raymond R. Cosner	<i>F/A-18 Aerodynamic Assessment</i> Co-investigators: Robert H. Bush, William W. Romer, and Paul G. Willhite McDonnell Douglas Corporation	37
Jerry E. Deese	<i>Launch Vehicle Flow-Field Simulation</i> Co-investigator: Ramesh K. Agarwal McDonnell Douglas Corporation	38
Daniel F. Dominik	<i>Space Shuttle Flow Fields with Plume Simulation</i> Co-investigators: K. Rajagopal, C. Olling, K. Mani, S. Vuong, J. Wisneski, G. Hock and J. Sikora Rockwell International, Space Systems Division	39

Principal Investigator	NAS Summary	Page
W. Kelly Londenberg	<i>Reynolds Number Effects on a Delta Wing</i> ViGYAN, Inc.	40
Christopher L. Reed	<i>High-Angle-of-Attack Aerodynamics</i> Lockheed Engineering and Sciences Company	41
Arvin Shmilovich	<i>Computational Studies of Advanced Wings at High Incidence</i> Co-investigators: K. C. Chang and R. A. Pelkman McDonnell Douglas Aerospace	42

Aeronautics: Propulsion

Alan B. Cain	<i>Simulation of Supersonic Jet Screech</i> Co-investigators: William W. Bower and Yutaka Ikeda McDonnell Douglas Corporation	45
Rodrick V. Chima	<i>Multiblock Solver for Turbomachinery Flows</i> NASA Lewis Research Center	46
Wei J. Chyu	<i>Airframe/Inlet Aerodynamics</i> Co-investigator: Tom I-P. Shih NASA Ames Research Center/Carnegie Mellon University	47
Frederik J. de Jong	<i>Turbine Blade Tip Clearance Flows</i> Co-investigator: Tony Chan Scientific Research Associates, Inc.	48
W. W. Follett	<i>Vortex Induced Mixing Behind Ramp Injectors</i> Co-investigators: J. V. Madison and S. Palaniswamy Rockwell International, Rocketdyne Division/Rockwell International Science Center	49
Karen L. Gundy-Burlet	<i>Unsteady Turbomachinery Computations</i> NASA Ames Research Center	50
Chunill Hah	<i>Unsteady Three-Dimensional Flow in a Transonic Compressor</i> Co-investigators: J. Loellbach, W. W. Copenhaver, and S. L. Puterbaugh NASA Lewis Research Center/ICOMP/Wright Patterson Air Force Base	51
Edward J. Hall	<i>Transonic Core Compressor Rotor/Stator Interaction</i> Co-investigators: Kurt F. Weber, K. V. Rao, and R. A. Delaney Allison Engine Company	52
Edward J. Hall	<i>Advanced Ducted Propfan Analysis Code Certification</i> Co-investigator: G. Scott McNulty Allison Engine Company	53
Edward J. Hall	<i>Fan Rotor/Endwall Treatment Interaction</i> Co-investigators: Andrew J. Crook and Kathy P. Nardini Allison Engine Company	54

Principal Investigator	NAS Summary	Page
Budugur Lakshminarayana	<i>Three-Dimensional Steady and Unsteady Turbulent Flows in Turbomachines</i> Co-investigators: S. Fan, J-F. Gallardo, Y-H. Ho, J. Luo, and W. S. Yu Pennsylvania State University	55
C. L. Merkle	<i>Computational Propulsion Applications</i> Co-investigators: S. Venkateswaran, J-Z. Feng, H-H. Tsuei, and J. M. Grenda Pennsylvania State University	56
Edward J. Reske	<i>Complex Three-Dimensional Flows in the Advanced Solid Rocket Motor</i> Co-investigators: Lee A. Kania and James W. Zuercher NASA Marshall Space Flight Center	57
William C. Rose	<i>High-Speed Inlet Design and Analysis</i> Rose Engineering and Research, Inc.	58
Balu Sekar	<i>Three-Dimensional Mixing Flows in High-Speed Combustors</i> Wright Patterson Air Force Base	59
Tom I-P. Shih	<i>Flow in Turbine-Blade Cooling Passages</i> Co-investigators: Mark A. Stephens and Kestutis C. Civinskas Carnegie Mellon University/NASA Lewis Research Center	60
Arvin Shmilovich	<i>Analysis of Nacelle/Pylon/Wing Installations</i> Co-investigator: Lie-Mine Gea McDonnell Douglas Aerospace	61
Clifford E. Smith	<i>Jets-in-Cross-Flow Mixing</i> Co-investigators: Daniel B. Bain and James D. Holdeman CFD Research Corporation/NASA Lewis Research Center	62
Robert H. Sues	<i>Parallel Multidisciplinary Stochastic Optimization</i> Co-investigator: Graham S. Rhodes Applied Research Associates, Inc.	63
R. C. Swanson	<i>Simulation of Scramjet Flow Fields</i> Co-investigators: J. Korte and E. Turkel NASA Langley Research Center/ICASE	64
Jong H. Wang	<i>Hydrocarbon Scramjet Combustor</i> Rockwell International, North American Aircraft Division	65
Scott Ward	<i>Reusable Launch Vehicle Flow Simulations</i> Co-investigator: Darren Fricker McDonnell Douglas Aerospace	66
Kurt F. Weber	<i>Chimera Domain Decomposition Applied to Turbomachinery Flow</i> Co-investigator: Dale W. Thoe General Motors Corporation, Allison Gas Turbine Division	67

Principal Investigator	NAS Summary	Page
Shaye Yungster	<i>National Aero-Space Plane Nozzles with External Burning</i> Co-investigator: Charles J. Trefny ICOMP/NASA Lewis Research Center	68

Aeronautics: Rotorcraft

W. J. McCroskey	<i>Calculations of High Performance Rotorcraft</i> Co-investigators: E. P. N. Duque, S. Ko, J. Ahmad, and A. C. B. Dimanlig NASA Ames Research Center/U.S. Army Aeroflightdynamics Directorate/ Sterling Software Systems/University of California, Davis	71
Roger C. Strawn	<i>Solution-Adaptive Computations of Helicopter Acoustics</i> Co-investigators: Rupak Biswas and Michael Garceau U.S. Army Aeroflightdynamics Directorate/NASA Ames Research Center/ RIACS/Stanford University	72

Aeronautics: Turbulence

David E. Ashpis	<i>Transition in a Highly Disturbed Environment</i> Co-investigator: Philippe R. Spalart NASA Lewis Research Center/Boeing Commercial Airplane Group	75
Brian J. Cantwell	<i>Incompressible Plane Wake Computation Comparisons</i> Co-investigators: Nagi N. Mansour, Rolf Sondergaard, and Eric Monsen Stanford University/NASA Ames Research Center	76
Haecheon Choi	<i>Numerical Simulation of Riblets</i> Co-investigators: Parviz Moin and John Kim Stanford University/NASA Ames Research Center	77
George E. Karniadakis	<i>Direct and Large-Eddy Simulation of Wake Flows</i> Co-investigators: D. Newman and R. D. Henderson Brown University	78
George E. Karniadakis	<i>Simulation of Complex-Geometry Wall-Bounded Flows</i> Co-investigators: Catherine H. Crawford and Ronald D. Henderson Brown University	79
Linda D. Kral	<i>Turbulence Modeling for Three-Dimensional Flow Fields</i> Co-investigators: John A. Ladd, Mori Mani, and John F. Donovan McDonnell Douglas Corporation	80
Thomas S. Lund	<i>Large-Eddy Simulation of Jet Combustors</i> Co-investigators: Parviz Moin and Knut Akselvoll Stanford University/NASA Ames Research Center	81
Nateri K. Madavan	<i>Boundary-Layer Transition on a Heated Flat Plate</i> MCAT Institute	82

Principal Investigator	NAS Summary	Page
Parviz Moin	<i>Direct Numerical Simulation of Shock/Turbulence Interaction</i> Co-investigators: Sanjiva K. Lele, Krishnan Mahesh, and Sangsan Lee Stanford University	83
Parviz Moin	<i>Large-Eddy Simulation of Separated External Flows</i> Co-investigators: Thomas S. Lund, Patrick Beaudan, and Haecheon Choi Center for Turbulence Research/Stanford University/NASA Ames Research Center	84
Parviz Moin	<i>Large-Eddy Simulation of Complex Flows</i> Co-investigators: Thomas S. Lund and Hans J. Kaltenbach Stanford University/NASA Ames Research Center	85
Steven A. Orszag	<i>Unsteady Turbulence Model Simulations</i> Co-investigator: William S. Flannery Cambridge Hydrodynamics, Inc.	86
Richard H. Pletcher	<i>Three-Dimensional Liquid Sloshing Flow Simulation</i> Co-investigators: S. Babu, F. J. Kelecý, and W-P. Wang Iowa State University	87
Man Mohan Rai	<i>Direct Simulation of Turbulent/Transitional Airfoil Flow</i> NASA Langley Research Center	88
Michael M. Rogers	<i>Self-Similar Turbulent Plane Wakes</i> Co-investigators: Robert D. Moser, S. Scott Collis, and Chris Rutland NASA Ames Research Center/Stanford University/University of Wisconsin, Madison	89
Bart A. Singer	<i>Origins of Near-Wall Turbulence</i> Co-investigator: Ronald D. Joslin High Technology Corporation/NASA Langley Research Center	90

**General: Aeroacoustics, Astronautics, Astronomy, Atmospheric Science,
Chemistry, Computer Science, Electromagnetics, Fluid Mechanics, Life Science,
Magnetospheric Physics, Reactive Flow, Space Science**

Aeroacoustic

Lyle N. Long	<i>Hybrid Massively Parallel Aeroacoustics Scheme</i> Pennsylvania State University	93
--------------	--	----

Astronautics

Creon Levit	<i>Evolution of Planetary Rings</i> NASA Ames Research Center	94
-------------	--	----

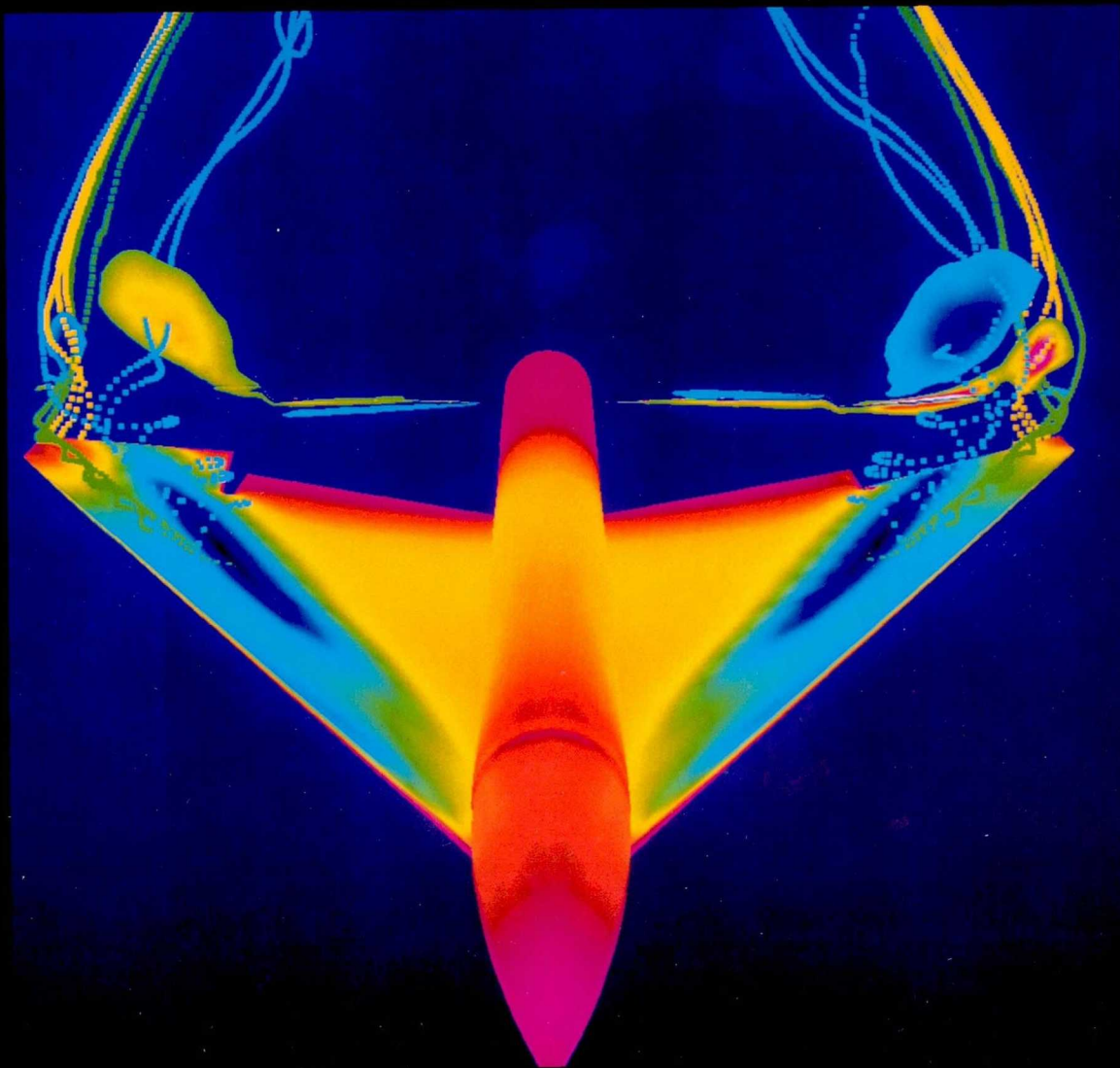
Astronomy

James Caristi	<i>Simulating the Cosmic X-Ray Experiment</i> Co-investigators: Brian Ramsey, Martin Weisskopf, and Jeff Youngen Valparaiso University/NASA Marshall Space Flight Center	95
---------------	--	----

Principal Investigator	NAS Summary	Page
Bruce F. Smith	<i>Studies of Galaxy Formation and Evolution</i> Co-investigators: Richard A. Gerber, Richard H. Miller, and Thomas Y. Steiman-Cameron NASA Ames Research Center/University of Chicago	96
Atmospheric Science		
Christian L. Kepenne	<i>Intraseasonal Atmospheric Oscillations</i> Jet Propulsion Laboratory	97
James B. Pollack	<i>Dynamics of the Martian Atmosphere</i> Co-investigator: Robert Haberle NASA Ames Research Center	98
Richard E. Young	<i>Simulation of Volcanic Aerosol Clouds</i> Co-investigators: O. B. Toon and H. Houben NASA Ames Research Center	99
Chemistry		
Sang-Wook Kim	<i>Chemically Reacting Compressible Shear Layer</i> University of Toledo	100
Computer Science		
Jerry Yan	<i>Automated Instrumentation and Monitoring System</i> Co-investigators: Pankaj Mehra, Sekhar Sarukkai, Cathy Schulbach, Melisa Schmidt, and Brian Vanvoorst Recom Technologies/NASA Ames Research Center	101
Electromagnetics		
Ramesh K. Agarwal	<i>Computational Fluid Dynamics Solution for Maxwell's Equations</i> Co-investigators: Dau-Sing Wang and Mark R. Axe McDonnell Douglas Corporation	102
Vijaya Shankar	<i>Computational Fluid Dynamics Approach to Computational Electromagnetics</i> Co-investigators: William Hall, Chris Rowell, and Alireza Mohammadian Rockwell International Science Center	103
John L. Volakis	<i>Electromagnetic Scattering by Airborne Structures</i> Co-investigator: Arindam Chatterjee University of Michigan	104
Alex C. Woo	<i>Computational Radar Cross Sections</i> Co-investigators: Michael Simon and Michael Schuh NASA Ames Research Center/Sterling Software Systems	105
Fluid Mechanics		
Joseph D. Baum	<i>Arbitrary Lagrangian-Eulerian Three-Dimensional Simulations</i> Co-investigator: Rainald Lohner	106

	Science Applications International Corporation/George Mason University	
Principal Investigator	NAS Summary	Page
Fred Stern	<i>Unsteady Viscous Marine Propulsor Hydrodynamics</i> Co-investigators: E. Paterson and B. Chen University of Iowa	107
Fred Stern	<i>Free-Surface Effects on Boundary Layers and Wakes</i> Co-investigators: Y. Tahara and J. Choi University of Iowa	108
Matthew E. Thomas	<i>Impeller Computational Fluid Dynamics Modeling</i> Co-investigators: Mahesh M. Athavale and Mark L. Ratcliff CFD Research Corporation	109
Life Science		
Jeffrey R. Hammersley	<i>Modeling of Pulmonary Fluid Dynamics</i> Co-investigators: Rama Reddy, Dan E. Olson, Boyd Gatlin, and Joe F. Thompson University of Arkansas/Medical College of Ohio/Mississippi State University	110
Andrew Pohorille	<i>Structure and Functions of Membranes</i> Co-investigator: Michael A. Wilson University of California, San Francisco	111
Muriel D. Ross	<i>Finite Volume Neuronal Modeling</i> Co-investigators: David G. Doshay, Samuel W. Linton, and Timothy J. Barth NASA Ames Research Center/Sterling Software Systems	112
Magnetospheric Physics		
Stephen H. Brecht	<i>Solar Wind Interaction with Mars</i> Co-investigator: John R. Ferrante Berkeley Research Associates	113
Reactive Flow		
K. Kailasanath	<i>Burner-Stabilized Flames in Microgravity</i> Co-investigator: G. Patnaik Naval Research Laboratory/Berkeley Research Associates	114
Space Science		
Jeffrey N. Cuzzi	<i>Protoplanetary Nebula Particle-Gas Dynamics</i> Co-investigators: Anthony R. Dobrovolskis, Robert C. Hogan, Joelle M. Champney, and Jennifer M. Dacles-Mariani NASA Ames Research Center/University of California, Santa Cruz/Synernet, Inc.	115

Aeronautics



Basic Research

Page intentionally left blank

Unstructured Grid Finite-Element Solutions

Ramesh K. Agarwal, Principal Investigator

Co-investigators: David W. Halt and David L. Marcum

McDonnell Douglas Corporation/Mississippi State University



Research Objective

To investigate the viability of unstructured grids in computing three-dimensional finite-element Euler and Navier–Stokes steady and unsteady flows.

Approach

The Euler or Reynolds-averaged Navier–Stokes equations are solved on an unstructured grid of tetrahedral elements. Space discretization is obtained from a Galerkin-weighted residual approximation. Time discretization uses either an explicit Lax–Wendroff scheme or an explicit multistage Runge–Kutta scheme. Turbulence effects can be modeled using a Baldwin–Lomax, Baldwin–Barth, or two-equation $k-\epsilon$ model. The incremental-point-insertion Delaunay method is used for grid generation and solution adaptation.

Accomplishment Description

An unstructured grid was generated for the Delta launch vehicle with nine attached boosters. The objective was to allow every third booster to separate symmetrically from the main body after the booster fuel was burned. The grid for a 120-degree section was generated with 88,325 grid points and 460,722 tetrahedra. The initial steady state solution is computed at a free-stream Mach number of 2.313 and 0 degrees angle of attack. The force and moments were integrated on each free booster with initial trajectories set and the unsteady flow solution was initiated. The unstructured grid was distorted as the free boosters separated from the main body. A continual cycle of unsteady flow analysis, integration of body forces and moments, calculation of the trajectory, and movement of the grid was repeated until the level of grid distortion required maintenance. This case required 15 megawords of memory and 9 Cray Y-MP microseconds per iteration for each node.

Significance

An unsteady Euler analysis of the Delta launch vehicle with separating boosters was demonstrated.

Future Plans

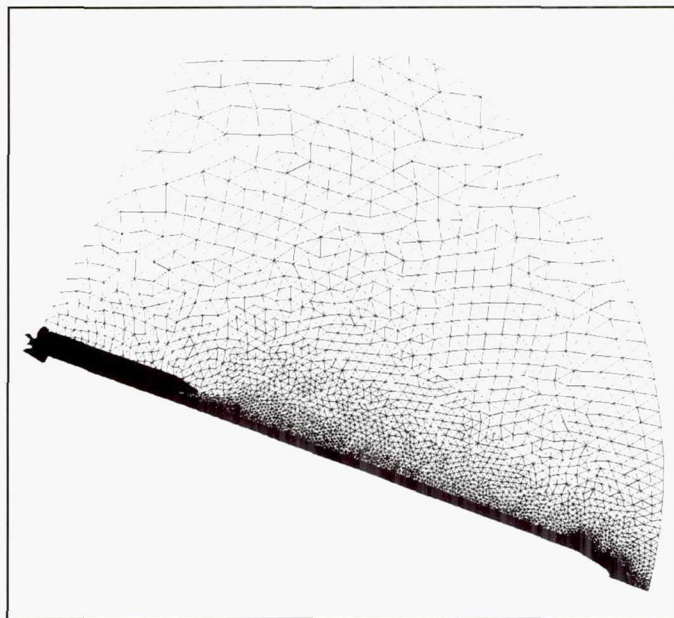
To calculate the viscous unsteady flow fields about multiple bodies in relative motion, such as a launch vehicle with separating boosters or an aircraft releasing a store.

Keywords

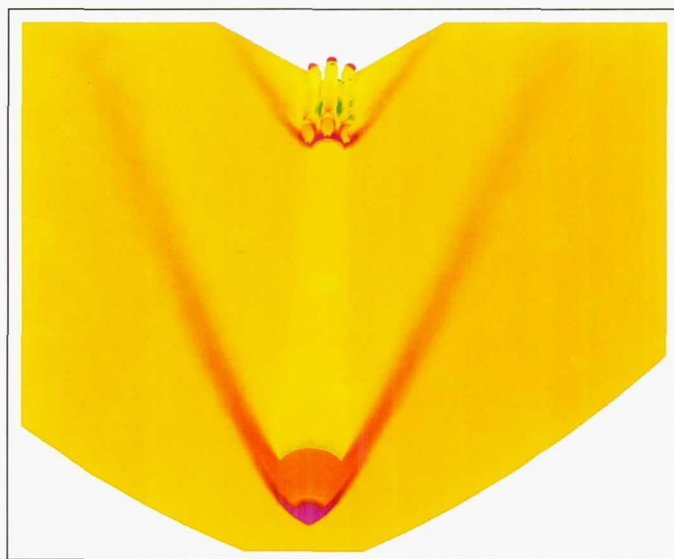
Computational fluid dynamics, Viscous flow, Finite element method

Publication

Marcum, D. L.; and Weatherill, N. P.: Finite Element Calculations of Inviscid and Viscous Flow Fields about Launch Vehicle Configurations. Eighth International Conference on Finite Elements in Fluids, Barcelona, Spain, Sept. 1993.



Surface grids for a launch vehicle with nine boosters.



Density contours for a launch vehicle with nine boosters.

Parallel Implementation of an Unstructured Mesh Navier–Stokes Solver

Timothy J. Barth, Principal Investigator

Co-investigator: Samuel W. Linton

NASA Ames Research Center/Sterling Software Systems



Research Objective

To develop a parallel implementation of an existing unstructured mesh Navier–Stokes solver.

Approach

A parallel implementation of an existing Navier–Stokes solver for the Cray computer was modified for the CM-5. The code utilizes a static mesh partitioning combined with a message passing protocol. In the baseline Cray code, the Navier–Stokes equations are discretized on arbitrary meshes using a finite-volume approach with upwind dissipation added to stabilize the scheme. A single-equation turbulence model is included to simulate the effects of turbulence on the mean flow. The algorithm exhibits second-order spatial accuracy on sufficiently smooth meshes. An implicit time-stepping strategy is used that approaches Newton's method for large time steps. This strategy requires the solution of a sequence of large, sparse matrix equations that are solved using a generalized minimum residual method with incomplete lower–upper preconditioning. The parallel implementation retains the discretization and Newton-like properties of the uniprocessor code.

Accomplishment Description

The figure shows typical results for subsonic flow over a high-lift airplane configuration. The subdivisions induced by the volume partitioning are shown on the body surface and cross plane.

Significance

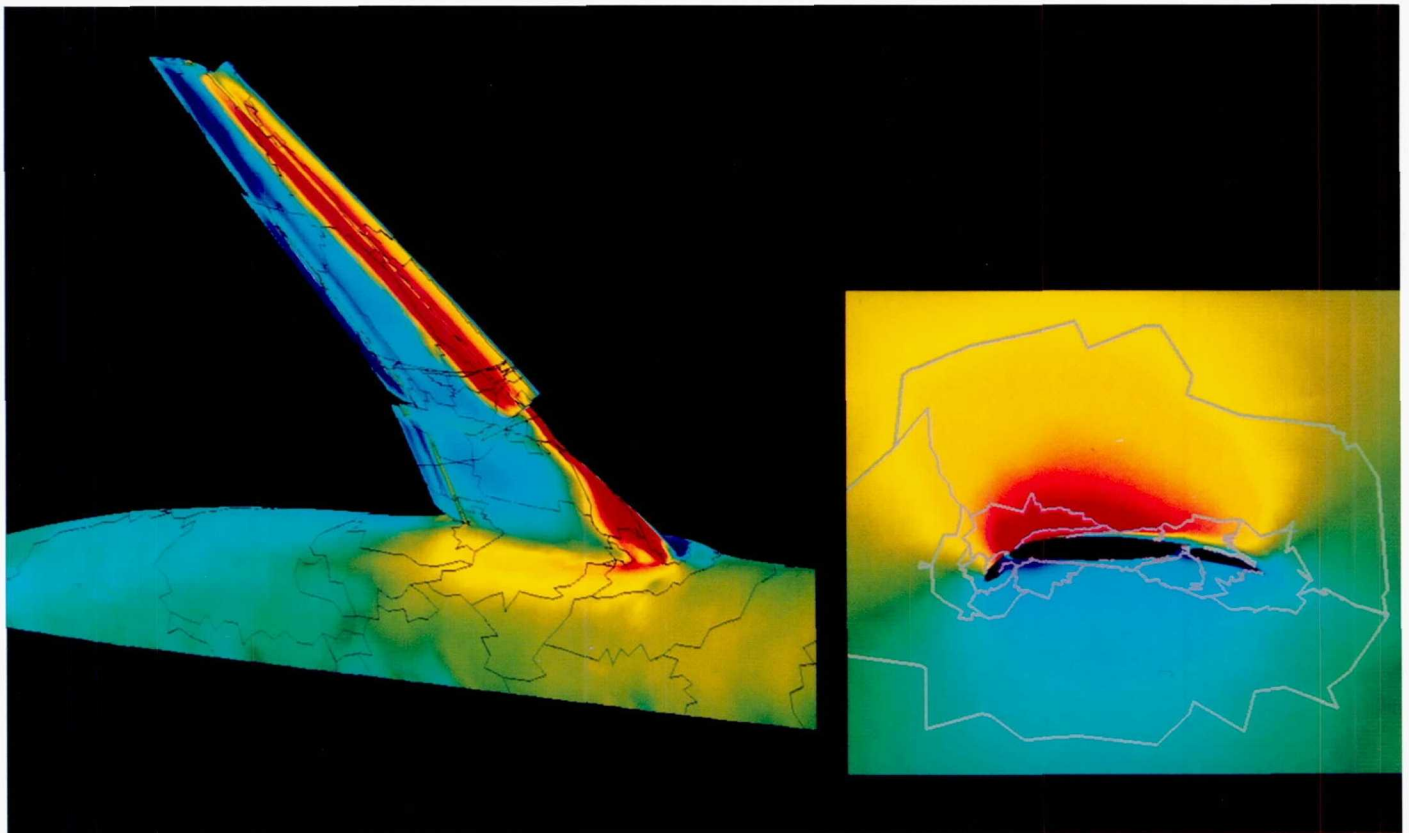
The use of unstructured meshes permits the calculation of aerodynamic flow over complex geometries. Moreover, the improved efficiency and scalability of the parallel algorithm permits the calculation of these flows using modest resources.

Future Plans

A shape optimization capability will be incorporated into the flow solver using an adjoint equation approach.

Keywords

Unstructured mesh, Navier–Stokes



Mach number Goursaud shading of surface and cross plane for subsonic flow calculation.

Applied Computational Fluid Dynamics

Farhad Ghaffari, Principal Investigator

Co-investigators: Brent L. Bates and James M. Luckring

NASA Langley Research Center/ViGYAN, Inc.



Research Objective

To assess the vortical-flow prediction capability of the state-of-the-art unstructured-grid methodology for a complex generic fighter wind tunnel model over a wide range of flow conditions.

Approach

The analytical description of a generic fighter wind tunnel model, known as modular transonic vortex interaction (MTVI), was used to generate the geometrical database from which the computational surface grid definition was derived for the entire geometry. The MTVI configuration incorporated a 60-degree sharp-edged cropped delta wing with segmented leading-edge flaps, chine-shaped fuselage, and twin vertical tails positioned on the aft-inboard region of the wings. The complete geometry was represented by about 28,000 surface triangles. The flow-field grid, generated using an advancing front method, consisted of about 825,000 tetrahedral cells. The grid spacing, distribution, and the extent of the far-field boundaries were consistent with an earlier calibration study performed on the isolated MTVI fuselage configuration. Since the subject vortical flow (emanating from sharp edges) is presumed to be mostly governed by inviscid flow phenomena, the present computational effort was performed based on an Euler formulation.

Accomplishment Description

Computational results were obtained for the MTVI configuration for a wide range of flow conditions using the flow solver USM3D. A typical solution obtained at 22 degrees angle of attack and a Mach number of 0.4 and superimposed over the computational surface grid is shown in the figure. The figure illustrates the total-pressure contours at several cross-flow planes along with the particle tracings within the core region for both primary vortex sys-

tems (one emanating from the chine forebody and the other from the wing leading-edge flaps). The figure clearly shows the geometric complexity, in particular the deflected wing leading-edge flaps (two inboard segments deflected at 30 degrees), and the predicted vortical-flow structures. This solution, initiated from the free-stream flow conditions, was advanced for 2,000 iterations during which the total residuals dropped about 1.5 orders of magnitude. The solution required approximately 150 megawords of memory and used about 10 hours of computational time on Cray Y-MP. Additional analysis has shown that the computed surface pressure coefficients, forces, and moments agree reasonably well with the measured experimental wind tunnel data.

Significance

The present unstructured-grid methodology provides reasonable flow predictions. The versatility of the methodology in grid generation for complex geometries makes it an efficient technique for routine analysis applications.

Future Plans

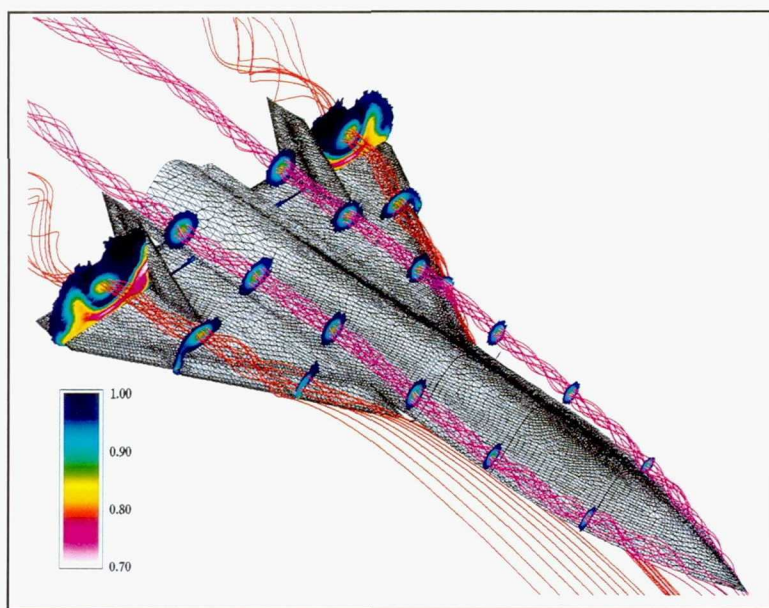
Computations will be extended to parametrically investigate the aerodynamic effects for various geometrical modifications such as the fuselage chine shapes, tail arrangements, and wing leading-edge flap deflections.

Keywords

Euler computations, Fighter configuration, High angle of attack, Vortex flows

Publication

Ghaffari, F.: On the Vortical-Flow Prediction Capability of an Unstructured-Grid Euler Solver. AIAA Paper 94-0163, Jan. 1994.



Total-pressure contours in various cross-flow planes and vortex core particle traces; $\alpha = 22$ degrees and free-stream Mach number = 0.4.

Design-by-Optimization Method

Philip B. Gingrich, Principal Investigator
Rockwell International, North American Aircraft Division



Research Objective

To develop and validate a three-dimensional (3-D) numerical optimization design method applicable to complete aircraft configurations.

Approach

A multiblock, implicit time-marching Euler and Navier–Stokes solver is coupled with a gradient-based, constrained optimization technique. Geometry perturbation functions, with an associated design variable, operate on the surface grid. The optimizer determines the design variable set, which minimizes a composite function formed with the objectives and constraints. The objective may be any aerodynamic variable such as drag or lift-to-drag (L/D) ratio. Constraint functions consist of both aerodynamic and geometric variables. To simulate an inverse procedure, the objective is the root-mean-square difference between current and specified target pressure distribution.

Accomplishment Description

A 3-D design-by-optimization method for application to complete aircraft configurations is expanded to increase geometric flexibility and to reduce computational time. The method was originally developed as an inverse design tool to derive a shape for a specified pressure distribution. Recent efforts have focused on deriving a wing shape for minimum drag in nonlinear flow regimes. The ONERA M6 wing, simulated with a coarse Euler

grid, was used as a test case. An Euler analysis of the baseline configuration at Mach = 0.84 and 3.06 degrees angle of attack is shown in the figure. Design studies were conducted to minimize drag with the total lift constrained. Shape functions were applied alternately to the upper surface and the mean camber plane with various spanwise distributions. A typical optimization result is shown in the figure. The L/D ratio, including estimated skin friction drag, increased from 11.24 to 12.35. An optimization for a 200,000 point grid required 1–2 Cray Y-MP hours and 20 megawords of memory.

Significance

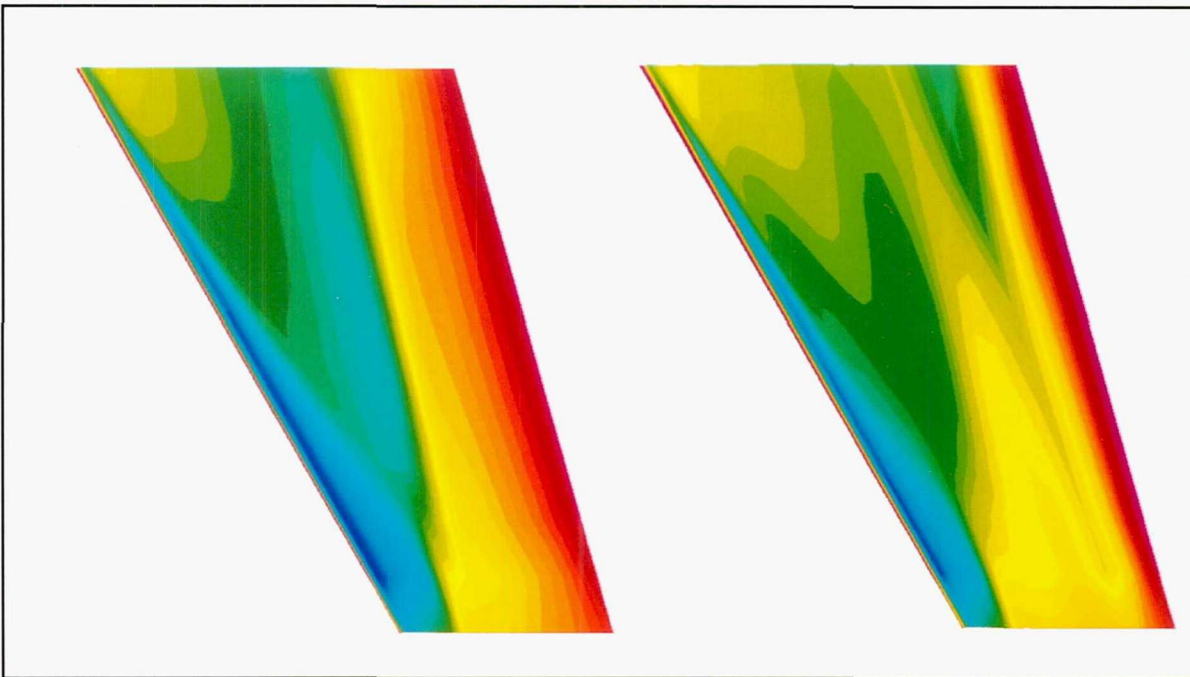
Nonlinear design methods have not kept pace with computational fluid dynamics analysis capability. Emerging direct inverse and numerical optimization techniques will reduce design cycle time for subsonic and supersonic aircraft.

Future Plans

Inclusion of analytically derived sensitivity derivatives will be investigated as a means of reducing computational time and reducing potential noise arising from finite-difference gradient computation.

Keywords

Aerodynamics, Computational fluid dynamics



Upper surface isobars on an ONERA M6 wing with $L/D = 11.24$ (left side); lift-constrained numerical optimization with $L/D = 12.35$ (right side) at Mach = 0.84 and 3.06 degrees angle of attack.

Simulation of Spatially Evolving Jets

Fernando F. Grinstein, Principal Investigator
Naval Research Laboratory



Research Objective

To characterize the underlying fluid-mechanical processes leading to the deformation and breakdown of vortex rings in rectangular jets, their dependence on aspect ratio, and their role in entrainment and transition to turbulence.

Approach

Monotonic algorithms on structured grids were used to develop a three-dimensional numerical simulation of rectangular jets developing in space and time. The model uses fourth-order flux-corrected transport algorithms and appropriate inflow and outflow boundary conditions for convective transport, finite-rate chemistry, and temperature- and species-dependent diffusive transport.

Accomplishment Description

The figures show simulation results of an isolated vortex ring with an aspect ratio of 4:1 as it is convected away from the nozzle. The evolution of the ring is visualized in terms of instantaneous iso-surfaces of the vorticity magnitude. The self-deformation of the ring first follows a pattern similar to that observed for the 2:1 jet, leading to a rectangular-shaped ring with its axis rotated 90 degrees relative to its initial cross section. As the ring moves farther downstream and away from the nozzle, the centers of its longer portions approach each other, vortex reconnection takes place, and the ring eventually bifurcates into two smaller vortex rings that are linked by very thin threads of vorticity. Vortex-ring bifurcation was suggested by laboratory experiments with 4:1 rectangular jets. The figures reveal that the detailed vorticity dynamics in this vortex "fission" process involve self-deformation and axis-switching followed by vorticity redistribution leading to the bridging of antiparallel portions of the vortex ring and the forming of threads linking the new vortex rings. This simulation used 23 megawords of memory and about 64 Cray Y-MP hours.

Significance

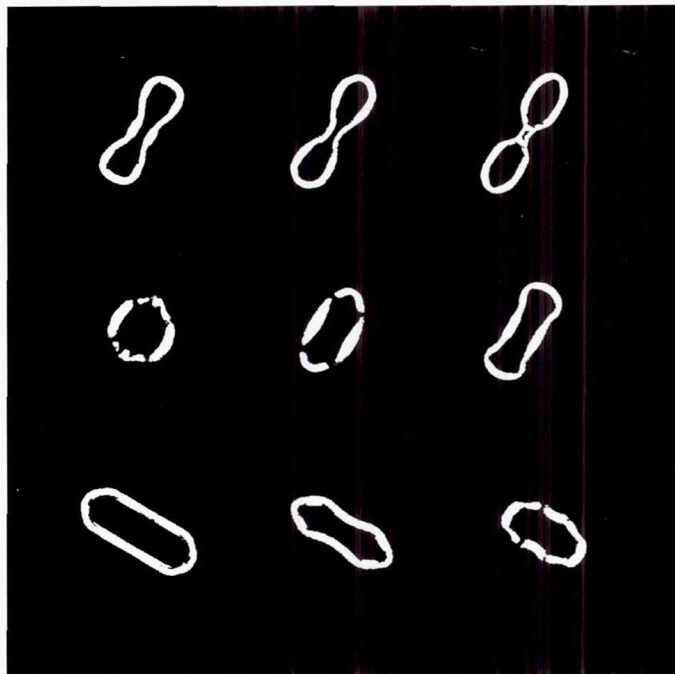
The simulations provide insight into the physics of large-scale coherent structures in rectangular jets and the mechanisms affecting entrainment and the transition to turbulence. The effort advances the state of the art of turbulent jet simulations.

Future Plans

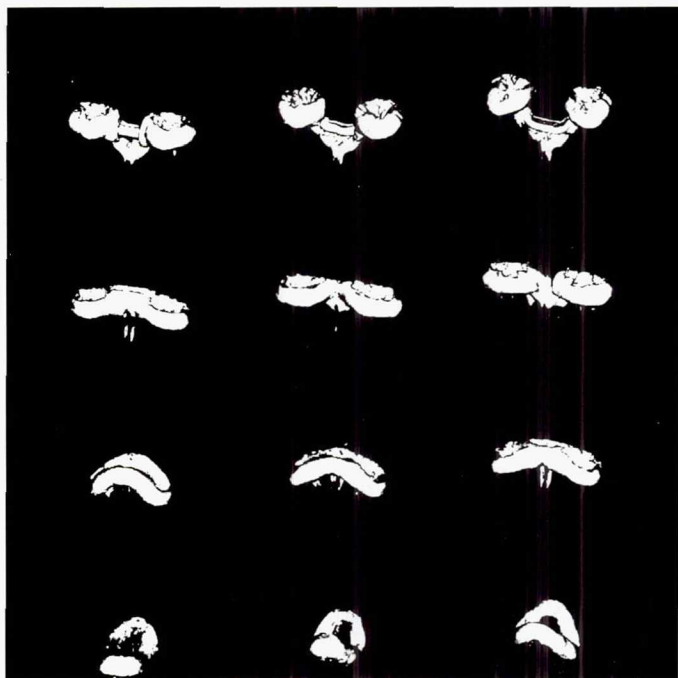
The study of reactive jets will continue and the flame extinction phenomena in jets will be investigated.

Keywords

Fluid mechanics, Vortex, Turbulence



Iso-surfaces of the vorticity magnitude equal to 40 percent of its initial peak value. Flow evolves spatially from bottom to top in each frame. Time increases from left to right in each row, and from the bottom row to the top row.



Iso-surfaces of the vorticity magnitude from a different perspective and for 15 percent of the peak vorticity value.

Aeroelasticity of Wing–Body–Control Configurations

Guru P. Guruswamy, Principal Investigator

Co-investigators: Chansup Byun, Eugene Tu, and Shigeru Obayashi

NASA Ames Research Center/MCAT Institute



Research Objective

To compute the aeroelasticity of wing–body–control configurations using the Navier–Stokes flow equations directly coupled with finite-element structural equations.

Approach

The finite-difference based three-dimensional Euler/Navier–Stokes equations of motion coupled with the finite-element plate/shell structural equations of motion were solved by using a time-accurate numerical integration scheme with configuration-adaptive dynamic grids. An accurate and robust domain decomposition method suitable for aeroelasticity associated with strong fluid/structural interactions was used.

Accomplishment Description

The computational domain was divided into fluid and structural domains. The information between domains were communicated using a robust grid-point (fluid) to element (structural) approach. A typical unsteady computation of a wing–body–control configuration with 1 million grid points required about 35 Cray C-90 hours and 33 megawords of memory.

Significance

This research has a major impact on the Advanced Subsonic Civil Transport (ASCT), High Speed Civil Transport (HSCT), and High Performance Computing and Communications programs. It can also be used for Department of Defense projects.

Future Plans

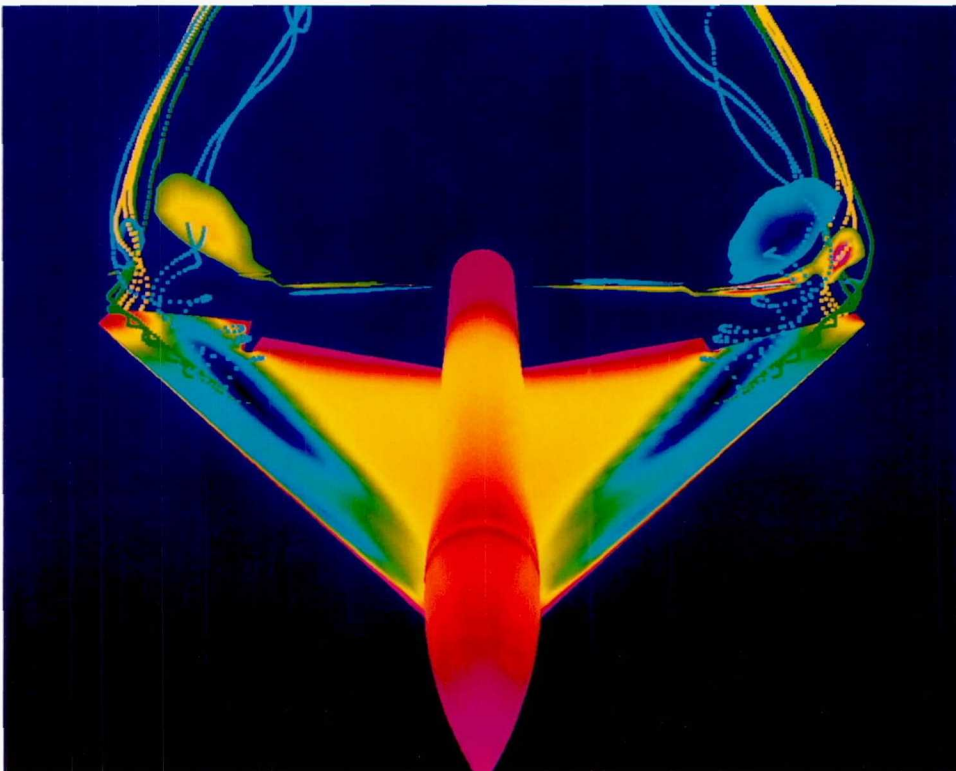
This technology will be extended to wing–body–control–empennage configurations for the ASCT and HSCT programs.

Keywords

Aeroelasticity, Controls

Publications

1. Guruswamy, G. P.; and Byun, C.: Fluid-Structural Interactions Using Navier–Stokes Flow Equations with Shell Finite-Element Structures. AIAA Paper 93-3087, 24th Fluid Dynamics Conference, Orlando, Fla., July 1993.
2. Obayashi, S.; Chiu, I.; and Guruswamy, G. P.: Navier–Stokes Computations on Full-Span Wing–Body Configurations with Oscillating Control Surfaces. AIAA Paper 93-3687, AIAA Atmospheric Flight Mechanics Conference, Monterey, Calif., August 1993.



Flow over an HSCT-type wing–body–control configuration with oscillating control surfaces.

Wing-Body Aeroelasticity

Guru P. Guruswamy, Principal Investigator
Co-investigator: Chansup Byun
NASA Ames Research Center/MCAT Institute



Research Objective

To perform aeroelastic computations on realistic configurations using the Intel iPSC/860 parallel computer.

Approach

The finite-difference-based three-dimensional Euler equations of motion coupled with the finite-element plate/shell structural equations of motion are solved by using a time-accurate numerical integration scheme with configuration adaptive dynamic grids. A domain decomposition method suitable for parallel computers is used. In this method, the computational domain is divided into fluids and structural domains. The information between domains is communicated using a robust grid-point (fluid) to element (structural) approach. The fluids domain is solved in parallel with the structural domain in a separate group (cube) of processors. Within each cube, computations are performed in parallel.

Accomplishment Description

A new version of the computer code ENSAERO that solves the Euler equations simultaneously with the finite-element structural equations of motion has been developed on the Intel iPSC/860 computer. The flow is modeled using H-O type grid topology using 250,000 grid points. The structures of the wing and body are modeled using plate and shell elements. This resulted in a structural matrix equation with 1,641 degrees of freedom. The fluids part of ENSAERO, including the moving grid, is computed in a cube of 32 processors and the finite-element structures are computed in a cube of 8 processors. A typical aeroelastic response (shown in the figure) required about 20 central processing unit hours. The same computation requires 8 Cray C-90 hours. The Intel iPSC/860 computer performed at an efficiency of about 10 percent for this practical problem.

Significance

The successful implementation of ENSAERO with finite-element structures on the Intel iPSC/860 is a major step in the development of general purpose computer codes to solve fluid/structures interaction problems on parallel computers.

Future Plans

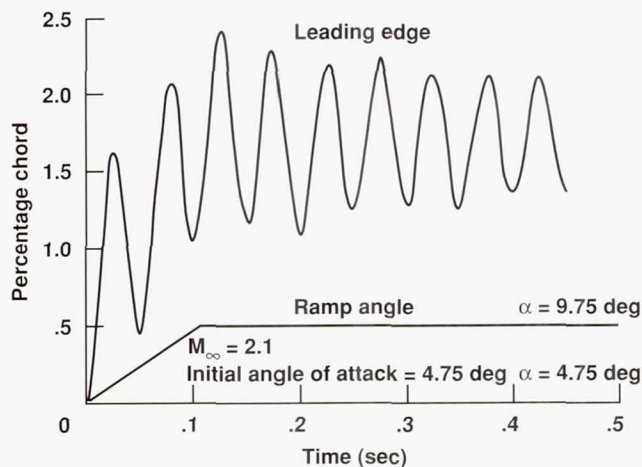
The structures solver will be improved because direct solvers do not scale well for larger problems. This technology will be extended to model more complex configurations using zonal grids for fluids and substructures for structures. Navier-Stokes capability with Baldwin-Lomax turbulence modeling, moving control-surface, and tail modeling capabilities will be added to ENSAERO. Transonic aeroelastic results will be computed for advanced subsonic civil transport configurations. Detailed finite-element capabilities including active controls and optimization disciplines will be implemented.

Keywords

Aeroelasticity, Finite elements, Euler equations

Publication

Byun, C.; and Guruswamy, G. P.: Wing-Body Aeroelasticity Using Finite-Difference Fluid/Finite-Element Structural Equations on Parallel Computers. AIAA Paper 94-1487, Apr. 1994.



Aeroelastic response of the Boeing 1807 high-speed civil transport model in pitch-up motion.

Multipoint Aerodynamic Design

Forrester T. Johnson, Principal Investigator

Co-investigators: Michael B. Bieterman, Craig L. Hilmes, William P. Huffman, Robin G. Melvin, and David P. Young
The Boeing Company



Research Objective

To demonstrate and evaluate a multipoint aerodynamic design capability for three-dimensional (3-D) aircraft configurations on Cray supercomputers. Interim objectives supporting these goals are the application and evaluation of recently developed techniques for improved aerodynamic analysis and single-point design of complex configurations.

Approach

The TRANAIR code, a full-potential/boundary-layer coupled code that uses solution adaptive local refinement of Cartesian grids to resolve flow fields about complex aircraft configurations, is used in this project. To solve the discrete system of flow equations, a Newton method is used that incorporates incomplete sparse matrix factorizations. A single-point design optimization methodology has been added to TRANAIR to enable treatment of many realistic constraints and objective functions. In this project, improvements that were made to TRANAIR's design analysis capabilities are applied, evaluated, and extended to multipoint design problems. Applications of particular interest are those involving high-speed civil transport (HSCT) configurations.

Accomplishment Description

One recently developed improvement that was tested on the Cray C-90 is second-order upwinding, which can result in substantially better accuracy in supersonic flow regions. This method is especially promising for HSCT problems requiring high resolution of flow features near the aircraft or for sonic boom, wind tunnels, and other simulations where accurate capture of shocks in the field away from the aircraft is of interest. A recently developed integral boundary layer coupling capability was evaluated. This capability allows the modeling of viscous effects and enables these effects to be incorporated into design objective functions and constraints. Drag accuracy, the use of drag minimization in single-point design, and recently implemented treatment of manufacturing, structural, and flow constraints were evaluated. This work contributed to the development of improved aerodynamic optimization formulations for HSCT configurations. A multipoint design optimization methodology was developed and applied to two-dimensional (2-D) problems in a workstation environment. Typical computer requirements for 3-D configurations in this project have been 2–4 Cray C-90 hours and 64–128 megawords of memory.

Significance

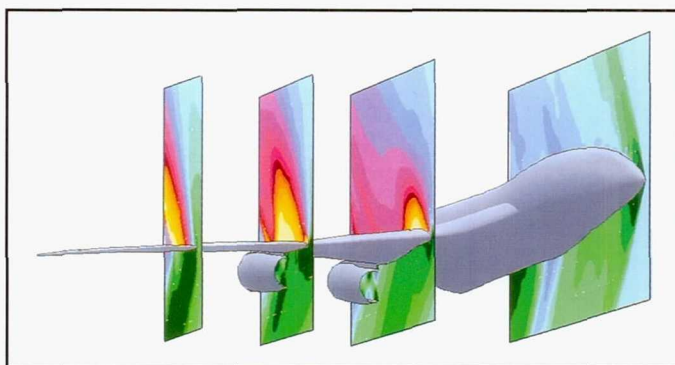
Competitive commercial transport aircraft designs require state-of-the-art aerodynamic performance under nominal cruise conditions and acceptable performance under "off-design" conditions. The design cycle time of such aircraft may be significantly shortened if computational fluid dynamics design tools that achieve some degree of optimality for multiple flow conditions are available early in the design cycle. Such cycle time reduction may be especially valuable for future aircraft such as the HSCT, where high performance in both supersonic and transonic flight regions would be desirable.

Future Plans

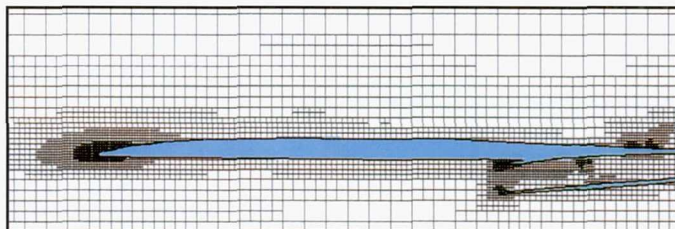
Evaluation of analysis and single-point design method improvements that are necessary for efficient and accurate multipoint design will continue. The multipoint design methodology tested for 2-D problems will be implemented and evaluated for 3-D aircraft configurations in the multiple-CPU Cray C-90 environment.

Keywords

TRANAIR, Adaptive grid, Boundary layer coupling



Mach contours of a TRANAIR solution of a high-speed civil transport problem; yellow = high and dark green = low.



Cross section of the inboard wing and nacelle on the 1.2-million-point computational grid.

Vortex-Flow Control

Steven B. Kern, Principal Investigator
Naval Air Warfare Center



Research Objective

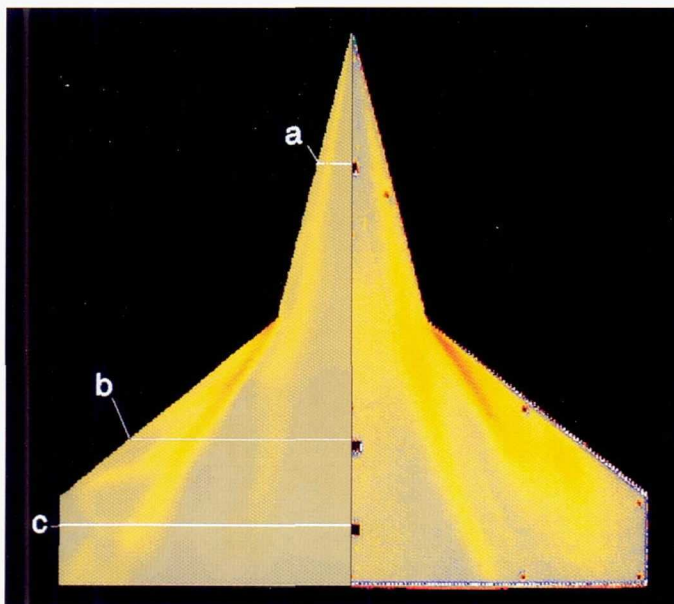
To investigate unique vortex-flow control concepts on a common configuration and to apply the most promising of these concepts to a complete aircraft configuration such as the F/A-18E.

Approach

A combined computational and experimental approach is used for this research. Applying the OVERFLOW and CFL3D codes, the three-dimensional Reynolds-averaged Navier-Stokes equations are used to simulate the vortical flow fields resulting from three unique vortex-flow control concepts: leading-edge extension/wing junction fillets, spanwise blowing to control the secondary vortex, and windward side modifications. These concepts are being investigated on a single delta wing and a cropped double delta wing. The most promising concepts are tested experimentally and, once validated, can be applied to a realistic fighter configuration.

Accomplishment Description

To date, a study of the effects of spanwise tangential blowing from a slot on the upper surface of a delta wing and a study on the effects of grid refinement and embedded grids on a cropped double delta wing configuration have been completed. Each run required an average of 32 megawords of memory and 7 Cray C-90 hours. Spanwise tangential slot blowing at the point of boundary layer separation was effective in completely eliminating the secondary separation vortex on the delta wing. The double delta wing with fillets was tested in the NASA Langley 7- by 10-Foot Transonic Wind Tunnel, 8-Foot Transonic Wind Tunnel, and Basic Aerodynamic Research Tunnel. The figure shows the computational surface pressure coefficients compared



Computational surface pressure coefficients compared to pressure sensitive paint and surface pressure taps at (a) 25, (b) 75, and (c) 90 percent chord stations.

to pressure sensitive paint and surface pressure taps at 25, 75, and 90 percent chord stations.

Significance

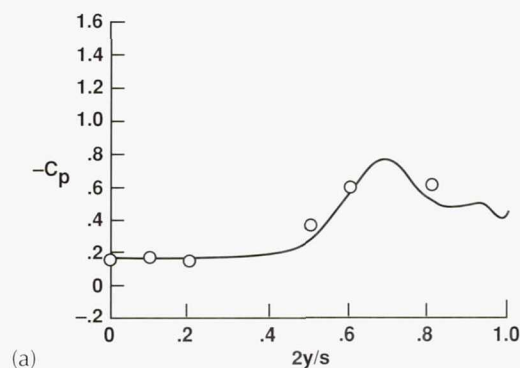
The control of vortices has the potential to increase lift and rolling moments on demand, which will enhance aircraft maneuverability, agility, and controllability.

Future Plans

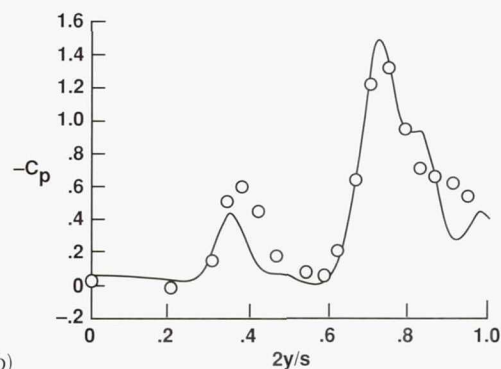
Vortex-flow control concepts on the complete F/A-18E aircraft at high angle of attack will be computed.

Keywords

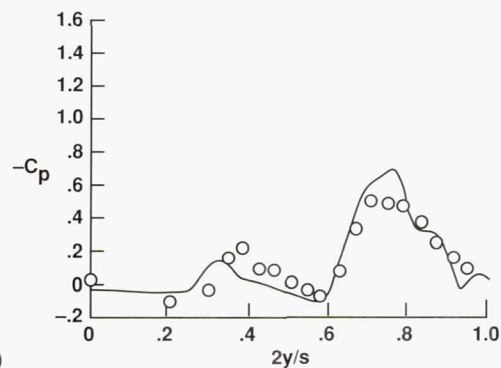
Vortex flows, Fighter configuration, High angle of attack



(a)



(b)



(c)

Skewed Compressible Mixing Layers

Sanjiva K. Lele, Principal Investigator

Co-investigator: Ganyu Lu

Stanford University



Research Objective

To establish the potential for enhanced mixing because of free-stream skewing.

Approach

Three-dimensional (3-D) unsteady Navier–Stokes equations are solved for skewed mixing-layer flows. The linear-stability analysis of the skewed 3-D flow is used to prescribe inflow disturbances. The unsteady dynamics of the large-scale structures and the overall statistical evolution of the flow is studied.

Accomplishment Description

Direct numerical simulations were conducted to study a particular subclass of skewed compressible mixing layers—mixing layers between streams with equal velocity magnitude, but skewed in the opposite directions. The inflow and initial conditions were prescribed by the linear stability eigenfunctions for the most unstable waves. Nonlinear spatial evolution of the vortex structures were then simulated. For these flows, a stationary spanwise wave was the most unstable wave for low-convective Mach numbers and was used as the inflow disturbance in the direct numerical simulation. The grid size of the simulation was $251 \times 189 \times 65$. The first figure shows the vortex lines and cuts of a passive scalar field for a skewed mixing layer with a 90-degree skewing angle. The free-stream Mach number is 0.6, which keeps the stabilizing compressibility effect at a small level. Near the inflow, the disturbance rolls up and forms a pattern of streamwise vortices. Further downstream, the straight concentrated vortex tubes suddenly spread out. The vortex breakdown can enhance the mixing between the two streams, which is shown quantitatively by the spreading of momentum thickness for different skewing angles. A typical simulation requires approximately 80 Cray C-90 hours, 15 megawords of central memory, and 110 megawords of disk scratch space.

Significance

Skewing the free streams offers a simple method for mixing enhancement. The skewing effects on mixing layers can now be estimated. Enhanced instability may lead to more effective mixing and its control.

Future Plans

The simulation will be extended to systematically explore the effects of skewing and compressibility on the mixing layer.

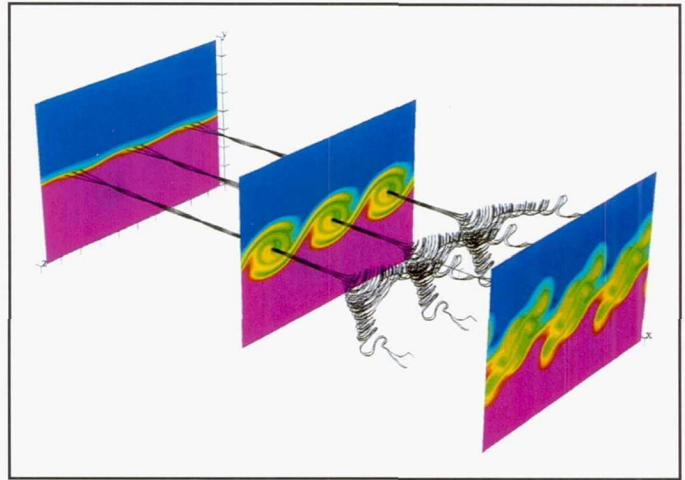
Keywords

Vortex breakdown, Mixing enhancement

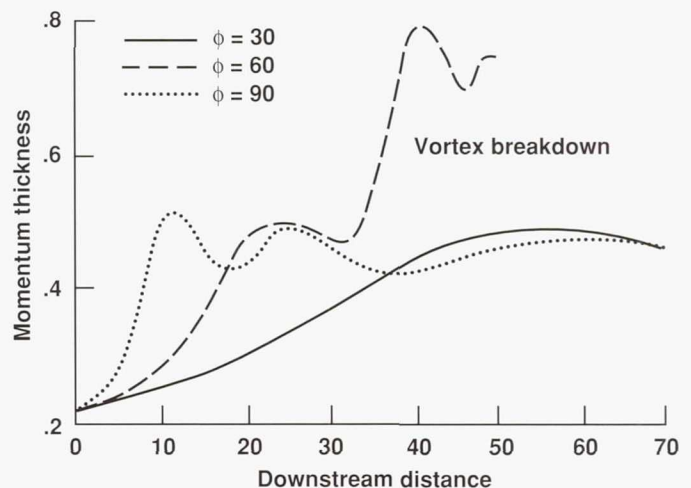
Publications

1. Lu, G.; and Lele, S. K.: Inviscid Instability of Skewed Compressible Mixing Layers. *J. Fluid Mech.*, vol. 249, Apr. 1993, pp. 441–463.

2. Lu, G.; and Lele, S. K.: Spatial Growth of Disturbances in a Skewed Compressible Mixing Layer. AIAA Paper 93-0214, 1993.
3. Lu, G.; and Lele, S. K.: Vortex Breakdown in Skewed Compressible Mixing Layers. AIAA Paper 94-0821, 1994.



Vortex lines and cuts of the passive scalar field of the skewed mixing layer with equal, but oppositely, skewed streams (red = lower-stream fluid, blue = upper-stream fluid, green = mixed fluid).



Momentum thickness for different skewing angles as a function of downstream distance.

Comparison of TLNS3D Computations with Test Data

Frank Marconi, Principal Investigator
Co-investigator: M. Siclari
Grumman Corporate Research Center



Research Objective

To validate five NASA-developed codes for use in aircraft design.

Approach

Five codes were selected for evaluation by NASA and the Multidisciplinary Analysis and Design Industrial Consortium (MADIC). This project concentrated on the evaluation of the thin-layer Navier–Stokes TLNS3D code. The code was designed for transonic external-flow computations. The application of the code to a transonic transport wing with a simple axisymmetric fuselage was studied. The configuration was realistic, but it excluded geometric complexities that cannot currently be resolved.

Accomplishment Description

The TLNS3D code was exercised to certify its applicability as a design tool, thus the ability of the code to predict aerodynamic forces and moments accurately was a major focus. To assure a detailed certification of the code, test data were selected that included significant surface pressure data and force and moment data. The flight conditions tested were typical of cruise. The configuration matched that tested in the Aircraft Research Association (UK) 9-ft by 8-ft wind tunnel. Significant surface pressure data and forces and moments were measured for a Mach test matrix α containing 14 points. The TLNS3D code was found to be user friendly and robust. The grid resolution required to capture the wing surface pressure distribution accurately was surprisingly fine and resulted in larger than expected running times. Although the experimental data were intended for computational fluid dynamics validation and were well documented, an unaccounted for aeroelastic effect caused a 10 percent error in lift. The investigation concentrated on the effects of free-stream conditions (Mach and angle of attack), numerical dissipation (matrix and scalar), and turbulence model and grid resolution. This code assessment was a snapshot in time; the code was exercised essentially in its current form (no major changes were made in the code during the evaluation).

Significance

The accuracy of the TLNS3D code was enhanced and the matrix form of the dissipation was made more robust.

Future Plans

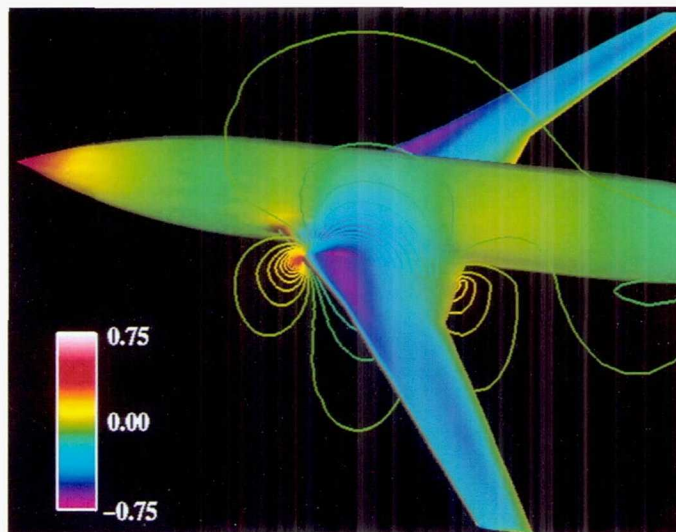
Code improvements will be identified.

Keywords

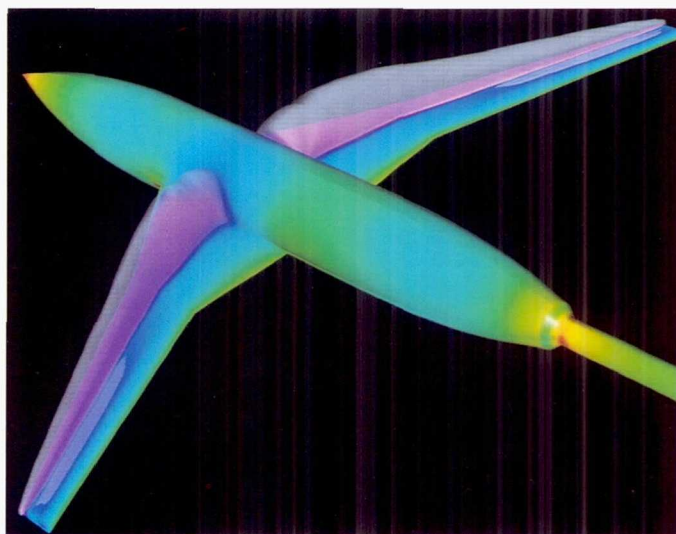
Aircraft design, External flow

Publication

Marconi, F.; Siclari, M.; Chow, R.; and Carpenter, G.: Comparison of TLNS3D Computations with Test Data for a Transport Wing/Simple Body Configuration. AIAA Paper 94-2237, 25th AIAA Fluid Dynamics Conference, Colorado Springs, Colo., June 1994.



Wing/simple body surface pressure ($M_\infty = 0.8$, $\alpha = -1.46$ degrees).



Wing/simple body translucent supersonic zone ($M_\infty = 0.8$, $\alpha = 2.02$ degrees).

Navier–Stokes Computations on Unstructured Grids

Dimitri J. Mavriplis, Principal Investigator
ICASE



Research Objective

To develop an accurate and efficient method for computing steady state turbulent viscous flows about complex three-dimensional (3-D) configurations.

Approach

The steady state Reynolds-averaged Navier–Stokes equations are solved on an unstructured mesh using a Galerkin finite-element discretization strategy. An edge-based data structure is employed to minimize memory overheads. An unstructured multigrid approach is employed to accelerate convergence to steady state. A combination of microtasking and autotasking has been employed to parallelize the solver on the shared memory architecture of the Cray Y-MP.

Accomplishment Description

The low overheads incurred by the present algorithm as well as the parallel implementation enable the solution of flows on very fine grids in rapid turnaround time. The turbulent flow over a high-lift wing geometry has been computed on a grid of 1.8 million points, or 10 million cells, using 320 megawords of memory in 1.5 hours of wall clock time on the 16-processor Cray Y-MP.

Significance

The ability to compute highly resolved flows over complex geometries is of extreme importance to the aircraft and propulsion industries. In particular, 3-D flows over high-lift geometries have proved particularly difficult to simulate in the past.

Future Plans

Improved multigrid unstructured mesh algorithms are being investigated. The inclusion of adaptive meshing techniques and computations over more complicated geometries are also planned.

Keywords

High lift, Turbulent flows, Complex geometries

Publication

Mavriplis, D. J.: A Three-Dimensional Multigrid Reynolds Averaged Navier–Stokes Solver for Unstructured Meshes. AIAA Paper 94-1878, June 1994.

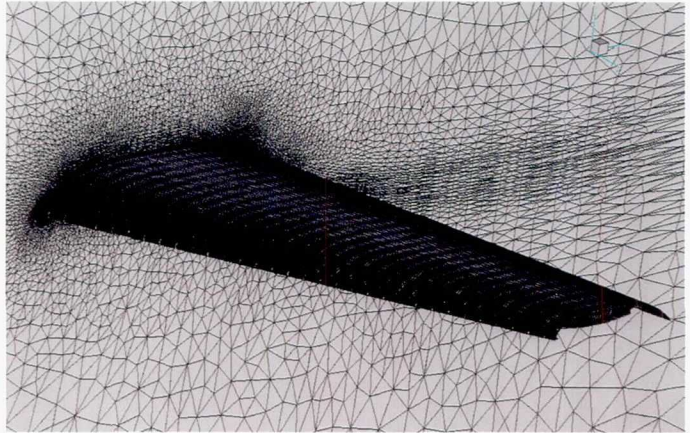
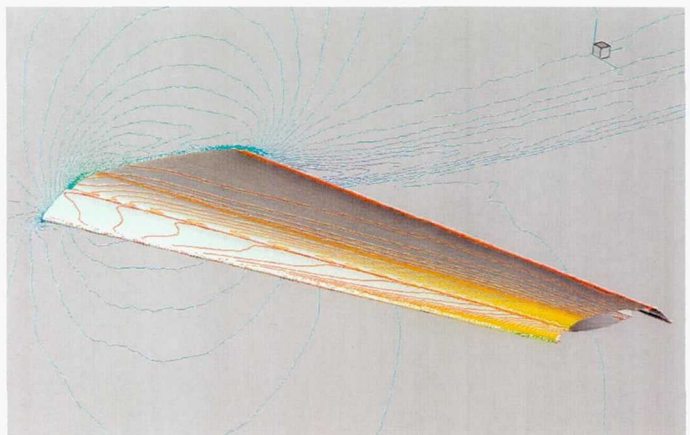


Illustration of fine mesh employed for 3-D high-lift configuration.



Computed Mach contours (symmetry plane) and density contours (wing surface) for 3-D flow over high-lift wing geometry.

CFL3D Code Evaluation

Pradeep Raj, Principal Investigator
Co-investigators: Tom Kinard and Richard Semmes
Lockheed Aeronautical Systems Company



Research Objective

To evaluate the capabilities of the CFL3D code for reliably predicting design and performance data in a timely and easy manner with established error measures over a clearly defined envelope of operating conditions. This research is in support of a joint project between NASA and the Multidisciplinary Analysis and Design Industrial Consortium on certifying NASA computational fluid dynamics (CFD) codes for use in multidisciplinary analysis, design, and optimization of aircraft configurations.

Approach

The approach to assess the accuracy, reliability, efficiency, responsiveness, and ease of use of CFL3D was to (1) apply the code to a set of test cases, (2) compare the computed results with measured data and solutions from other codes, and (3) conduct sensitivity studies for grid size, turbulence models, and boundary conditions. Data were generated for three configurations: a Wing C, an ogive-cylinder (axisymmetric) boat-tail, and a two-dimensional C-D nozzle.

Accomplishment Description

The Wing C configuration was analyzed for two flow conditions: Mach number = 0.82 and angle of attack = 5 degrees, and Mach number = 0.84 and angle of attack = 4.62 degrees. Both flows were at Reynolds number = 10 million. Grid sensitivity was inves-

tigated using two single-block C-O topology grids; one grid had 578,641 nodes and the other had 1,356,225 nodes. Solutions on both grids agreed well. The pressure distribution on the upper surface and plane of symmetry are shown in the first figure for the first Wing C configuration. The second figure shows sensitivity of surface pressures (at a wing station halfway between the root and the tip) to four turbulence models. The boat-tail configuration was analyzed as an axisymmetric body at Mach number = 1.2, Reynolds number = 0.13 million, and a nozzle pressure ratio of 12.06. A three-block grid with 17,135 nodes and the Baldwin-Lomax turbulence model were used.

Significance

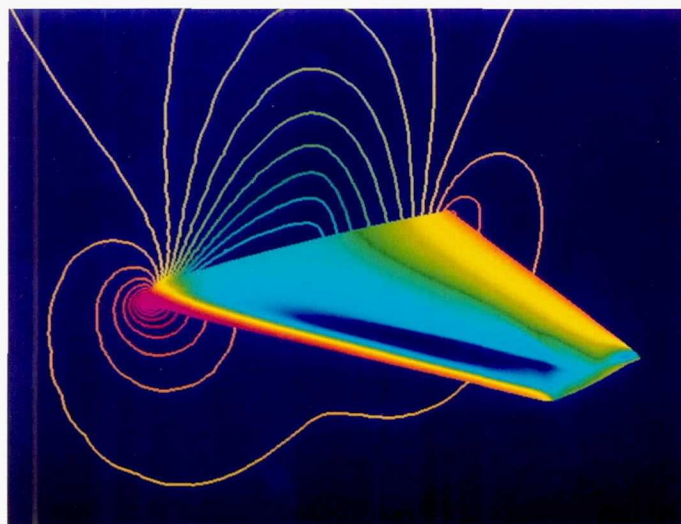
This work will accelerate the acceptance and integration of NASA CFD codes into the industrial design environment by providing industry an assessment of NASA technology and by providing NASA with future code development requirements.

Future Plans

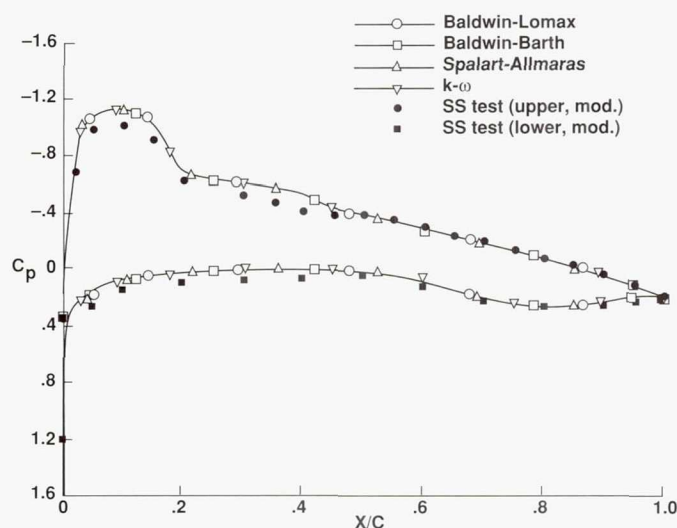
Additional sensitivity studies involving grids, turbulence models, and Reynolds numbers are planned.

Keywords

Computational fluid dynamics, Aircraft configurations



Pressure distribution on the upper surface and plane of symmetry for a Wing C configuration. Mach number = 0.84, angle of attack = 4.62, Reynolds number = 10 million.



Wing C sensitivity of surface pressures to four turbulence models.

Prediction of the Unsteady F-18 Flow Field

Yehia Rizk, Principal Investigator

Co-investigator: Scott Murman

NASA Ames Research Center



Research Objective

To predict the unsteady flow field around the F-18 aircraft at high angle of attack using computational fluid dynamics (CFD), including a study of the effects of simulating more details of the engine inlet and refining the grid on the vortex burst location. The effect of grid refinement on the tail buffet and the structural response of the tail with and without a leading-edge extension (LEX) fence is examined.

Approach

A Chimera scheme is used to discretize the computational space around the complete F-18 aircraft including the inlet duct, splitter plate, and boundary layer vent (first figure). A time-accurate flow solver (F3D) is used to simulate the unsteady flow field by solving the Reynolds-averaged Navier-Stokes equations. The structural response of the flexible vertical tail is computed using modal analysis. The fine mesh calculations include about 2 million grid points. A coarse mesh of about 1 million grid points is constructed as a subset of the fine mesh for the grid sensitivity study.

Accomplishment Description

Fine grid calculation with more details of the engine inlet components improves prediction of the vortex burst location (second figure). The results indicate a strong coupling of the external and inlet flows, especially at the maximum power engine setting. The time-accurate fine-mesh tail buffet computations show the same trend observed in the coarse mesh calculations—tail buffet occurs because the airload dominant frequency coincides with the tail's first natural frequency of bending. Also, installing the LEX fence introduces an unsteady vortex interaction that results in reducing the airload dominant frequency (third figure). Coarse grid computations typically take about 50 Cray C-90 hours and require about 12 megawords of central memory for each case. Fine grid computations typically require twice as much time and memory as the coarse grid computations.

Significance

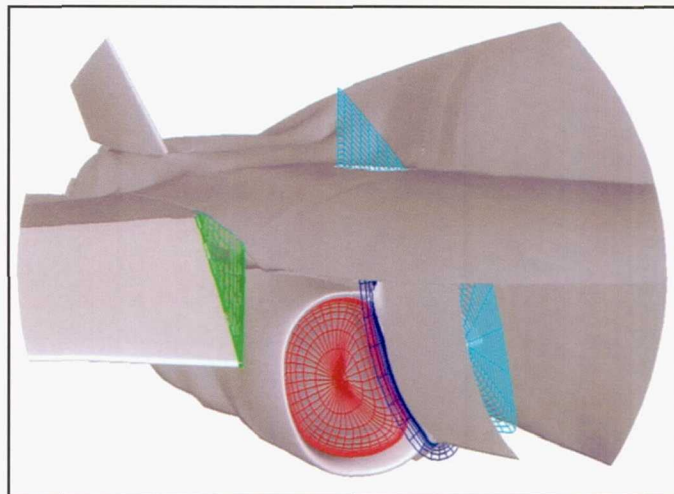
This study provides a better understanding of the F-18 flow field and the phenomenon of the vortex/tail interaction. Understanding of the buffet phenomenon will lead to more effective means to control or alleviate buffet and prevent premature tail structural fatigue for the F-18 and other twin-tail aircraft.

Future Plans

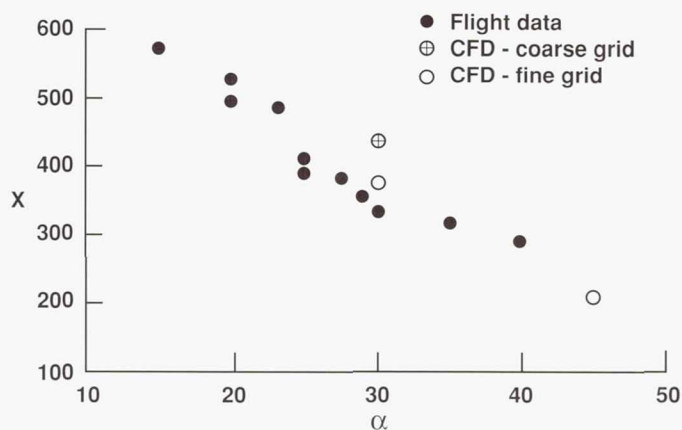
The highly unsteady flow field around the F-18 aircraft at angles of attack between 45 and 60 degrees will be computed. The results will be compared with the flight data obtained from the F-18 High-Angle-of-Attack Research Vehicle with thrust vectoring.

Keywords

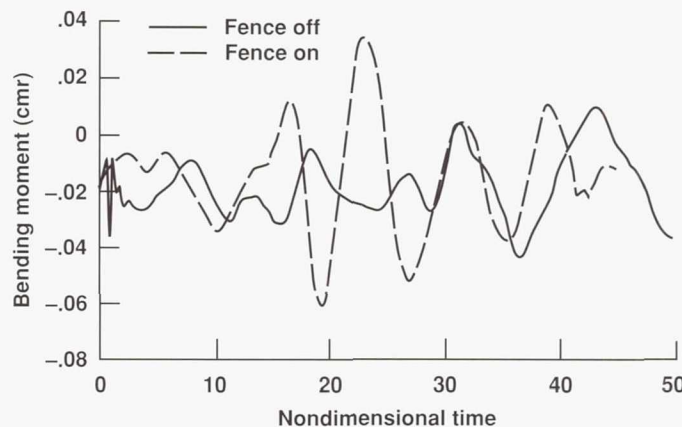
Tail buffet, High angle of attack, Engine inlet



Details of the grid near the engine inlet.



Vortex burst location comparison.



Effect of the LEX fence on vertical tail loading for the fine grid.

Analysis of High-Speed Civil Transport Transient Response

David M. Schuster, Principal Investigator
Lockheed Engineering and Sciences Company



Research Objective

To analyze the aerodynamic and structural response of future high-speed civil transport (HSCT) aircraft by coupling computational fluid dynamics (CFD) methods with computational structural mechanics (CSM) algorithms.

Approach

An existing HSCT aircraft concept, the NASA Langley Mach 2.4 HSCT, was analyzed. The Euler/Navier–Stokes three-dimensional Aeroelastic (ENS3DAE) method was used to perform a quasi-steady analysis of the HSCT performing a specified maneuver by choosing flight conditions at discrete points in the maneuver, assuming the flow was steady at these points, and performing a steady, rigid aerodynamic analysis at each condition. Aerodynamic loads were computed at each point in the trajectory, and these data were transferred to a dynamic, finite-element CSM method to compute the structural response of the vehicle throughout the maneuver. Coupling of the CFD and CSM methods involved transfer of loads from the aerodynamic grid to the finite-element structural model through a conservative load-beaming technique and the transfer of surface deflections from the structural model back to the aerodynamic grid using interpolation.

Accomplishment Description

A loose coupling of the CFD and CSM methods was accomplished and aerodynamic loads on the HSCT concept vehicle were computed. These loads were successfully transferred to the corresponding finite-element structural model and structural

deflections were computed. The figure shows contours of the vertical component of the aerodynamic load and the respective aerodynamic and structural models on which these loads were applied. The aerodynamic and structural models were independent and a structured single-zone aerodynamic grid was used to compute the loads, while a grid composed of triangles served as the structural finite-element model for computing deflections. Slight differences were seen in the loading pattern because the values displayed were absolute loads and were dependent on the local panel areas. Differences in grid refinement and surface point distribution affect the local load values.

Significance

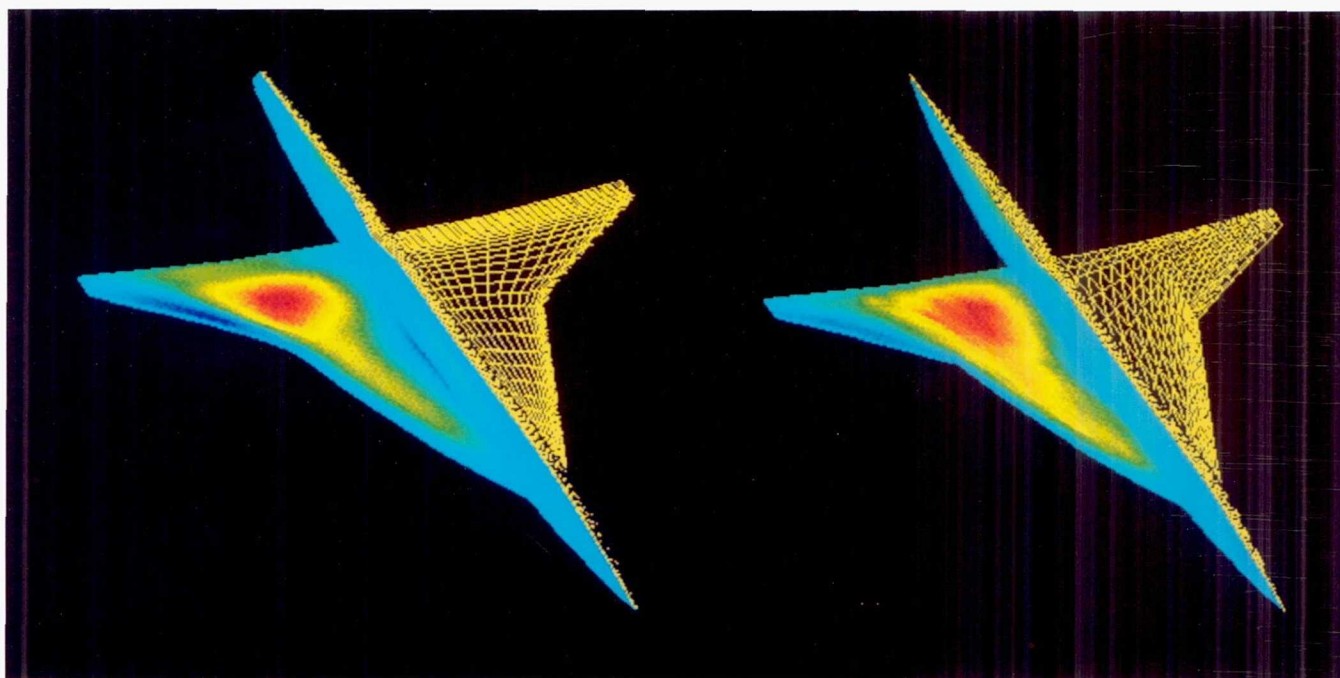
This research provides a method for performing structural analysis using detailed aerodynamic surface loads as input. Transient loads caused by aircraft maneuvers or gusts and computed by the CFD analysis are used by the CSM method to predict structural deformations and stresses. These data are important to the design of efficient, lightweight aircraft structures.

Future Plans

Strong coupling of the CFD and CSM methods to calculate dynamic aeroelastic loads, structural deformation, and stress will be performed.

Keywords

Computational fluid dynamics, Computational structural mechanics, High-speed civil transport



Contours of the computed vertical load component on the aerodynamic (left) and structural (right) models; Mach number = 2.4, angle of attack = 2.0 degrees. Magenta represents a large load into the page and blue represents a large load out of the page.

Complete F-18 Hybrid Solution

James L. Thomas, Principal Investigator

Co-investigators: Robert T. Biedron, Christopher L. Rumsey, W. Kyle Anderson, and Daryl L. Bonhaus

NASA Langley Research Center



Research Objective

To perform unsteady three-dimensional (3-D) Reynolds-averaged Navier–Stokes computations for aerodynamic configurations at high angles of attack in support of the High Alpha Technology Program.

Approach

Two algorithms have been merged using a hybrid zonal technique. The CFL3D code solves the compressible 3-D Reynolds-averaged Navier–Stokes equations using a structured-grid finite-volume scheme. The UNS3D code solves the Euler equations using an implicit unstructured-grid finite-volume scheme. To solve the linearized system, the GMRES code is used. Both CFL3D and UNS3D employ flux-difference splitting for treating the convective terms. The viscous terms in CFL3D are centrally differenced.

Accomplishment Description

Computations were performed for several high-alpha flows past a complete F-18 configuration. The solutions were obtained by using a hybrid zonal technique, and they were a preliminary study of the tail buffet problem on the F-18 aircraft. For this hybrid approach, the flow field was divided into two primary zones: a structured zone over the forebody/leading-edge extension (LEX) where the Navier–Stokes equations were solved in order to model vortex roll-up, and an unstructured zone over the aft part of the aircraft where the Euler equations were solved to model the convection of the forebody/LEX vortices. Earlier calculations for a simple delta wing indicated little difference between the vortex path obtained from a similar hybrid zonal approach as compared to the vortex path obtained using a single Navier–Stokes zone. CFL3D was used to compute the solution in the structured zone and UNS3D was used to compute the solution in the unstructured zone; communication between the zones was established using a modified Chimera grid scheme. The accompanying figures show the solution obtained for 30 degrees angle of attack. The vortex bursts between the canopy and the wing leading-edge/fuselage juncture. This burst position qualitatively agrees with flight-test data. The comparison between the computed results and flight-test data for the LEX surface pressures is also shown. Quantitative agreement between the computation and the flight test was obtained. The computation was performed using a grid with approximately 325,000 grid points in the structured section and approximately 90,000 nodes in the unstructured section. The computation took 12 Cray Y-MP hours and required storage of 64 megawords.

Significance

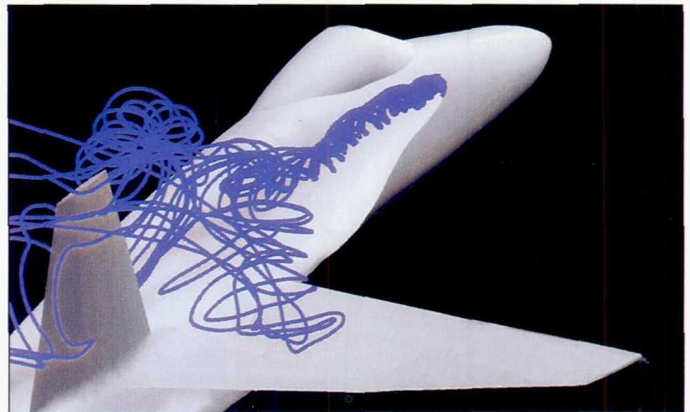
The hybrid structured/unstructured approach relieves many of the grid-generation difficulties associated with using a structured grid over the entire configuration, but it retains the ability to track the forebody/LEX vortices for tail-buffet studies.

Future Plans

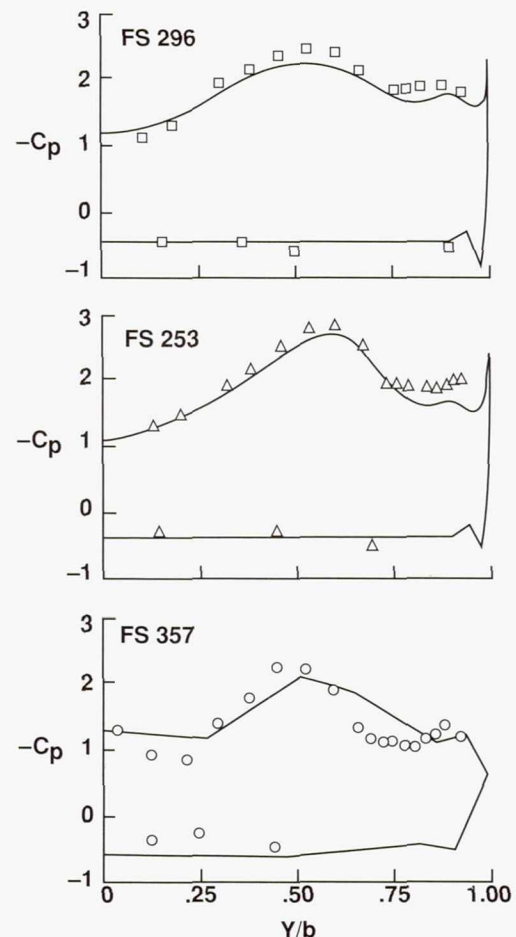
The scheme will be modified to perform time-accurate computations of the F-18 tail-buffet problem.

Keywords

High angle of attack, Finite-volume scheme, Tail buffet



Vortex core streamlines of F-18 hybrid solution at 30 degrees angle of attack.



Comparison between the computed surface pressures with those from flight at three stations on the LEX and at 30 degrees angle of attack.

Flow Simulation about Attack Aircraft

Chung-Jin Woan, Principal Investigator

Co-investigator: John D. Duino

Rockwell International, North American Aircraft Division



Research Objective

To demonstrate a computational fluid dynamics (CFD) capability of computing the complex flows about a highly integrated aerodynamics/propulsion/low-observable vehicle, and to obtain a better understanding of the physics of this class of flow phenomena. The effects of wind tunnel supporting sting on the vehicle aerodynamic characteristics will also be investigated.

Approach

A Navier–Stokes solver was used to simulate the flow about a highly integrated aerodynamics/propulsion/low-observable attack experimental vehicle and correlate the prediction with the wind tunnel test data.

Accomplishment Description

A Navier–Stokes solution was obtained for a high-performance/low-observable inlet/duct with a bell mouth at a static sea level condition simulating a wind tunnel test condition. The computational grid consists of four blocks of approximately one million grid points. The solution took 43 Cray C-90 hours and required 28 megawords of memory. Also completed was an Euler flow simulation for a wind tunnel model of an advanced aircraft configuration with sting at Mach number 0.85 and 3.3 degrees angle of attack. Four blocked grids were used with 714,580 total grid points. The computation used 16 Cray-2 hours and 20 megawords of memory for an average Euler run. The predicted force and drag divergence Mach number compared favorably with the wind tunnel data.

Significance

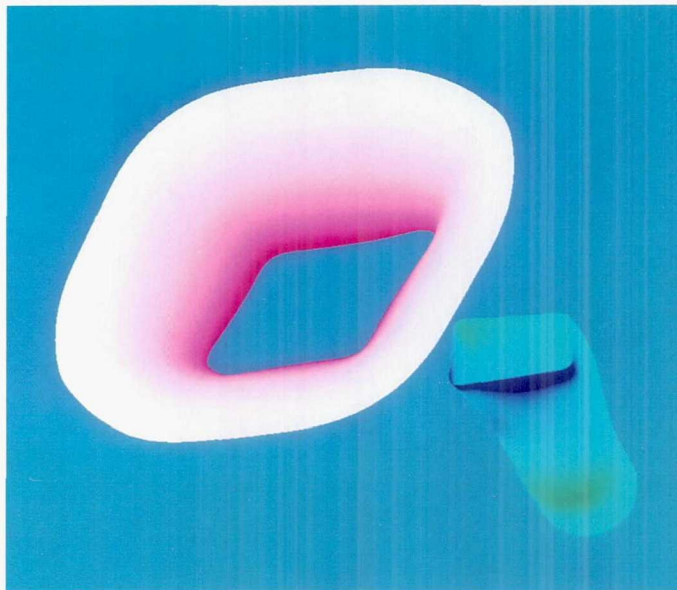
The CFD combined with advanced computer graphics can provide aerodynamic configuration designers with details of flow around complex geometry and vivid flow visualization for easy, quick, and detailed analysis. Such detailed flow information and visualization are generally difficult or too expensive to obtain in experiments. The calculated results assisted in determining the instrumentation locations on the tested wind tunnel model.

Future Plans

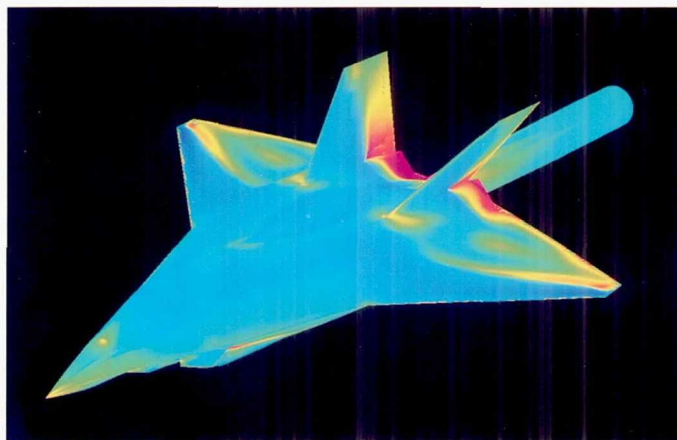
Effort will be made to obtain a Navier–Stokes solution for the aircraft model to investigate the effects of the wind tunnel supporting sting on the vehicle aerodynamic characteristics.

Keywords

Aerodynamics, Computational fluid dynamics, Propulsion



Pressure contours on a high-performance/low-observable inlet/duct with a bell mouth (the middle section is not shown); black = low pressure and white = high pressure.



Mach contours on a wind tunnel model of a fighter with sting; blue = low pressure and red = high pressure.

Multiple-Body Aerodynamics

David T. Yeh, Principal Investigator
Rockwell International, North American Aircraft Division



Research Objective

To assess the feasibility and technical challenges facing the numerical methods development for simulating the crew escape process at low-supersonic, low-altitude conditions, and to develop a better understanding of the aerodynamic and dynamic aspects of the ejection system.

Approach

The existing overset grid techniques were used and requisite improvements were made to model the pilot and seat in and out of an aircraft configuration. The overset grid approach was chosen because it provides the geometric and computational freedom to simulate multiple-body separation processes with the versatility to modify design alternatives with minimal regridding effort. The OVERFLOW code was used to simulate the flow phenomena. This code solves the three-dimensional Reynolds-averaged Navier-Stokes equations through a finite-difference, central-differencing scheme for structured overlapping grids. The F-16A aircraft was the primary focus of this study because of the existing wind tunnel results database.

Accomplishment Description

The future trends in designing ejection seats point to high-speed, low-altitude flight conditions. A test case was conducted to assess the numerical capability in predicting the flow field around an ejection seat in the vicinity of the F-16A aircraft. Because the flow condition of interest is in the supersonic regime, only the forebody geometry was included in the calculation. Overlapping volume grids were generated that consisted of the F-16A forebody, a cavity representing the seating compartment, and a generic seat. The first figure shows the centerline grid arrangement. An additional grid over the cavity was generated to provide the necessary communication between the cavity and the other grids. A flow solver intergrid connectivity file was generated to obtain the interface boundary conditions among the overlapping grids. A Reynolds-averaged Navier-Stokes solution was obtained for a static case where the seat was fixed at a prescribed location. The second figure shows the surface grid and associated pressure contours and some particle traces emanating from the seat. A typical computation required 16 megawords of memory and 12 Cray Y-MP hours.

Significance

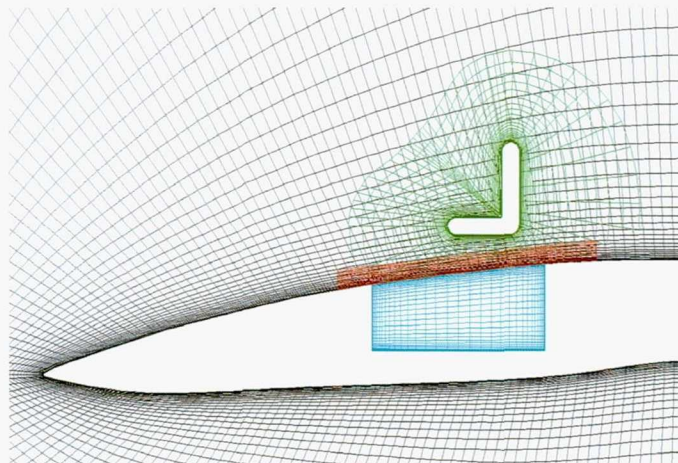
Wind tunnel tests are used extensively to analyze the ejection devices that can sufficiently reduce wind blast pressure on the pilot and correct the stabilization problems associated with high-speed ejection. The high cost involved in testing limits the number of concepts and conditions that can be evaluated with limited knowledge of their effectiveness prior to testing. In spite of significant advances in computational fluid dynamics analysis, continuing effort is required to bring promising procedures and techniques to maturity and to facilitate applications in design.

Future Plans

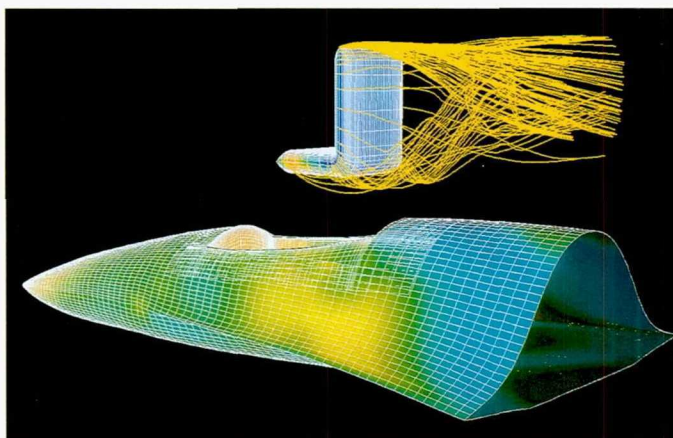
Sixth-degree-of-freedom rigid body dynamic analysis and moving/unsteady grid coupling for multiple-body separation applications will be investigated.

Keywords

Overset grids, Crew escape

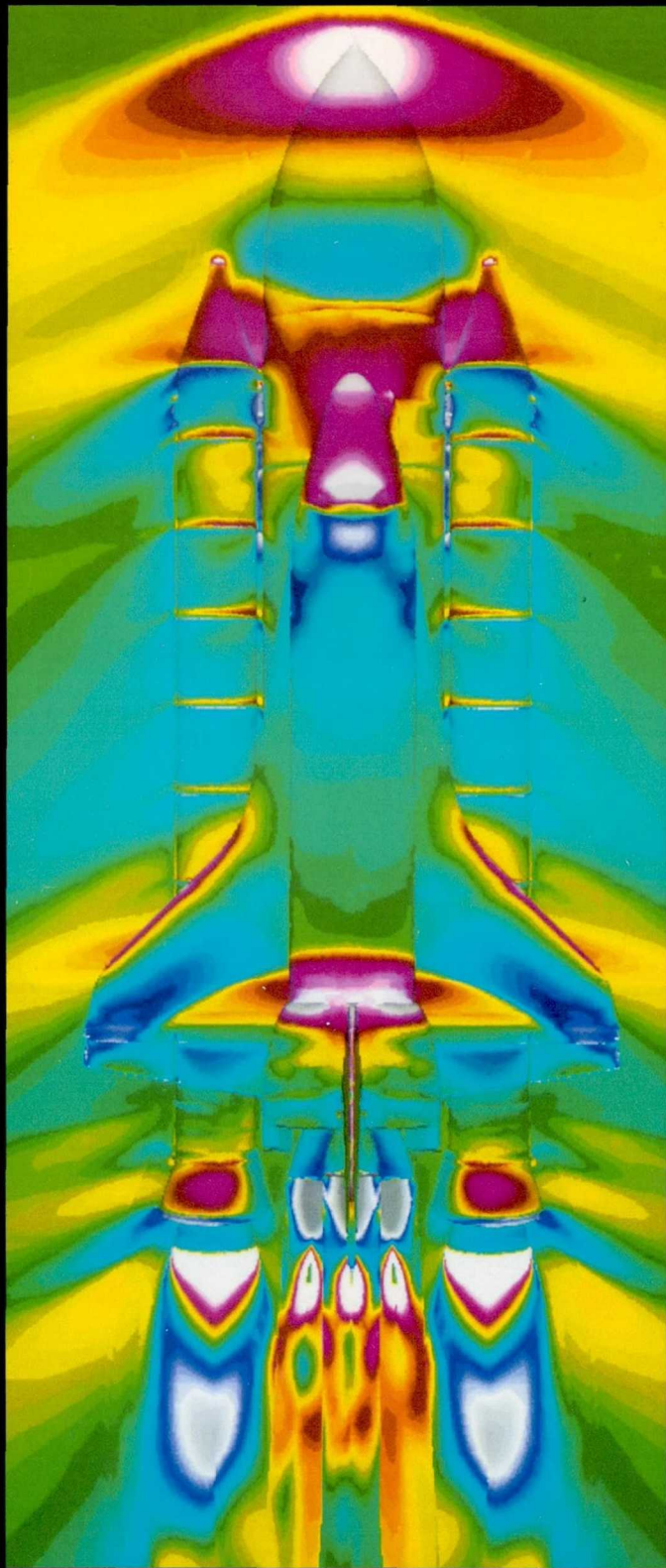


Centerline overlapping grids arrangement.



Flow field about an ejection seat in the vicinity of an F-16A aircraft; Mach number = 1.5 and Reynolds number = 1 million.

Aeronautics



Hypersonics
Subsonics
Supersonics
Transonics

Page intentionally left blank

Time-Accurate Simulation of Hypervelocity Wakes

Andrew Anagnost, Principal Investigator
Stanford University



Research Objective

To modify traditional implicit algorithms for solving blunt body flow fields so that they map efficiently to the message passing paradigm, and to apply this capability to the time-accurate simulation of hypervelocity base flows.

Approach

The block implicit Gauss–Seidel line relaxation technique is employed to solve the Navier–Stokes equations for an unsteady laminar flow over a blunt body at hypervelocity. The technique accounts for the physical propagation of information across the computational domain. If information is only allowed to transverse a block of processors in a single time step, then only the processors within that block need to communicate in a global, coupled fashion. By limiting communication, large performance gains are possible and the stability limitations are only moderately more severe than fully coupled implementation.

Accomplishment Description

Experimentally consistent oscillations are computed for an axisymmetric base flow at Mach 14, and they are the first time-dependent simulations of hypervelocity base flows that demonstrate unsteady behavior. The laminar mechanism of unsteadiness in the computed solutions agrees well with qualitative and quantitative experimental observations. Gridding and resolution requirements for capturing the unsteady features of the flow field are determined and their impact on the character of unsteadiness is assessed. The line relaxation technique results in simulation times on 128 nodes of the iPSC/860 that are two times faster than a traditional Gauss–Seidel solver running on a single pipe of the Cray C-90.

Significance

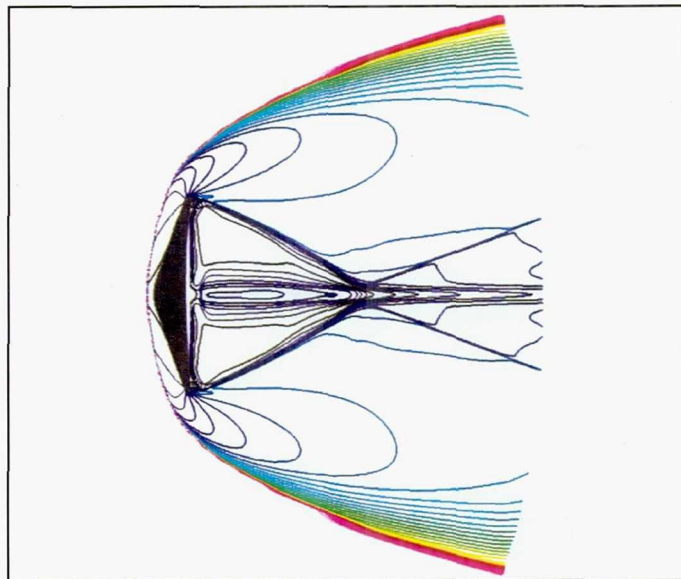
Implicit algorithms can be mapped to parallel supercomputers with significant performance gains without significantly increasing the computational work load. Also, unsteady behavior of hypervelocity base flows can be predicted computationally, which will help in the design of thermal protection systems.

Future Plans

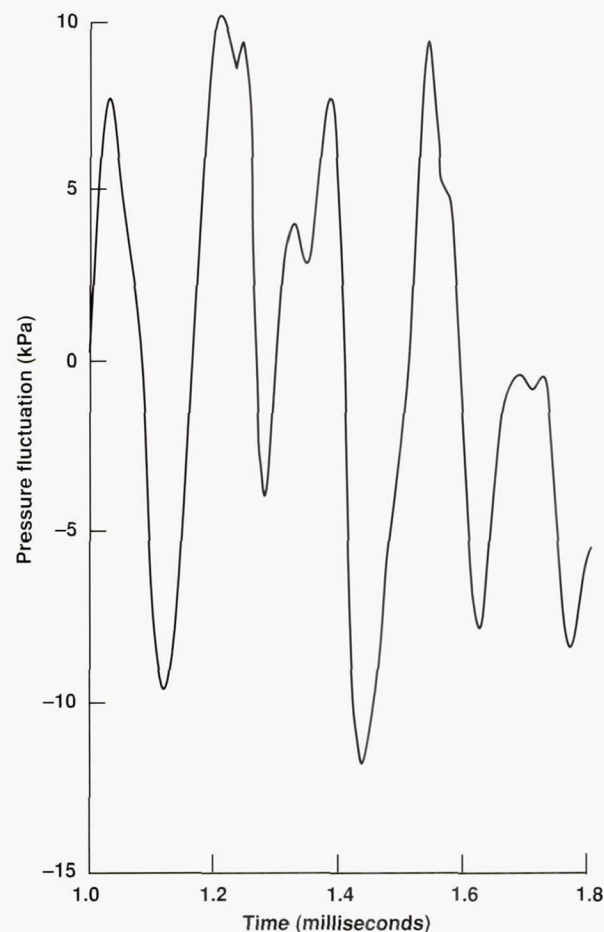
Research will focus on the impact of vehicle geometry and free-stream Reynolds numbers on computed unsteadiness. The geometry used in this study was not fully representative of a flight vehicle. The free-stream conditions were based on ballistic range experiments with known levels of unsteady behavior. Simulations will be performed to determine if the same behavior observed in a ballistic range is observed in flight.

Keywords

Hypersonics, Wakes, Parallel algorithms, Time-dependent simulation



Computed Mach contours for a blunt body base flow at free-stream Mach number 14.



Computed pressure fluctuations at the wake neck.

Effects of Roll Angle on Vortex Breakdown

Neal M. Chaderjian, Principal Investigator

Co-investigators: Lewis B. Schiff, John A. Ekaterinaris, and Yuval Levy

NASA Ames Research Center/Naval Post Graduate School/Stanford University



Research Objective

To determine if the Reynolds-averaged Navier–Stokes equations (RANS) can simulate an experimentally observed nonlinear variation of rolling moment with static roll angle.

Approach

The time-dependent, three-dimensional RANS equations are used to compute the flow about a 65 degree swept delta wing at high incidence. The Navier–Stokes simulation (NSS) code integrates the RANS equations using the implicit Beam–Warming algorithm. The diagonal algorithm may result in spurious vortex asymmetries at high angles of attack. Turbulent flow conditions are treated with the Baldwin–Lomax turbulence model with the Degani–Schiff modification, which properly accounts for cross-flow separation at high incidence.

Accomplishment Description

The NSS code is used to compute vortical flow about a delta wing with a free-stream Mach number of 0.27 at 30 degrees angle of attack and a Reynolds number of 3.67 million based on the wing root chord. Static roll angles up to 42 degrees are investigated. The first figure shows an instant streamline visualization of the leeward-side vortices that form when the delta wing is held at -5 degrees of roll. There is a sudden growth of the vortex-core diameters, which indicates that vortex breakdown occurs on both sides of the wing. The helical path of the streamlines indicates a spiral-type breakdown. The flow downwind of the initial breakdown positions is highly nonsteady. There was good agreement between the computed and experimental breakdown positions. The second figure shows that the computed and experimental time-averaged rolling moment coefficients compare well. Note the nonlinear variation of the rolling moment coefficient with roll angle. There are five trim points (zero moment)—three that are statically stable (negative slope) and two that are statically unstable (positive slope). Some differences between the computation and experiment are attributed to the need for finer grids.

Significance

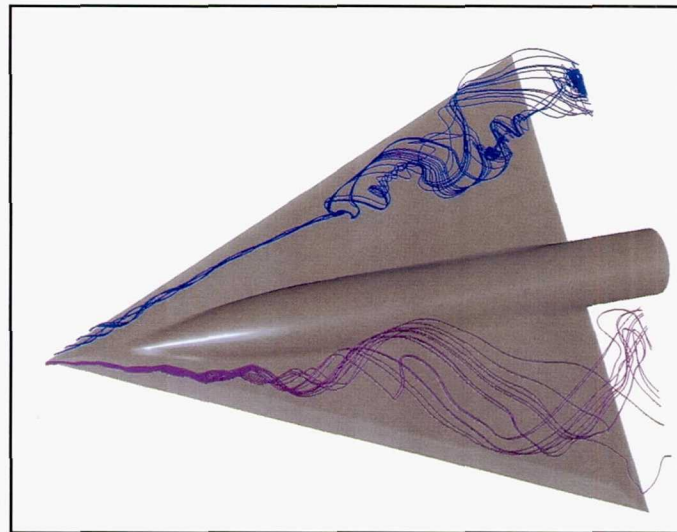
This study extends the validity of the present approach to higher angles of attack and advances the goal of using numerical simulation to study aircraft maneuver aerodynamics at high angles of attack.

Future Plans

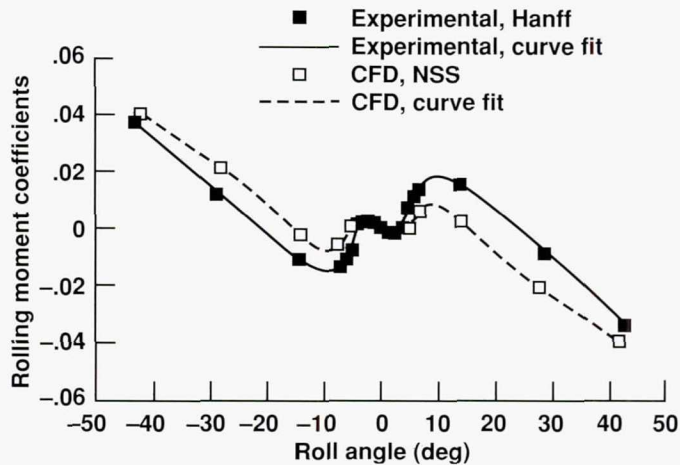
Forced and free-to-roll motions of a delta wing at high incidence will be simulated and the effects of grid refinement will be determined.

Keywords

High angle of attack, Unsteady flow, Vortex breakdown



Planform view of leeward-side vortices visualized with instant streamlines. Flow conditions: Mach number = 0.27, angle of attack = 30 degrees, roll angle = -5 degrees, Reynolds number = 3.67 million.



Computed and experimental time-averaged rolling moment coefficients. Flow conditions: Mach number = 0.27, angle of attack = 30 degrees, Reynolds number = 3.67 million.

Jet Interaction Effects on Aerodynamic Control of Missiles

Robert R. Chamberlain, Principal Investigator
Co-investigators: Anthony Dang and Ken Xiques
Adaptive Research Corporation



Research Objective

To study the effects of a single supersonic pitch control jet and the associated jet interaction (JI) phenomena on the aerodynamic forces and moments experienced by an ogive/cylinder missile configuration. Investigation of the scaling of cold jet wind tunnel data to the hot jet flight environment is of particular interest.

Approach

To study the scaling from tunnel to flight, a parametric study involving the variation of the control jet thrust coefficient was carried out. Computational fluid dynamics (CFD) predictions for the forces and moments both with and without a cold jet were compared to tunnel data to verify the grid (2.7 million nodes) and the computational procedure. Flight cases at the same free-stream Mach number (2.2) and angle of attack (-6 degrees), including a separate species for the hot jet exhaust, were also computed over a wide altitude range to determine the effects on stability and control of the full-scale prototype. Individual surface pressure contributions to the integrated aerodynamic coefficients were isolated for the missile body and the fins to identify the JI effects.

Accomplishment Description

Favorable agreement with experiment was obtained for all tunnel cases computed. The flight cases indicated that, at the higher altitudes, control of the missile is dominated by the thrust of the jet alone (JI effects are negligible). At low altitudes, however, JI effects become significant because of the confinement of the jet shock within the body bow shock and the resulting low-pressure region immediately behind the jet. The pitching moment is up to two times over that because of the jet thrust alone. The jet plume/fin interaction accounts for a significant portion of the moment amplification and also depends substantially on whether the jet exhaust is hot (flight) or cold (tunnel). The size, shape, and position of the plume as it passes over the fins dictates how the cross flow wraps around the body and determines the resulting surface pressure distribution on the fins. A typical run for this problem requires 64 megawords of memory and 80 Cray C-90 hours.

Significance

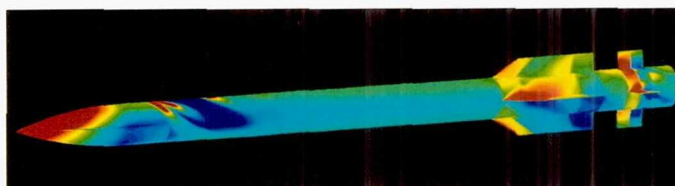
Battlefield engagement simulations, autopilot design, and guidance and control algorithms all depend upon reliable full-scale flight information about JI control effectiveness. CFD predictions for the increment to the aerodynamic coefficients in flight caused by JI effects significantly enhance confidence in current scaling procedures for obtaining the required data from cold gas wind tunnel tests. In some cases, new scaling procedures were suggested based on the CFD results.

Future Plans

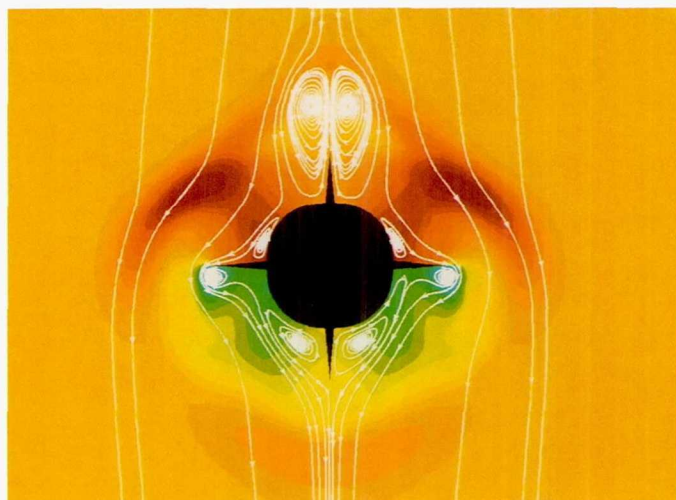
Additional work is planned to examine the influence of Mach number, angle of attack, and altitude on JI control effectiveness, particularly when wind tunnel data indicate an instability or some other unfavorable interaction. The effect of exhaust gas temperature and composition will also be investigated.

Keywords

Aerodynamic control, Missile aerodynamics



Pressure coefficients on the missile with the jet turned on.



Recirculation in the JI plume and pressure contours in a cross-flow plane through the first set of fins. Streamwise velocity goes into the page.

Transition Model for High-Speed Flow

Hassan A. Hassan, Principal Investigator

Co-investigator: Eric S. Warren

North Carolina State University



Research Objective

To develop a transition model that incorporates information from linear stability theory and accurately reproduces experimental data for transitional flows over a wide range of Mach numbers. Previous work has established a model for including the effects of first-mode disturbances into a transition model. An objective of the present work is the extension of this model to account for Mach number effects. Additionally, the present work includes the effects of second-mode disturbances that dominate the transition process at hypersonic speeds.

Approach

The model is based on the fact that the stress in the transitional region can be expressed as a function of the turbulent and nonturbulent stresses. The nonturbulent stress is a result of first- and second-mode oscillations. The transition model was incorporated into a Reynolds-averaged Navier-Stokes solver with a one-equation turbulence model. A variable turbulent Prandtl number was developed and included in the approach. A finite-volume method was used to evaluate the spatial terms in the Navier-Stokes equations. An upwind approach based on Roe's flux-difference splitting was used along with MUSCL differencing. The solution was stepped in time using a modified Runge-Kutta method until a steady state was obtained.

Accomplishment Description

Available experimental results for transitional flows are well predicted by the transition model. Moreover, the results of the model illustrate the inadequacies of using a constant turbulent Prandtl number for high-speed flow. Typical runs took an average of 1 Cray C-90 hour with central memory requirements of about 3–5 megawords.

Significance

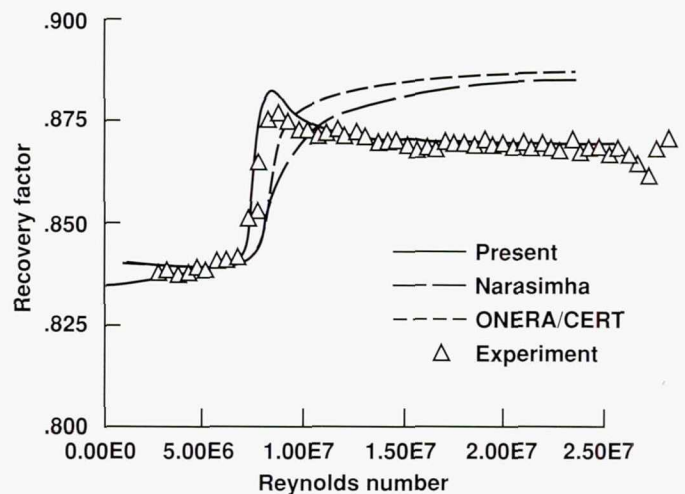
The study of high-speed transition is important for the efficient design of hypersonic vehicles, which encounter flows that may be transitional over a significant portion of the vehicle. Within this transitional region, design parameters such as skin friction and heat transfer are rapidly increasing or are maximum.

Future Plans

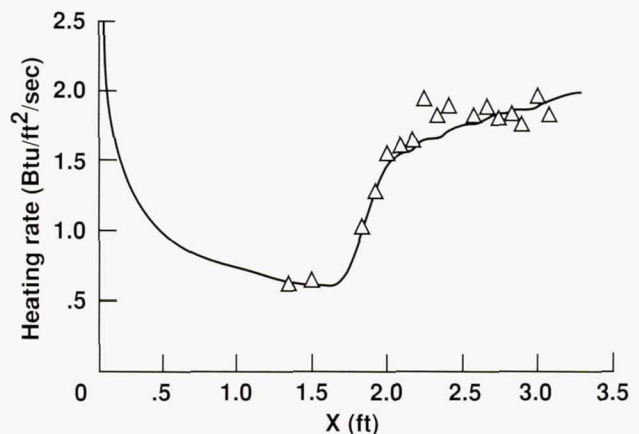
Efforts are focused on predicting the transition onset location. A method based on the reduced Navier-Stokes equations is being developed with the goal of simulating the transition onset location and transition region. Additional work is beginning on an improved turbulence model that more adequately accounts for the presence of pressure gradients.

Keywords

Transitional flow, High-speed flow, Hypersonic



Comparison of model with experiment and linear combination transition models for Mach 3.5 flow over a 5-degree half-angle cone.



Comparison of model with experiment for Mach 8 flow over a 7-degree half-angle flared cone.

Titan Entry Flow Field of the Cassini–Huygens Probe

John Rakiewicz, Principal Investigator

Co-investigators: Scott Ward, Darren Fricker, and David Wyn-Roberts

Jet Propulsion Laboratory/McDonnell Douglas Aerospace/European Space Agency



Research Objective

To use state-of-the-art computational techniques to characterize the forebody and wake flow-field environment about the Cassini–Huygens probe as it enters the Titan atmosphere.

Approach

The McDonnell Douglas Navier–Stokes code designated MDNS3D/ULTRA was used for this study. The code uses a structured zonal grid approach to discretize the full set of Reynolds-averaged Navier–Stokes equations and includes a generalized fully coupled finite-rate chemical kinetics model and a fully coupled two-equation turbulence model. The equations are solved in a time-dependent manner using second-order-accurate central differencing in space and an explicit fourth-order-accurate time advancement algorithm. When used with an appropriate total-variation-diminishing scheme, the applicability of the code extends into the Mach 30+ range. To model the chemical kinetic effects of the Titan atmosphere (composed of approximately 86.5 percent nitrogen, 10 percent argon, and 3.5 percent methane), a nine-species, seven-reaction finite-rate chemistry model was implemented.

Accomplishment Description

Simulations were concentrated on the maximum total heating trajectory point. Analyses completed at zero angle of attack provide detailed aerothermodynamic and chemical composition data that address the effects of small perturbations in the free-stream chemical composition (because of uncertainties in the concentration of argon in the Titan atmosphere). A 5 degree angle-of-attack solution was also completed to assess the effects of the nonaxisymmetric forebody and wake flow-field structure on vehicle heating. All the solutions provide connective heating results and the flow-field temperature and chemical composition distributions necessary to calculate the radiative component of the total heat flux to the probe surface. A typical four-zone, angle-of-attack solution of the forebody and wake flow fields required approximately 30 megawords of memory and 100 Cray C-90 hours.

Significance

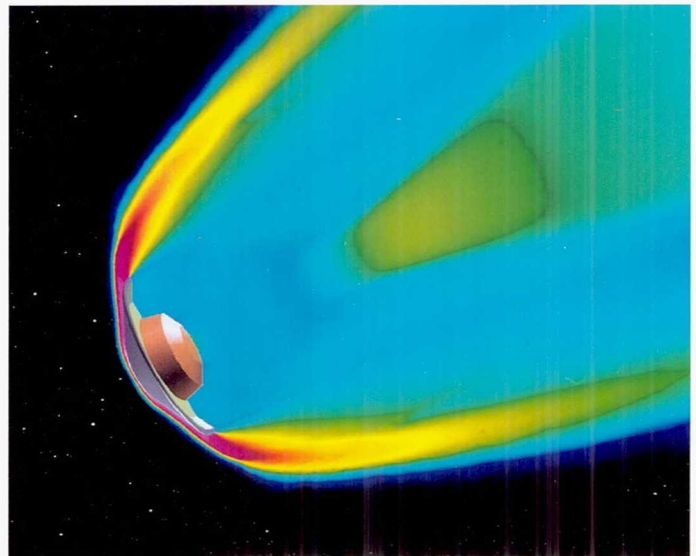
The computational fluid dynamics (CFD) predictions provide direct assessment of the severity of the environments that will be encountered during the Cassini–Huygens probe entry into the Titan atmosphere. The data provided by these simulations cannot be reproduced using any means other than CFD or measurement during the actual mission.

Future Plans

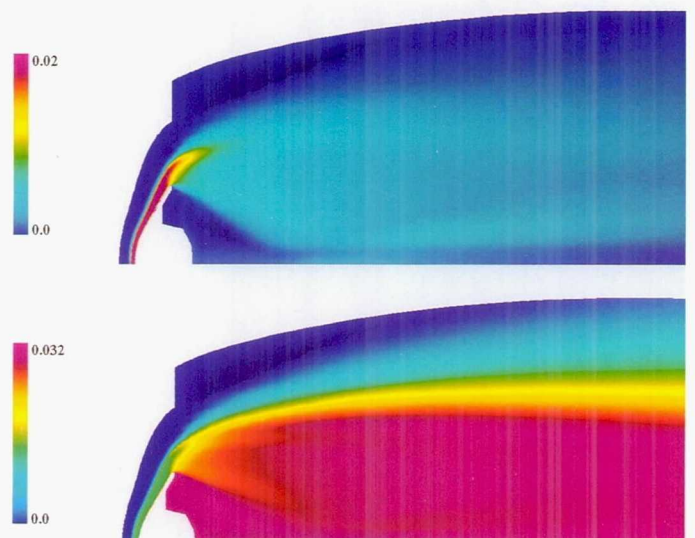
This work is complete.

Keywords

Hypersonic, Planetary probe, Aerobrake, Nonequilibrium chemistry



Pressure distribution around Cassini–Huygens probe entering the Titan atmosphere.



CN (top) and C (bottom) chemical composition distributions (mole fractions) around probe.

Simulation of Rarefied Jet Interaction

S. H. Konrad Zhu, Principal Investigator

Co-investigator: Leonardo Dagum

Rockwell International, Rocketdyne Division/NASA Ames Research Center



Research Objective

To characterize the flow field produced by two interacting free jets expanding into a vacuum and to establish an analytic model to predict the flow field for the Space Station design.

Approach

The direct simulation Monte Carlo method was employed and PSiCM, a three-dimensional (3-D) particle simulation code for rarefied flows, was used to perform a parametric study with a wide range of the penetration Knudsen number.

Accomplishment Description

PSiCM was validated in a previous work by comparison to experimental results for the interaction between two rarefied free jets, which shows excellent agreement. The present parametric study on the jet plume interactions in the transitional regime has revealed that a similarity does exist for the secondary jet resulting from the interaction of two primary jets. The separation distance between the primary jets is a proper length scale in studying the plume interaction. The study also showed that predicting multiple plume flow field as a linear superposition of each single plume is not accurate, but the inaccuracy decreases as the interaction approaches the free molecular regime. The study required 500 CM-5 hours and 2 gigabytes of memory.

Significance

This work is a continuation of a task prompted by the Space Station design and the concern of possible excessive loads on the solar array from the Orbiter reaction control system (RCS) plume impingement. An analytical model is needed to determine the flow field resulting from multiple RCS firings for the design of the station and the proximity maneuver of the Orbiter. This study provides a theoretical basis for establishing the model and a method for quantifying the errors using the linear superposition prediction.

Future Plans

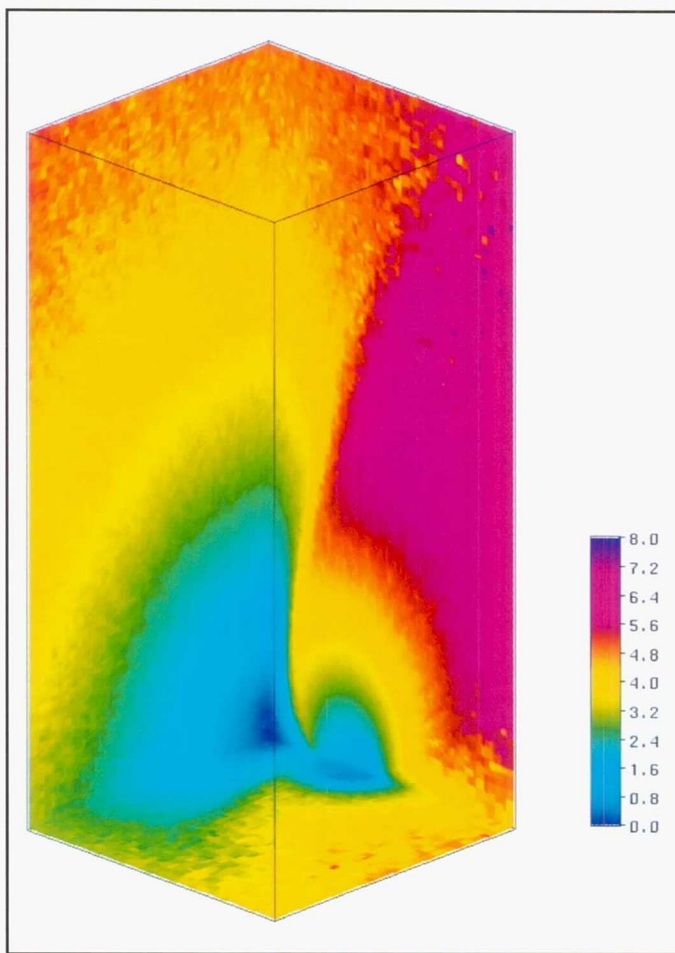
The simulation will be extended further downstream and the range of the penetration Knudsen number will be expanded. Eventually, the analytic model will be established, and the impingement from the multiple plume interactions will be investigated.

Keywords

Flow field, Plume interaction

Publications

1. Dagum, L.; and Zhu, S.: Three Dimensional Particle Simulation of High Altitude Rocket Plumes. AIAA Paper 92-2913, July 1992.
2. Dagum, L.; and Zhu, S.: DSMC Simulation of The Interaction Between Rarefied Free Jets. AIAA Paper 93-2872, July 1993.
3. Zhu, S.; and Dagum, L.: A Parametric Study of Rarefied Jet Interaction Using DSMC. AIAA Paper 94-2046, June 1994.



Mach number field from interaction of two rarefied free jets separated by a distance of three exit diameters.

Subsonic High-Lift Analysis

Kenneth M. Jones, Principal Investigator

Co-investigators: Victor Lessard, Simha Dodbele, Kevin Kjerstad, Steve Yaros, and Mamad Takallu

NASA Langley Research Center/ViGYAN, Inc./Lockheed Engineering and Sciences Company



Research Objective

To provide accurate analyses of complex high-lift systems for advanced subsonic transport configurations and high-speed research (HSR) configurations. The long-term goal of the project is to assess a variety and hierarchy of methods for their usefulness as analysis and design tools for three-dimensional (3-D) high-lift systems.

Approach

Two approaches for analyzing high-lift systems were pursued. One approach was to use a multiblock Chimera grid scheme with a 3-D finite-volume Navier–Stokes code (CFL3D). The two-dimensional (2-D) option of the code was used with Chimera grids to analyze a multi-element airfoil. The second approach was to use a 3-D unstructured-grid Euler solver (USM3D) to analyze a vortex-flow leading-edge-flap configuration that included a partial span trailing-edge-flap deflection.

Accomplishment Description

The CFL3D code was used in the 2-D mode to analyze a three-element high-lift airfoil using a Chimera gridding technique. Five grids were used to model the configuration (first figure). The analyses were performed over an angle-of-attack range of 4–21 degrees and at Reynolds numbers of 5 and 9 million. The analyses were performed with the Baldwin–Lomax and Spalart–Allmaras turbulence models. The surface pressure distributions for both models compare well with experimental data. The Spalart–Allmaras model produced more accurate results, particularly in the leading-edge region of each element. The analyses required up to 3 Cray-2 hours and 8 megawords of memory. The USM3D code was used to model leading-edge vortex flaps coupled with deflected trailing-edge flaps on an HSR configuration. Experimentally obtained force, moment, and flow visualization results were compared with the computed solution. The analysis performed with the original unstructured grid generated for this configuration produced reasonable force and moment comparisons, but did not match the experimentally observed flow-field pattern—there was no clearly defined reattachment line for the primary leading-edge vortex. The grid was reclustered in the vicinity of the core of the vortex, which produced an improved solution (second figure). The analyses required 122 megawords of memory and 8 Cray-2 hours.

Significance

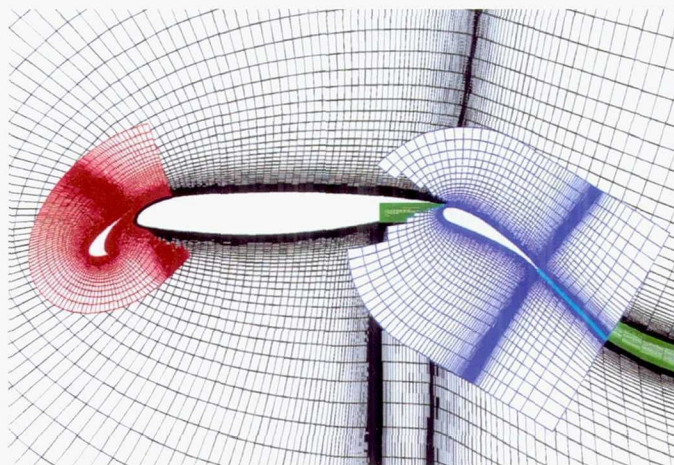
Structured Navier–Stokes and unstructured Euler methods are viable candidates for analyzing complex high-lift systems for subsonic transports and HSR configurations.

Future Plans

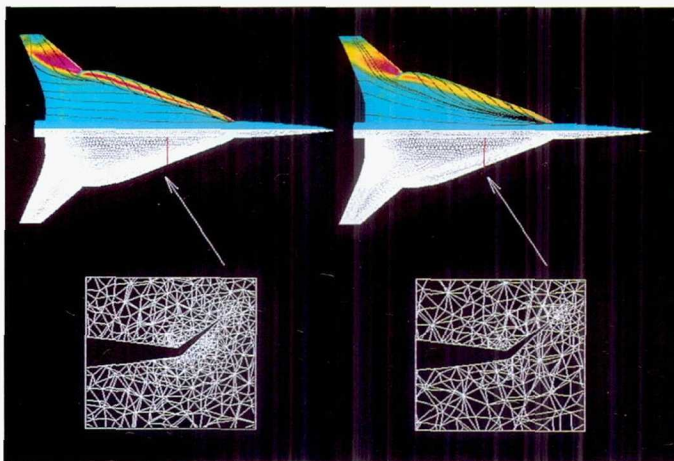
The Chimera approach will be extended to a 3-D high-lift system using the CFL3D. The unstructured Euler analysis will be extended to include viscous effects by tying in the Euler solution with a boundary layer method or by employing an unstructured-grid Navier–Stokes solver.

Keywords

Navier–Stokes, Chimera, Unstructured grids, Euler



Five-block Chimera grids used to analyze the three-element airfoil.



Unstructured flow-field grids (original and modified) and surface pressure distributions with surface streamlines for an HSR configuration. Mach number = 0.22, angle of attack = 16.0.

Investigation of Forebody Flow Control

Lewis B. Schiff, Principal Investigator

Co-investigators: Ken Gee and Roxana Agosta

NASA Ames Research Center/MCAT Institute



Research Objective

To determine the effectiveness of forebody tangential slot blowing for flow control on rounded forebodies.

Approach

Time-accurate solutions and a range of free-stream Mach number and jet exit condition solutions are obtained for an isolated F-18 forebody. Solutions are obtained using the generic chined forebody at different angles of attack, slot locations, and jet exit conditions. A multizone, thin-layer Navier-Stokes code is used to compute the flow fields and the computational results are compared with corresponding wind tunnel experimental data.

Accomplishment Description

At very low values of mass flow ratio (MFR), little or no yawing moment occurs. At moderate values of MFR, the jet remains attached to the forebody surface and generates a low-pressure region. This effect, coupled with the movement of the nose vortices, results in a significant yawing moment. Jet underexpansion occurs at high MFR resulting in early separation of the jet and leveling off of the yawing moment with increased MFR. Similar results are obtained from the generic chined forebody solutions. At low blowing rates on the chined forebody, moment reversal is observed. At very high blowing rates, there is a sharp decrease in the yawing moment. The differences in the effect of blowing are partly due to the different body geometries. Each solution required an average of 20 hours Cray C-90 time and 16 megawords of central memory.

Significance

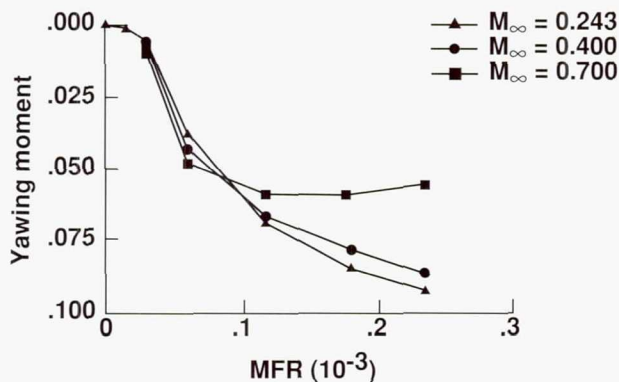
Tangential slot blowing remains an effective method of generating yawing moment at transonic Mach numbers and over a range of mass flow ratios.

Future Plans

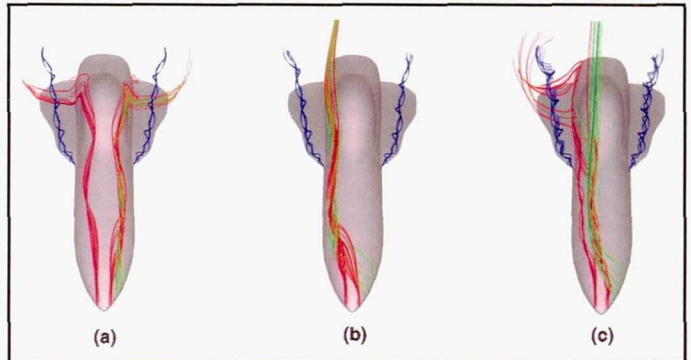
Analysis is under way to fully understand the flow physics of tangential slot blowing and force and moment generation.

Keywords

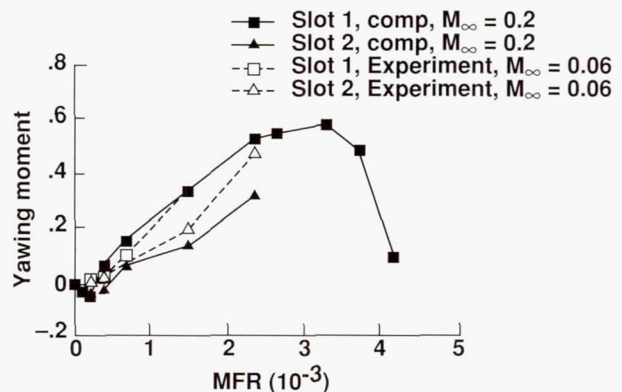
High angle of attack, Tangential slot blowing



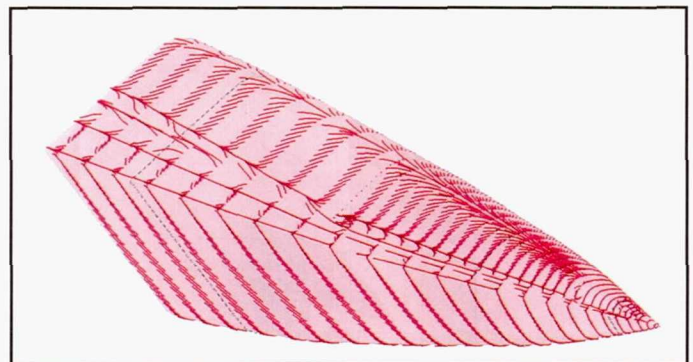
Tangential slot blowing is effective over a range of free-stream Mach numbers and blowing rates.



The effect of jet blowing rates on the flow field: (a) low, (b) moderate, and (c) high.



Comparison with experimental data shows that the effect of tangential slot blowing on a generic chined forebody can be accurately predicted using computational methods.



The surface flow pattern shows how blowing changes the flow field near the surface of the generic chined forebody.

Evaluation of Navier–Stokes Codes for Transport Configuration Analysis

N. J. Yu, Principal Investigator

Co-investigators: H. V. Cao and S. R. Allmaras

Boeing Commercial Airplane Group



Research Objective

To evaluate numerical and turbulence modeling capabilities of Navier–Stokes codes for transport configuration analysis, and to validate the direct iterative surface curvature (DISC) inverse design method for wing and isolated nacelle design.

Approach

The multiblock Navier–Stokes codes TNS3DMB and CFL3D were used to analyze the 747-200 configuration and other advanced technology wing/body configurations. Existing wind tunnel data were used to assess the accuracy of the codes and the applicability of various turbulence models for cruise and off-design analysis. DISC was incorporated in the Navier–Stokes system for wing and isolated nacelle design. The incompressible Navier–Stokes code INS2D was evaluated and enhanced for two-dimensional (2-D) multi-element airfoil analysis.

Accomplishment Description

The TNS3DMB and CFL3D codes were evaluated for transport wing/body configurations. Using the same turbulence model, the codes provide comparable wing pressure results over a wide range of flow conditions. The two codes also give similar velocity profiles within turbulent boundary layers. At cruise design conditions, computed results using the Johnson–King, Spalart–Allmaras, and $k-\omega$ models agreed well with test data. For off-design analysis, both the Spalart–Allmaras and $k-\omega$ models provide improved results over the Johnson–King model. The DISC inverse design method was tested for cruise wing and isolated nacelle designs. Wings with improved cruise-condition pressure distributions, and nacelles with nearly shock-free pressure distributions were designed based on this method. An example of a

wing design to improve outboard loading is shown in the figure. A typical design run required 3 Cray C-90 hours and 60 megawords of memory. The INS2D code was tested on various high-lift, multi-element airfoil configurations over a wide range of flow conditions. It was incorporated in a 2-D Navier–Stokes analysis system that consisted of an automatic multiblock grid generator for multi-element airfoils and a method for predicting boundary layer transition. Numerical studies were conducted to determine the effects of grid distribution, boundary layer transition, Reynolds number, turbulence models, and wind tunnel walls. The results of the numerical studies led to a better interpretation of the 2-D wind tunnel data and, in many instances, a better understanding of the physics of high-lift systems.

Significance

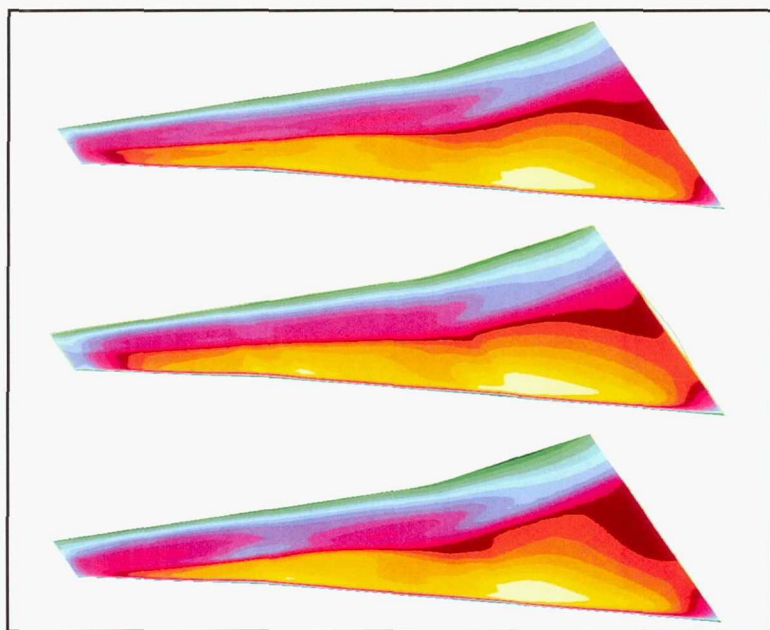
Evaluation and improvement of 2-D and 3-D Navier–Stokes codes are important steps toward transferring the technology from CFD developers to airplane designers. Designers can use validated codes in the airplane design process. This project works well for cruise-wing and high-lift wing design.

Future Plans

The feasibility of using Navier–Stokes codes for stability and control problems, such as airplane pitch up, and spoiler aerodynamic reversals, will be explored. Evaluation of the OVERFLOW and INS2D codes for complex configuration analysis, such as high-lift systems, is planned.

Keywords

Transonic, High lift



Wing design using DISC method for input (top), target (middle), and design (bottom); light yellow = low pressure and green = high pressure.

Supersonic Laminar Flow Control Experiment

Michael C. Fischer, Principal Investigator
Co-investigator: Chandra S. Vemuru
NASA Lewis Research Center/AS&M, Inc.



Research Objective

To develop detailed grids and to analyze F-16XL flight configurations to reduce risk for the F-16XL supersonic laminar flow control experiment.

Approach

Three-dimensional Euler and Navier–Stokes codes were used to analyze the F-16XL configurations. The GRIDGEN program was used to generate the grids for the F16-XL shock-fence configurations.

Accomplishment Description

Using GRIDGEN, a 27-block grid was generated containing approximately 2 million grid points. A family of shock fences of varying height and length were modeled to determine the minimum height required to effectively block the shock originating from the inlet diverter. Without the fence, the computational fluid dynamics (CFD) solution revealed a strong shock that traversed the lower surface and caused undesirable, peaky upper-surface leading-edge pressures downstream of the intersection with the leading edge. These peaky pressures prevent the achievement of laminar flow on the upper surface. With a fence of adequate height and length at the 65-in. wingspan location, the shock was blocked and was reflected toward the fuselage. Before, at the end of the fence, the shock disturbance wrapped around the fence and traversed outboard, but with the fence it crossed the leading edge outboard of the laminar flow glove region. The CFD predictions with and without the fence agree well with precursor F-16XL flight data. Each analysis used about 70–80 megawords of memory and approximately 4 Cray C-90 hours.

Significance

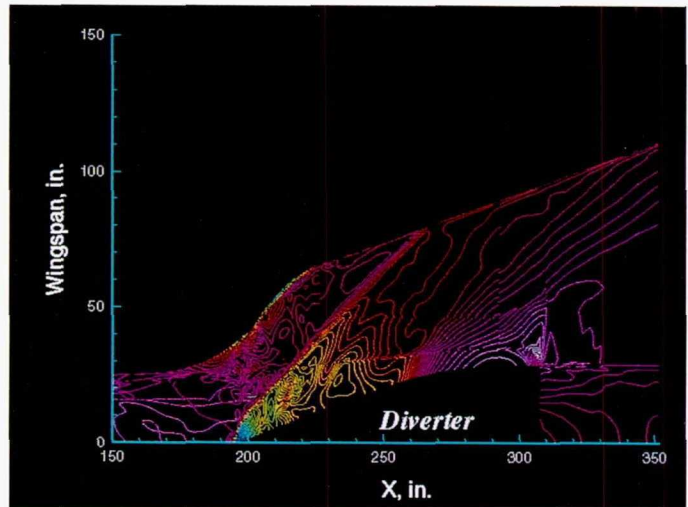
A baseline fence configuration was selected and is being evaluated on a 1:15 scale F-16XL model in the Langley Research Center Supersonic Unitary Plan Wind Tunnel. This fence design will greatly reduce the F-16XL flight experiment risk.

Future Plans

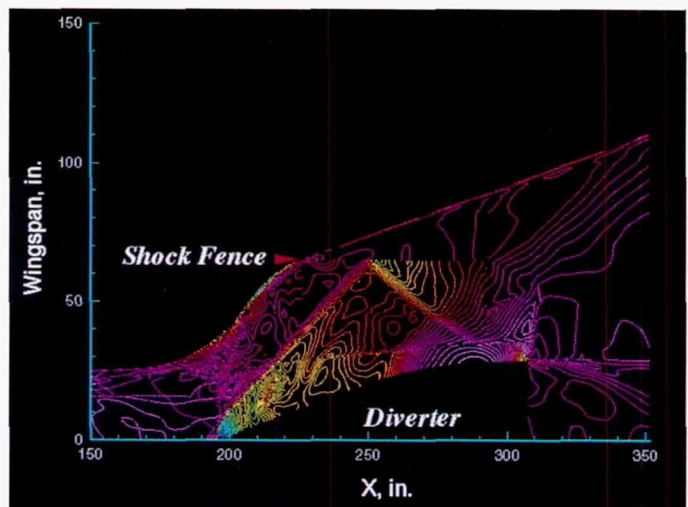
Refinements to the fence design to improve its effectiveness may be explored. Other unique F-16XL experiment-related flow problems will be modeled to develop workable solutions that reduce risk or provide design information.

Keywords

High-Speed Research Program, High-speed civil transport, Laminar flow



F-16XL lower-surface isobar contours.



F-16XL lower-surface isobar contours with 20-in. shock fence at 65-in. wingspan location.

Unstructured Grid/Flow Solver Calibration

Steve L. Karman, Jr., Principal Investigator

Co-investigators: Tracy J. Welterlen, Elizabeth A. Fuchs, and Doug Howlett
Lockheed Engineering and Sciences Company



Research Objective

To validate a Cartesian unstructured grid Euler/Navier-Stokes solver for complex three-dimensional (3-D) geometries with special emphasis on weapons separation.

Approach

An unstructured Cartesian grid computational fluid dynamics (CFD) code is used to analyze complex 3-D multibody flow fields. The grids are generated by recursively refining a root Cartesian cell that encompasses the entire domain. The grid generation is initially based on user-defined boundary spacing and is later refined based on flow-field gradients. The flow solver uses upwind differencing for inviscid fluxes and central differencing for viscous fluxes. A point implicit scheme, which makes use of Jacobi subiterations for improved stability, is used to advance the solution to steady state. Prismatic grids can be added for resolving the boundary layer regions near the bodies in viscous flow analyses. The outer layer of the prismatic grids interfaces with the Cartesian grid in a conservative manner.

Accomplishment Description

The 3-D version of the code was tested on several simple single- and multiple-body configurations. Calibration of the results for the ONERA M6 wing showed that the code was in agreement with the experimental data. The inviscid analysis of an MK-84 bomb separating from a fully loaded F-16 began in late 1993. Computation of the captive case is nearly completed. The

analysis compares the forces and moments on the MK-84 to wind tunnel balance results. The current solution is limited to 850,000 cells and is shown in the figure. A shedding vortex inboard of the MK-84 pylon makes determining forces difficult. The amount of memory required for this case is 220 megawords and a run of 100 iterations requires 2.9 Cray C-90 hours.

Significance

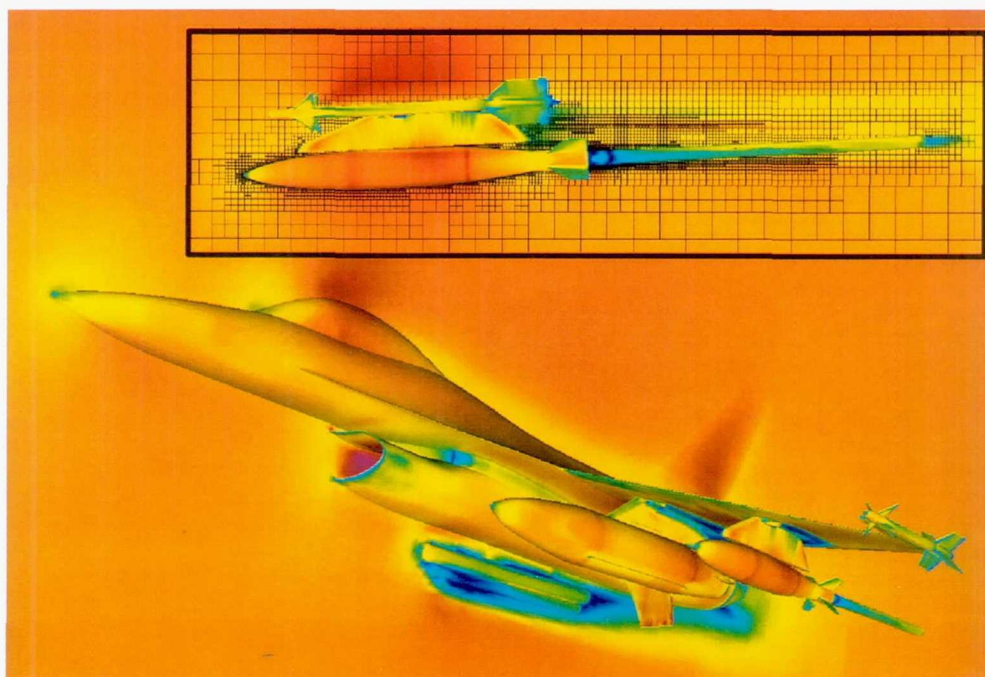
The development of this unstructured CFD capability reduces the analysis time for complex 3-D geometries and flow fields. The automatic grid generation capability permits rapid problem setup and configuration changes, enabling the timely evaluation of parametric studies of complex geometries and analysis of phenomena such as store separation.

Future Plans

The calibration of the 3-D Cartesian-based unstructured grid code will continue. The analysis of the MK-84 bomb at several instances in time will be compared with the wind tunnel captive trajectory simulation results. A quasi-steady trajectory simulation will be performed using the integrated CFD forces and moments and a six-degree-of-freedom package. The computed trajectory will be compared with the experimental result.

Keywords

Store separation, Adaptive



Mach number contours displayed on solid surfaces and the symmetry plane. A cutting plane through the MK-84 centerline (inset) shows the grid adaptation results and Mach number contours.

Laminar Flow Supersonic Wind Tunnel

E. Tu, Principal Investigator

Co-investigator: G. H. Klopfer

NASA Ames Research Center/MCAT Institute



Research Objective

To develop computational tools so that the design of a test model and its placement within the test section of the Laminar Flow Supersonic Wind Tunnel (LFSWT) can be verified by numerical simulation of the Navier–Stokes equations before the model is constructed. For transition studies in the supersonic Mach regime it is important to know the extent of clean and undisturbed flow over the test model.

Approach

Modified versions of the upwind parabolized Navier–Stokes (UPS) and the compressible Navier–Stokes finite volume (CNSFV) codes were used to solve the thin-layer Navier–Stokes equations for laminar flow about the test model inside the LFSWT. The faster UPS code was used for the higher Mach numbers investigated and the multizonal CNSFV for the lower supersonic Mach regime.

Accomplishment Description

Computations were performed for a NACA 64A010 wing with a 70-degree leading-edge sweep mounted on the top wall of the LFSWT at Mach 1.6 for inviscid and viscous flows with the UPS and CNSFV codes. Various model locations were studied to verify that the top wall mounted position provided the largest extent of undisturbed flow on the model. The figure shows the inviscid

shock pattern obtained with the UPS code. Shown are the impinging shocks on the tunnel walls and the model. The undisturbed region on the model is the triangular region in front of the reflected shock wave impinging on the model. The flow field behind the impinging shock wave is no longer undisturbed and the part of the model behind the shock is useless for any natural transition study.

Significance

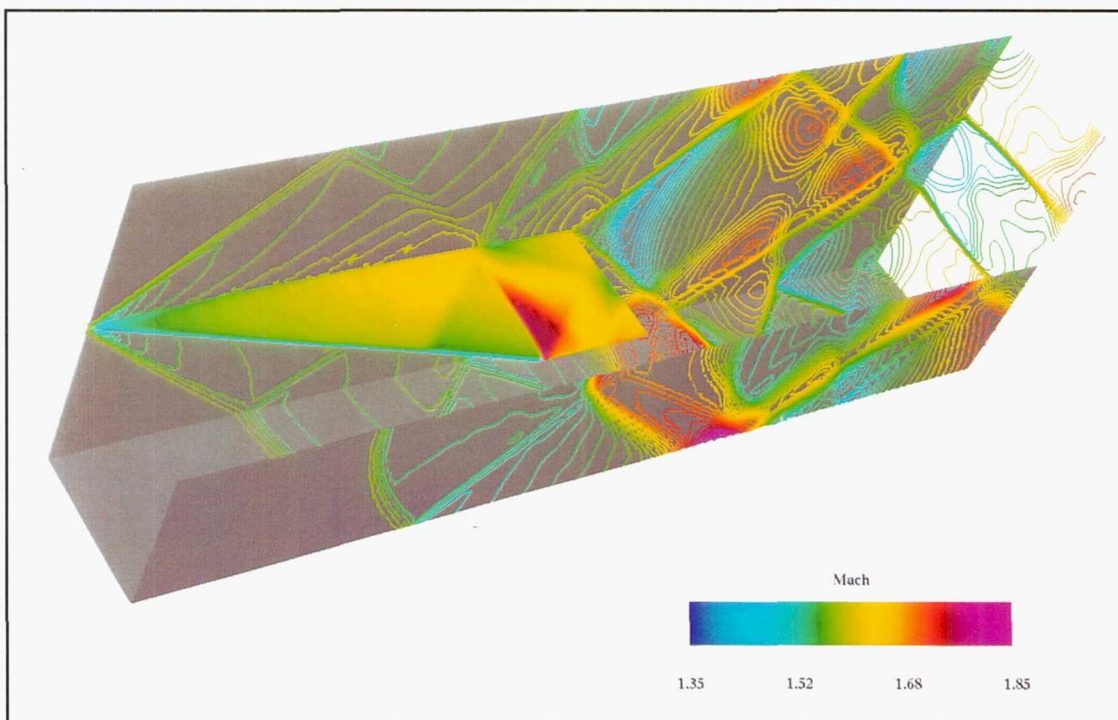
An accurate prediction of the flow field inside the LFSWT with various test models is important for maximizing the usefulness of the tunnel, especially when relatively small test sections are considered. Numerical simulation can be used for designing tunnel modifications and innovative passive and active tunnel devices to minimize the impact of reflected shock waves on the test model. This is a cost-effective means of increasing the usable size of the LFSWT.

Future Plans

The CNSFV code and technique will be extended to unsteady flows to study test model blockage and tunnel unstart problems.

Keywords

Laminar flow control, Supersonic



Numerical verification of the LFSWT shock pattern of a 70-degree sweep NACA 64A010 wing at Mach 1.6.

Transonic Flows Around Complex Geometries

Jassim A. Al-Saadi, Principal Investigator

Co-investigators: Peter A. Cavallo and William D. Smith

NASA Langley Research Center/George Washington University



Research Objective

To accurately and efficiently compute transonic flows around complex subsonic transport aircraft geometries.

Approach

An unstructured Euler code, USM3D, was used to predict pressure distributions and flow characteristics over advanced subsonic transport configurations. An interacting boundary layer (IBL) method was added to USM3D to improve pressure predictions in the transonic range. A high-wing transport with engine nacelles, pylons, and winglets was analyzed with the Euler code to assess engine interference effects against previous clean-wing solutions. The interacting boundary layer code was applied to this complex configuration and to a low-wing transport to compare its ability to predict pressure distributions against the Euler code alone.

Accomplishment Description

The Euler code successfully captured shocks at the wing/pylon intersections and other flow characteristics observed in wind tunnel tests of the high-wing transport. The grid for the full high-wing configuration contained 1.4 million cells. Both the Euler and Euler/IBL solver solutions required 4 Cray C-90 hours and 250 megawords of memory. Addition of the IBL method to the Euler code results in a marked improvement in the high-wing transport pressure distribution predictions when compared with experimental data. Accurate prediction of winglet/wing interac-

tion required the IBL method. To verify the utility of the Euler/IBL solver, a low-wing transport solution was obtained with a grid of 286,000 cells. This solution took 1 Cray C-90 hour and required 50 megawords of memory. The IBL method also showed significant improvements in pressure predictions for the low-wing transport configuration.

Significance

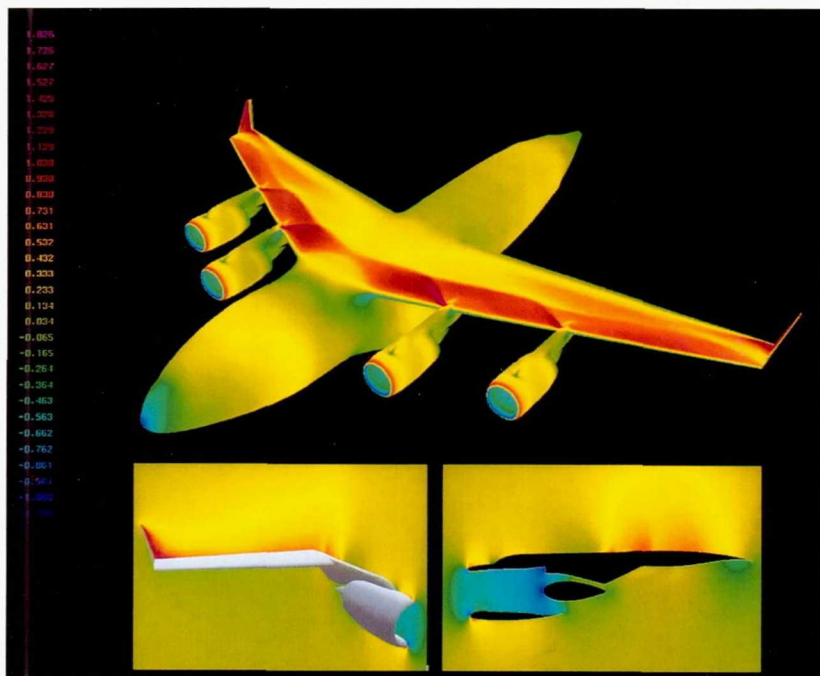
Unstructured-grid Euler methods can effectively compute transonic flows over complex transport aircraft configurations. The addition of a boundary layer calculation for viscous flow simulation further improves pressure predictions for complex geometries without requiring the grid generation time associated with structured-grid Navier-Stokes solvers.

Future Plans

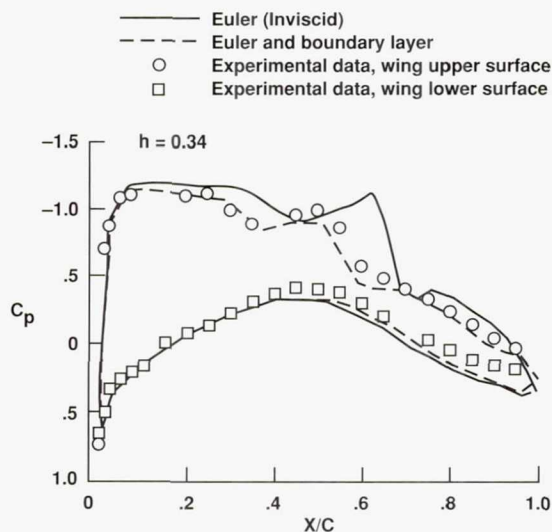
Reynolds number effects with either the unstructured Euler/IBL solver or a structured Navier-Stokes solver will be investigated. Work is under way to predict propulsion installation effects using a structured-grid Navier-Stokes solver on a low-wing transport configuration. The full viscous solutions will be compared against the unstructured-grid Euler and Euler/IBL solutions and experimental data.

Keywords

Unstructured grids, Propulsion integration, Interacting boundary layer



Pressure contours on a high-wing subsonic transport at cruise Mach number.



Effect of interacting boundary layer on pressure predictions for a low-wing transport.

Simulation of Coupled Fluid and Flightdynamic Systems

Christopher A. Atwood, Principal Investigator
Overset Methods, Inc.



Research Objective

To develop and demonstrate a multidiscipline simulation capability involving the nonlinear coupling of aerodynamics, flight dynamics, and controls.

Approach

This effort addresses the nonlinear interaction of multidiscipline problems through numerical simulation. The disciplines of aerodynamics (Reynolds-averaged Navier–Stokes equations), body dynamics (Euler rigid body dynamics equations), and controls (state-feedback controls model) are included. The simplifications typically used in computing aerodynamic interactions and loads for control law design are not included in this study. In order to assess the accuracy of the initial computations, a problem that could be compared against analytic and experimental results was chosen—a cavity store separation problem with and without active control of a canard control surface was used.

Accomplishment Description

Application of the control law to both two- and three-dimensional (3-D), three-degree-of-freedom cavity store separation problems revealed improved trajectory characteristics as

compared to canard-fixed simulations. However, because of the high store ejection rate, the improvement was modest. The accompanying figure shows the 3-D controlled store during the separation process. A typical 3-D simulation required 16 megawords of main memory and approximately 70 Cray C-90 hours on a single processor.

Significance

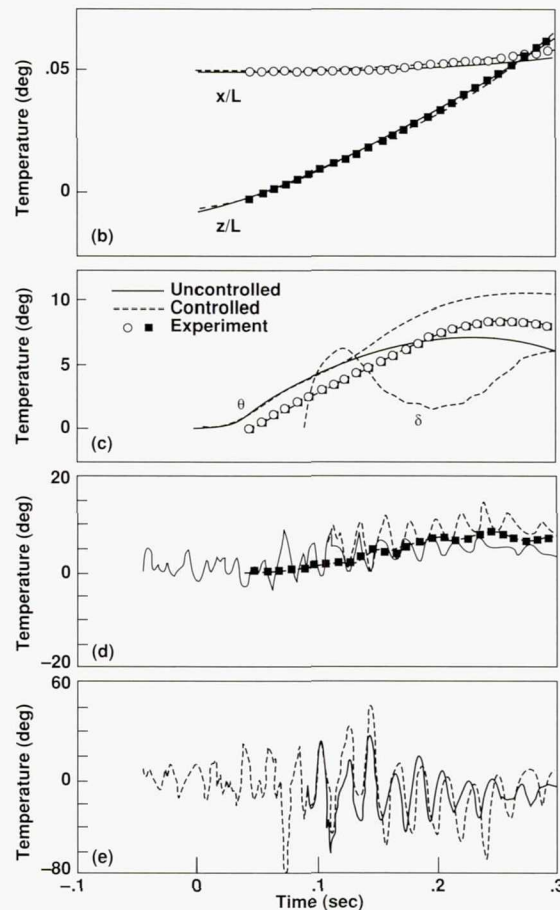
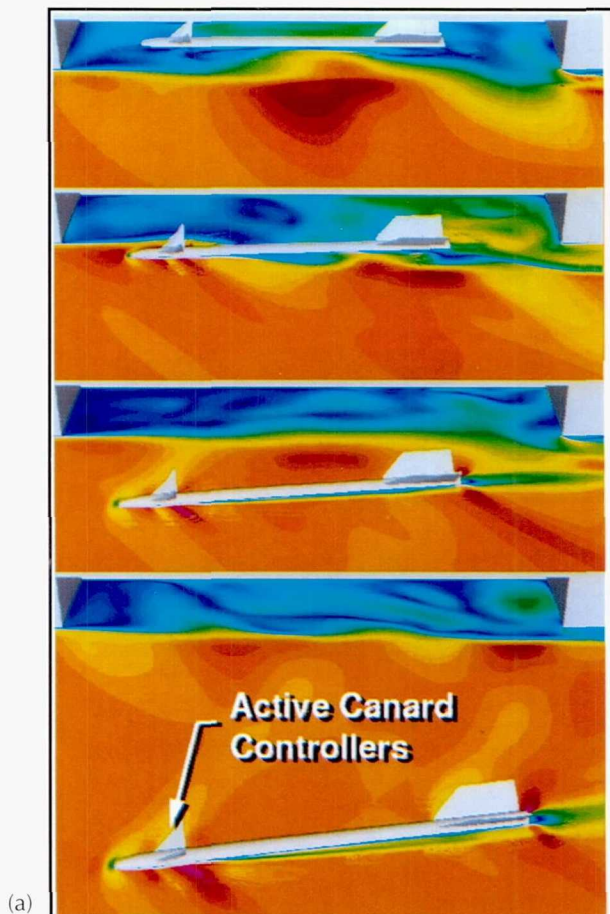
This computation represents one of the first 3-D simulations to couple complex viscous aerodynamics and control models together in the same computation. This capability, when fully developed, offers a means of reducing aircraft design cycle time and cost while enhancing safety and performance.

Future Plans

More detailed simulations involving reasonably complete aircraft and the inclusion of a structural dynamics model to allow for aircraft flexibility will be completed.

Keywords

Unsteady, Controls, Navier–Stokes



Three-dimensional controlled store: (a) Mach contours on symmetry plane, (b) center of gravity position, (c) body attitude (θ) and canard deflection (δ), (d) force coefficient, and (e) moment coefficient.

F/A-18 Aerodynamic Assessment

Raymond R. Cosner, Principal Investigator

Co-investigators: Robert H. Bush, William W. Romer, and Paul G. Willhite

McDonnell Douglas Corporation



Research Objective

To predict the model support hardware impact on the measured performance of the F/A-18.

Approach

Parallel computational fluid dynamic (CFD) and experimental predictions of the sting and distortion performance increment will be performed to determine if CFD can adequately predict this increment. The CFD study precisely paralleled the experimental study, including the exact wind tunnel model geometry, the wind tunnel walls, and wing tip mounting system in the calculations. Non-overlapping grids were used to model the geometry. Zone breaks in the aft end region isolated the grid changes to areas where the geometry changed from the real to the distorted aft end. The modified differential approximation proprietary code NASTD, using the Baldwin–Barth turbulence model option, was used to compute the flow field. The Arnold Engineering Development Center wind tunnel wall porosity model was implemented for this study to ensure consistency between the wind tunnel and CFD wall effects.

Accomplishment Description

This study demonstrates the ability of CFD to accurately predict sting and distortion performance increments. Accurate increment predictions require tight controls on the geometry, grid topology and resolution, and consistent application of the flow solver to

the incremented cases. The flow solver took approximately 200 Cray C-90 hours for each run and used 50 megawords of memory. The figure shows predicted surface pressure contours on a boom-supported, distorted, F/A-18A model at Mach 0.85.

Significance

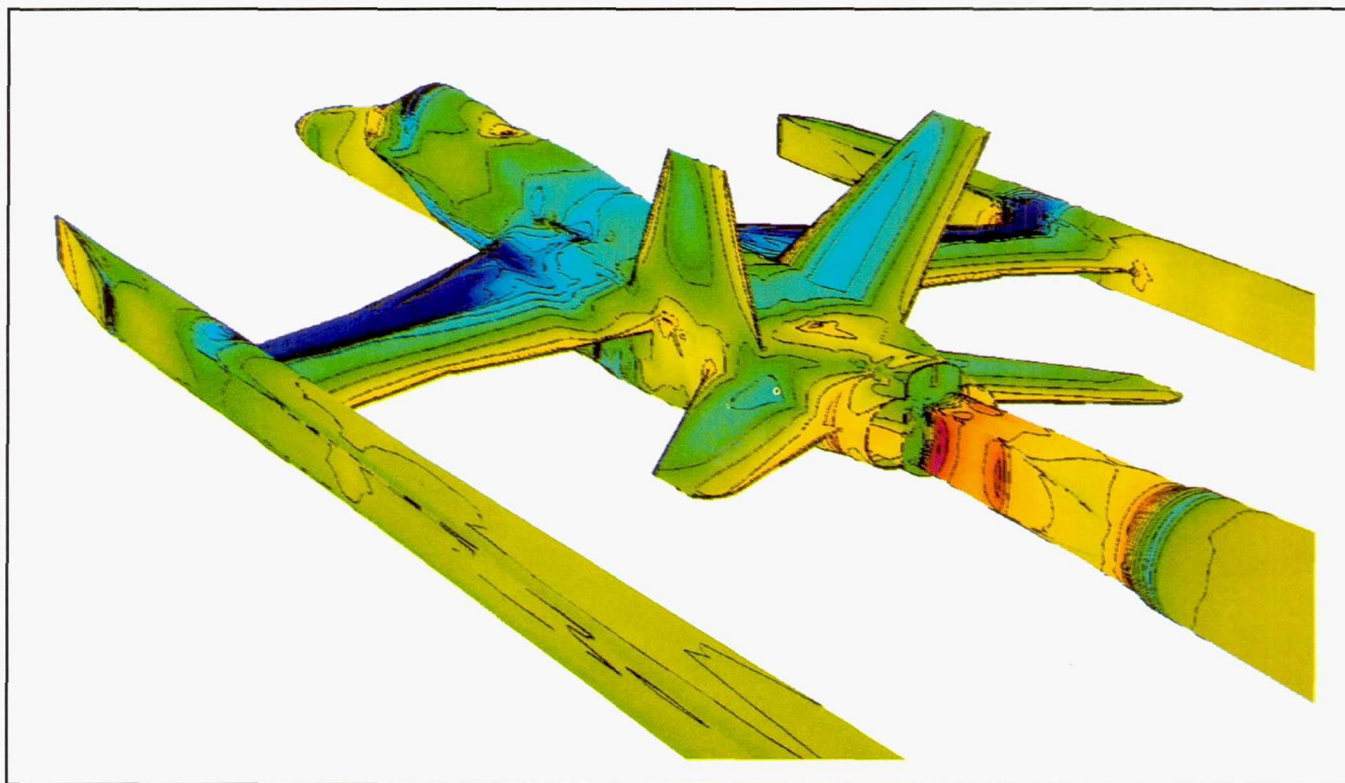
The ability to accurately predict sting and distortion increments with CFD provides a cost effective means of correcting wind tunnel performance data for sting and distortion effects.

Future Plans

The ability of CFD to quantitatively predict the performance of full configuration aircraft configurations opens an array of potential applications. Future work will focus on further validation of the accuracy of CFD for complex steady and unsteady flows of engineering interest.

Keywords

Wind tunnel interference, Sting and distortion increments, Afterbody drag



A full configuration Navier–Stokes calculation of a distorted aft end flow field provides quantitative performance predictions.

Launch Vehicle Flow-Field Simulation

Jerry E. Deese, Principal Investigator
Co-investigator: Ramesh K. Agarwal
McDonnell Douglas Corporation



Research Objective

To develop accurate and efficient methods for the prediction of flow fields over complete launch vehicle configurations including the effects of plumes.

Approach

The Reynolds-averaged Navier–Stokes equations are solved on body-conforming curvilinear grids using a finite-volume Runge–Kutta time-stepping algorithm. Euler, thin-layer, slender-layer, and full Navier–Stokes options are available. Complex configurations are modeled with a multiblock zonal implementation. The code includes algebraic, Johnson–King, and two-equation turbulence models. Chemistry models for nonequilibrium air, hydrogen/air, and hydrocarbon/air are available.

Accomplishment Description

This effort was focused on the prediction of multiple body launch vehicle flow fields. A number of calculations were run for multiple body configurations that consist of a core vehicle with solid rocket boosters attached. The surface pressure distribution on a 120-degree segment of a three-booster configuration is shown in the figures. Initial calculations modeled the solid rocket plumes with hot air; a 15-species, 13-reaction solid rocket motor chemistry model is being added to the code for improved plume modeling. Typical runs required 100–200 megawords of memory and 50 Cray C-90 hours.

Significance

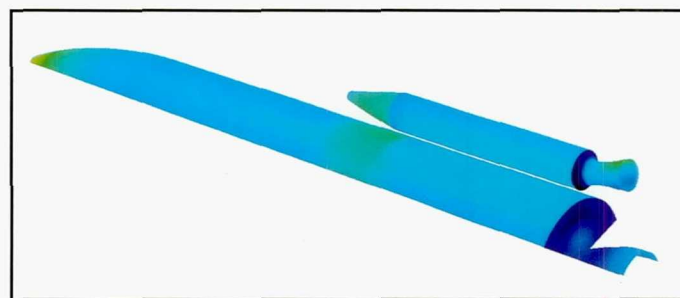
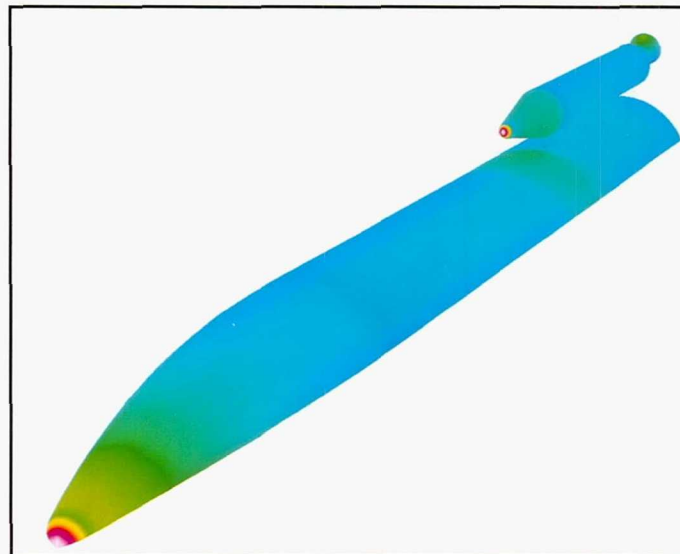
The ability to predict complete configuration flow fields allows designers to take component interference into account and optimize the aerodynamic performance of the complete vehicle. An accurate prediction method allows designers to build an aerodynamic performance database for new configurations that have not been tested experimentally.

Future Plans

Flow solver and chemistry model validation with experimental data will continue. The code will be applied to the analysis of new launch vehicle configurations. Once the methodology is established for steady flows, attention will turn to unsteady flows for application to booster-stage separation.

Keywords

Transonics, Navier–Stokes, Base flows



Front view (top) and aft view (bottom) of the surface pressure distribution on a 120-degree segment of a three-booster configuration.

Space Shuttle Flow Fields with Plume Simulation

Daniel F. Dominik, Principal Investigator

Co-investigators: K. Rajagopal, C. Olling, K. Mani, S. Vuong, J. Wisneski, G. Hock and J. Sikora

Rockwell International, Space Systems Division



Research Objective

To predict transonic aerodynamic loads for the Space Shuttle Launch Vehicle (SSLV) during ascent by performing Navier–Stokes computations with plume simulation at full-scale flight Reynolds number.

Approach

A model with fine geometry details of the SSLV was built using ICEM, a computational fluid dynamics (CFD) computer aided design grid software. Most of the interzonal boundaries were aligned. The numerical solutions were obtained using the Reynolds-averaged Navier–Stokes formulation of the USA-RG3D code with the algebraic Baldwin–Lomax turbulence model. Calculations include simulation of the three Space Shuttle main engine (SSME) plumes and the two solid rocket booster (SRB) plumes. Results were correlated with available flight-test and wind tunnel data.

Accomplishment Description

The SSLV model simulated the forward and rear attach hardware connecting the Orbiter, the external tank, and the two SRBs. The primary protuberances on the body surfaces, including the liquid oxygen feed line on the right side of the external tank, were modeled to enhance the accuracy of the multibody flow-field simulation. The complete, asymmetric grid model contained 269 zones and approximately 6 million points. The USA-RG3D flow solver was used to simulate the turbulent, flight Reynolds number transonic flow over the geometry. The model was broken into 6 sections so that no section required more than 64 megawords of main computer memory. Each section had overlapping zones and the solutions were updated by cycling through the sections to ensure proper communication. Numerical solutions were computed for the redesigned solid rocket booster at Mach = 1.25 with -5.1 and -3.3 degrees of angle of attack, and the advanced solid rocket booster at Mach = 1.25 with -5.1 degrees of angle of attack. Variable specific heat gases were simulated for the SRB and SSME plumes; the plumes affect the flow field in the aft half of the vehicle and increase the wing loads.

Significance

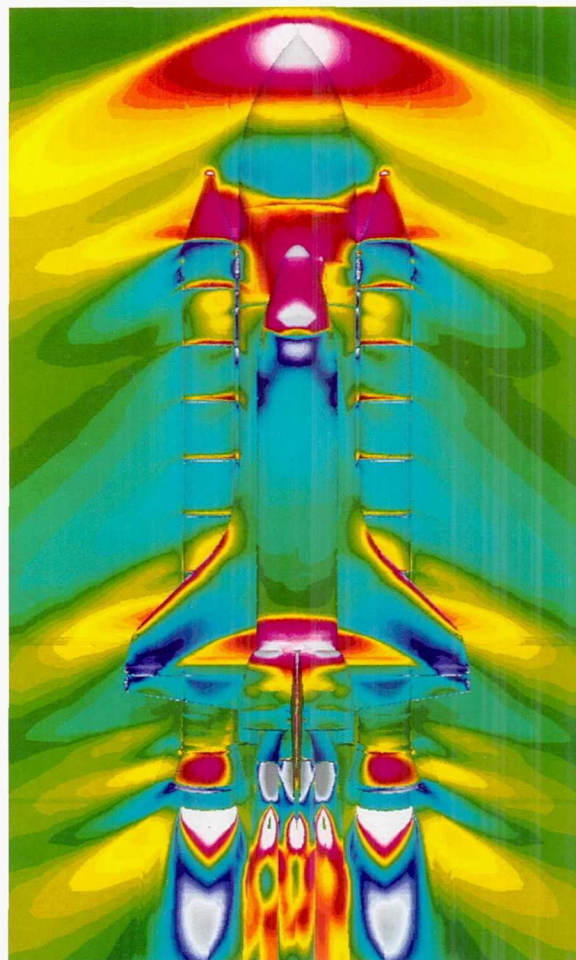
In transonic flow regimes, the influence of plumes can significantly alter the forebody load distributions. These computations demonstrate the CFD simulation of engine plumes and their effect on the flow field. However, the pressures were over predicted on the Orbiter base and on the wing lower surface. Better comparison between CFD results and flight data will require a better turbulence model, plume chemistry model, and grid resolution.

Future Plans

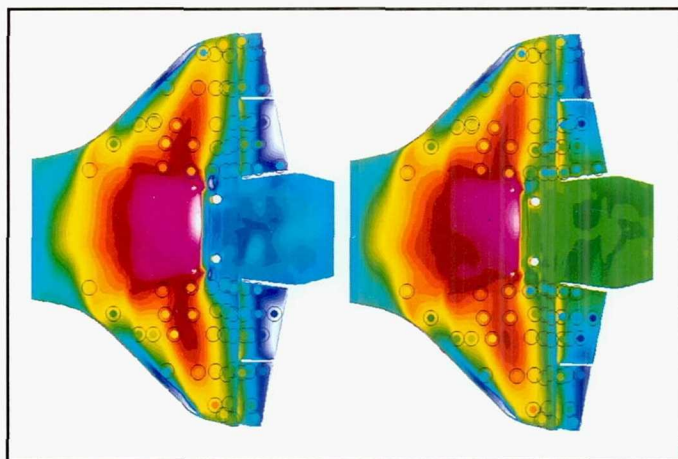
SSLV flow fields will be simulated with a turbulence model better suited for multiple shear flows.

Keywords

Plume effects, Multibody flow fields



Pressure coefficient at Mach = 1.25, angle of attack = -5.1 degrees; blue = -0.4 and magenta = 0.55.



Pressure coefficient on Orbiter wing lower surface at Mach = 1.25, angle of attack = -5.1 degrees with plumes inactive (left) and active (right). CFD in contours and flight data in circles; blue = -0.4 and magenta = 0.55.

Reynolds Number Effects on a Delta Wing

W. Kelly Londenberg, Principal Investigator
ViGYAN, Inc.



Research Objective

To continue the calculations for a grid about a delta wing with a medium leading-edge radius including the sting at varying Reynolds numbers and angles of attack. The calculations will be assessed on how well Reynolds number, angle of attack, and geometrical effects on the flow over a highly swept wing are computationally predicted.

Approach

Calculations were performed using the CFL3D code. This multi-block code solves the thin-layer approximations to the three-dimensional, time-dependent, compressible Navier–Stokes equations. Coupled with this code are the Baldwin–Lomax algebraic and the Spalart–Allmaras one-equation turbulence models.

Accomplishment Description

Numerous solutions were obtained for a 65-degree delta wing configuration using the CFL3D code. Initial pressure coefficients obtained using the Baldwin–Lomax algebraic turbulence model compared well with experiment for attached flow conditions at 6×10^6 Reynolds number, but the solution became unsteady at separated conditions. Solutions obtained using the Spalart–Allmaras one-equation turbulence model predicted pressure distributions that compared equally well for attached flow cases, and steady solutions were obtained for separated flow conditions. Using the one-equation turbulence model, solutions were

obtained for Reynolds numbers $6 \times 10^6 \leq 120 \times 10^6$ for several angles of attack. The predicted pressure distributions compared very well with experiment at all Reynolds numbers for attached flow conditions. The code, however, predicted separation aft of the experimental location. This resulted in the predicted vortex forming later than in the experiment, which resulted in a weaker vortex being computed. Also, the cross-flow shock apparent in the experiment was not predicted. On average, the solutions required 6.33 Cray C-90 hours for convergence and used approximately 60 megawords of memory.

Significance

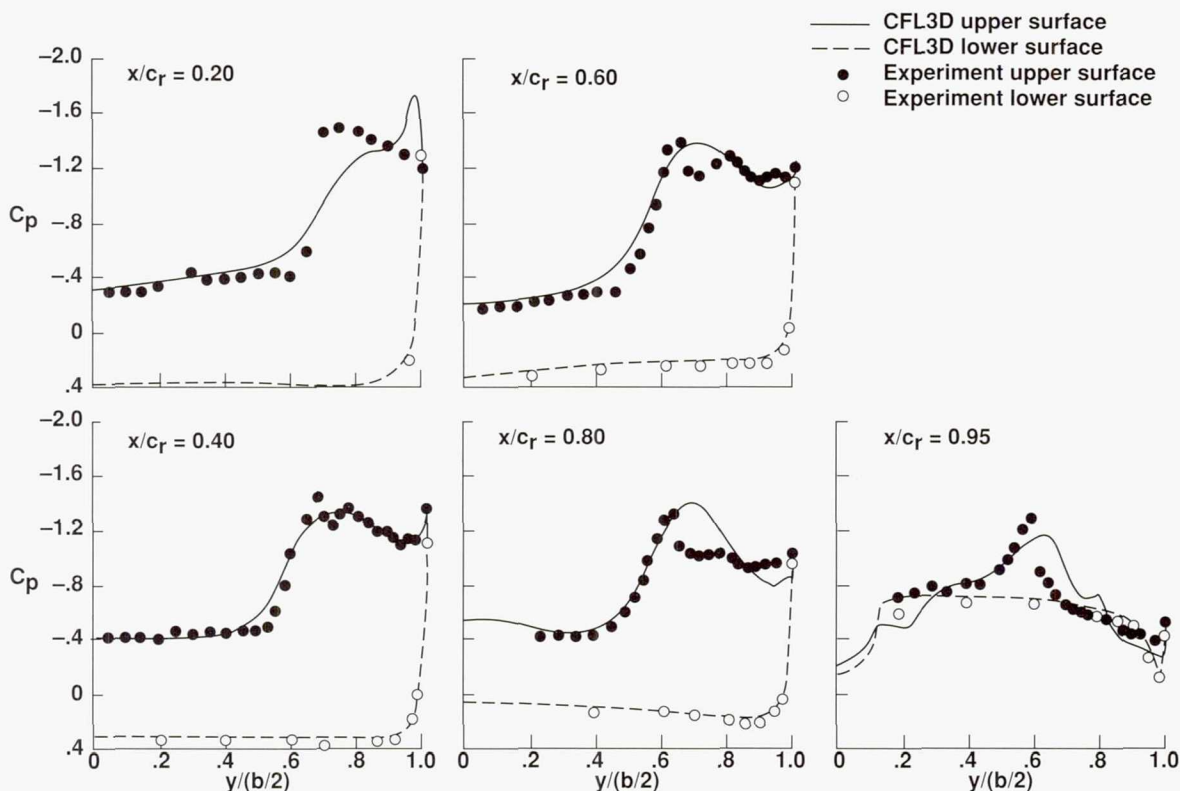
Even though the vortex location is predicted well, the Spalart–Allmaras one-equation turbulence model does not predict the separation location accurately for this geometry.

Future Plans

Methods to improve the comparisons will be investigated. The use of advanced one- and two-equation turbulence models for comparison improvement will be studied. The effect of transition location will also be investigated.

Keywords

Computational fluid dynamics, Turbulence models, Transonic flow



Predicted pressure distributions show poor comparison with experiment for separated flow case. Large-radius leading edge, Spalart–Allmaras turbulence model, Mach = 0.85, $\alpha = 16.59$ degrees, Reynolds number = 120 million.

High-Angle-of-Attack Aerodynamics

Christopher L. Reed, Principal Investigator
Lockheed Engineering and Sciences Company



Research Objective

To develop and validate three-dimensional computational fluid dynamics (CFD) techniques for the aerodynamic analysis of bodies at arbitrary attitudes.

Approach

CFD analysis techniques were developed starting with a simple configuration at relatively benign attitudes and then progressing to more complex configurations at extreme attitudes. The analyses results were compared with experimentally obtained force and moment data. These analyses are completed using a central difference finite-volume Navier-Stokes analysis code. The code uses a diagonalized lower-upper implicit technique to solve the governing equations. A two-equation k - ϵ turbulence model was employed with a wall layer model along no-slip walls.

Accomplishment Description

An extensive wind tunnel test was completed for a 920,000 point symmetric grid and a 1.8 million grid point full grid for a 600 gallon F-22 tank plus pylon configuration. This allowed a significant number of analysis-to-experiment comparisons. The analyses were run at Mach 0.9 and 1.2, from 0 to -90 degrees angle of attack, and with sideslip angles from 0 to 40 degrees. A typical analysis required approximately 5,000 iterations to reduce the mean flow residual 3 to 4 orders of magnitude. The normal force, axial force, and pitching moment were also monitored to determine solution convergence. Each case required approximately 50 megawords of memory and 34 Cray C-90 hours. Comparisons with the test data were very favorable.

Significance

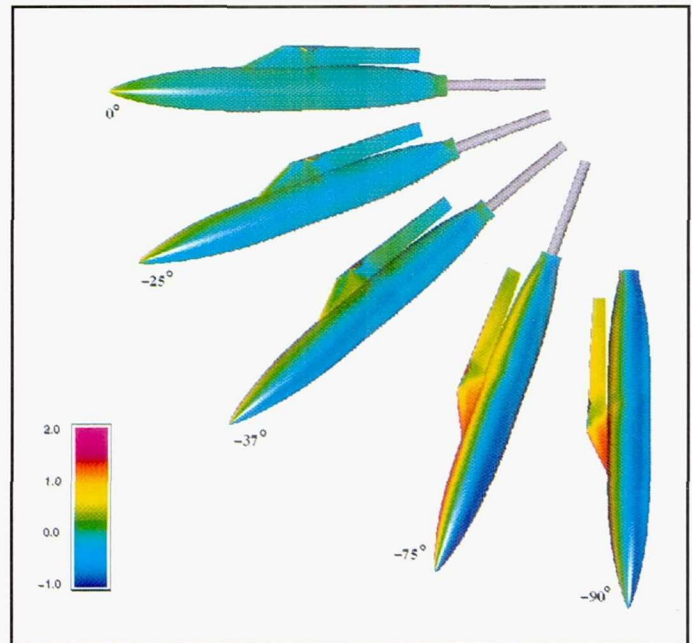
The capability to analyze bodies at arbitrary attitudes is important (particularly to store separation engineers). Bodies ejected during flight achieve extreme attitudes compared to flight vehicles. Methods that can accurately predict store trajectories are desirable and CFD analysis promises to fill that requirement. Methods exist that use a number of steady-state solutions to aid in the prediction of store trajectories. Lessons learned from steady state predictions will aid in the development of fully time-dependent methodologies. It is believed that significant gaps will exist in the F-22 store force and moment database because of test limitations. The ability to accurately provide these data using CFD may significantly impact the F-22 program.

Future Plans

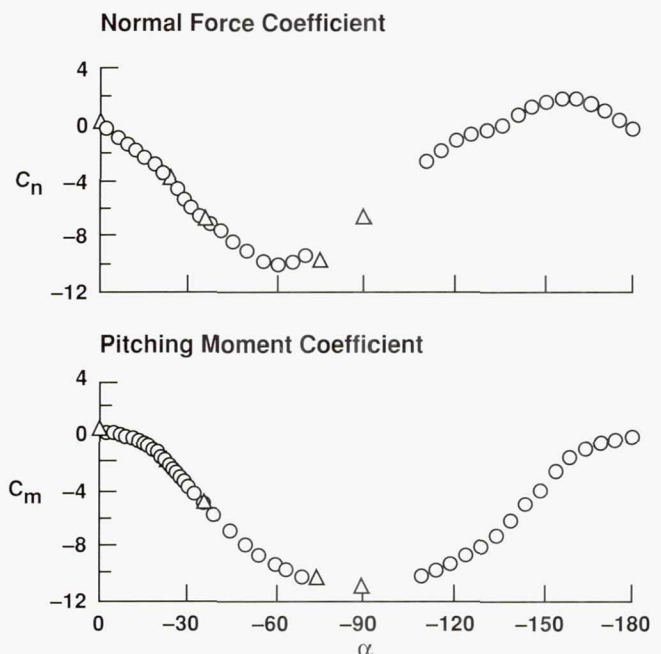
The methodology will be further developed and validated. A low-speed test will be completed using the F-22 600 gallon tank plus pylon configuration. The configuration will have a number of pressure taps and force and moment balances. This will allow more extensive comparisons. The test program will include runs at extreme attitudes.

Keywords

Store separation, Computational fluid dynamics



An F-22 tank with pylon is colored by pressure and shown at various angles of attack. Mach = 1.2 and Reynolds number = 1.2 million.



Comparisons with available test data indicate excellent agreement for normal force coefficient (top) and pitching moment coefficient (bottom). The triangles represent the CFD analysis and the circles represent the Arnold Engineering Development Center test data.

Computational Studies of Advanced Wings at High Incidence

Arvin Shmilovich, Principal Investigator

Co-investigators: K. C. Chang and R. A. Pelkman

McDonnell Douglas Aerospace



Research Objective

To calibrate advanced computational fluid dynamics (CFD) methods with various turbulence models for simulating flow fields about wing/fuselage configurations at buffet conditions.

Approach

The one-half-equation turbulence model of Johnson-King and the one-equation models of Baldwin-Barth and Spalart-Allmaras were used to evaluate numerical methods for predicting wing separated flows at transonic buffet. The models were implemented in TLNS3D and CFL3D.

Accomplishment Description

Several wing/body configurations representing contemporary wing designs and advanced wing concepts were used to evaluate the turbulence models in TLNS3D and CFL3D. Comparisons of the numerical predictions with wind tunnel and flight-test data were made for conditions representing cruise-to-buffet and for a range of Reynolds numbers. Results indicate that better predictions can be obtained for separation-dominated flows using one-equation turbulence models, and thus the capability of the numerical schemes to simulate flows beyond buffet onset is improved. For a grid of about 1 million points, a typical run required 2 Cray C-90 hours and approximately 60 megawords of memory.

Significance

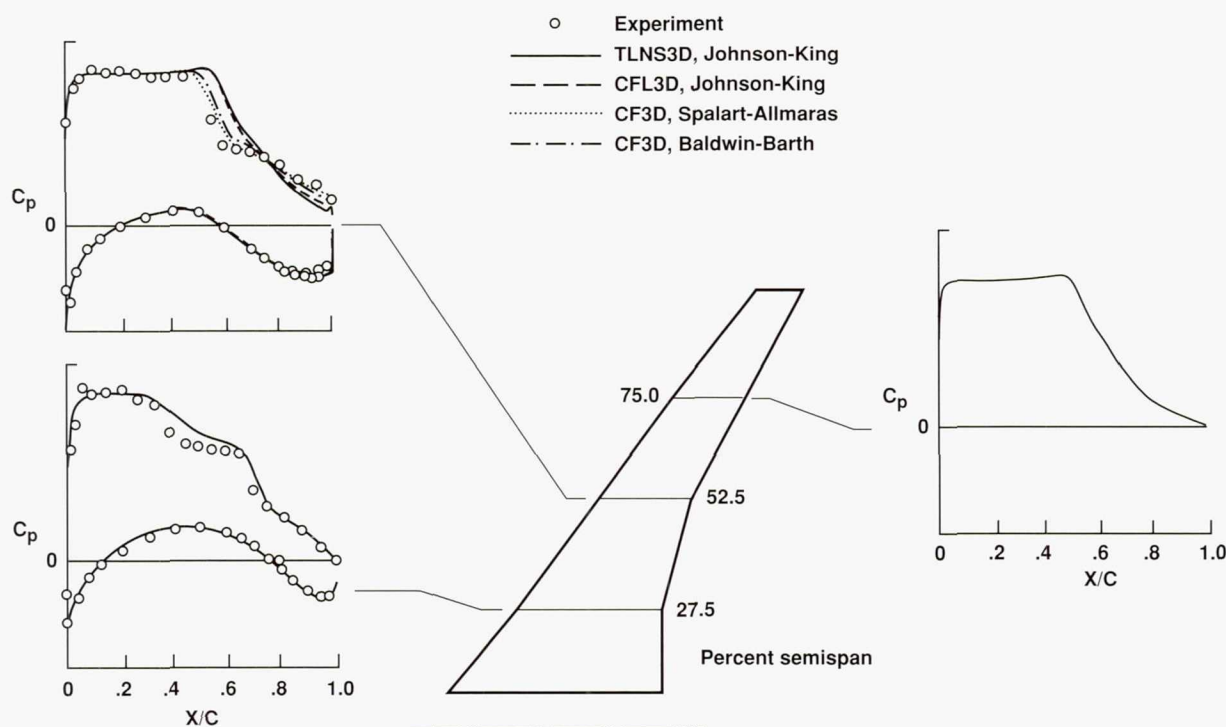
In contrast to the success accomplished for attached flow conditions and for flows with mild separation, in general, computational tools are of limited use for predicting flow fields at conditions that result in sizable separated flow regions because the predictions gradually depart from the experimental data. The flow conditions examined in this study at buffet onset and post buffet indicate improved correlations with the aid of new turbulence models.

Future Plans

The validation study will be extended to include other promising turbulence models. Possible extensions of the turbulence models to include more adequate wake modeling will be investigated. Proper wake modeling is a crucial element for the treatment of buffet flows because the attainment of acceptable accuracy is contingent on the ability to simulate the interaction between the shear layers and the wake during flow reversal conditions.

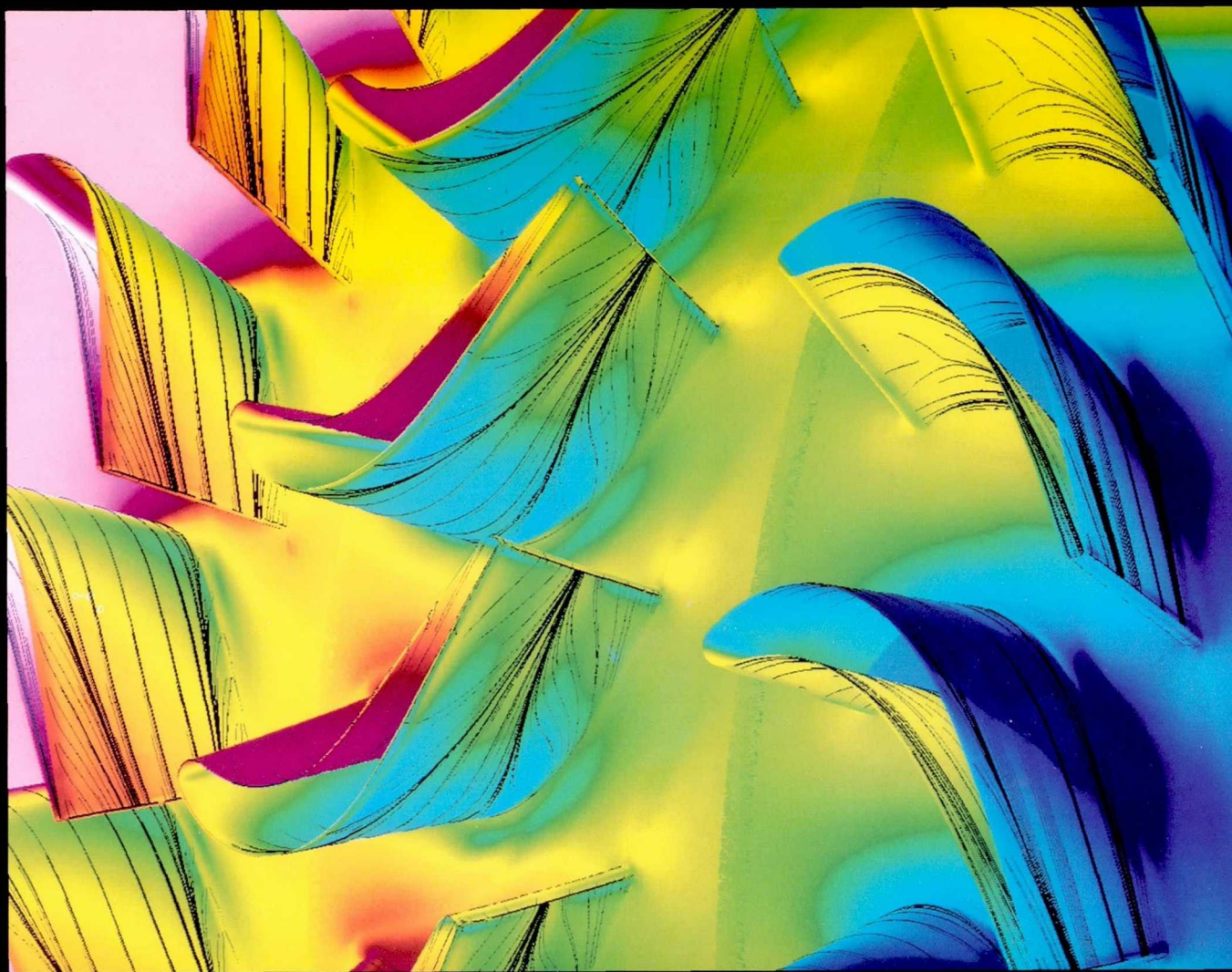
Keywords

Separation, Turbulence, Buffet



CFL3D and TLNS3D advanced wing predictions with various turbulence models at transonic buffet (same incidence and free-stream velocity).

Aeronautics



Propulsion

Page intentionally left blank

Simulation of Supersonic Jet Screech

Alan B. Cain, Principal Investigator

Co-investigators: William W. Bower and Yutaka Ikeda

McDonnell Douglas Corporation



Research Objective

To simulate supersonic jet screech to provide modeling information on the receptivity and acoustic radiation from the shock-vortex interaction.

Approach

A conservation, finite-volume formulation of the Navier-Stokes equations are solved using an upwind biased spatial scheme together with a Runge-Kutta time integration. A hole cut grid permits the needed grid smoothness to be achieved with the compromise of multizone interfaces. Damping is added near the computational boundaries to minimize boundary reflections because of imperfect boundary conditions.

Accomplishment Description

The basic three-dimensional simulation of a self-sustained oscillation in a round jet flow was demonstrated. This is the first of the necessary steps to establish an accurate simulation of screech. The geometry of this demonstration case matches that of a laboratory study at NASA Langley. The early stages of this work were based on two-dimensional and axisymmetric cases. A single case requires about 200 Cray Y-MP hours and 64 megawords of memory.

Significance

Screech acoustic amplitudes can reach 160 dB and are known to produce damage to the aft end of certain military aircraft. An accurate and rapid analytical design tool is needed to ensure that future designs will not produce screech at an amplitude that results in structural damage. Numerical simulation is the only method of obtaining detailed information to validate or guide analytical models of the acoustic radiation produced by the shock-vortex interaction.

Future Plans

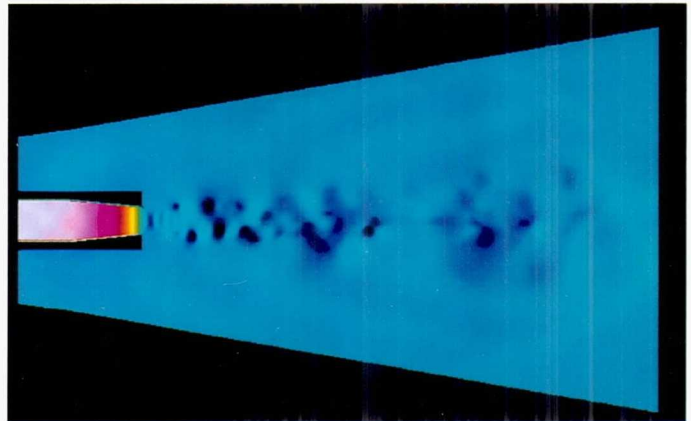
Numerical simulations will be used to guide or verify analytical modeling of nozzle-lip receptivity and shock-vortex interactions.

Keywords

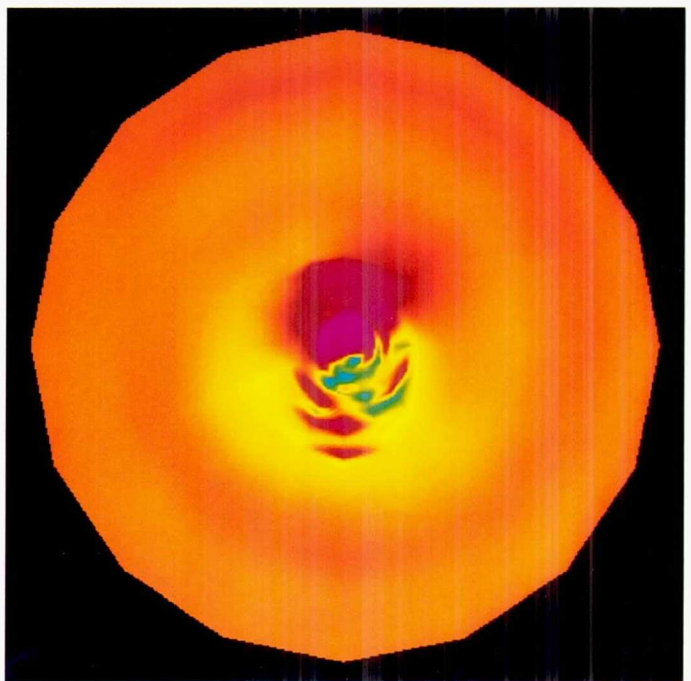
Acoustic resonance, Jet plumes

Publication

Cain, A. B.: Computation of Supersonic Jet Screech. Proceedings of the 14th IMAC World Congress, Atlanta, Ga., July 1994.



Pressure contours of a streamwise cut through the jet centerline; dark blue = low pressure and white-red = high pressure.



Density contours of an axial cut through the jet; yellow = low density and red = high density.

Multiblock Solver for Turbomachinery Flows

Rodrick V. Chima, Principal Investigator
NASA Lewis Research Center



Research Objective

To develop and validate a multiblock Navier–Stokes code for analysis of three-dimensional viscous flows in turbomachinery.

Approach

The SWIFT multiblock code solved the thin-layer Navier–Stokes equations with the Baldwin–Lomax turbulence model using a finite-difference scheme. An explicit, multistage Runge–Kutta scheme with implicit residual smoothing was used to solve the flow equations. The code uses H-type grids for inlet duct regions, periodic C-type grids around the blade and in the wake, and O-type grids in the tip clearance region above the blades. Asynchronous input/output is used on the Cray to move the grid and solution blocks between the solid state storage device and the core memory used by the solver.

Accomplishment Description

A transonic compressor rotor (NASA rotor 37) was analyzed as part of a blind test case for turbomachinery codes developed by the American Society of Mechanical Engineers. Detailed experimental measurements of the rotor flow field were withheld from

the test case participants until the computational results were submitted. The computational grid had just over 1 million grid points in 3 blocks, with 13 points across the tip clearance gap. Nine operating points along the 100 percent speed line were computed. Required processing time was about 4 Cray C-90 hours for each operating point.

Significance

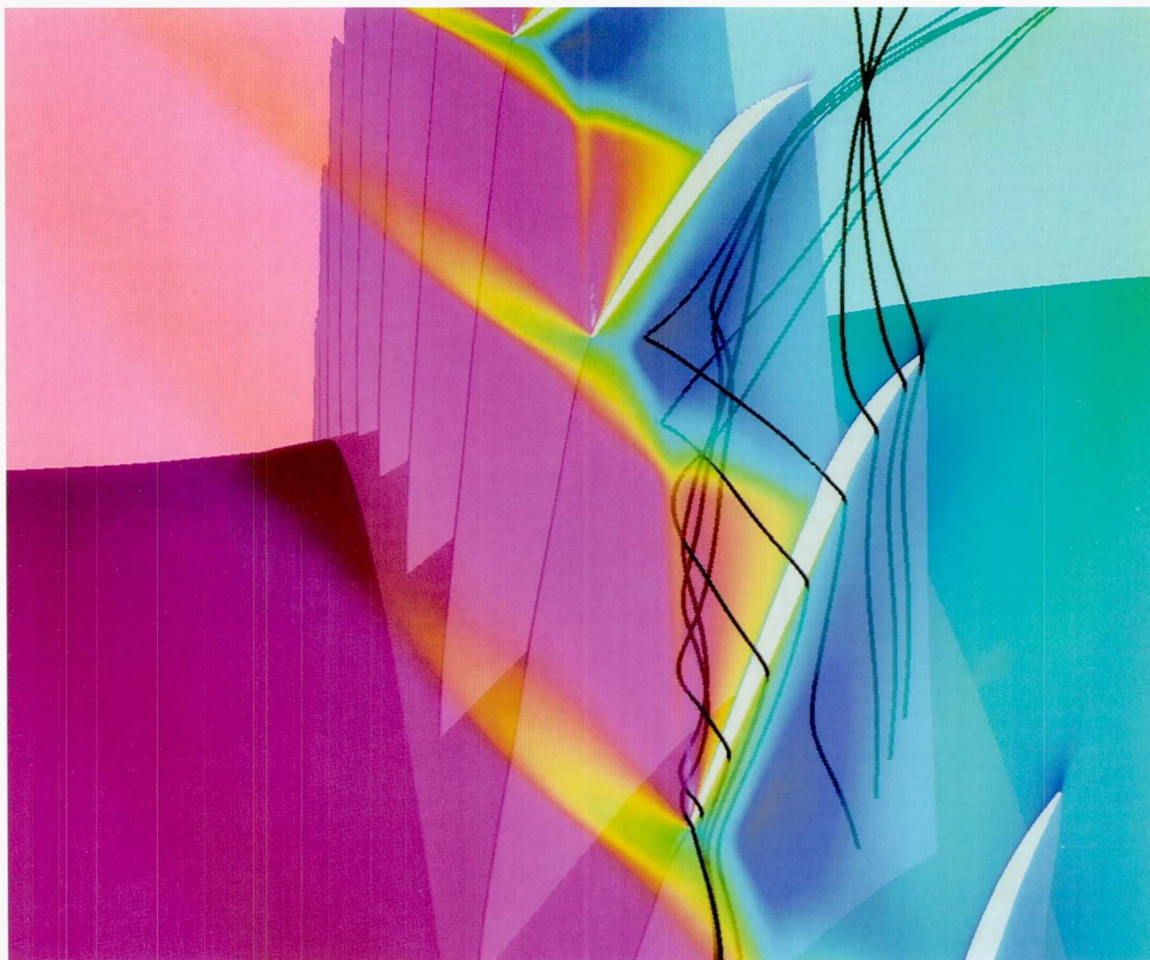
High-resolution solutions of the flow in the tip clearance region allow detailed study of the losses because of tip leakage and also allow evaluation of simpler tip models used in other codes.

Future Plans

Detailed comparisons will be made with the experimental data to verify the code. The SWIFT code will be extended to allow steady calculations of multiple stages using an averaging plane approach.

Keywords

Turbomachinery, Compressors, Tip clearance



NASA rotor 37 near stall showing clearance vortex passage–shock interaction.

Airframe/Inlet Aerodynamics

Wei J. Chyu, Principal Investigator

Co-investigator: Tom I-P. Shih

NASA Ames Research Center/Carnegie Mellon University



Research Objective

To develop an analytical capability to predict integrated performance of forebody/inlet systems for highly maneuverable aircraft.

Approach

The OVERFLOW Navier–Stokes code is used to study inlet bleed systems. The PEGSUS code Chimera grid-embedding techniques are used to integrate grids encompassing bleed holes and free-stream and plenum flow fields. A variety of two-equation turbulence models are evaluated to identify the most robust model.

Accomplishment Description

The inlet bleed process under experimental investigation is numerically studied in a case where the fluid in the boundary layer was bled through multiple staggered rows of circular holes into a plenum to control shock-induced flow separation. The modeling techniques use symmetry boundary conditions to simulate an infinite row of holes. Turbulence models based on the standard $k-\epsilon$ and $k-\omega$ formulations were developed and incorporated into the Navier–Stokes code. The capability of the models to predict separated flows is being studied.

Significance

This study permits analysis of complex inlets, making possible the investigation of a broader range of design variables associated with the integrated forebody and inlet systems and the evaluation of inlet performance as influenced by the boundary-layer control.

Turbulence models validated for accurate flow prediction are essential in the computation of viscous-dominated inlet flow fields.

Future Plans

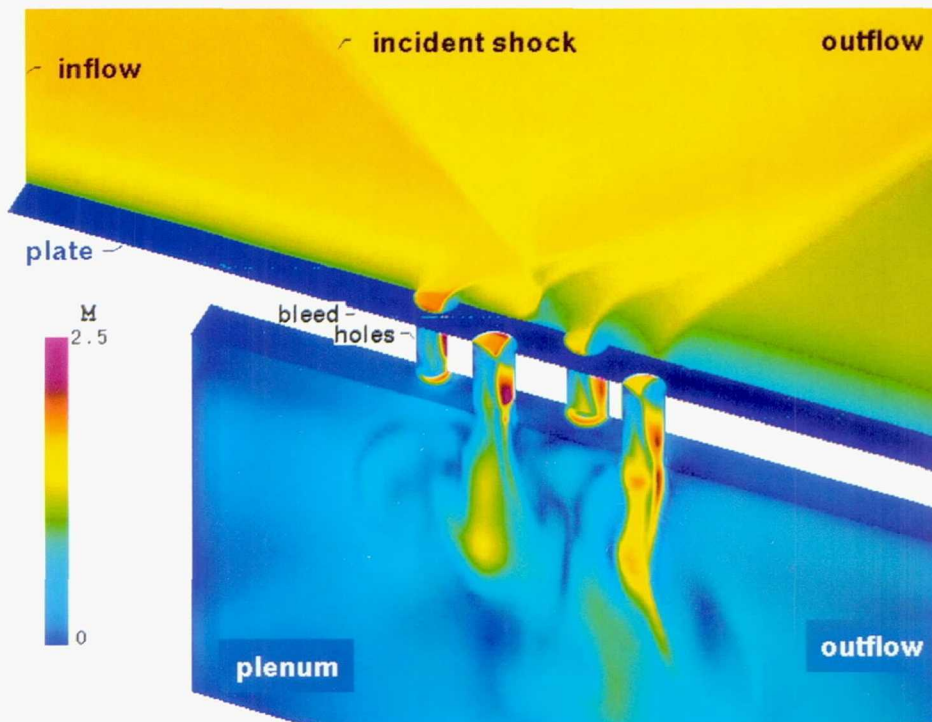
The study will be extended to other experimentally investigated bleed configurations. The effects of critical design parameters on bleed-system efficiency will be studied. Turbulence models will be investigated for their ability to predict inlet performance and associated flow physics.

Keywords

Inlet, Bleed, Turbulence

Publications

1. Mysko, J. M.; Chyu, W. J.; and Chow, C. Y.: Navier–Stokes Simulation of External/Internal Transonic Flow on the Forebody/Inlet of the AV-8B Harrier II. AIAA Paper 93-3057, July 1993.
2. Chyu, W. J.; Rimlinger, M. J.; and Shih, T. I-P.: Effects of Bleed-Hole Geometry and Plenum Pressure on Three-Dimensional Shock-Wave/Boundary-Layer/Bleed Interactions. AIAA Paper 93-3259, July 1993.
3. Rimlinger, M. J.; Shih, T. I-P.; and Chyu, W. J.: Three-Dimensional Shock-Wave/Boundary-Layer Interactions with Bleed Through Multiple Holes. AIAA Paper 94-0313, Jan. 1994.



Boundary layer bleed through multiple staggered rows of circular holes.

Turbine Blade Tip Clearance Flows

Frederik J. de Jong, Principal Investigator

Co-investigator: Tony Chan

Scientific Research Associates, Inc.



Research Objective

To analyze the tip clearance region flow for the gas generator oxidizer turbine (GGOT) blade, and to study advanced concepts proposed in an effort to reduce tip clearance losses.

Approach

Turbine blade tip flow fields were computed by solving a finite difference form of the compressible, three-dimensional Navier–Stokes equations for a single blade row in a rotating frame of reference using a linearized block-implicit alternating-direction implicit procedure. The grids were generated by stacking a series of two-dimensional grids from hub to casing; grid points were clustered near solid boundaries and in the tip clearance region. At the inflow boundary flow profiles were specified, while at the outflow boundary the static pressure was prescribed.

Accomplishment Description

Previously, results were obtained for the baseline GGOT blade at the full-scale Reynolds number on a grid containing approximately 216,000 points. Particle traces in the near-tip region show vortical flow behavior of the fluid that passes through the clearance region and exits at the downstream edge of the gap. In an effort to reduce clearance flow losses, the mini-shroud concept was proposed, which adds a fence to the pressure side of the blade at the blade tip. However, calculations performed on the GGOT geometry with the mini-shroud indicate that the mini-shroud has only a marginal effect on the tip clearance losses at

the design tip clearance. Additional calculations were performed at two and four times the design tip clearance, both with and without the mini-shroud, to assess the effect of tip clearance. The analysis of these calculations is in progress. Each calculation required approximately 10 Cray Y-MP hours on a single processor and 11 megawords of memory.

Significance

The ability to accurately predict the tip clearance flow and to perform parametric studies on changes in the geometry (both blade shape and tip clearance) is essential to the design of high-performance turbines.

Future Plans

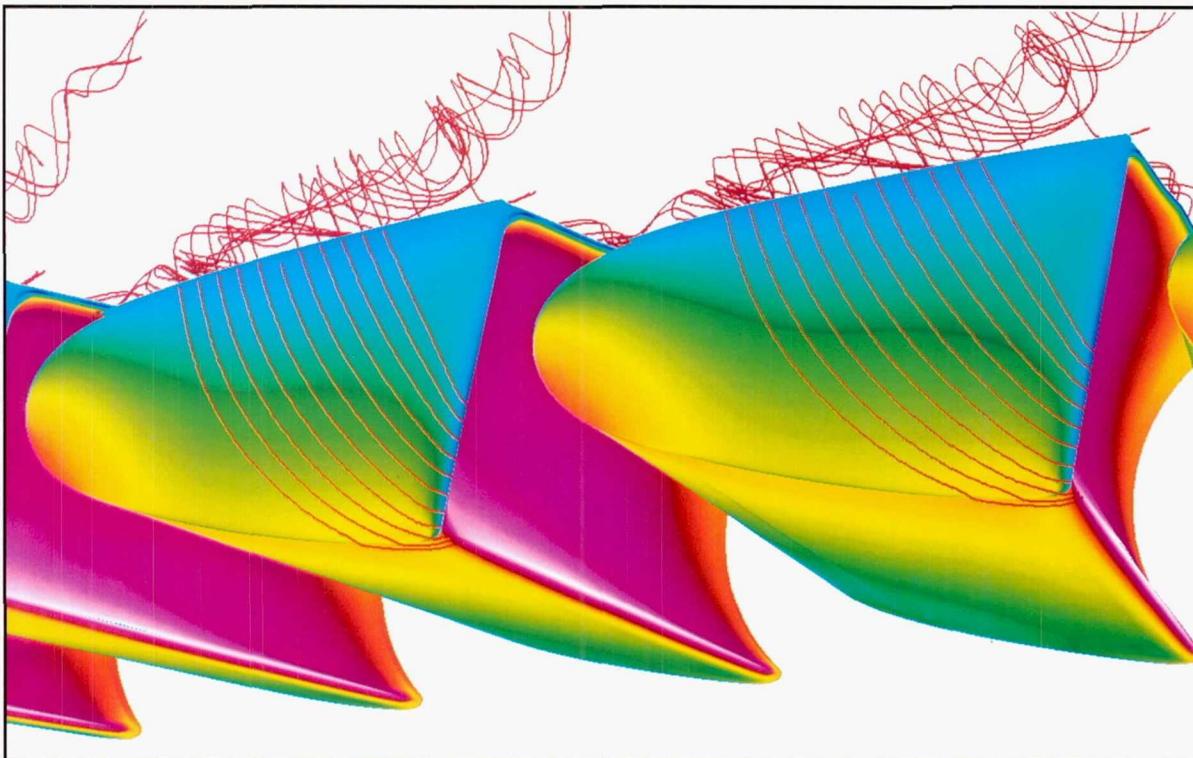
The present code will be applied to the study of aircraft engine compressor tip treatments.

Keywords

Rocket propulsion, Navier–Stokes analysis, Computational fluid dynamics

Publication

Chan, Y.-T.; and de Jong, F. J.: Navier–Stokes Analysis of an Oxidizer Turbine Blade with Tip Clearance with and without a Mini-Shroud. 11th Workshop for Computational Fluid Dynamics Applications in Rocket Propulsion, NASA CP-3221, Part 2, Apr. 1993, pp. 1,397–1,422.



Pressure contours and particle traces on the GGOT blade with the mini-shroud and at twice the design clearance.

Vortex Induced Mixing Behind Ramp Injectors

W. W. Follett, Principal Investigator

Co-investigators: J. V. Madison and S. Palaniswamy

Rockwell International, Rocketdyne Division/Rockwell International Science Center



Research Objective

To investigate the effects of geometry and aspect ratio of ramp injectors for high-speed vortex mixing through numerical modeling.

Approach

The unified solution algorithm (USA) was used to compute the flow fields of several axial ramp injector elements. The USA code uses the third-order accurate total-variation-diminishing (TVD) scheme in space, Roe's approximate Riemann solver for convective fluxes, and the scalar approximate factorization scheme for time advancement. Once the computational fluid dynamics (CFD) code is validated with the test data, it will be used to design an optimal ramp injector geometry. The velocities of the injection jet were matched to the free stream to minimize the effects of shear mixing and to isolate the vortex structure and its interaction with the fuel jet.

Accomplishment Description

Four sets of three-dimensional tip-to-tail solutions were obtained for simulating ramp injectors at an inlet Mach number of 2.07 with an axial injection jet of iodine seeded air at Mach 1.7. The geometries included a 10-degree swept ramp with 9.5-degree swept sidewalls and a base aspect ratio of 1.4, and a 10-degree straight sidewall ramp with base aspect ratios of 2.0, 1.0, and 0.71. All ramps had the same length and base height and were run with the same free-stream and injection conditions. Each calculation used a 3-zone grid with 820,000 cells and required approximately 32 megawords of memory and 12 Cray Y-MP hours. Solutions were run two ways—either laminar or as a Baldwin-Lomax turbulence model to determine the impact on the vortex development and persistence. All solutions showed reasonable agreement with the experimental data. The first figure shows the wall static pressure contours and the vortex/jet particle traces for the swept ramp configuration. The second figure shows the same quantities for the high-aspect-ratio straight ramp.

Significance

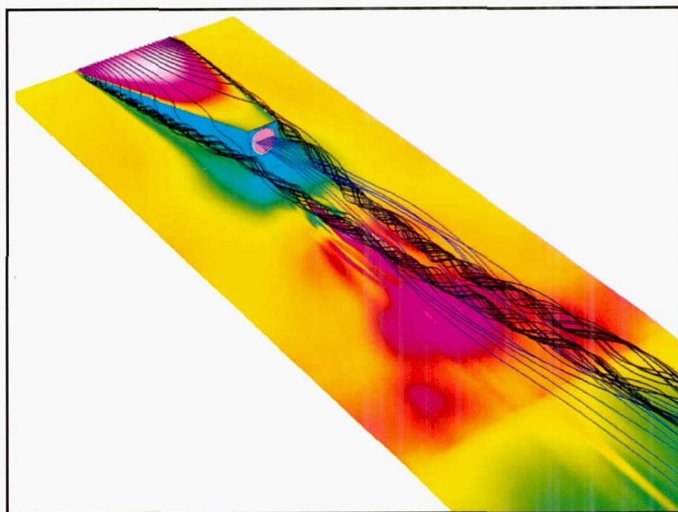
The solutions provide insight into the structure of complex vortical flow fields generated by ramp injectors, which will aid in developing an optimal configuration for high-speed fuel injectors. Validation of the methodology with experimental data was accomplished, and it justifies the extension to higher enthalpy flight conditions. Applying CFD to this class of problems is necessary because of the expense and difficulties associated with full-scale testing for high-Mach-number flows.

Future Plans

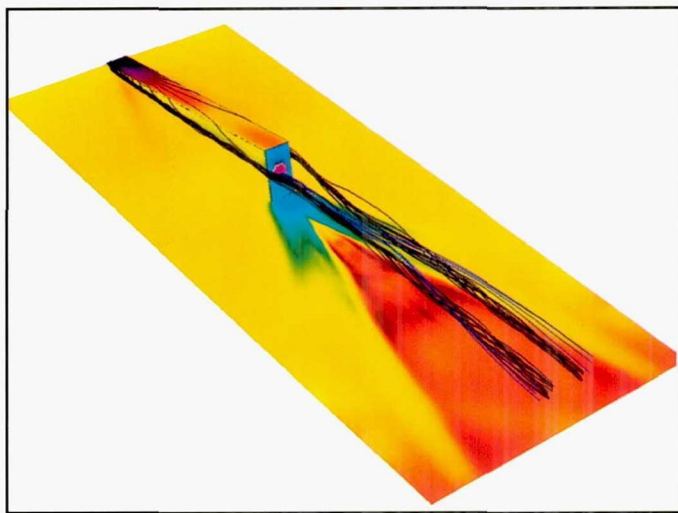
The effects of higher Mach number and higher enthalpy flows will be investigated. A more refined one-equation turbulence model will be implemented to determine the impact of physical modeling on vortex strength and persistence. More complex geometries will be simulated to study interference effects.

Keywords

Mixing, Numerical modeling



Particle traces show the vortex structure and jet interaction for the 10-degree swept ramp case. Wall static pressures vary from 22 psf (dark blue) to 1,150 psf (white).



Particle traces and wall static pressure contours for the high-aspect-ratio straight ramp injector. Wall static pressures vary from 22 psf (dark blue) to 1,150 psf (white).

Unsteady Turbomachinery Computations

Karen L. Gundy-Burlet, Principal Investigator
NASA Ames Research Center



Research Objective

To investigate unsteady rotor/stator interaction in multistage turbomachines.

Approach

The three-dimensional (3-D) Navier–Stokes codes STAGE-3 and Rotor-4 incorporate the most modern, high-order upwind-biased schemes for solving thin-layer Navier–Stokes equations. The schemes are set in an iterative implicit framework. The codes use a multizone grid with some zones moving relative to others. Information is transferred between the various zones using temporally and spatially accurate zonal boundary conditions.

Accomplishment Description

A fine-grid 3-D calculation of a 1.5 stage turbine was completed. Results from the code compare well with experimental data for time-averaged surface and cross-flow pressure distributions and time-averaged surface streamlines. The code requires 93 megawords of main memory for the 2.7 million point grid. This 1.5 stage turbine calculation required approximately 500 Cray C-90 hours for the time-averaged solution to converge. The figure shows time-averaged surface pressures overlaid with surface streamlines within the turbine.

Significance

Unsteady turbomachinery flow fields are extremely complex, especially in the latter stages of multistage turbomachines. Wake/wake and wake/airfoil interactions cause complex time-varying forces on the downstream airfoils. It is important to understand these interactions in order to design turbomachines that are light, compact, reliable, and efficient.

Future Plans

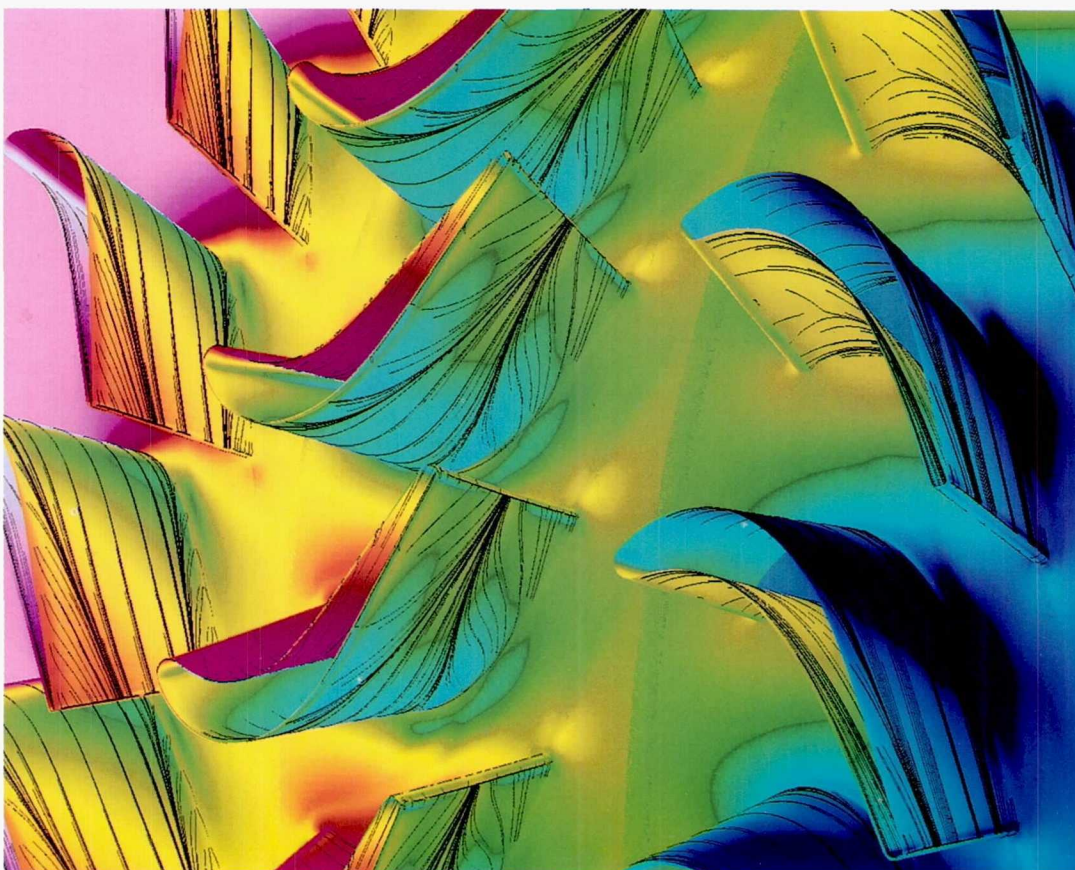
A fine-grid, 3-D computation of a 2.5 stage compressor is in progress. The results of the 2.5 stage compressor computation will be compared with experimental data from a 2.5 stage compressor. Future computations will include a 4.5 stage compressor geometry, a multistage/multi-airfoil turbine computation, and an investigation of the effects of 3-D hot streaks on the flow within the 1.5 stage turbine.

Keywords

Turbine, Multistage

Publication

Gundy-Burlet, K. L.; Rai, M. M.; and Madavan, N. K.: Unsteady Three-Dimensional Navier–Stokes Simulations of Multistage Turbomachinery Flows. AIAA Paper 93-1979, June 1993.



Time-averaged pressures and surface streamlines within a 1.5 stage turbine.

Unsteady Three-Dimensional Flow in a Transonic Compressor

Chunill Hah, Principal Investigator

Co-investigators: J. Loellbach, W. W. Copenhaver, and S. L. Puterbaugh

NASA Lewis Research Center/ICOMP/Wright Patterson Air Force Base



Research Objective

To numerically simulate the unsteady flow field inside a transonic, high-through-flow axial compressor stage, and to compare the computed results with experimental data.

Approach

The three-dimensional, unsteady Navier–Stokes equations are solved on structured grids using second-order accurate implicit time integration, third-order accurate upwind differencing for the inviscid fluxes, and second-order accurate centered differencing for the viscous fluxes. A two-equation turbulence model with a low-Reynolds-number modification is used for turbulence closure.

Accomplishment Description

The flow field inside a transonic, low-aspect-ratio compressor rotor was numerically analyzed by solving the unsteady, Reynolds-averaged Navier–Stokes equations. Previous experimental studies have indicated that some inherent flow unsteadiness exists near the shock and shock-boundary layer interaction areas even though the compressor rotor was tested as an isolated blade row. In order to study the origins of the unsteadiness, especially of the shock oscillations, an unsteady calculation of the

flow field as an isolated rotor was performed. Computed distributions of the time-averaged static pressure and the nondimensionalized pressure fluctuation parameter are shown near the shroud in the figures. The tip-clearance vortex with particle traces is shown in the first figure. These numerical results agree well with the unsteady pressure measurements. The unsteady results from the isolated rotor calculation will be compared with results from an unsteady rotor/stator stage calculation.

Significance

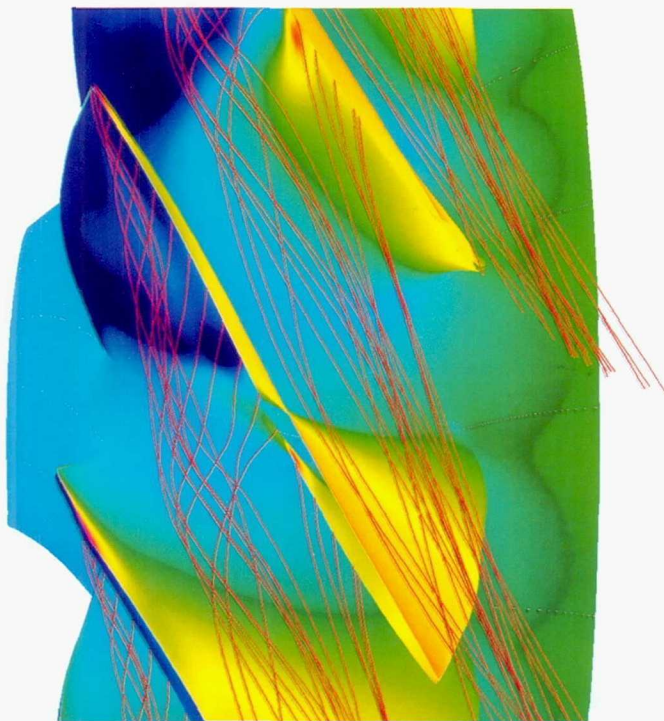
This work is a direct extension to unsteady flow analysis of an existing steady Navier–Stokes solver that has been tested and applied to a wide range of turbomachinery flows. Unsteady analysis is necessary for accurate flow-field prediction for closely coupled blade rows within a stage or between successive stages.

Future Plans

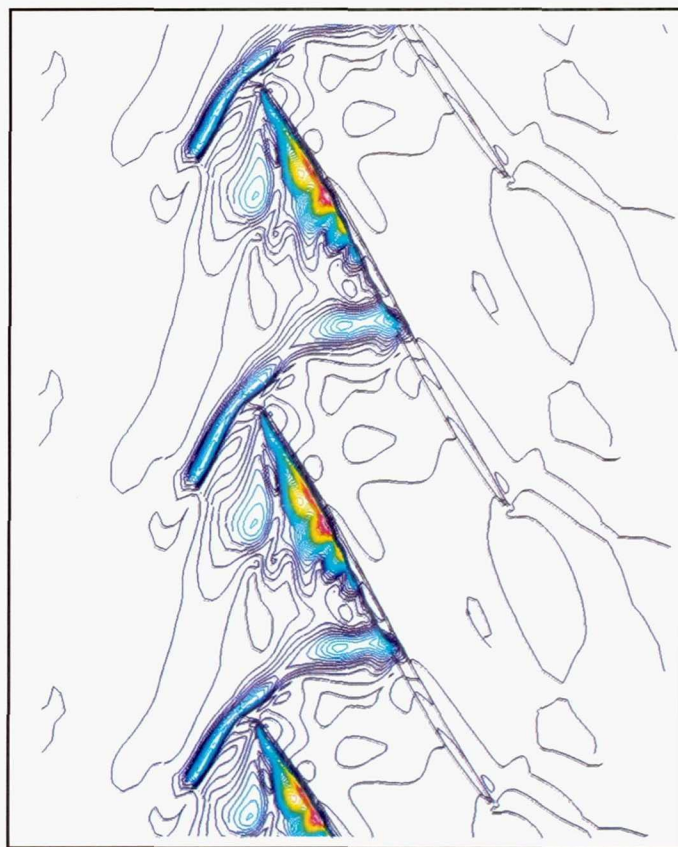
Efforts are under way to analyze the unsteady effects of inlet distortions and to perform parametric studies for design optimization.

Keywords

Navier–Stokes, Tip clearance



Contours of the time-averaged static pressure inside the tip gap.



Contours of the unsteady pressure fluctuation parameter inside the tip gap.

Transonic Core Compressor Rotor/Stator Interaction

Edward J. Hall, Principal Investigator

Co-investigators: Kurt F. Weber, K. V. Rao, and R. A. Delaney

Allison Engine Company



Research Objective

To assess the effect of rotor/stator interaction on the aerodynamic performance of aircraft engine axial compressors. Existing compressor data show a significant effect on performance of the unsteady interaction between rotors and stators in axial compressors. Substantial performance gains can be achieved by optimizing the spacing between adjacent blade rows.

Approach

The analytical tool utilized in this study was the advanced ducted propfan analysis code (ADPAC). ADPAC was developed for steady state and time-dependent flow-field simulation of advanced turbofan engines. The code employs a flexible, multi-blocked mesh discretization scheme. The block gridding technique permits coupling of complex multiple-region domains with common grid interfaces, and permits simultaneous coupling of solutions for adjacent, relatively rotating blade rows. The solution procedure employs a finite-volume numerical formulation and a Runge-Kutta time-marching procedure.

Accomplishment Description

Numerical solutions were obtained for the very high pressure ratio, two-stage axial compressor design advanced small turboshaft compressor (ASTC). Numerical solutions were obtained for individual blade rows operating independently, as well as time-averaged solutions employing the circumferential averaging concept. A time-dependent solution was generated for a realistic representation of the two-stage compressor. The original compressor blade row airfoil counts were slightly modified to permit a reduced geometric representation of the whole machine

(the unsteady problem can be reduced to one quarter of the entire wheel with circumferential periodicity). The unsteady solution requires modeling 4 blade passages of the first rotor, 9 blade passages of the first stator, 8 blade passages of the modified second rotor, and 15 blade passages of the second stator. The final mesh contained over 2,000,000 points and required approximately 400 Cray C-90 hours and 125 megawords of central memory to reach a quasi-time periodic state. An instantaneous snapshot of the computed velocity field from the time-dependent solution for the advanced two-stage compressor is shown in the figure. The interaction between the bow-shock system in the second rotor and the trailing edge of the first stator is evident, and comparisons of the time-dependent prediction and the time-averaged predictions for compressor performance show substantial differences.

Significance

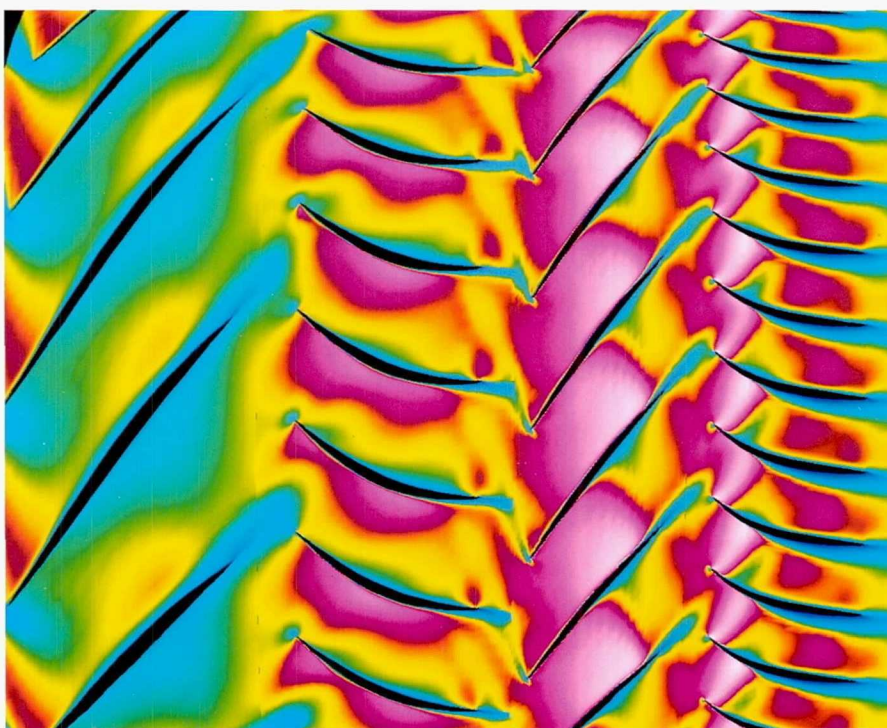
Optimization of the blade row spacing in advanced highly loaded axial compressors is essential for minimizing performance degradation associated with rotor/stator aerodynamic interaction. This research is relevant to aerodynamic aspects of the Integrated High Performance Turbine Engine Technology goal of doubling the thrust-to-weight ratio of fighter engines by the year 2000.

Future Plans

Detailed comparisons of the time-dependent predictions with measured test data for the ASTC compressor will be performed.

Keywords

Compressor, Interaction



Instantaneous predicted velocity contours at midspan for the ASTC compressor.

Advanced Ducted Propfan Analysis Code Certification

Edward J. Hall, Principal Investigator
Co-investigator: G. Scott McNulty
Allison Engine Company



Research Objective

To certify a three-dimensional (3-D) Navier–Stokes code for turbomachinery flow computations intended to form the basis for an aerothermodynamic/structural optimization program for turbomachinery airfoils planned by the Multidisciplinary Analysis and Design Industrial Consortium. Certification is required to establish an accurate, robust, user-friendly solver that can be used in an optimization environment. Particular emphasis was placed on accurate prediction of airfoil surface aerothermodynamics and overall aerodynamic performance.

Approach

The 3-D Navier–Stokes advanced ducted propfan analysis code (ADPAC) was selected for the investigation because it is applicable to a wide variety of turbomachinery flow/heat transfer problems. Certification of the code was performed by obtaining detailed comparisons of numerical predictions with experimental data for two test cases. A transonic fan rotor, NASA Rotor 67, was tested to provide data for code validation. The rotor has 22 low-aspect-ratio blades, a design relative tip Mach number of 1.38, and a design mass flow rate of 73.3 pounds per second. Laser anemometer measurements taken within the rotor provide excellent definition of the passage shock structure at the peak efficiency and near-stall operating points. To assess the ADPAC's ability to predict turbine airfoil heat transfer, the C3X turbine cascade was used. The C3X airfoil, representative of a vane section from a transonic turbine vane row, was tested in a rectilinear cascade. Both aerodynamic and heat transfer data were acquired for a range of expansion ratios, Reynolds numbers, and wall-to-gas temperature ratios. The computations were performed on grids that were fine enough to yield grid independent heat transfer solutions.

Accomplishment Description

An array of numerical predictions was obtained for the NASA Rotor 67 and C3X turbine vane cascade. The rotor calculations were performed on H-type and body-centered O-type mesh systems. Details of the tip clearance flow were computed using a

degenerate O-type mesh that discretized the clearance flow region. Mesh-independent heat transfer predictions were defined for the C3X turbine cascade by comparing solutions on successively finer meshes. Essentially mesh independent heat transfer predictions could be achieved when the near-surface mesh spacing resulted in a turbulent velocity profile y^+ value of 3 or less. Typical calculations required 1 Cray C-90 hour and 16 megawords of central memory.

Significance

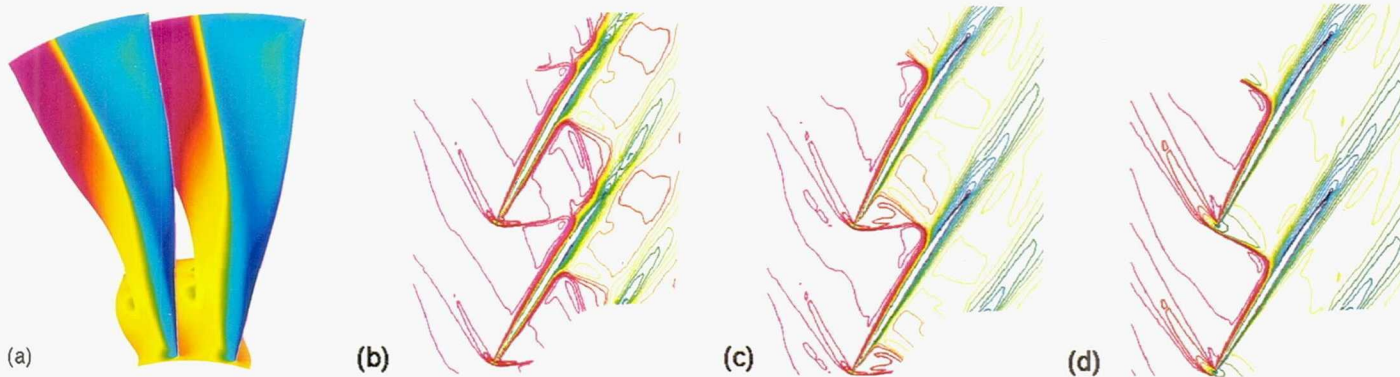
The use of modern aerothermodynamic analytical techniques requires extensive validation to achieve the levels of confidence necessary to base decisions related to design trade-off studies on numerical simulations. This program is the first step to incorporate an advanced aerothermodynamic analytical tool into a multidisciplinary optimization design program for turbomachinery airfoils. The program is relevant to the Integrated High Performance Turbine Engine Technology goal of doubling the thrust-to-weight ratio of fighter engines by the year 2000, and is applicable to the High Performance Computing and Communication Program initiative.

Future Plans

Additional compressor and turbine validation tests will be performed.

Keywords

Advanced ducted propfan analysis code, Optimization, Fan, Turbine



Predicted results for NASA Rotor 67; (a) 3-D surface pressure contours at near stall, (b) blade-to-blade Mach number contours for choke, (c) peak efficiency, and (d) near stall at 90 percent span.

Fan Rotor/Endwall Treatment Interaction

Edward J. Hall, Principal Investigator

Co-investigators: Andrew J. Crook and Kathy P. Nardini

Allison Engine Company



Research Objective

To determine the effects of endwall treatments (slots, grooves, embedded vanes) on the aerodynamic performance of aircraft turbofan engine fan rotors. Existing fan rotor performance data indicate a significant improvement in fan stall margin with end-wall treatment compared to a similar untreated geometry.

Advanced Navier–Stokes analysis techniques can aid in the understanding of the complex time-dependent rotor/endwall treatment aerodynamic interactions that determine the overall performance gains associated with endwall treatments.

Approach

The analytical tool utilized during this study was the advanced ducted propfan analysis code (ADPAC). ADPAC was developed for steady state and time-dependent flow-field simulation of advanced high-bypass turbofan engines. The code employs a flexible, multiblocked mesh discretization scheme. The block gridding technique permits coupling of complex, multiple-region, relatively rotating domains with common grid interfaces. The solution procedure employs a finite-volume numerical formulation and a Runge–Kutta time-marching procedure.

Accomplishment Description

Numerical solutions were obtained for a modern turbofan engine fan rotor design with and without endwall treatments. Fan pressure ratio and efficiency versus mass flow operating characteristics were predicted at the design speed to determine the baseline rotor stall characteristics. Similar results were generated for various endwall treatments to determine the effectiveness of the treatments on enhancing stall margin. Several solutions were obtained using a time-averaged fan rotor/endwall treatment cou-

pling technique as well as a complete time-dependent solution of the rotor/treatment aerodynamic interaction problem. Time-dependent solutions for the rotor/treatment interaction analysis typically required 100 Cray C-90 hours and 64 megawords of central memory.

Significance

Effective application of endwall treatments permits high levels of blade aerodynamic loading while maintaining adequate stall margin safety. This research is relevant to aerodynamic aspects of the Integrated High Performance Turbine Engine Technology goal of doubling the thrust-to-weight ratio of fighter engines by the year 2000, and has significant applications for reducing acoustic signatures of advanced subsonic transport engines.

Future Plans

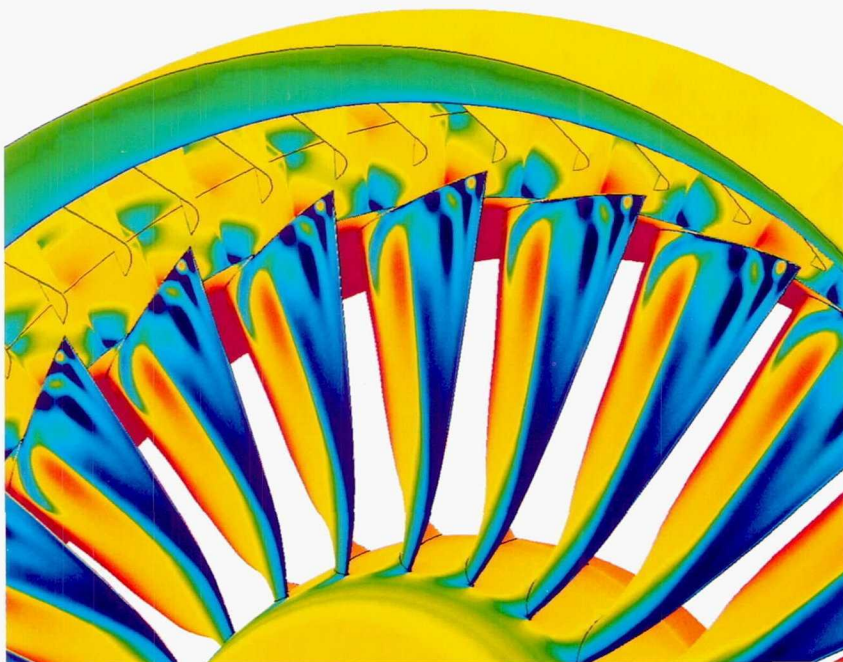
Additional calculations are under way to examine the effectiveness of endwall treatments for fan rotors operating in the presence of inlet aerodynamic distortion. Inlet distortion can drastically reduce engine stall margin. Endwall treatments may ultimately be designed to accommodate off-design rather than design-flow conditions.

Keywords

Fan, Casing treatment, Stall

Publication

Hall, E.; Crook, A.; and Delaney, R.: Aerodynamic Analysis of Compressor Casing Treatment with a 3-D Navier–Stokes Solver. AIAA Paper 94-2796, June 1994.



Instantaneous surface static pressure contours for rotor/endwall treatment aerodynamic interaction analysis.

Three-Dimensional Steady and Unsteady Turbulent Flows in Turbomachines

Budugur Lakshminarayana, Principal Investigator

Co-investigators: S. Fan, J-F. Gallardo, Y-H. Ho, J. Luo, and W. S. Yu
Pennsylvania State University



Research Objective

To develop advanced turbulence models and efficient numerical techniques for the prediction of complex steady and unsteady turbulent and thermal fields in turbomachinery applications.

Approach

Three-dimensional (3-D) time-marching and pressure-based Navier–Stokes codes are used to predict steady and unsteady flow and heat transfer fields in turbomachines. In the pressure-based technique, a predictor-corrector type algorithm is applied to the governing equations to ensure the time accuracy. The time-marching technique incorporates 3-D steady and unsteady nonreflecting boundary conditions based on characteristics theory. A variety of turbulence models have been incorporated in these codes to capture complex turbulent flow features such as the effect of rotation, curvature and anisotropy, and unsteady effects.

Accomplishment Description

The codes were used to predict a variety of turbomachinery flow fields, providing validation of the turbulence models and numerical techniques. A subsonic cascade flow subject to vortical incoming waves was computed to demonstrate the effectiveness of the unsteady nonreflective boundary conditions at the inlet and the outlet of the flow field. A typical unsteady Euler solution requires about 1 Cray Y-MP hour and nearly 3 megawords of memory. The pressure-based method was used to investigate the structure of secondary flows in a turbine rotor cascade. The development of secondary flow is captured accurately, including blade-to-blade variation of all three components, pitch and yaw angles, and losses and blade static pressures. Each flow computation required approximately 8 Cray Y-MP hours and 28 megawords of memory. The turbulent flow in a strongly curved turn-around duct has been computed using various turbulence models and the results were compared with experimental data. The Reynolds stress model (RSM) and algebraic Reynolds stress model (ARSM) successfully captured the convex curvature effects and the large anisotropy of the turbulence through the bend. Significant improvement was obtained with the $k-\epsilon$, ARSM, and RSM models with a modified dissipation equation. The computation required about 2 Cray Y-MP hours and 4 megawords of memory.

Significance

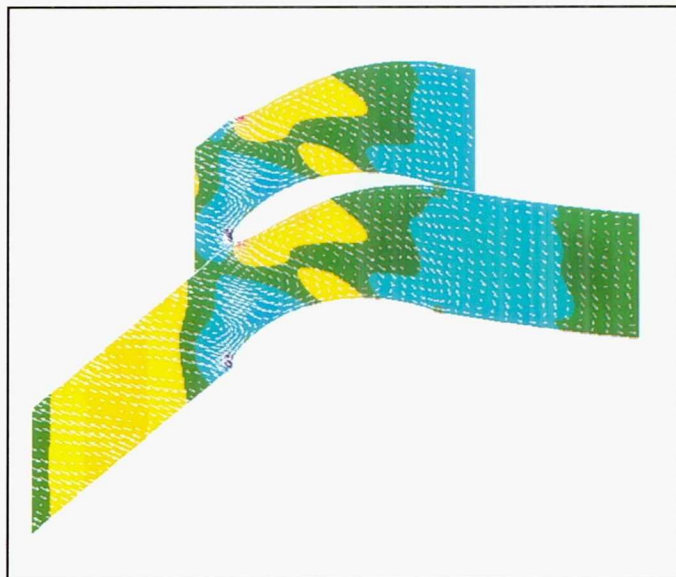
The ability to simulate the unsteady viscous flow inside the blade passages is important in understanding the rotor/stator interaction effects in turbomachinery. Improved understanding of the complex flow field inside the turbomachinery leads to more efficient turbomachinery design.

Future Plans

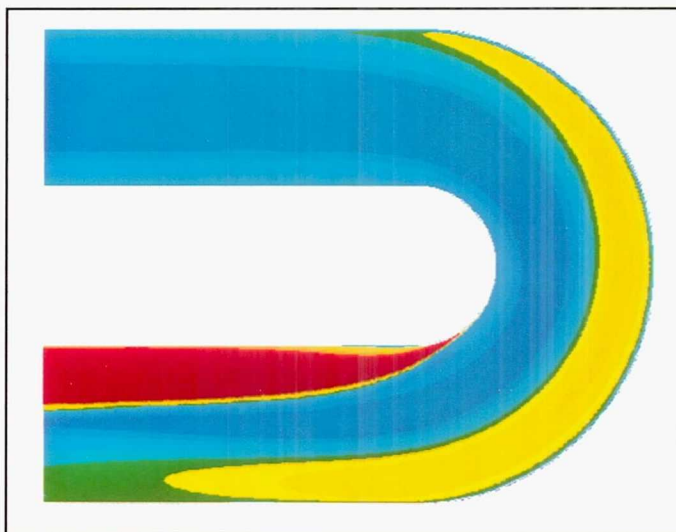
Three-dimensional time-accurate predictions of unsteady flow caused by rotor/stator interaction are being investigated. The emphasis is to understand the effects of upstream rotor wakes, secondary flow, and tip leakage flow on the blade row.

Keywords

Turbomachines, Turbulent flow, Thermal fields



Unsteady pressure and velocity fields caused by wake/blade interaction.



Turbulent intensity distribution in a 180-degree duct.

Computational Propulsion Applications

C. L. Merkle, Principal Investigator

Co-investigators: S. Venkateswaran, J-Z. Feng, H-H. Tsuei, and J. M. Grenda
Pennsylvania State University



Research Objective

To enhance physical understanding in three areas of propulsion application—film-cooled chemical thrusters for auxiliary propulsion, super-critical coolant channel flow fields, and combustion instability in liquid rocket engines.

Approach

All three problems involve solutions of the Navier–Stokes equations coupled to additional physics in two and three dimensions. The chemical thruster analysis involves detailed hydrogen/oxygen chemistry along with three-dimensional (3-D) and unsteady effects in the reacting shear layer adjacent to the thruster walls. The combustion instability problem is 3-D, time-dependent, and involves two-phase effects. A Lagrangian droplet-tracking model is coupled to the Eulerian gas phase. The coolant channel analysis is also 3-D and involves high-speed flow of super-critical hydrogen.

Accomplishment Description

Several representative calculations for the three problems were performed. For the chemical thruster problem, a series of unsteady reacting computations were completed for the wall-bounded shear layers and full-engine geometry. Parametric trends of the effects of molecular weight and wall proximity have been established (see figures). Typical memory requirements for the calculations (for 15 periods of oscillation) are 12 megawords and about 40 Cray-2 hours. For the combustion instability problem, 3-D response to incipient instability and bombs were simulated including the effects of droplet atomization and vaporization. For the coolant channel analysis, heat transfer and pressure drop have been characterized at several representative Reynolds numbers. Calculations typically required about 50 Cray-2 hours and 64 megawords of memory.

Significance

In the auxiliary chemical thruster engines, more than 50 percent of the fuel is used for wall-film cooling. Computations provide insight into fuel-film integrity and combustion performance of the engines. The combustion instability results demonstrated that droplet vaporization is a likely mechanism for triggering unstable pressure response in liquid rocket engines.

Future Plans

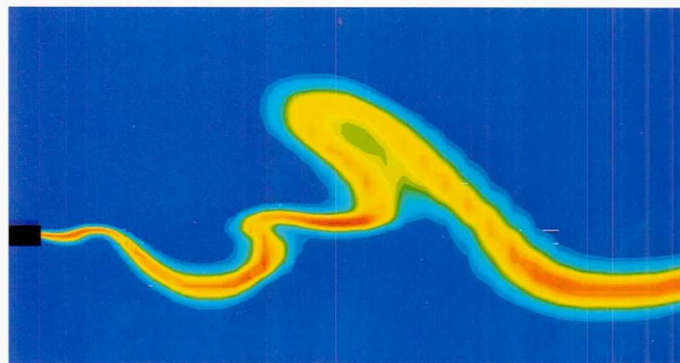
Computations of 3-D chemical-thruster geometry including turbulence and finite rate chemistry are being performed. Unsteady reacting computations with large-eddy simulation models for subgrid turbulence will also be performed. For the coolant channel analysis, bifurcated channels and coupled heat transfer in solid walls and fluid dynamics are being studied.

Keywords

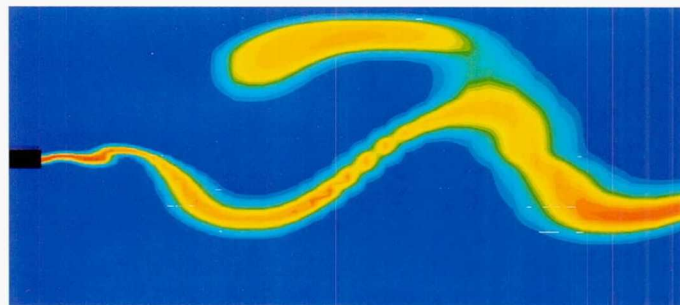
Combustion, Instability

Publications

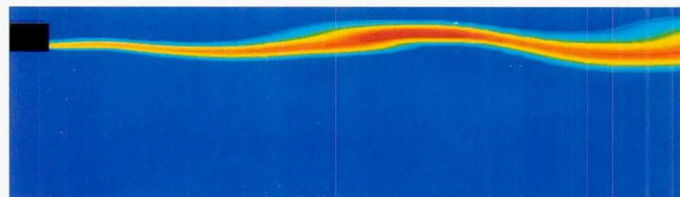
1. Grenda, J. M.; Venkateswaran, S.; and Merkle, C. L.: Analysis of Liquid Rocket Instabilities Using a Computational Testbed. Presented at the International Symposium on Combustion, Irvine, Calif., July 25–31, 1994.
2. Tsuei, H-H.; and Merkle, C. L.: CFD Analyses of Combustor, Nozzle and Plume Flowfields. AIAA Paper 94-0553, Jan. 1994.
3. Yagley, J. A.; Feng, J.; and Merkle, C. L.: CFD Analyses of Coolant Channel Flowfields. AIAA Paper 93-1830, June 1993.



(a)



(b)



(c)

Instantaneous radical contours in unsteady reacting (hydrogen/oxygen) shear layer with effects of wall proximity. Distance of wall from shear layer: (a) 2 cm, (b) 1 cm, and (c) 1 mm.

Complex Three-Dimensional Flows in the Advanced Solid Rocket Motor

Edward J. Reske, Principal Investigator

Co-investigators: Lee A. Kania and James W. Zuercher

NASA Marshall Space Flight Center



Research Objective

To characterize the internal flow environment and internal nozzle aerodynamics for the advanced solid rocket motor (ASRM).

Three-dimensional (3-D) computational fluid dynamic (CFD) models are tools to address key design issues.

Approach

A 3-D Navier–Stokes flow solver was used to analyze complex flows in the aft segment and nozzle of the ASRM. Input on physical reference quantities and boundary conditions was obtained from the Joint Army–Navy–NASA–Air Force Solid Performance Prediction Ballistics program.

Accomplishment Description

Gimballing a submerged nozzle in a solid rocket motor produces a pressure differential and subsequent circumferential flow in the aft-dome region. The hot gases entering, swirling in, and then exiting the aft-dome region can produce severe environments for motor components. A fine-grid CFD analysis has been conducted for the ASRM aft segment with an 8-degree gimbaled nozzle to assess the thermal environment and heat transfer to components in the ASRM, such as the flex seal, case-to-nozzle joint, and casing insulation. The CELMINT Navier–Stokes flow solving code has been used to model the flow and thermal environment on a numerical grid of 311 axial points \times 127 radial points \times 37 circumferential planes (1.46 meter grid points). Such a large grid was needed because the computational domain has a length scale of 600 inches and diameter scales of 54.5–130.0 inches, whereas the smallest grid spacing was required to be a thou-

sandth of an inch to enable sufficient boundary layer resolution to facilitate the calculation of heat transfer (despite the fact that wall functions were being used). This calculation required 125 Cray C-90 hours and 64 megawords of memory. A code validation effort has been performed to benchmark the CELMINT code for use in modeling the internal aerodynamics of submerged nozzles in solid rocket motors by comparing it with the 8 percent ASRM cold flow model. Flow in the cold flow model was simulated by running CELMINT on a numerical grid consisting of 160 axial points \times 85 radial points \times 37 circumferential planes. Good agreement was obtained for the static wall pressures predicted by CELMINT and the experimental values. The model required 25 Cray C-90 hours and 24 megawords of memory.

Significance

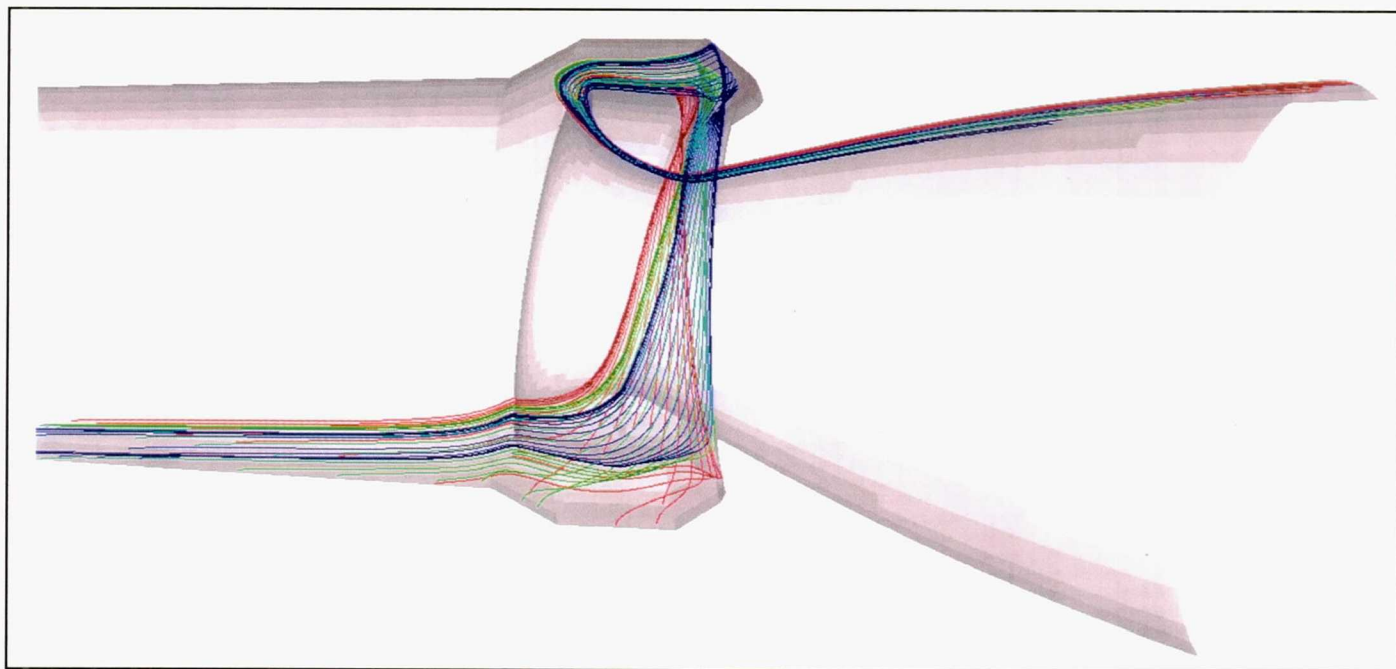
The results from these models have provided useful tools and results needed for designing the ASRM. In particular, these models allow designers to address key issues for the ASRM, such as the internal environment and nozzle aerodynamics.

Future Plans

The results of the CFD analyses performed over the past three years will be documented and submitted for publication in professional journals. The results from this work will provide a basis for the solid rocket motor community to address key design issues for future solid rocket motor projects.

Keywords

Computational fluid dynamics, Nozzle aerodynamics



Flow visualization for the ASRM fine-grid model showing circumferential flow in the aft-dome region when the nozzle is gimbaled 8 degrees. Mach number = 0.224, $\alpha = 0.0$, Reynolds number = 4.42×10^6 .

High-Speed Inlet Design and Analysis

William C. Rose, Principal Investigator
Rose Engineering and Research, Inc.



Research Objective

To examine the flow in a subsonic diffuser located downstream of a high-speed inlet.

Approach

The three-dimensional (3-D) flow code OVERFLOW is used to obtain the solution through the supersonic inlet and then determine the flow characteristics (with the attendant thick boundary layers) within an S-duct diffuser as the flow transitions from a rectangular to a circular shape.

Accomplishment Description

The OVERFLOW code was used to solve the flow within several prospective diffusers. The general shape of a diffuser is shown in the first figure. The diffuser area ratio and the amount of S-duct offset were varied to achieve a reasonable diffusion rate and flow quality measurement at the outlet of the subsonic diffuser. The

second figure shows the Mach number contours from a 3-D solution for half of the symmetrical inlet.

Significance

This study shows the technical feasibility of using the OVERFLOW code to calculate subsonic diffuser flows very rapidly. Each solution takes approximately 15 minutes. The rapid solution turnaround time allows the code to be used in an iterative, parametric manner to arrive at a manually optimized design in a very short period of time.

Future Plans

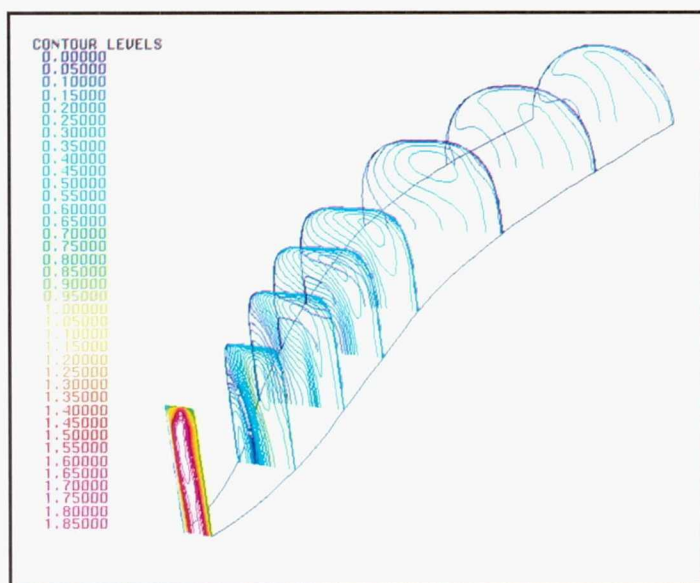
The study is temporarily suspended pending funding for fiscal year 1995.

Keyword

Subsonic diffuser flow



View of the surface geometry for the transitioning, S-duct subsonic diffuser.



Mach number contours obtained with the OVERFLOW code in a representative diffuser. Mach number = 5.020, $\alpha = 0.0$, Reynolds number = 1.85×10^6 .

Three-Dimensional Mixing Flows in High-Speed Combustors

Balu Sekar, Principal Investigator
Wright Patterson Air Force Base



Research Objective

To apply the state-of-the-art three-dimensional (3-D) computer codes to predict the flow development and performance of the high-speed propulsion components, such as supersonic combustors and nozzles.

Approach

The 3-D, time-dependent, compressible Navier-Stokes equations were solved with algebraic turbulence models and with fully coupled chemistry for various reaction mechanisms to compute the mixing and diffusion phenomena that occur in a typical scramjet combustor.

Accomplishment Description

The GASP code was used to simulate the parallel injection of air from a swept-ramp base into a Mach 2 free stream of air. GASP has the capability of computing complicated flows by a general multiblock (zonal) feature that allows piecing the individual blocks of grids so that they align. The ease of applying various boundary conditions to complex 3-D arbitrary internal/external configurations and the implementation of efficient numerical algorithms make this code particularly attractive and suitable for high-speed combustor modeling. Numerical studies carried out for the swept-ramp combustor configuration were used to determine the key performance parameters, such as penetration and mixing. The figures show the computed pressure, injected air mass fraction distribution inside the combustor, and the axial decay distribution of the injectant at the symmetric plane. Flow convergence for this configuration of 6 zones with 656,850 grid points was obtained with 16 Cray C-90 hours on a single processor and 6 megawords of memory. The computed flow compares moderately well with the experiments.

Significance

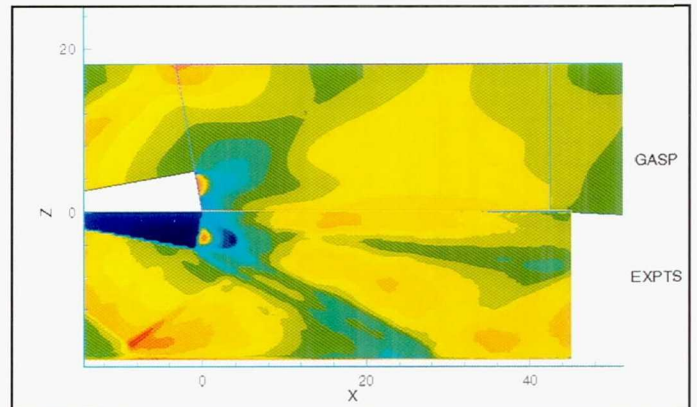
Numerical modeling of the complex 3-D flows is necessary to understand the critical issues associated with fuel mixing. The validated numerical model aids in pre- and posttest analysis and gives an in-depth analysis of the complexities of these flows. These studies are essential tools for the improved design and development of supersonic combustors with increased mixing.

Future Plans

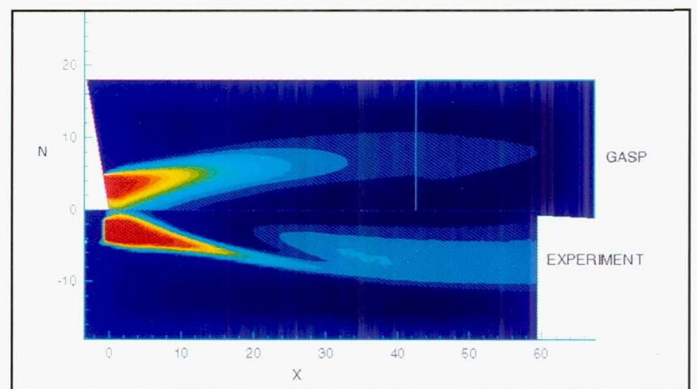
Research is under way to determine the relative performance, improvements of different combustors, and fuel injector conceptual designs applicable to scramjet propulsion. This will enhance the operating characteristics of the propulsion systems because of increased mixing and combustion and the reduction in the net flow loss.

Keywords

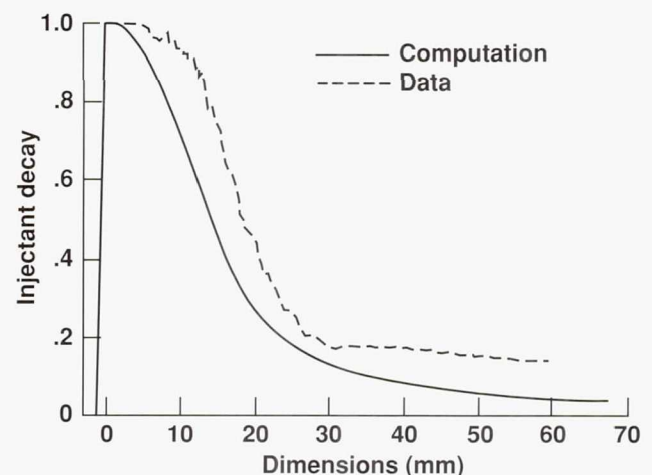
High-speed propulsion, Supersonic combustion, Mixing, Diffusion



Computed and measured pressure contours in the symmetry plane.



Computed and measured injectant mass fraction in the symmetry plane.



Computed injectant decay in the symmetry plane.

Flow in Turbine-Blade Cooling Passages

Tom I-P. Shih, Principal Investigator

Co-investigators: Mark A. Stephens and Kestutis C. Civinskas
Carnegie Mellon University/NASA Lewis Research Center



Research Objective

To develop, evaluate, and apply advanced computational tools to study three-dimensional (3-D) flow and heat transfer inside cooling passages of turbine blades.

Approach

When 3-D flow fields inside geometrically complex turbine-blade cooling passages are computed, the hours involved in the grid generation process account for most of the time required to obtain a solution. To reduce grid generation time, overlapping structured (Chimera) grids were employed. Solutions to the compressible Navier-Stokes equations on the Chimera grids were obtained using a modified version of the OVERFLOW code.

Accomplishment Description

The OVERFLOW code was adapted to compute flow fields in cooling passages of turbine blades that have steady state solutions with respect to a rotating frame of reference. Solutions for flow and heat transfer were obtained for several cooling passages including a branched duct where experimental data are available for code validation and a cooling passage inside a rotating radial turbine blade. These computations elucidate physics as a function of design and operating parameters. The 3-D solution for the branched duct with 1.6 million grid points required 28 megawords of memory and 10 Cray C-90 hours. The 3-D solution for the cooling passage inside the rotating radial turbine blade with 0.7 million grid points required 16 megawords of memory and 5 Cray C-90 hours.

Significance

Currently, cooling passages are designed by using either quasi-one-dimensional analyses or multidimensional analyses with simplified geometries. This study produced a code that allows the correct geometry to be analyzed in a timely and cost-effective manner. Also, application of the code produced better understanding of flow physics.

Future Plans

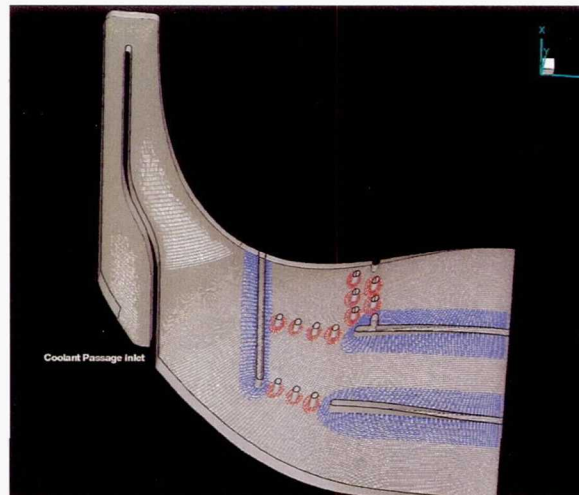
The accuracy of predictions will be improved by using turbulence models that account for rotation and streamline curvature. Physics of flow and heat transfer inside coolant passages as a function of design and operating parameters will be studied.

Keywords

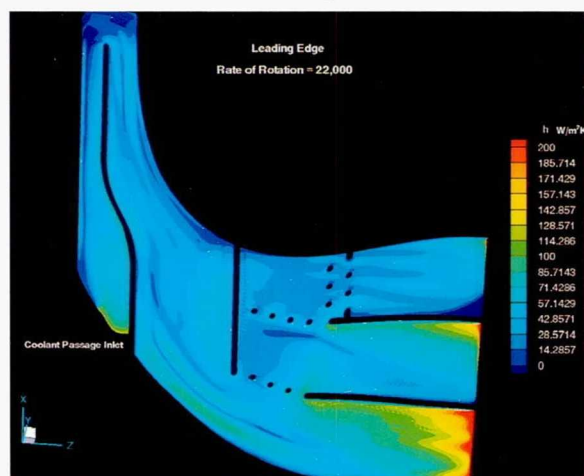
Internal blade cooling, Heat transfer

Publication

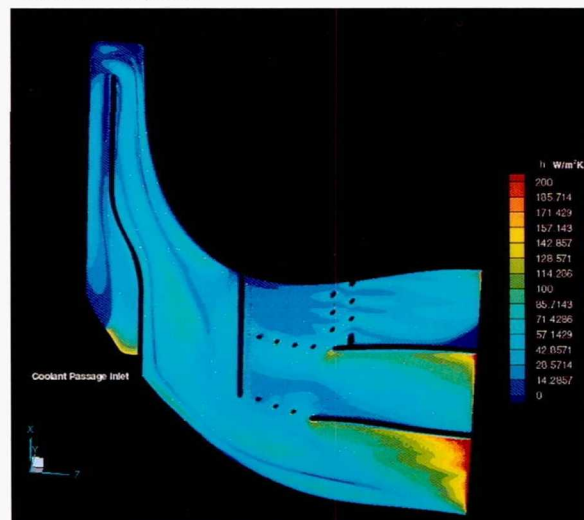
Stephens, M. A.; Rimlinger, M. J.; Shih, T. I-P.; and Civinskas, K. C.: Chimera Grids in the Simulation of Three-Dimensional Flowfields in Turbine-Blade-Coolant Passages. AIAA Paper 93-2559, June 1993.



One view of the 3-D Chimera grid.



Heat transfer coefficient on a leading surface. Rate of rotation = 22,000.



Heat transfer coefficient on a trailing surface. Rate of rotation = 22,000.

Analysis of Nacelle/Pylon/Wing Installations

Arvin Shmilovich, Principal Investigator

Co-investigator: Lie-Mine Gea

McDonnell Douglas Aerospace



Research Objective

To validate the OVERFLOW/Chimera code for the transonic analysis of multicomponent wing/fuselage/nacelle/pylon/winglet configurations.

Approach

A major difficulty in using computational methods for the integration of new engine technology on advanced wings is solving the flow problem in regions of complex geometrical shapes. Combined with the requirement to achieve proper scales of discretization, it is desirable to generate a set of structured grids with each grid adequate for the flow discretization about an individual component. In the Chimera approach the analysis is performed independently on each component grid and it allows for proper interaction within the regions of overlap. OVERFLOW solves the time-averaged Navier-Stokes equations using an implicit approximate factorization scheme.

Accomplishment Description

Several contemporary and advanced wing/fuselage/nacelle/pylon configurations were used to calibrate OVERFLOW and the Chimera approach. Strategies for generating the individual component grids and prescribing the overset regions were established to ensure proper communication among the individual subgrids.

For all configurations analyzed, the OVERFLOW/Chimera results were in excellent agreement with test data.

Significance

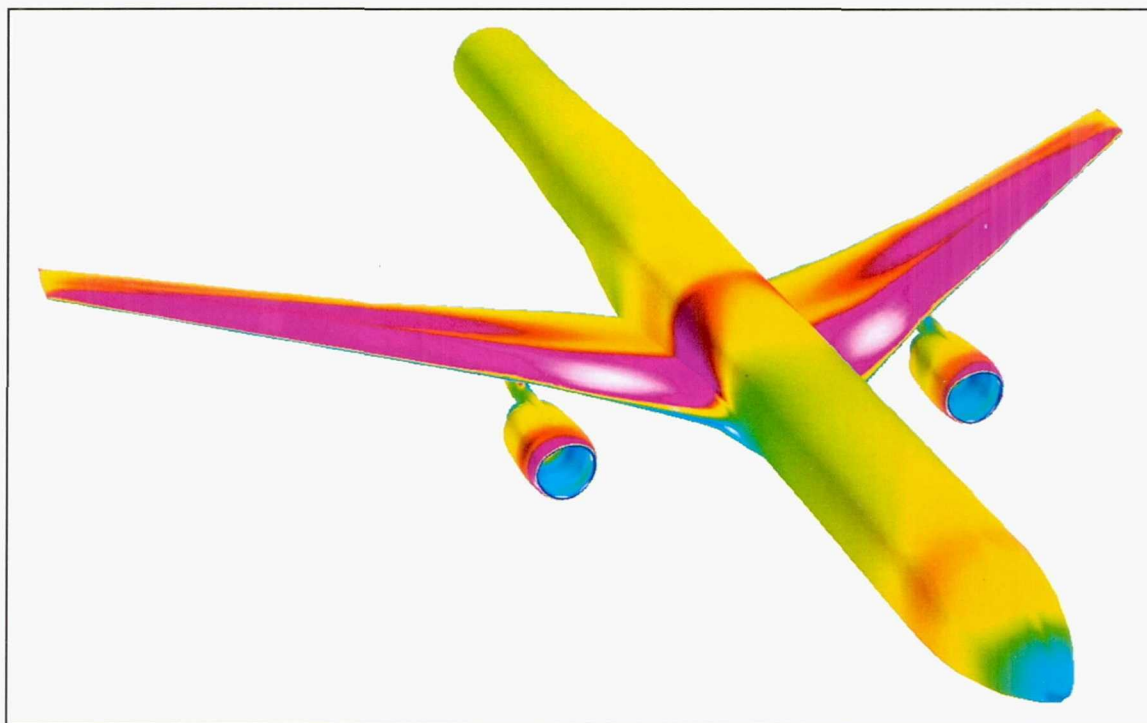
Considerations of both noise and propulsive efficiency have enhanced the attractiveness of high-bypass-ratio engines. This trend, coupled with the accompanying requirements toward higher cruise speeds, is making the task of efficiently integrating the advanced engines with modern wings very complex. OVERFLOW can analyze these flow situations and its Chimera implementation offers great geometric flexibility. This study demonstrates the ability of the code to predict the impact of nacelle/pylon installation on the wing flow development. OVERFLOW predictive capabilities for wing/winglet installation analyses were also established.

Future Plans

Further studies of the advanced wing installation effects for engines of very-high-bypass ratio (up to 12) will be completed using OVERFLOW to establish the range of applicability.

Keywords

Overset grids, Engine integration



Velocity contours for a complex advanced wing/fuselage/nacelle/pylon configuration at transonic conditions; blue = low velocity and white = high velocity.

Jets-in-Cross-Flow Mixing

Clifford E. Smith, Principal Investigator

Co-investigators: Daniel B. Bain and James D. Holdeman

CFD Research Corporation/NASA Lewis Research Center



Research Objective

To identify improved mixing schemes for rich burn/quick mix/lean burn (RQL) combustors applicable to advanced supersonic aircraft engines, and to assess the effects of design parameters on mixing effectiveness and emission reduction.

Approach

Numerical parametric studies were performed to assess the effect of varying key design parameters. The computational tool used was a three-dimensional Navier–Stokes flow solver (CFD-ACE) designed to analyze turbulent reacting flows in complex geometries. The computational results were examined using the interactive software visualization package, CFD-VIEW.

Accomplishment Description

The CFD-ACE code was used in analyzing over 30 parametric mixing simulations. The analysis was performed to identify the effect of orifice aspect ratio and jet mass flow ratio on jet mixing in rectangular geometries. The geometry modeled consisted of a rectangular duct with inline rows of jets on the top and bottom walls. The computations were performed assuming isothermal and reacting flow conditions. The numerical calculations in this study used grids varying in size from 50,000 to 100,000 nodes. An average parametric case took 2–4 Cray C-90 hours and 8–12 megawords of memory.

Significance

The computations show that the slot aspect ratio had little effect on the jet penetration and overall mixing. Circles and equivalent area slots (e.g., squares and 4:1 slots) were shown to have similar mixing characteristics. The jet wake recirculation region increased in size as the slot aspect ratio was reduced. Jet mass flow ratio was shown to significantly affect jet penetration; the design correlation parameter for optimum mixing (orifice spacing-to-duct height ratio \times the square root of the jet-to-cross-flow momentum flux ratio) increased by a factor of two as the jet-to-cross-flow mass flow ratio increased from 0.5 to 2.0. These results were used to design advanced RQL combustors.

Future Plans

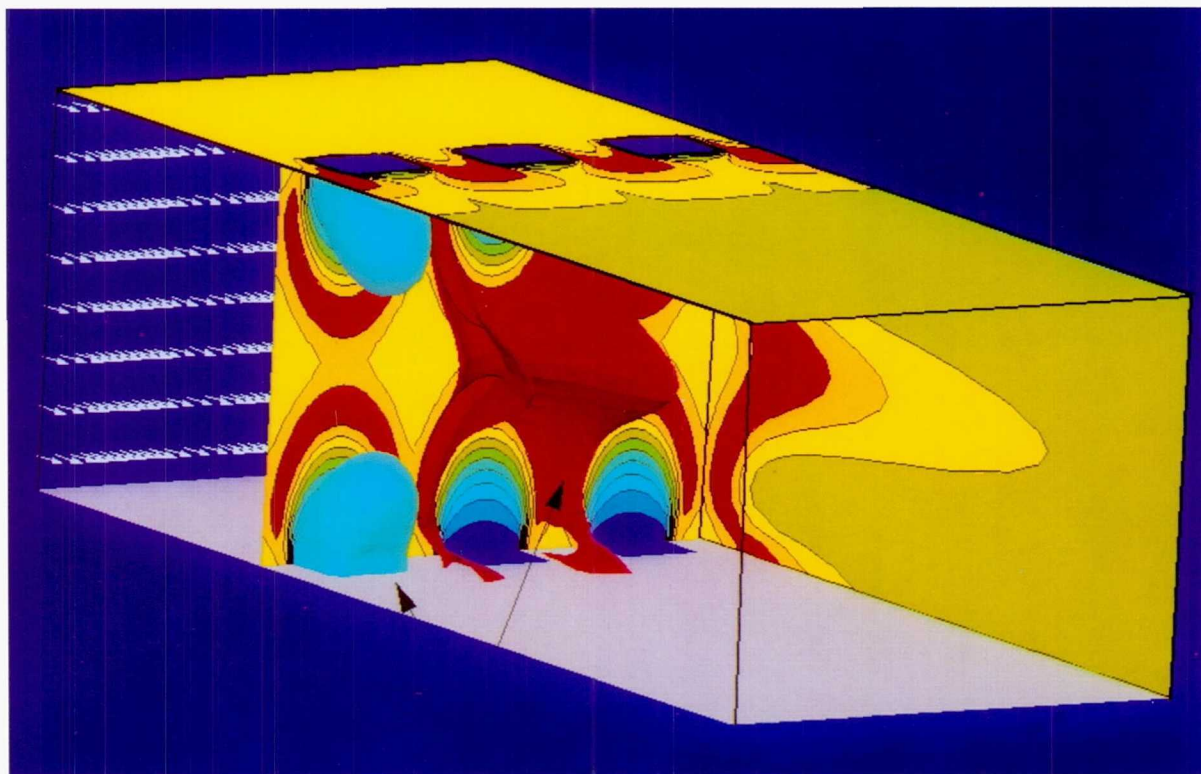
Continuing analysis will focus on turbulent reacting flow in jets in cross flow. The calculations will assess what effect heat release has on jet mixing. Jet mixing configurations that reduce gaseous emissions will also be studied.

Keywords

Combustors, Cross flow

Publication

Bain, D. B.; Smith, C. E.; and Holdeman, J. D.: CFD Assessment of Orifice Aspect Ratio and Mass Flow Ratio on Jet Mixing in Rectangular Ducts. AIAA Paper 94-0218, Jan. 1994.



Numerical simulation of jet mixing in a rectangular geometry. Inline square orifices: $S/H = 0.425$, $J = 36$, mass flow ratio = 2.0. Temperature: red = 2,550 K and blue = 950 K.

Parallel Multidisciplinary Stochastic Optimization

Robert H. Sues, Principal Investigator
Co-investigator: Graham S. Rhodes
Applied Research Associates, Inc.



Research Objective

To develop a general purpose parallel computing environment for large-scale multidisciplinary stochastic optimization (MSO) problems encountered in the design of advanced, high-performance aerospace systems.

Approach

A problem was formulated on the aerodynamic design of an advanced propfan blade. A single-processor code representing key components of the MSO methodology was developed. Probabilistic analysis was performed using Monte Carlo simulation. The finite-element code, NIKE3D, was used for structural analysis, and a linear-potential panel-method code was used for aerodynamic analysis. The Automated Design Synthesis library was used for optimization. Parallel implementations of the single-processor code were developed using the parallel virtual machine programming language. These implementations exploited the multiple levels of parallelism inherent in MSO problems. Performance was evaluated on the 128-processor Intel iPSC/860 hypercube and on a network of 32 IBM RS/6000 workstations.

Accomplishment Description

The feasibility of effectively parallelizing some of the key computational elements of MSO problems was demonstrated. Influence coefficients were computed in parallel to determine blade surface pressure coefficients. An average analysis required 5 minutes to process (using 32 hypercube processors) and 2 megabytes of memory per processor. High speedups achieved on the hypercube and workstation networks demonstrate the portability and parallel processing potential of the methodology. High speedups were also achieved for the sensitivity coefficient computations. The effect of multilevel parallel processing was investigated. Optimization was performed in clusters of processors to compute each sensitivity coefficient, and each processor in a cluster computed a group of influence coefficients. Speedup results for single- and multilevel parallel processing of the sensitivity coefficients are shown in the figure. Single-level speedup results reach a plateau at 20 processors because there are only 20 sensitivity coefficients to compute.

Significance

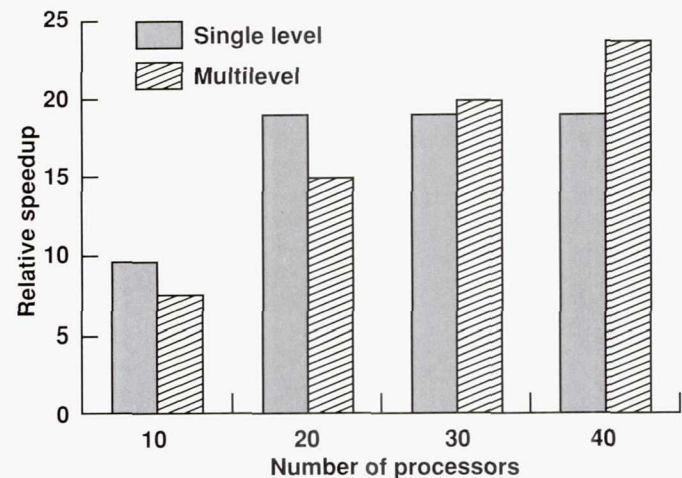
There are several levels of parallelism in MSO problems that must be fully exploited to maximize parallel processing performance. MSO can be applied to high-speed civil transport and advanced propulsion systems research to reduce design and development time and test costs.

Future Plans

A fully integrated design system for solving MSO problems on parallel computers will be developed. The system will integrate several principal components of parallel processing technology. Efficient multilevel parallel algorithms will be developed to effectively distribute aerodynamic and structural analysis computations across multiple processors.

Keywords

Turbomachinery, Turbojet, Propfan, Turboprop



Relative speedup results for multilevel parallelism.

Simulation of Scramjet Flow Fields

R. C. Swanson, Principal Investigator
Co-investigators: J. Korte and E. Turkel
NASA Langley Research Center/ICASE



Research Objective

To develop and apply the Langley Research Code for Chemical Kinetics (LARCK) for the solution of the three-dimensional (3-D) compressible Navier-Stokes equations for turbulent high-speed flows with and without chemistry.

Approach

A cell-centered, finite-volume spatial discretization with upwind-biased differencing was used. A multistage time-stepping scheme with implicit support was used as a smoother in a multigrid process to obtain stationary solutions and a multiblock capability was included to provide flexibility for treating complex geometries.

Accomplishment Description

Before considering high-speed flows with complex flows, LARCK was evaluated for a Mach 14.1 flow over a 3-D compression ramp at an angle of 24 degrees. The Reynolds number was 72,000, the free-stream temperature was 160 °R, and the wall temperature was 535 °R. This problem has viscous/inviscid interactions typical of those found in the flow field within the propulsion system of a hypersonic vehicle. In addition, it has separated flow, which makes convergence to a stationary solution more difficult. The difficulty is a consequence of significant changes in

the downstream solution with the evolution (in pseudo-time) of the separation bubble. The figure shows the computed pressure contours on a mesh of 53 points in the streamwise direction, 41 points in the normal direction, and 33 points in the cross-flow direction. The leading-edge shock, separation shock, and shock/shock interaction region are shown and the separation extent is delineated. A comparison of the predicted wall pressures in the symmetry plane with experimental data exhibits fairly good agreement.

Significance

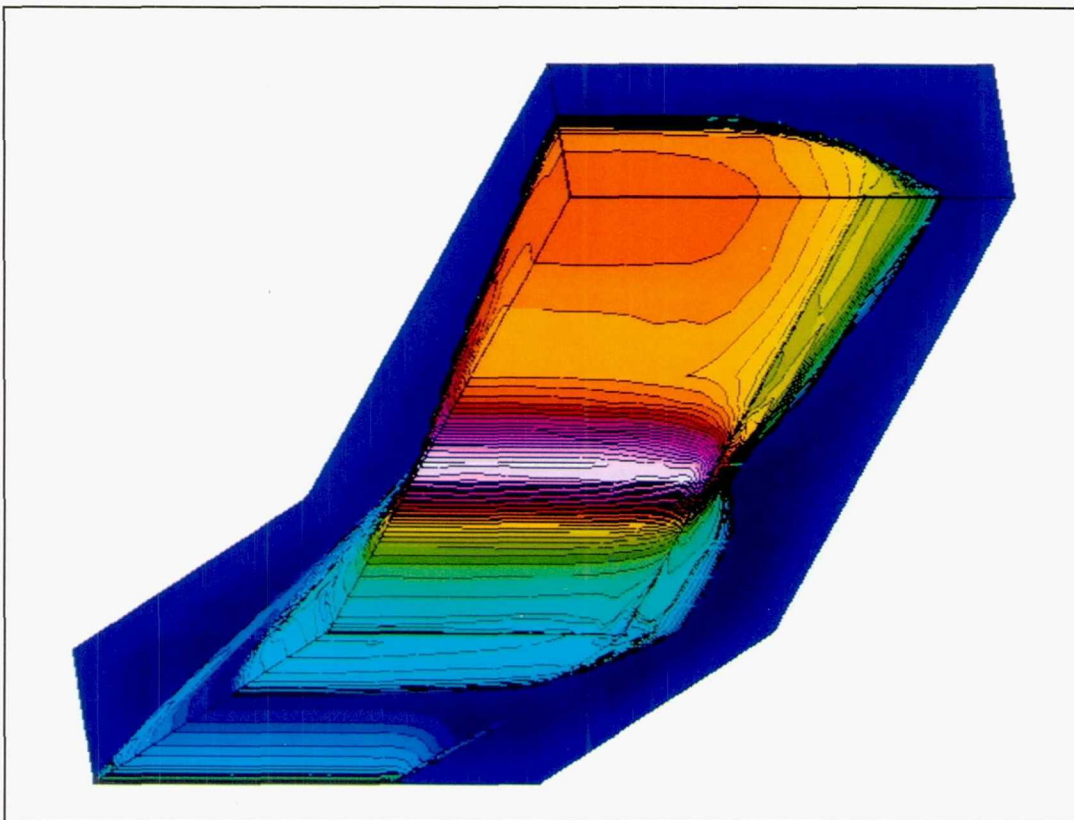
This project provided a capability to effectively compute high-speed flows with a multigrid/multiblock method and upwind-biased spatial differencing. The LARCK code was used to obtain good predictions for flows similar to those occurring in hypersonic propulsion systems.

Future Plans

The ability of the present 3-D flow solver to efficiently compute high-speed flows with chemistry will be demonstrated.

Keywords

Hypersonic, Propulsion



Mach 14.1 laminar flow over a compression ramp.

Hydrocarbon Scramjet Combustor

Jong H. Wang, Principal Investigator
Rockwell International, North American Aircraft Division



Research Objective

To validate Navier-Stokes methodology for predicting hydrocarbon scramjet combustor flows.

Approach

The unified solution algorithms code is applied to existing combustor-flow test cases to validate the code and to provide direction for future numerical and chemical model development.

Accomplishment Description

A dual-mode direct-connect hydrocarbon scramjet combustor was numerically investigated. The combustor was first modeled as a two-dimensional (2-D) flow with the fuel injector opening adjusted for a correct fuel-air ratio. At a fuel-air ratio of 1 in the injection zone, the 2-D model underpredicted the measured pressure data by about 50 percent. This deviation indicated that the mixing for the 2-D numerical model was much less than that for the physical flow model. A study was also performed to investigate the effects of three-dimensional (3-D) flow. The detailed configuration of the combustor, including all the fuel injectors, was considered in the numerical model. The grid system consisted of 347,030 points. The model required 19 megawords of memory, the solutions took 76 Cray C-90 seconds for each iteration, and the entire process took about 60 hours to converge. The predicted temperature contours in the combustor are shown in the first figure. The predicted distributions of centerline wall static pressure are compared with data in the second figure. The present 3-D numerical model gives predictions that are in good accord with experimental data.

Significance

Efficient hypersonic combustors are essential to the design of air-breathing hypersonic vehicles. Flow physics complexity and effi-

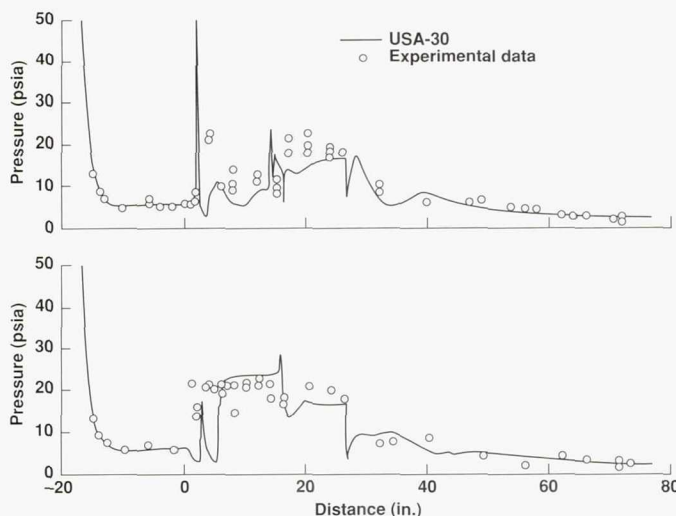
cient mixing and combustion require an accurate and robust computational tool.

Future Plans

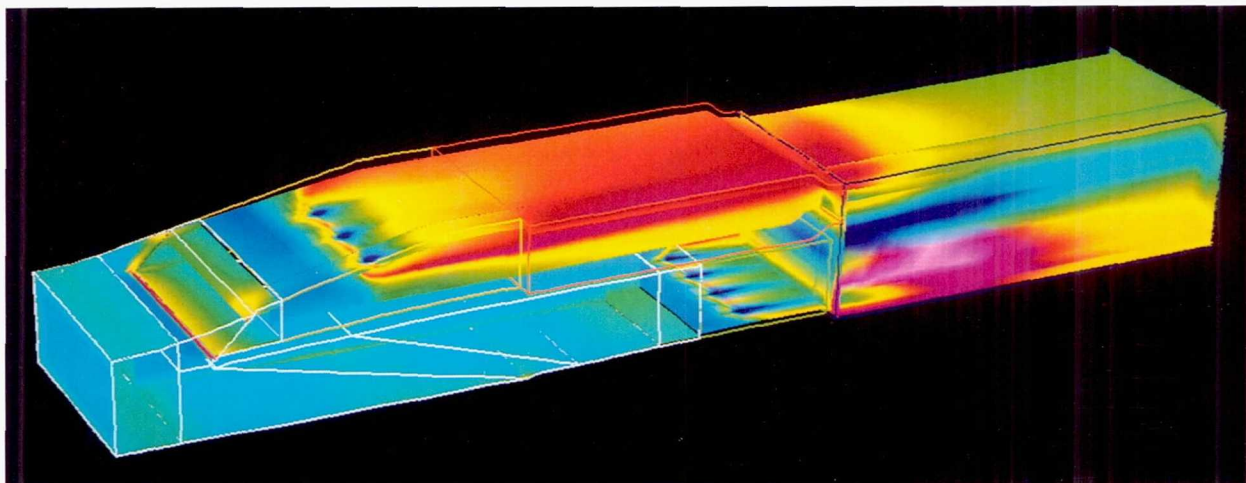
Based on the 3-D numerical results, an injection model will be devised for the 2-D computations. The injection model is necessary for promoting mixing in the 2-D numerical model.

Keywords

Propulsion, Scramjet combustor, Combustion



Predicted temperature contours in the scramjet combustor.



Comparisons of predictions with data for pressure on port side (top) and starboard side (bottom) combustor walls.

Reusable Launch Vehicle Flow Simulations

Scott Ward, Principal Investigator

Co-investigator: Darren Fricker

McDonnell Douglas Aerospace



Research Objective

To use state-of-the-art computational techniques to predict the aerodynamic and aerothermal performance of advanced launch vehicle configurations including power-on effects.

Approach

The Navier–Stokes code MDNS3D/ULTRA uses a structured zonal grid approach to discretize the full set of Reynolds-averaged Navier–Stokes equations and includes a generalized fully coupled finite-rate chemical kinetics model and a fully coupled two-equation turbulence model. The equations are solved in a time-dependent manner using second-order-accurate central differencing in space and an explicit fourth-order-accurate time advancement algorithm. Total-variation-diminishing dissipation ensures stability of the central difference scheme.

Accomplishment Description

Analysis of a nonaxisymmetric low-fineness-ratio multi-engine reusable launch vehicle configuration with and without power effects was conducted. The complex structure of the fundamentally unsteady base flow field, characterized by large regions of separation and entrainment into the engine exhaust flows, was studied. Base pressure and total vehicle force predictions from perfect gas simulations were compared to the pre-existing ground test database for a range of different ascent power settings. Although the large, essentially unsteady regions of separated flow reduced code convergence rates for most power-on cases, agreement between predictions and test data was good. Typical perfect gas solutions required approximately 8 Cray C-90 hours and 15 megawords of memory.

Significance

A computational fluid dynamics capability to model the complex base flow field for a multi-engine reusable launch vehicle was validated. This capability augments the existing ground test database by allowing a detailed study of underlying flow features not recorded by test instrumentation. The necessity for further ground testing may also be diminished.

Future Plans

A hydrogen/oxygen plus air chemical kinetics model will be implemented and several ascent cases calculated. Results will be compared to the perfect gas simulations to obtain increments that may be used to scale ground test data to flight conditions. Aero-thermal studies of other mission critical trajectory points will be undertaken.

Keywords

Computational fluid dynamics, Aerodynamics, Aerothermodynamics, Propulsion, Base flow



Surface pressure contours (red = high pressure and blue = low pressure) and flow-field streamlines for the Delta Clipper experimental single-stage-to-orbit vehicle during power-on ascent. Free-stream Mach number = 0.3, altitude = sea level.

Chimera Domain Decomposition Applied to Turbomachinery Flow

Kurt F. Weber, Principal Investigator

Co-investigator: Dale W. Thoe

General Motors Corporation, Allison Gas Turbine Division



Research Objective

To upgrade the POVERFLOW code for turbomachinery applications, apply it to conventional and unconventional turbomachinery applications, and evaluate its performance and accuracy.

Approach

Domain decomposition was applied using Chimera grid embedding to couple the calculated solutions of local flow fields in gas turbine fans and compressors. The equations were solved using Pulliam's diagonal version of the Beam-Warming implicit approximate factorization algorithm. A composite mesh for complex flow fields was generated using the Chimera grid embedding technique. The code worked with the output from the multiple-grid data management code PEGSUS, which established the interpolation between individual grids. The flow field was geometrically decomposed and grids were generated for the individual elements of a turbomachinery flow field that cannot be handled with a single mesh (blade rows for a compression system or air feed pipes for an engine test cell). PEGSUS was run to set up the interpolations for the mesh boundary communication. For parallel processing, data decomposition was applied and the parallel processors distributed so that the solution on each mesh was calculated concurrently.

Accomplishment Description

Upgrades to account for source terms due to a constant rotation rate were completed. Coding to calculate time varying metrics for a rotating mesh system, and an inlet boundary procedure specifying radial profiles of total pressure, total temperature, and velocity components were added. Exit boundary procedures and periodic boundary procedures for O-grids, C-grids, and H-grids were completed. The most computationally intensive calculation was for the flow through the six feed pipes and plenum and into the bell mouth inlet to the test section for an Allison Engine Company Test Cell 886. The calculation involved 8 grids, 904,000 points, and it required 116 processors with 8 megabytes of storage each. The calculation was run for 6,000 iterations and it required the equivalent of fifty 32-node iPSC/860 hours. The accompanying figure shows particle traces released at the inlets of the six pipes that feed the plenum supplying the air to the bell mouth inlet. The calculation confirmed the degree of total pressure distortion at the inlet of the engine test section.

Significance

The use of three-dimensional flow codes for aerodynamic design improvements in aircraft gas turbine engine compressors and fans is widespread. There is increasing emphasis on extending the capability of analyses by coupling previously isolated flow-field calculations to determine the effect of coupling on component performance. With cost-effective parallel computers, more complex turbomachinery flow calculations can be used in the routine design process.

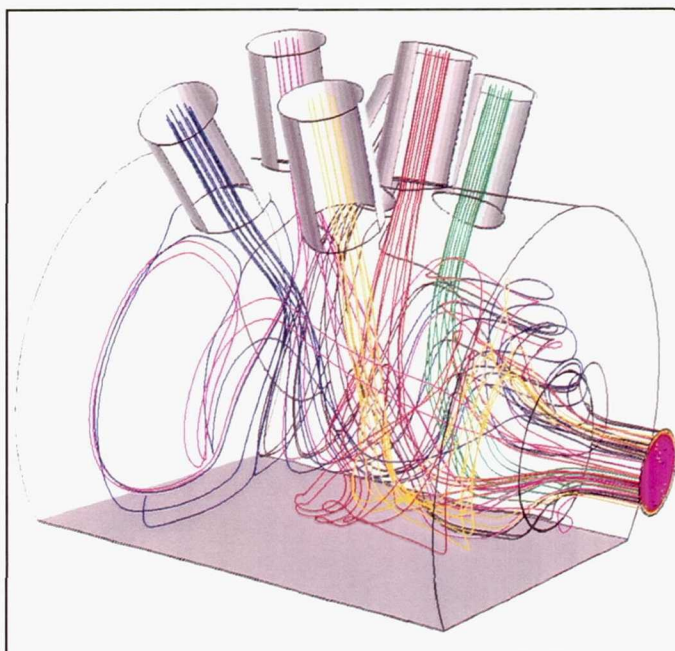
Future Plans

The routine written specifically for turbomachinery and the accuracy of the code for calculating the flow through transonic

fans and compressors will be verified. Calculated values of overall performance characteristics and blade-to-blade mass averaged quantities will be compared with component rig test data for NASA rotor 37 and NASA stage 37.

Keywords

Turbomachinery, Domain decomposition



Particle traces released at the inlets of the six feed pipes supplying air to an Allison Engine Test Cell 886. The traces show the extent of mixing and swirl in the test cell plenum.

National Aero-Space Plane Nozzles with External Burning

Shaye Yungster, Principal Investigator
Co-investigator: Charles J. Trefny
ICOMP/NASA Lewis Research Center



Research Objective

To develop computational fluid dynamics (CFD) prediction techniques to study the subscale and full-scale performance of external burning nozzles at transonic flight conditions.

Approach

The Reynolds-averaged Navier–Stokes equations with finite-rate chemistry were solved using two- and three-dimensional multi-block, fully implicit codes. The spatial discretization was based on a second-order total variation diminishing scheme and the LU-SSOR implicit factorization scheme. The study focused on the effects of external heat addition and introduced a simplified injection and mixing model based on a control volume analysis. Using this simplified approach, different configurations were analyzed quickly and inexpensively.

Accomplishment Description

A CFD tool for analyzing single-expansion ramp nozzles with or without external burning was developed. Extensive code validation studies were conducted for several nozzle configurations. These configurations included a baseline and an extended cowl with and without the use of a flame holder. The computed pressure distributions, axial and normal forces, and general flow features were in very good agreement with experimental data. The first figure shows a typical pressure coefficient distribution along the expansion ramp surface. The results were compared with experimental data given at the centerline and off-centerline (61 percent semi-width) locations. A parametric study of nozzle performance as a function of nozzle pressure ratio at different Mach numbers was completed. A parametric study of nozzle performance as a function of external burning fuel injection pressure was also completed. The second figure shows Mach number contour plots for two different external burning fuel pressures. One of the main effects of increasing the fuel pressure is a reduction in the amount of overexpansion on the initial part of the ramp. An analysis of the external burning flow field at full scale was completed, and axial and normal forces and Isp estimates were provided for all the cases studied. A typical calculation required about 2 Cray Y-MP hours and 8 megawords of memory.

Significance

National aero-space plane nozzles are highly overexpanded at transonic speeds, which results in significant drag increases. One way to eliminate this drag is to increase the pressure along the afterbody by using external combustion. This investigation provides a method for determining the subscale and full-scale performance of external burning nozzles at transonic flight conditions.

Future Plans

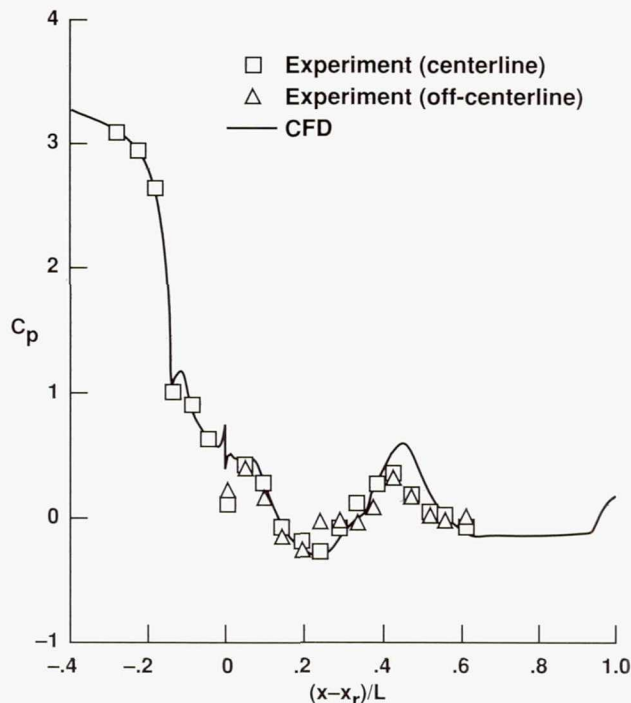
This study is complete.

Keywords

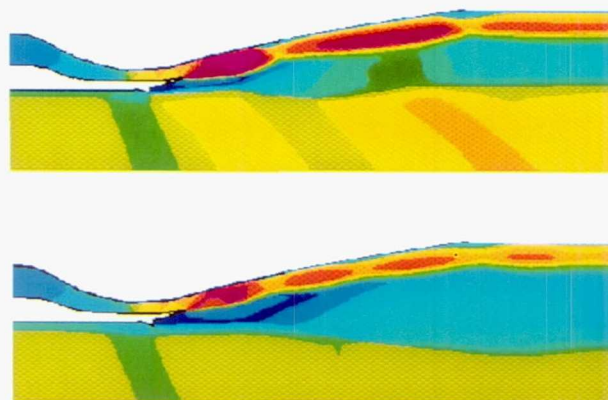
External burning, Transonic drag reduction

Publication

Yungster, S.; and Trefny, C. J.: Computational Study of Single-Expansion-Ramp Nozzles with External Burning. NASA TM-106550, April 1994.

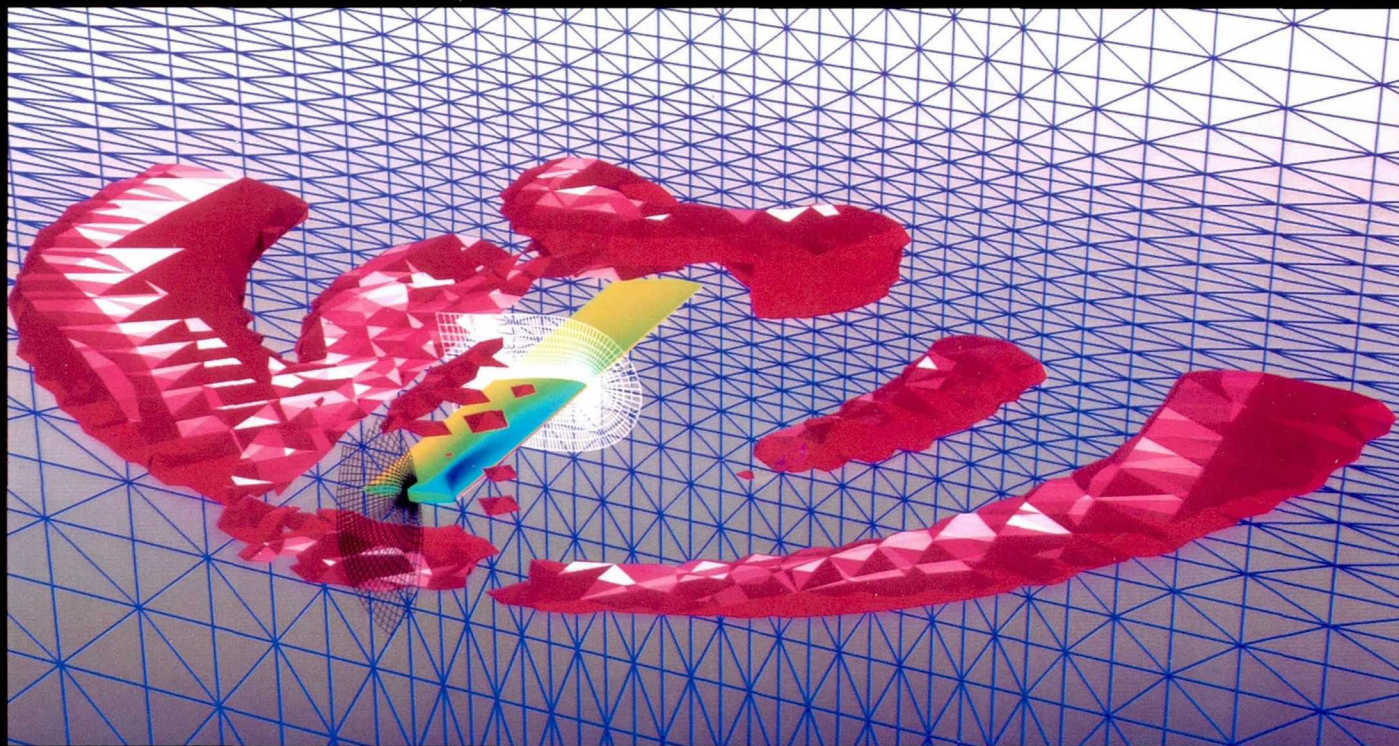


Pressure coefficient along the expansion ramp: Mach number = 1.8, nozzle pressure ratio = 8.58, external burning fuel pressure = 113 psi.



Mach number contours for two external burning fuel pressures (top = 50 psi and bottom = 250 psi). Mach number ranges from blue (0.0) to magenta (2.4).

Aeronautics



Rotorcraft

Page intentionally left blank

Calculations of High Performance Rotorcraft

W. J. McCroskey, Principal Investigator

Co-investigators: E. P. N. Duque, S. Ko, J. Ahmad, and A. C. B. Dimanlig

NASA Ames Research Center/U.S. Army Aeroflightdynamics Directorate/Sterling Software Systems/University of California, Davis



Research Objective

To compute the viscous, three-dimensional (3-D), unsteady flow field around advanced helicopters with particular emphasis placed on the aerodynamics of high-performance rotor blade tips, vortical wake structure, and rotor-body aerodynamic interference.

Approach

The unsteady 3-D Euler/Reynolds-averaged Navier-Stokes equations are solved by embedded structured-grid, unstructured-grid, and hybrid embedded structured/unstructured methods. The codes are validated through detailed comparisons with experimental data.

Accomplishment Description

The Reynolds-averaged thin-layer Navier-Stokes code OVERFLOW was used to solve the flow field of the Comanche helicopter in forward flight. The first figure illustrates the surface pressure distribution over the fuselage and at the main rotor disk. The main and tail rotors are approximated by an actuator disk with a constant pressure jump based on a given rotor thrust. Significant progress was made in coupling an unstructured-grid rotor code to a structured-grid rotor code. In this case, a structured grid optimized for viscous dominated flows was used for the near-body flows, whereas the unstructured grid was used for the inviscid flow fields away from the body. The two grid systems were embedded into each other with the flow quantities passed between the grid systems by interpolation. The second figure shows the structured/unstructured grid system for a rotor in hover with surface pressure contours and pressure along a cross section of the blade surface. In addition, an iso-surface of vorticity illustrates the structure of the computed wake.

Significance

The Comanche helicopter is the newest Army aircraft. Viscous fuselage calculations provide detailed flow-field information unattainable by other methods. These calculations can be used to help evaluate and improve aircraft performance. The hybrid structured/unstructured method incorporates the best features of each technology. Generally, structured grids perform better for near-body flows because the grid can cluster near the walls without severe time-step limits. The unstructured grids can refine flow features more readily than the structured grids. This feature potentially allows more accurate wake calculations.

Future Plans

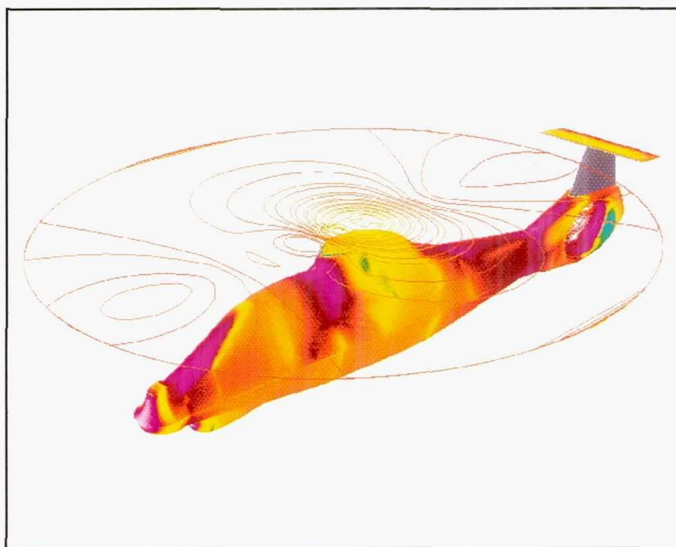
The unsteady flow field of the Comanche, including the rotor hub and blades in forward flight, will be computed and compared with future experiments. The structured/unstructured methodology will be validated for hover and forward flight including realistic motion of the blades. Dynamic grid adaptation of the unstructured mesh will be implemented and demonstrated.

Keywords

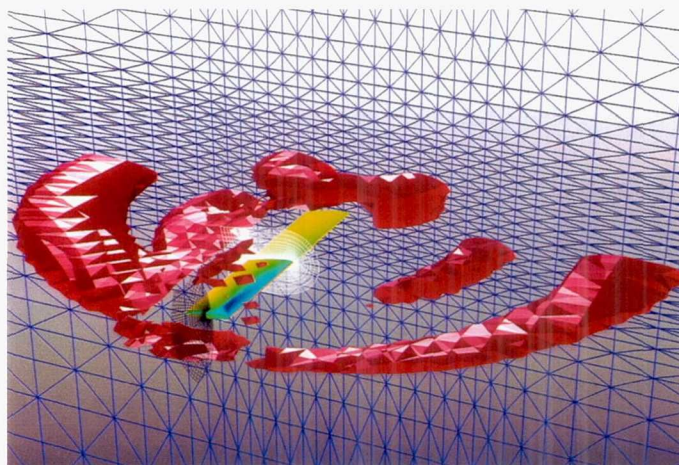
Unstructured embedded grids, Tip vortex, Wakes, Solution adaptation, Unsteady rotor-body interaction

Publications

1. Berry, J. D.; Chaffin, M. S.; and Duque, E. P. N.: Helicopter Fuselage Aerodynamics Predictions: Navier-Stokes and Panel Method Solutions and Comparison with Experiment. 1994 AHS Aeromechanics Specialists Conference, San Francisco, Calif., Jan. 19-21, 1994.
2. Duque, E. P. N.; and Dimanlig, A. C. B.: Navier-Stokes Simulation of the RAH-66 (Comanche) Helicopter. 1994 AHS Aeromechanics Specialists Conference, San Francisco, Calif., Jan. 19-21, 1994.
3. Duque, E. P. N.: A Structured/Unstructured Embedded Grid Solver for Helicopter Rotor Flows. AHS 50th Annual Forum, Washington, D.C., May 11-13, 1994.



Comanche helicopter in forward flight; free-stream Mach number = 0.26, free-stream Reynolds number = 14.0 million, and rotor thrust = 0.009.



Rotor in hover using the structured and unstructured grid pressure contours at the blade and an iso-surface of constant vorticity.

Solution-Adaptive Computations of Helicopter Acoustics

Roger C. Strawn, Principal Investigator

Co-investigators: Rupak Biswas and Michael Garceau

U.S. Army Aeroflightdynamics Directorate/NASA Ames Research Center/RIACS/Stanford University



Research Objective

To develop innovative solution-adaptive methods to accurately convect vorticity and acoustic waves in helicopter aerodynamics computations. Successful calculations require that numerical dissipation be kept to a minimum.

Approach

An unstructured-grid flow solver for the Euler equations is used to model helicopter aerodynamics and acoustics. An initial solution is obtained on a coarse tetrahedral mesh and local error estimates determine where additional mesh resolution is required. Mesh points are locally added or deleted to capture vortices and acoustic waves with an efficient distribution of grid points.

Accomplishment Description

A new three-dimensional mesh coarsening and refinement procedure was developed for tetrahedral meshes. Several demonstration cases show this procedure to be a highly efficient and effective way to adaptively resolve helicopter flow-field features in three dimensions. One of these cases is shown in the figure, where a solution-adaptive surface mesh and pressure contours are shown for a high-speed hovering rotor. In addition to the high resolution of the shock wave on the rotor surface, this solution shows excellent resolution of the acoustic wave that extends radially from the blade tip. This solution required approximately 5 Cray C-90 hours and 50 megawords of memory.

Significance

Noise reduction is one of the major problems facing the designers of future civilian and military rotorcraft. Accurate prediction of helicopter noise is a key component in its reduction and control. Helicopter acoustic signals require extremely fine-grid resolution away from the rotor blades. Solution-adaptive grids provide a computationally efficient method for obtaining this grid resolution in the far field.

Future Plans

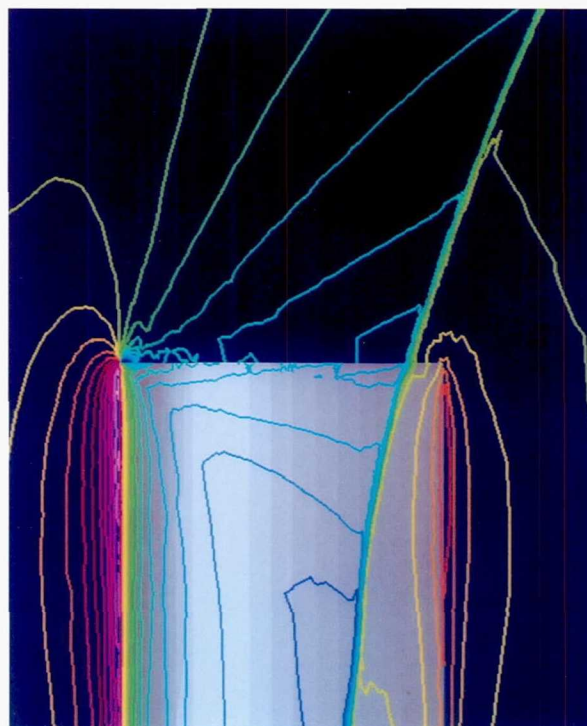
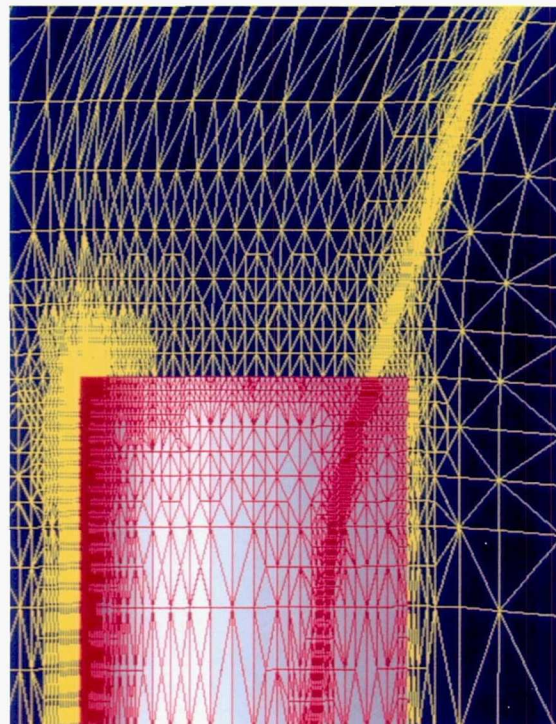
Future computations will use the newly developed dynamic mesh adaption scheme to compute rotor tip vortices and acoustic waves. Development of local error indicators for vortex-dominated flow fields is also a goal.

Keywords

Unstructured, Acoustics, Tip vortex, Wakes, Solution adaption, Euler solver, Tetrahedra

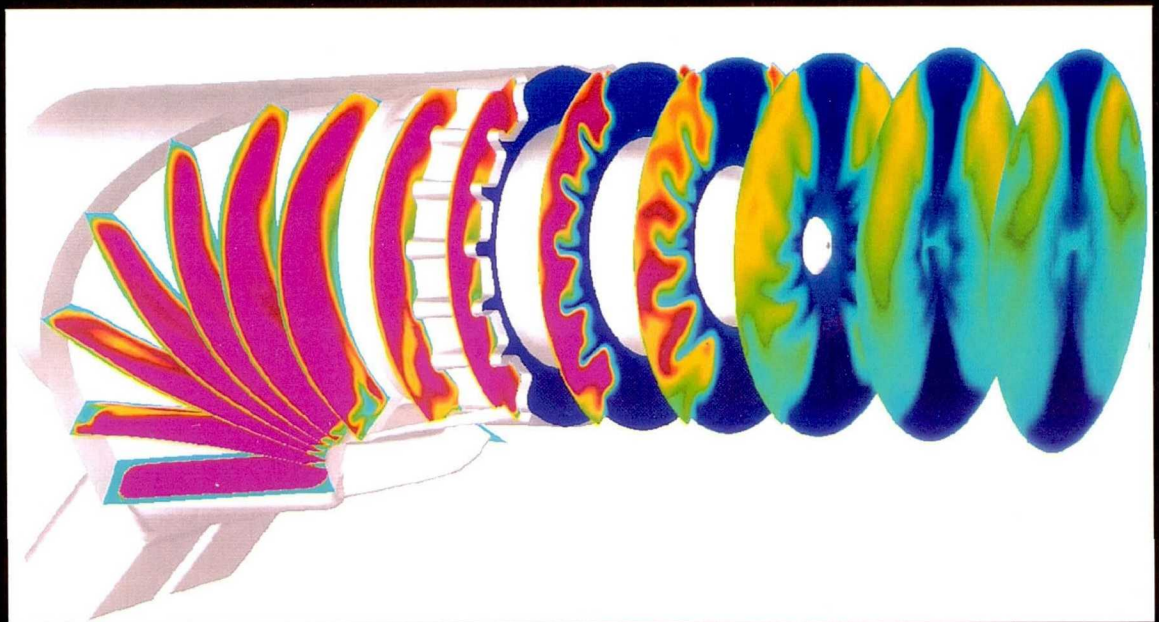
Publications

1. Biswas, R.; and Strawn, R. C.: A New Procedure for Dynamic Adaption of Three-Dimensional Unstructured Grids. Appl. Num. M., vol. 13, 1994, pp. 437-452.
2. Strawn, R. C.; Garceau, M.; and Biswas, R.: Unstructured Adaptive Mesh Computations of Rotorcraft High-Speed Impulsive Noise. AIAA Paper 93-4359, Oct. 1993.



Solution-adaptive mesh (top) and pressure contours (bottom) near the tip of a hovering rotor blade. Results are shown in the plane of the rotor. The hover-tip Mach number = 0.95 and the blade aspect ratio = 13.71.

Aeronautics



Turbulence

Page intentionally left blank

Transition in a Highly Disturbed Environment

David E. Ashpis, Principal Investigator

Co-investigator: Philippe R. Spalart

NASA Lewis Research Center/Boeing Commercial Airplane Group



Research Objective

To understand the physical mechanisms of nonlinear stability and bypass transitions to provide guidance for engineering model developers.

Approach

Direct numerical simulations of controlled disturbances in the boundary layer were performed. Spatial simulations were performed using a Spalart's "fringe code." Numerical experiments simulating single-frequency excitation (two-dimensional (2-D) vibrating ribbon, harmonic point source) and broadband excitation (blowing pulse) were performed. The disturbances are introduced on the wall by specifying localized suction and blowing. The flow field, frequency, and wave-number spectra were computed for incompressible Blasius boundary layer flow.

Accomplishment Description

The fringe code was modified to allow specification of time-dependent wall boundary conditions. The prior series of 2-D and three-dimensional (3-D) runs were continued for a range of disturbance frequencies, amplitudes, and Reynolds numbers. New simulations of harmonic-point-source excitations were performed. Parameters of these simulations matched prior calculations and experiments. The simulations were performed for a range of excitation amplitudes, from linear to nonlinear. Observations demonstrated the differences between linear and nonlinear disturbances. Computing resources varied according to the domain size, grid resolutions, and the length of simulation. Typical runs required 4–32 megawords of memory and 4–20 Cray Y-MP hours.

Significance

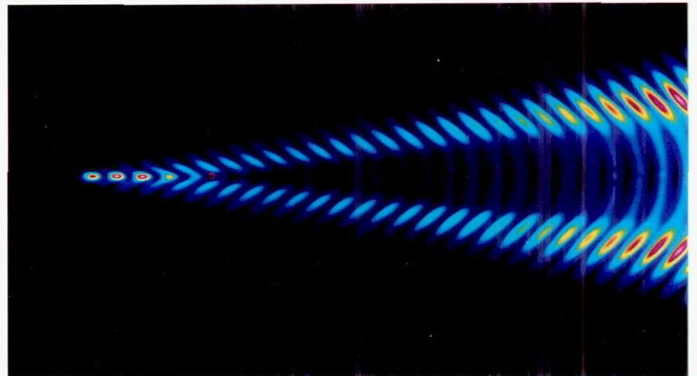
A highly disturbed environment prevails in the gas turbine flow. The simulations of the associated nonlinear and bypass stability mechanisms are valuable for developers of models for applied engineering calculations. The harmonic-point-source simulations reveal the effects of a single frequency in 3-D flow without the complexity of a broadband excitation spectrum.

Future Plans

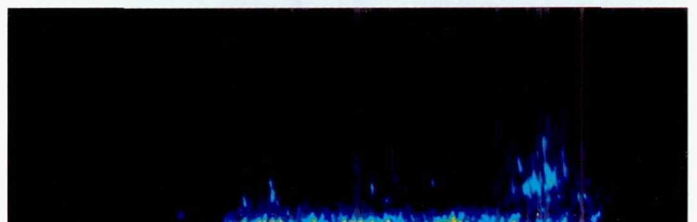
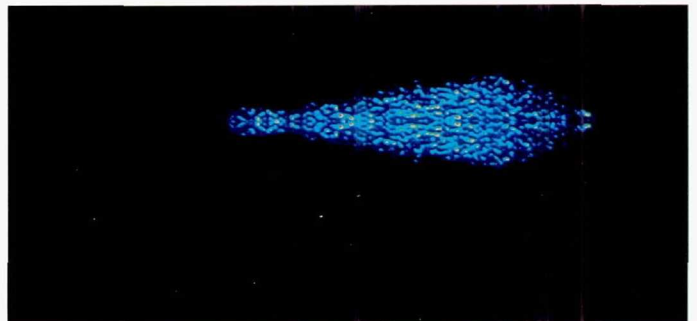
Postprocessing will continue with the data acquired. The effects of pressure gradients and curvature will be examined. The studies will be extended to flows with heat transfer.

Keywords

Disturbances, Receptivity, Bypass transition, Stability, Turbulence, Point source, Excitation



Disturbance energy for harmonic-point-source excitation in a Blasius boundary layer. Frequency parameter is 60. Excitation amplitude is 0.0001 of free-stream velocity. The top shows the X-Z plane and the bottom shows the X-Y plane at the centerline. Linear response is observed.



Disturbance energy for harmonic-point-source excitation in Blasius boundary layer. Frequency parameter is 60. Excitation amplitude is 0.01 of free-stream velocity. The top shows the X-Z plane and the bottom shows the X-Y plane at the centerline. Nonlinearities and breakdown to turbulence are evident.

Incompressible Plane Wake Computation Comparisons

Brian J. Cantwell, Principal Investigator

Co-investigators: Nagi N. Mansour, Rolf Sondergaard, and Eric Monsen
Stanford University/NASA Ames Research Center



Research Objective

To gain an improved understanding of the linkage between the late stages of wake development and properties of the initial flow field. Topological methods will be developed for revealing the significant flow-field features contained in large data sets and universal features will be sought.

Approach

Direct numerical simulations of the three-dimensional (3-D) incompressible wake using a Fourier spectral algorithm for flows with one infinite and two periodic directions have been run. Parameters such as Reynolds number and initial disturbance fields were varied to study the effects of changes in the early flow field on the development and structure of later turbulence. Matching simulations have been run on the Cray C-90 and the Intel iPSC/860 to compare performance.

Accomplishment Description

A code for direct numerical simulation of planar free shear flows was run on the Cray C-90 and Intel iPSC/860. Simulation comparison showed excellent agreement. A typical moderate Reynolds number simulation up to a convective time of 150 required approximately 20 Cray C-90 hours and 12 megabytes of memory. A matching simulation on the iPSC/860 using the parallel code required approximately ten 32-node hours. Wakes started from a variety of initial conditions were run on both machines. The computations showed that (1) the presence of an oblique disturbance had a significant effect on initial 3-D development in the wake; (2) flow Reynolds number had a strong effect on the late time growth of the wake; (3) the presence of longer wavelength disturbances allowed scale changes in the flow; and (4) the relative phase of initial disturbances had an effect on the detailed structure of the wake, but only a minor effect on the growth rate. The simulations studied included incompressible and compressible isotropic turbulence, sheared turbulence, and mixing layer flows.

Significance

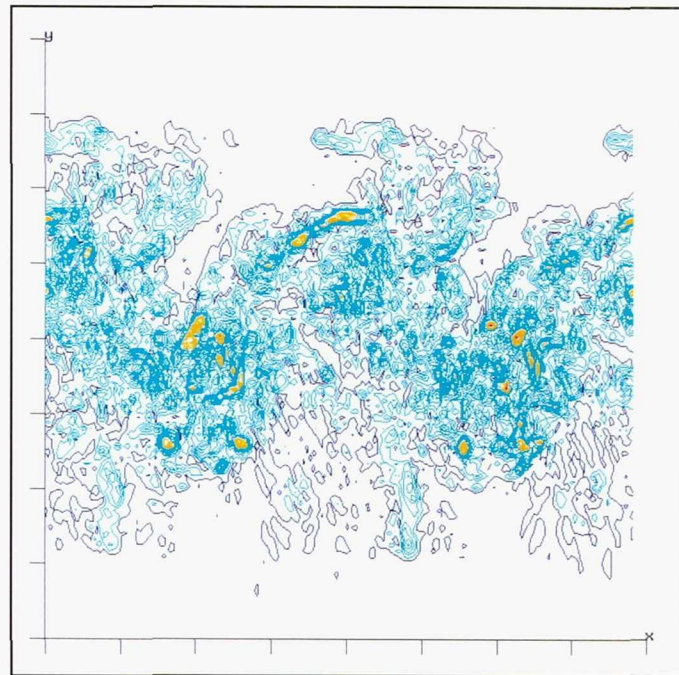
Improved understanding of turbulence development and the fine scale motions in inhomogeneous turbulent flows is necessary before improved subgrid-scale turbulence models can be developed. This project significantly improved the understanding of the role of subharmonic disturbances on wake growth.

Future Plans

Direct numerical simulation of several high Reynolds number 3-D incompressible planar shear flows will be performed to further study the effect of initial conditions on the late stages of flow development. Of particular interest is the effect of initial conditions on the fine scale topology of the turbulence.

Keywords

Wake, Turbulence, Parallel



Entropy contours for a vertical cut through a Reynolds number 2,768 wake at a time of 101.0. Contour levels are 0.1 (blue) to 5.0 (red). Free-stream flow is from left to right.

Numerical Simulation of Riblets

Haecheon Choi, Principal Investigator

Co-investigators: Parviz Moin and John Kim

Stanford University/NASA Ames Research Center



Research Objective

To provide an accurate estimate of drag reduction performance by riblet configurations supplied by the Boeing Company.

Approach

Direct numerical simulation is used to simulate turbulent flows over longitudinal riblets. A second-order-accurate finite difference method is used to solve unsteady incompressible Navier–Stokes equations in generalized coordinate systems.

Accomplishment Description

Direct numerical simulations of turbulent flows over riblets were performed at Reynolds number 180 based on the flat plate shear velocity and channel half-width. Two sawtooth riblet configurations (one with and one without a flat valley) in turbulent channel flow were considered. Both had riblet spacing of $s^+ = 15$, which is an optimum size for drag reduction. Twelve riblets were included in the computational domain, and 32 grid points for each riblet were used in the spanwise direction to accurately predict skin friction on the surface of riblets. The computations revealed about 9 percent drag reduction by the riblet with the flat valley and about 3 percent drag reduction by the riblet without the flat valley. The grid contained $16 \times 129 \times 384$ grid points in the streamwise, wall-normal, and spanwise directions. A typical run required 300 Cray C-90 hours and 10 megawords of memory.

Significance

Direct numerical simulation is an important tool in predicting complex turbulent flow phenomena occurring in a configuration of practical interest.

Future Plans

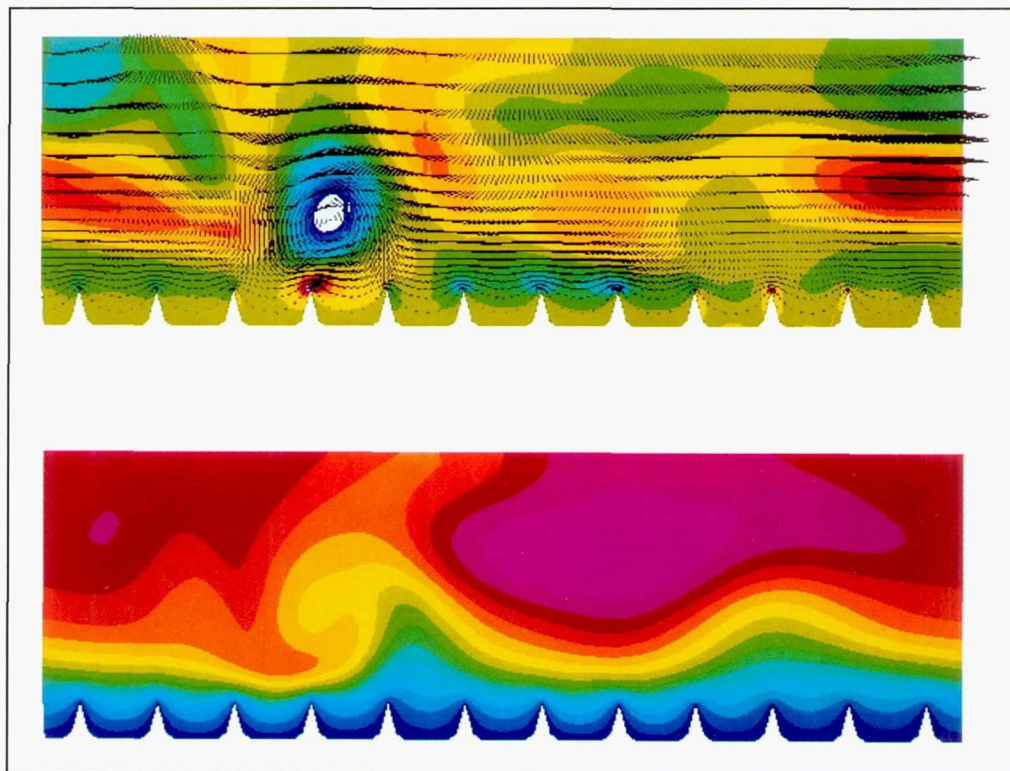
The direct numerical simulation range of applicability is limited to low Reynolds numbers. Large-eddy simulation and the dynamic subgrid-scale model will be used to access higher Reynolds number flows.

Keywords

Drag reduction, Turbulent boundary layer

Publications

1. Choi, H.; Moin, P.; and Kim, J.: On the Effect of Riblets in Fully Developed Laminar Channel Flows. *Phys. Fluids A*, vol. 3, 1991, p. 1,892.
2. Choi, H.; Moin, P.; and Kim, J.: Direct Numerical Simulation of Turbulent Flow Over Riblets. *J. Fluid Mech.*, vol. 255, 1993, p. 503.



Flow field above a riblet-covered wall. Streamwise vorticity with cross velocity (top) and streamwise velocity (bottom).

Direct and Large-Eddy Simulation of Wake Flows

George E. Karniadakis, Principal Investigator
Co-investigators: D. Newman and R. D. Henderson
Brown University



Research Objective

To understand and model turbulent wakes formed behind bluff bodies of arbitrary shape using high-order direct and large-eddy simulations (LES).

Approach

The numerical simulations were performed using the NEKTAR code, which is based on a new generation of spectral element algorithms. NEKTAR uses triangular instead of quadrilateral spectral elements and a hierarchical expansion basis, which produces well-conditioned matrix systems for high-order polynomial expansions. In the NEKTAR code, the entire three-dimensional (3-D) field is decomposed into Galerkin modes in all directions that can be used to identify which scales are resolved, at what accuracy, and how the quality of the solution can be improved by adaptively varying the hierarchical basis. In such a framework it is much more natural to implement subgrid models for LES. This adaptive strategy also provides a more efficient approach in direct numerical simulations (DNS) because its resolution requirements are optimal. In turn, this implies that a higher Reynolds number regime can be accurately investigated.

Accomplishment Description

Direct and large-eddy simulations of turbulent wakes were completed for a family of nominally two-dimensional planar and axisymmetric bluff bodies including circular and half-cylinders,

ellipses of different aspect ratios, flat plates, and spheres. Comparisons were performed with results obtained in companion experiments for vorticity- and velocity-averaged and instantaneous fields. Three topics were addressed in this study: (1) validation of the hybrid DNS-LES approach where the laminar boundary layer on the body is entirely resolved and the turbulent wake is modeled at the subgrid level; (2) investigation of spanwise variations of the time-averaged flow in wakes associated with instabilities of the large-scale turbulence structure; and (3) simulation of vortex-induced vibrations in 3-D flow past cylinders and spheres.

Significance

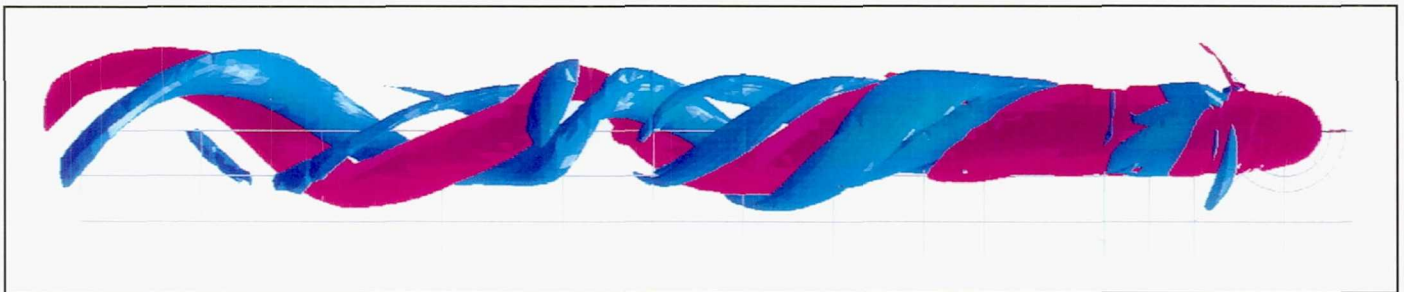
Bluff-body wake flows are perhaps the most common flows in aeronautical engineering; however, there are no numerical models for predicting the dynamics of such flows nor even the average body forces. The current work is an attempt to systematically simulate bluff-body flows and provide low-dimensional predictive models for turbulent wakes.

Future Plans

High-Reynolds number turbulent wake and flow-structure interactions will be studied.

Keywords

Turbulent wakes, Spectral elements, Simulations



Iso-surfaces of streamwise vorticity for flow over an axially spinning sphere at Reynolds number 300.

Simulation of Complex-Geometry Wall-Bounded Flows

George E. Karniadakis, Principal Investigator

Co-investigators: Catherine H. Crawford and Ronald D. Henderson
Brown University



Research Objective

To correlate turbulent structures in the near-wall region of complex-geometry flows with drag-reducing and drag-inducing flow events using high-order direct and large-eddy simulations.

Approach

Direct numerical simulations of turbulent flow over riblet-mounted surfaces were performed using an unstructured spectral element flow solver. This high-order flow solver used nonconforming spectral elements so that a large degree of mesh adaptivity and mesh refinement resolved the small-scale structures of the turbulence, especially the flow features near the riblet tips. The first figure shows a channel domain with its lower wall mounted with V-shaped grooves or riblets. The riblet geometry was chosen to correspond with available experimental data. The channel dimensions and mesh structure were chosen after a study of the resolution requirements for a spectral element simulation for a channel with two smooth walls.

Accomplishment Description

Direct numerical simulations of turbulent flow over riblets at a moderate Reynolds number were completed for both conforming and nonconforming riblet meshes. Turbulence statistics for both the lower riblet wall and the upper smooth wall were collected and averaged over 250 convective units. The riblets for this case did not reduce or induce drag at the wall. Because the riblet wall had over twice the wetted area as the smooth wall, there was a reduction in the skin friction. The turbulence intensity profiles and Reynolds stress profiles showed a slight reduction of the streamwise intensity and Reynolds stress at the riblet wall. The statistics from the smooth wall were in excellent agreement with previous numerical and experimental results. A quadrant analysis study was done to understand how small-scale turbulent structures were altered by the presence of a riblet wall. The riblets seemed to redistribute the instantaneous velocity and vorticity at about $y^+ = 10$ at the riblet wall compared to $y^+ = 10$ at the smooth wall. Also, the drag-enhancing events for both walls were correlated using instantaneous wall-shear distributions and velocity vector plots. The near-wall sweep events caused an instantaneous increase in the wall shear, while the near-wall ejection events caused an instantaneous decrease in the wall shear.

Significance

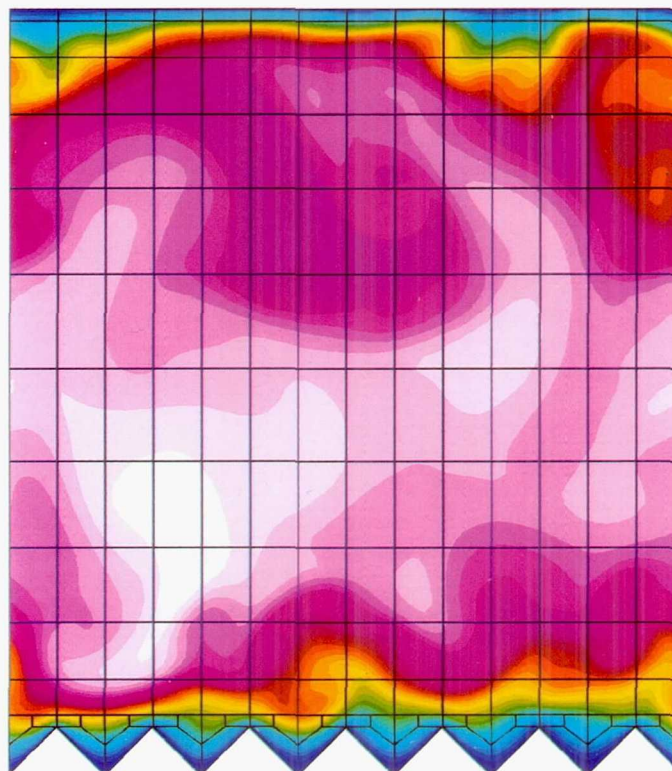
Although most researchers now agree that riblets of the correct height and span geometries do cause drag reduction, there exists no consistent explanation of why this happens. Through studies of the velocity and vorticity quadrant analysis and the identification of flow structures associated with increased or decreased drag, an explanation for riblet drag reduction and the drag reduction found in other near-wall flows will be found.

Future Plans

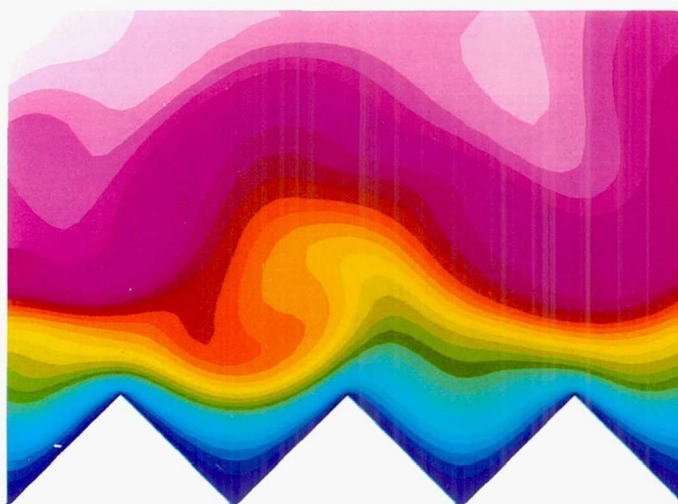
Higher Reynolds number turbulent flows and different riblet geometries will be studied. The hypothesis that the drag reduction could be caused by flow randomization will be validated.

Keywords

Near-wall turbulence, Drag reduction, Spectral elements, Simulations



Streamwise velocity contours in the riblet domain. Note the unstructured mesh at the riblet wall.



Close-up of streamwise velocity contours at the riblet wall.

Turbulence Modeling for Three-Dimensional Flow Fields

Linda D. Kral, Principal Investigator

Co-investigators: John A. Ladd, Mori Mani, and John F. Donovan

McDonnell Douglas Corporation



Research Objective

To investigate turbulence models used in numerical simulations of complex viscous flows for critical aircraft components such as the forebody, wing, nozzle, inlet, diffuser, and afterbody. The focus is on computations of turbulent, three-dimensional (3-D) flows using one-equation and two-equation turbulence models.

Approach

The 3-D zonal Navier–Stokes code, NASTD, was used to predict the turbulent flow fields around flight vehicles. An implicit, approximately factored, upwind scheme is employed to solve the 3-D, compressible, Favre-averaged Navier–Stokes and energy equations together with the k - ϵ two-equation turbulence model. Three zero-equation algebraic models and two one-equation models are available in the code. Six low-Reynolds number forms of the k - ϵ turbulence model are available. The Wilcox k - ω model and the Menter baseline and shear-stress transport-blended k - ω / k - ϵ models were included for evaluation. The Sarkar compressibility correction for free-shear layers was also employed.

Accomplishment Description

A hot-gas-exhaust mixing system was successfully analyzed using the Baldwin–Barth one-equation turbulence model. The analysis started from the hot engine exhaust, included ejector air at the turning duct inflow, continued through the mixing flanges, and out to the end of the tail boom where a back pressure was specified. Surface static temperatures of the mixer assembly and downstream duct are shown in the first figure. Prediction of downstream core temperature agreed with empirical predictions, and calculated surface temperatures indicate adequate mixing of the exhaust and bypass gases (second figure). The solution indicates there is significant cross flow near the approach to the mixing flanges, which could be minimized by proper vane placement. The exhaust mixer system calculation required 2.5 million points in 16 zones and nearly 20 Cray C-90 hours.

Significance

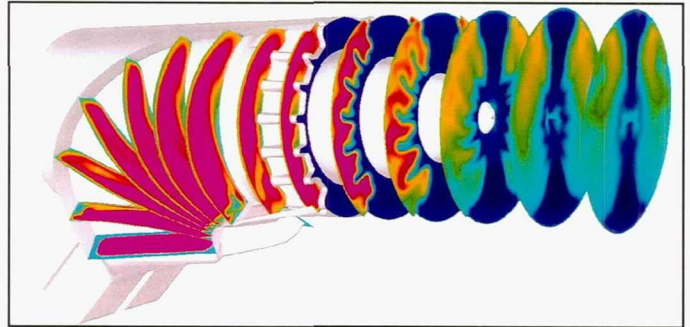
The data used to develop turbulence models were obtained from canonical flows and it is not clear how these turbulence models will perform for more realistic geometries. Successful simulation of turbulent flows of the complexity found on aircraft will be a valuable design tool.

Future Plans

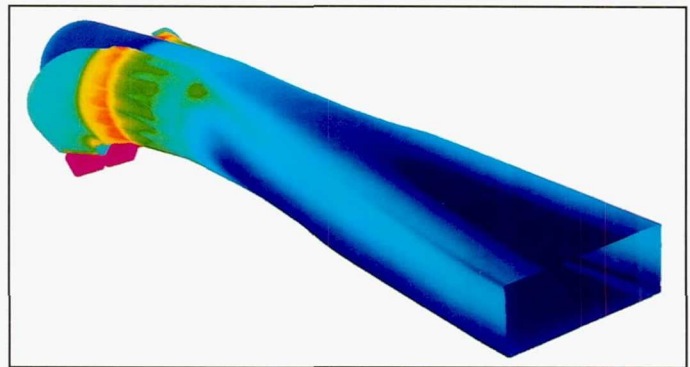
The Spalart–Allmaras one-equation model, the k - ϵ low-Reynolds number models of So and Huang–Coakley, and the Menter blended two-equation model will be evaluated. Corrections for curvature and compressibility will also be evaluated.

Keywords

k - ϵ , One-equation, Two-equation



Surface static temperature of the mixer assembly and downstream duct region; red = high temperatures and blue = low temperatures.



Temperature contours of the mixer showing the quick mixing present as the exhaust and fan air come together aft of the mixing flanges; red = high temperatures and blue = low temperatures.

Large-Eddy Simulation of Jet Combustors

Thomas S. Lund, Principal Investigator
Co-investigators: Parviz Moin and Knut Akselvoll
Stanford University/NASA Ames Research Center



Research Objective

To study mixing of fuel and air in a coaxial jet combustor to better understand the mechanisms responsible for lean blowout.

Approach

A passive scalar was used to trace the mixing of fuel and air in nonreacting jet combustors. Reynolds numbers on the order of 10^4 were considered and corresponded to those numbers achieved in laboratory experiments. Because of the relatively high Reynolds number, the large-eddy simulation (LES) approach was adopted. The dynamic subgrid scale model accounts for the effect of the unresolved turbulent motions. The code is based on finite differences and is second-order accurate in space and time.

Accomplishment Description

First, LES was used to calculate turbulent flow over a backward facing step to assess the accuracy and suitability of the dynamic subgrid scale model in a complex flow geometrically similar to the jet combustor. Simulations of the backward facing step were performed at Reynolds numbers of 5,100 and 26,000, based on step height and inlet free-stream velocity. For the low Reynolds number case, the mesh contained $192 \times 48 \times 32$ points in the streamwise, wall-normal, and spanwise direction, respectively. A typical run required about 20 Cray C-90 hours and used about 2.5 megawords of memory. For the high Reynolds number case, $244 \times 96 \times 96$ grid points were used, and about 70 Cray C-90 hours and 9 megawords of core memory were required. Both simulations are in excellent agreement with experimental data. The low Reynolds number simulation also agrees well with direct numerical simulation data. The second part of the study involved the simulation of mixing in a planar jet combustor. The geometry differs from the coaxial jet combustor only in that it is planar

rather than axisymmetric. This part of the study was undertaken to evaluate the dynamic subgrid-scale model for the residual scalar flux and to gain some insight into the mixing characteristics of jet combustors. The grid contained $192 \times 76 \times 16$ points. A typical run required about 20 Cray C-90 hours and about 2 megawords of memory. To prepare for the coaxial combustor simulation, an axisymmetric code was written and validated for turbulent pipe flow.

Significance

The LES technique, used in conjunction with the dynamic subgrid scale model, can accurately predict a complex turbulent flow at low and high Reynolds numbers. This technique also successfully describes the convection and diffusion of a passive scalar.

Future Plans

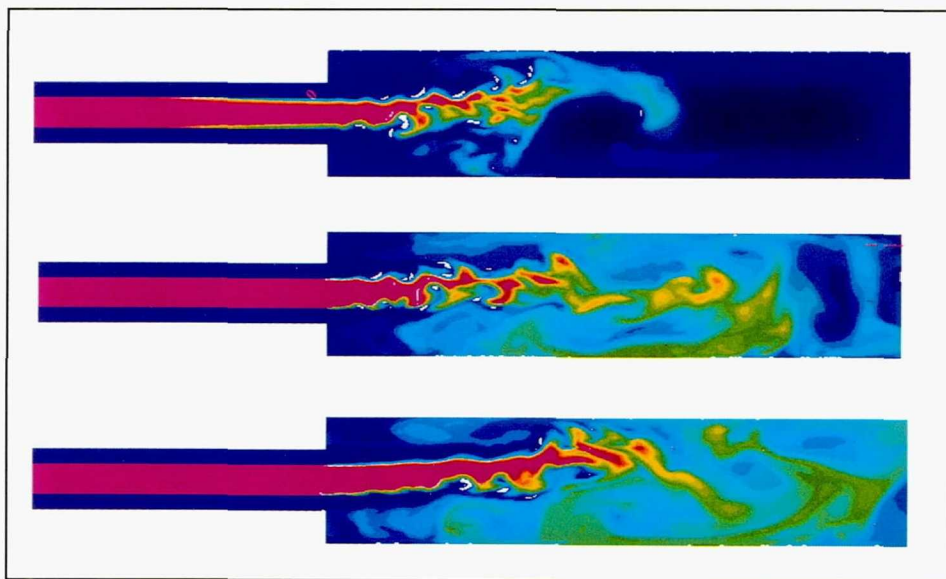
The coaxial jet combustor at Reynolds number 35,000 will be simulated and the mixing of fuel and air will be studied. Mechanisms responsible for lean blowout will be identified and control strategies aimed at preventing this condition will be investigated.

Keywords

Backward facing step, Scalar transport

Publication

Akselvoll, K.; and Moin, P.: Application of the Dynamic Localization Model to Large Eddy Simulation of Turbulent Flow Over a Backward Facing Step. Engineering Applications of Large Eddy Simulations, 1993, S. A. Ragab and U. Piomelli, eds., ASME Fluids Engineering Conference, Washington, D.C., June 20–24, 1993.



Passive scalar contours show mixing of fuel and air in the planar combustor; red = fuel, blue = air. Three times are shown from earliest (top) and latest (bottom).

Boundary-Layer Transition on a Heated Flat Plate

Nateri K. Madavan, Principal Investigator
MCAT Institute



Research Objective

To conduct direct numerical simulations of boundary layer transition on a heated flat plate with elevated free-stream turbulence.

Approach

The present approach uses a high-order-accurate, upwind-biased, finite-difference technique in conjunction with an iterative-implicit time advancement scheme to solve the unsteady Navier–Stokes equations in nonconservative form. The iterative time advancement ensures that the fully implicit form of the equations are solved at each time step. Factorization and linearization errors are thus driven to zero at each time step. Zonal methodologies are used to allow selected regions of the flow field to be resolved more accurately. The methods being used can be extended to general geometries.

Accomplishment Description

An existing computer code was modified for this effort. A coarse-grid computation (16 million grid points) was completed and the results were encouraging. The coarse-grid computation was obtained in stages, starting from an initial solution obtained on an

extremely coarse grid and then interpolating to successively finer grids. This interpolation helped reduce the computation time. For each grid point, the code requires 6 microseconds of single-processor Cray C-90 time for each iteration.

Significance

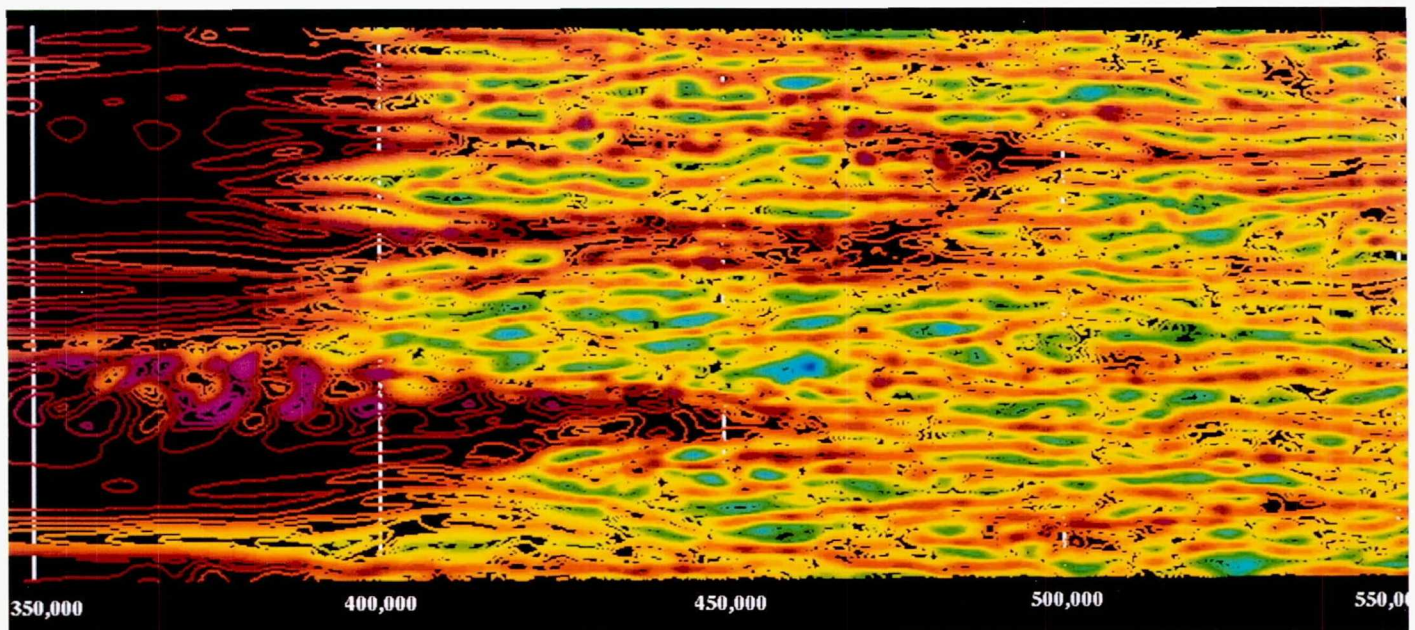
When completed, this work will provide valuable insight into the physics of transition and turbulence in high free-stream disturbance environments. This work has a wide range of applications, including gas turbine cooling system design, and it lays the foundation for future efforts toward direct or large-eddy simulations in complex configurations at more realistic Reynolds numbers.

Future Plans

After a larger statistical sample is acquired on the present grid, computations will be initiated on a finer grid (24 million grid points).

Keywords

Direct simulation, Turbulence



Spanwise vorticity contours in an (X-Z) plane very close to the plate ($y^+ = 1.0$). The Reynolds number transition region is between 350,000 and 550,000.

Direct Numerical Simulation of Shock/Turbulence Interaction

Parviz Moin, Principal Investigator

Co-investigators: Sanjiva K. Lele, Krishnan Mahesh, and Sangsan Lee

Stanford University



Research Objective

To guide turbulence model development for the interaction of shock waves with turbulent shear flows.

Approach

The three-dimensional Navier–Stokes equations were numerically solved. The sixth-order Pade scheme was used to compute spatial derivatives and the third-order Runge–Kutta scheme was used for time advancement. The shock wave could be treated either through resolution of its thickness using a nonuniform mesh or by using a high-order shock-capturing scheme. Turbulent fluctuations were specified at the inflow boundary, nonreflecting boundary conditions were specified at the outflow and normal boundaries, and the spanwise direction was homogeneous.

Accomplishment Description

The interaction of a shock wave of mean Mach number 1.2 with a developed shear flow was computed. A mesh of $191 \times 65 \times 65$ was used to resolve both the turbulence and the thickness of the shock wave. The code ran at 300 MFLOPS with 10 Cray C-90 seconds for each time step. The computation

required about 325 Cray C-90 hours, 8 megawords of core memory, and 40 megawords of scratch disk space. The results were consistent with a linear analysis that predicted large amplification of turbulent kinetic energy and a drop in the Reynolds shear stress across the shock wave (a behavior not predicted by current models). The computation also clearly illustrated the importance of entropy fluctuations in the interaction of shear flows with a shock wave. Currently, shock capturing is used to compute the interaction of a Mach 2 shock with a shear flow.

Significance

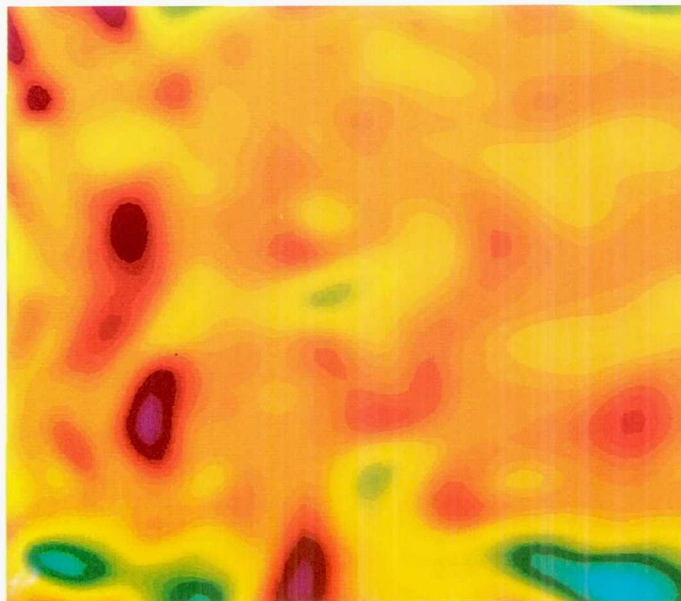
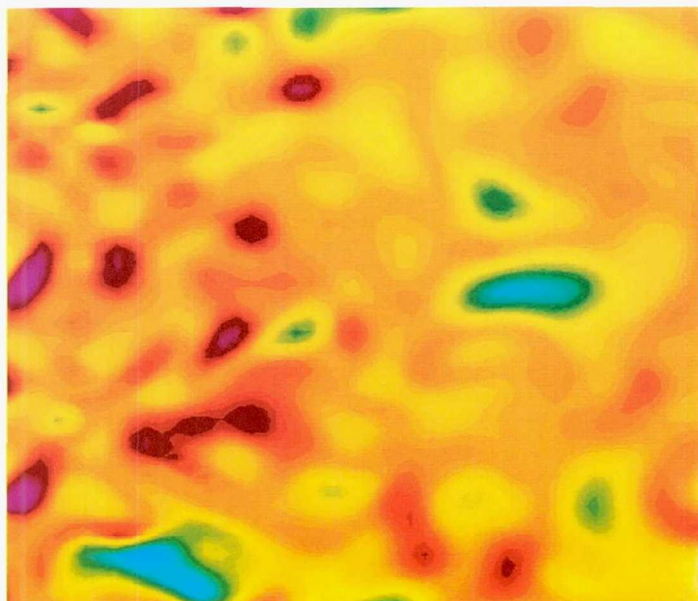
The simulations provide a valuable data base to validate turbulence models as well as to examine the physics involved.

Future plans

Shock capturing will be used to complete computation of shock wave/shear flow interaction.

Keywords

Turbulence, Shock wave, Shear



Instantaneous Reynolds shear stresses in an X-Z plane. The mean flow is from left to right and the shock wave is at the center of the domain. Note the presence of more regions of positive shear stress immediately behind the shock wave.

Large-Eddy Simulation of Separated External Flows

Parviz Moin, Principal Investigator

Co-investigators: Thomas S. Lund, Patrick Beaudan, and Haecheon Choi
Stanford University/NASA Ames Research Center



Research Objective

To assess the accuracy of the dynamic subgrid-scale model for the large-eddy simulation of separated external flows.

Approach

Large-eddy simulations were performed for two external separated flows: a circular cylinder and an airfoil at high angle of attack. A fifth-order-accurate upwind-biased finite-difference scheme was used for the circular cylinder, and a second-order finite-difference scheme was used to simulate the airfoil. For the cylinder wake, simulation statistics were compared with experimental data to assess the effectiveness of the subgrid-scale turbulence model.

Accomplishment Description

Three large-eddy simulations of the circular cylinder flow were performed with a dynamic model, a conventional Smagorinsky model, and a no-subgrid-scale model. The mesh contained $144 \times 136 \times 48$ points in the radial, azimuthal, and spanwise directions, respectively. The wake was resolved accurately for a distance of 10 diameters downstream from the cylinder. Each simulation required approximately 300 CPU hours and about 10 megawords of core memory on the Cray C-90. The simulation with the dynamic model predicts the mean velocity and the random and periodic components of the Reynolds stresses more accurately than the other two models. The figure shows the time- and spanwise-averaged subgrid-scale eddy viscosity obtained

with the dynamic and conventional Smagorinsky model. The dynamic model predicts a maximum level of eddy viscosity near the bubble closure, where mean turbulent production is maximum. Correct prediction of the eddy viscosity in the shear layers is necessary to simulate the transition process accurately, and the dynamic model simulation is superior in this regard. Simulation of flow over a NACA 4414 airfoil at Reynolds number 1.6 million and 12 degrees angle of attack was completed. A closed separation bubble appears near the trailing edge for these conditions. The grid contains $257 \times 70 \times 65$ points in the streamwise, normal, and spanwise directions, respectively. A typical simulation takes 50 Cray C-90 hours and requires 26 megawords of core memory.

Significance

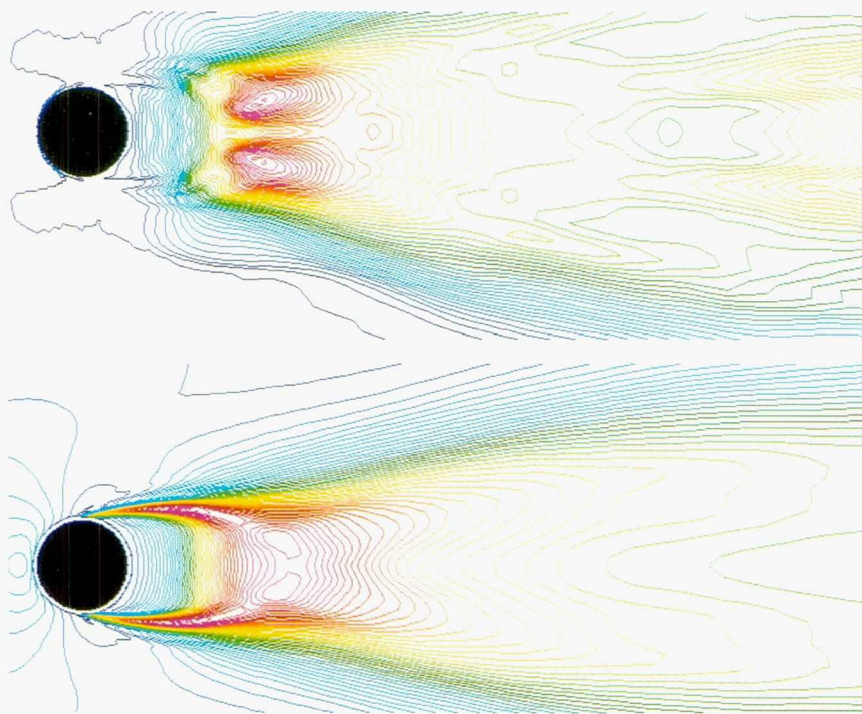
Large-eddy simulation in conjunction with the dynamic subgrid-scale model accurately predicts external flows involving separation. The dynamic model shows a clear advantage over a conventional Smagorinsky model for regions of laminar-turbulent transition.

Future Plans

Simulations of the airfoil at high angles of attack will continue and results will be compared with experimental data.

Keywords

Subgrid-scale modeling, Wake flow, Airfoil



Contours of time- and spanwise-averaged subgrid-scale eddy viscosity normalized by the molecular value; dynamic model (top) and conventional Smagorinsky model (bottom).

Large-Eddy Simulation of Complex Flows

Parviz Moin, Principal Investigator

Co-investigators: Thomas S. Lund and Hans J. Kaltenbach

Stanford University/NASA Ames Research Center



Research Objective

To evaluate the technique of large-eddy simulation in conjunction with the dynamic subgrid-scale model for complex turbulent flows where Reynolds-averaged techniques are subject to considerable error.

Approach

Simulations were performed for two complex turbulent flows: the boundary layer flow over a concave wall and the separated flow in a diffuser. The incompressible Navier–Stokes equations are solved in a curvilinear coordinate system using second-order finite differences. The time advancement is fully implicit and is also second order. The dynamic subgrid-scale model is used to account for the effect of the unresolved turbulent motions.

Accomplishment Description

A large-eddy simulation was conducted where a flat-plate boundary layer encountered a 90-degree constant radius of curvature bend. The Reynolds number based on the momentum thickness of the boundary layer at the start of the curve was 1,200 and the radius of curvature was 18 boundary layer thicknesses. Streamwise Taylor–Görtler vortices induced by the convex curvature were found to significantly alter the mean velocity and turbulent stress profiles and resulted in a 35 percent increase in skin friction. Comparisons with experimental data indicate that the simulation provides an accurate prediction of this flow and shows an improvement over the results of a full Reynolds stress transport model. The mesh contained $178 \times 40 \times 64$ points in the streamwise, wall-normal, and spanwise directions, respectively. A typical run required about 20 Cray C-90 hours and 16 megawords of memory. A second simulation of turbulent flow through a one-sided, 10-degree plane diffuser was performed. Fully developed channel flow enters the diffuser at Reynolds number 18,000 based on bulk velocity and inlet channel height. Results show a significant separation in the rear part of the diffuser and attendant losses in pressure recovery. The mesh contained $160 \times 64 \times 64$ grid points. A typical run required roughly 40 Cray C-90 hours and 12 megawords of memory.

Significance

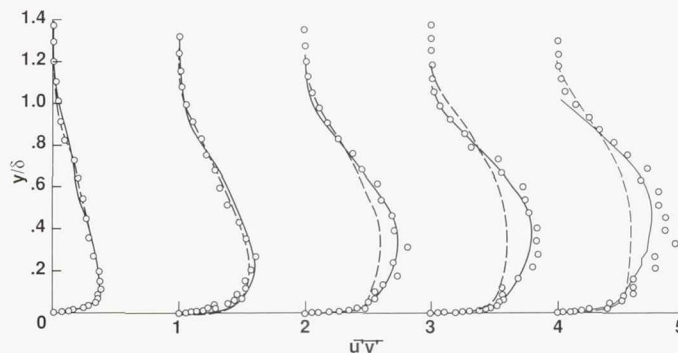
The results of the two simulations indicate that the technique of large-eddy simulation, used in conjunction with the dynamic subgrid-scale model, can accurately predict complex turbulent flows for which Reynolds-averaged techniques are inaccurate.

Future Plans

The relaxation of a boundary layer undergoing transition from convex curvature to a flat section will be simulated. Reynolds-averaged models are inaccurate for this flow. Disturbances will be added to the diffuser flow at the corner in an attempt to control the separation in the aft portion of the device. The simulations will be used to determine optimal disturbance waveforms and to test feedback control strategies.

Keywords

Subgrid-scale modeling, Boundary layer, Diffuser



Reynolds shear stress profiles for the curved-wall boundary layer. From left to right: a flat section that is 8 boundary layer thicknesses ahead of the curve, and 15-, 30-, 45-, and 60-degree stations along the curve. Solid line = large-eddy simulation, dashed line = full Reynolds stress transport model, dots = experimental data.



Instant spanwise velocity for the diffuser flow.

Unsteady Turbulence Model Simulations

Steven A. Orszag, Principal Investigator
Co-investigator: William S. Flannery
Cambridge Hydrodynamics, Inc.



Research Objective

To assess the importance of developing unsteady turbulence transport models for application to real-world engineering problems.

Approach

A very-large-eddy simulation (VLES) model, using turbulence transport equations based on the renormalized group (RNG) theory of turbulence and implemented in the commercial code FLUENT, was used to perform the computations.

Accomplishment Description

The incompressible flow past a simulated compressor trailing edge was considered as a prototype unsteady turbomachinery application. The Reynolds number for the flow was 56,400 based on the diameter of the half-cylinder trailing edge. The inlet was taken at 10.6 diameters upstream where a symmetrical zero pressure gradient turbulent boundary layer was set to match the experimental conditions. A grid of 30,000 cells was used. The time-dependent computations were run until a quasi-steady state was achieved and typically required 25–30 periods of the final shedding cycle. Approximately 8 megawords of memory and about 2 Cray-2 hours were required for each period. The first figure shows the vortex shedding behavior in the wake. Steady state computations of the trailing edge failed to predict the strength of the vortex in the wake and yielded significantly over-predicted wake base pressures. The results were identical to those obtained with a splitter plate in the wake. In the second figure, the time-averaged VLES computation gives rise to a strong pressure minimum in the wake, as does the experiment. The computed Strouhal frequency is 0.2 and is in reasonable agreement with experiment. Also shown in the second figure is a time-averaged computation using the standard $k-\epsilon$ model. Apparently, excessive turbulent production leads to large-eddy viscosities and mean wake vortices that are too weak. The base pressure in the wake is significantly overpredicted by the standard model.

Significance

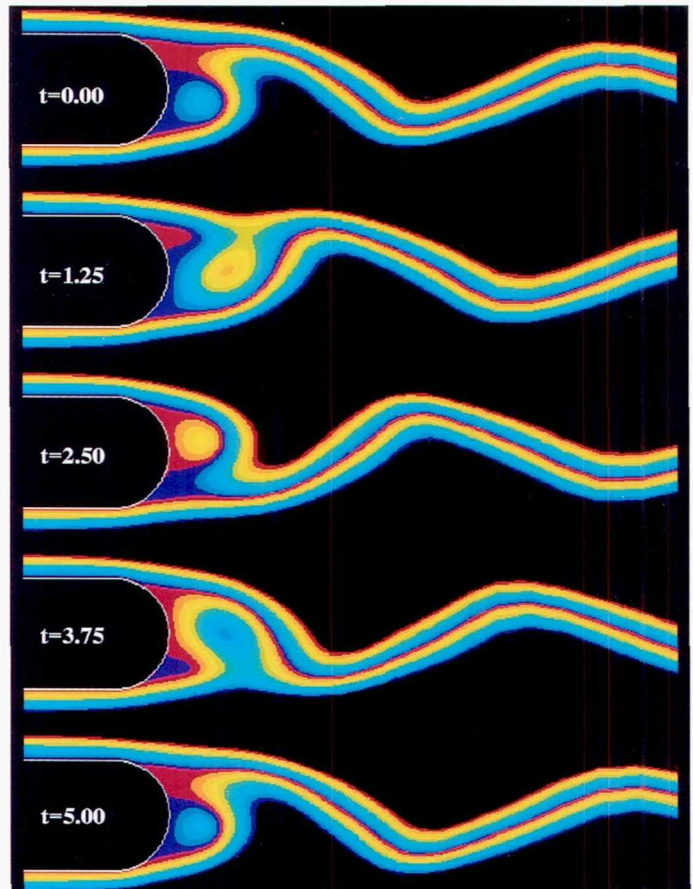
Unsteady simulations are required to accurately predict the effects of large-scale time-dependent structures. The RNG VLES models compute these flows and provide an accurate prediction of unsteady effects.

Future Plans

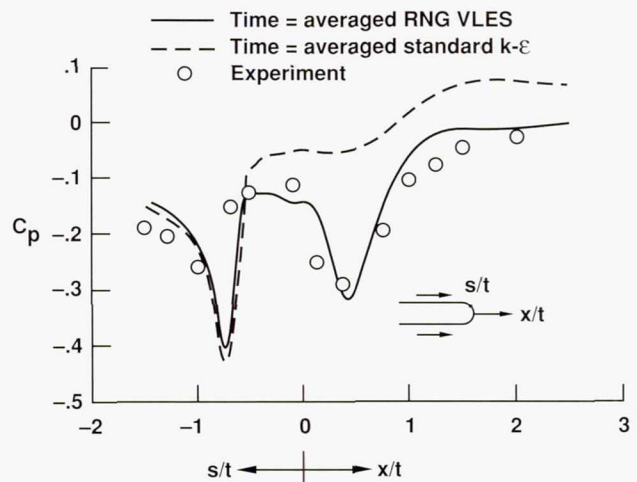
Further studies of other unsteady flows are planned to understand what time-dependent behavior the VLES models capture. In addition to two-dimensional flows, three-dimensional effects on nominally two-dimensional problems will be explored. Finally, some fully three-dimensional studies will be performed.

Keywords

Very-large-eddy simulation, Turbulence transport equations



Streamlines in the wake of a compressor trailing edge over a shedding cycle (Reynolds number = 56,400).



Comparison of time-averaged distributions of pressure with experiment for the flow past a compressor trailing edge (Reynolds number = 56,400).

Three-Dimensional Liquid Sloshing Flow Simulation

Richard H. Pletcher, Principal Investigator

Co-investigators: S. Babu, F. J. Kelecy, and W-P. Wang

Iowa State University



Research Objective

To develop accurate and efficient simulation methods for flows having a free surface, particularly liquid sloshing flows in moving containers, and to evaluate the predictive capability of large-eddy simulations (LES) to accurately resolve flows with complexities such as heat transfer and recirculation.

Approach

Current free-surface research focused on using surface fitting and surface capturing to compute three-dimensional (3-D) liquid sloshing flows in moving containers. The incompressible Navier–Stokes equations were solved using the artificial compressibility method and a fully coupled, implicit discretization in both schemes. The LES study employed a preconditioned (for low-Mach number efficiency), fully coupled, upwind finite-volume discretization of the filtered compressible Navier–Stokes equations in primitive variables. The convective terms were discretized with third-order quick-type upwinding while fourth-order central differencing was used for the viscous terms.

Accomplishment Description

A new calculation procedure that iteratively approaches second-order temporal resolution of the free-surface motion was devised. Results for the 3-D broken dam problem were in good agreement with experimental data (first figure). Several free-surface flows were computed using the surface capturing approach, including the broken dam problem, the Rayleigh–Taylor instability, and an axisymmetric spin-up in a spherical tank. The current LES approach was tested on a planar channel flow and was in reasonable agreement with published results. LES of channel flow with a low level of heat transfer (with both the uncoupled passive scalar equation and the coupled fully compressible energy equation) was accomplished. A typical computation used 250,000 grid points with 50–90 megawords of memory and 25–50 Cray C-90 hours. The second figure shows the instantaneous temperature contours at different spanwise locations for the case of compressible LES channel flow with low heat transfer rate and a Mach number of 0.01.

Significance

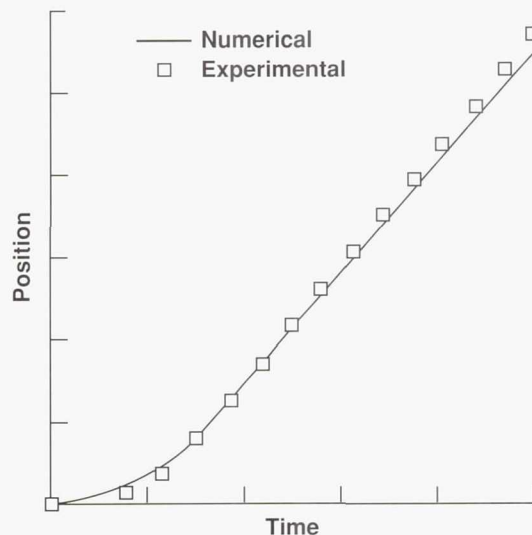
The ability to numerically simulate the motion of liquids in partially filled containers and the resulting interactions with structures is important for the design of liquid management systems for many space applications and more traditional applications. Turbulent flow represents one of the major pacing items restricting the usefulness of computational fluid dynamics for realistic design applications. A goal of the LES research is to take advantage of rapidly developing computer technology to advance the predictive capabilities of the approach toward larger and more relevant problems.

Future Plans

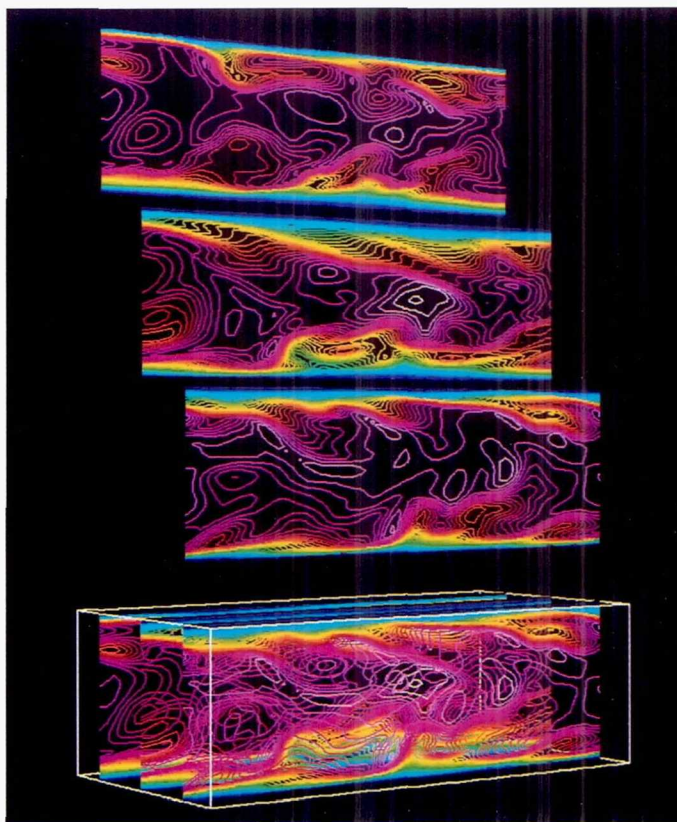
The surface fitting code will be used to compute flows under microgravity environments. Work is under way to perform the LES of variable-property channel flow with massive heat transfer to study the changes in turbulent statistics.

Keywords

Large-eddy simulation, Free surface, Turbulence



Comparison of predicted and measured surge front location for the 3-D broken dam problem.



Instantaneous nondimensionalized temperature contours at three spanwise locations; blue = low temperature and red = high temperature. Flow is from left to right.

Direct Simulation of Turbulent/Transitional Airfoil Flow

Man Mohan Rai, Principal Investigator
NASA Langley Research Center



Research Objective

To perform direct simulations of turbulent/transitional flow over a turbine airfoil.

Approach

High-order-accurate, upwind-biased, finite-difference methods were used to perform direct simulations of compressible turbulent/transitional flows over complex geometries.

Accomplishment Description

A program to compute turbulent/transitional flows over an airfoil cross section was developed. This code was used to compute the flow over a turbine airfoil cross section using a grid with about 20 million points (a grid with 40 million grid points probably will be required for the final computation). The figure shows instantaneous velocity contours very near the airfoil surface. The figure shows the isolated patches of vorticity immersed in relatively quiescent regions (near the leading edge). Further downstream there is an abrupt appearance of vortical structures indicating that the transition process is essentially complete.

Significance

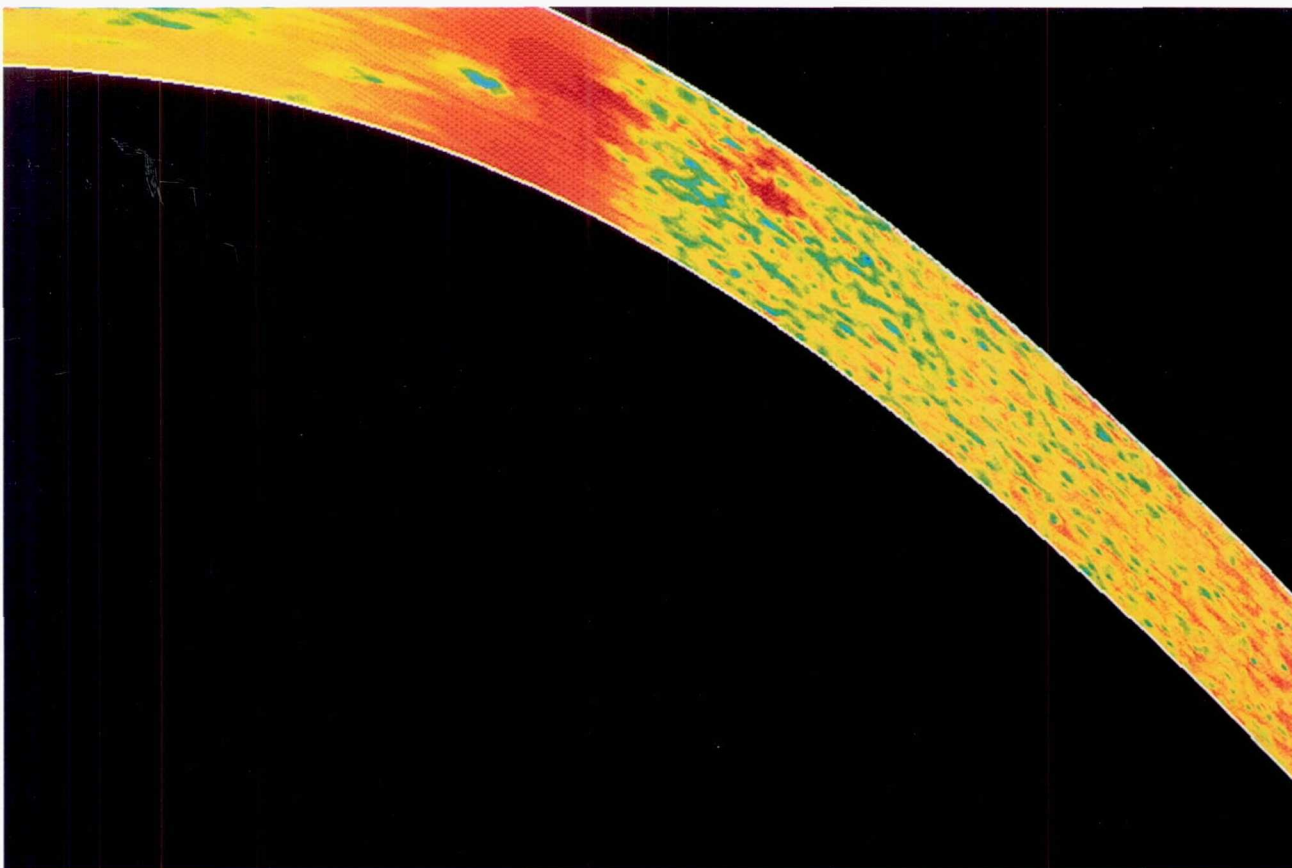
When complete, this work will be the first direct simulation of this kind for turbulent/transitional flow over an airfoil cross section. The computed data will be used to understand the transition process on a turbine airfoil and also to develop improved turbulence and transition models for large-eddy simulations and Reynolds-averaged Navier–Stokes simulations. The methodology and computer program developed during this effort will serve as a basis for future direct simulations of flow over complex geometries.

Future Plans

This computation will be continued on a grid with approximately 40 million grid points and a statistical sample will be obtained.

Keywords

Direct simulation, Turbulence



Instantaneous velocity contours just above the suction surface ($y^+ = 1.0$) of a turbine airfoil with flow direction from left to right. The leading edge is at the upper left section of the figure and the trailing edge is at the lower right section of the figure.

Self-Similar Turbulent Plane Wakes

Michael M. Rogers, Principal Investigator

Co-investigators: Robert D. Moser, S. Scott Collis, and Chris Rutland

NASA Ames Research Center/Stanford University/University of Wisconsin, Madison



Research Objective

To study the effects of two-dimensional (2-D) forcing on structures, statistics, and chemical reactions in incompressible fully turbulent self-similar plane wakes.

Approach

Direct numerical simulations of temporally evolving incompressible turbulent plane wakes were generated with various levels of 2-D forcing, using previously simulated turbulent boundary layers to provide a realistic turbulent initial condition. Pseudo-spectral numerical methods were used to solve the three-dimensional Navier–Stokes equations.

Accomplishment Description

Two fully turbulent wakes with half-width/velocity-deficit Reynolds numbers of about 2,000 were simulated. A passive scalar quantity was also computed to permit the study of “fast” chemical reactions. In one case, no 2-D forcing (beyond what is present in the initial boundary layers) was used, whereas the other case was strongly forced. The unforced case evolved self-similarly, with mean velocity and Reynolds stress profiles that collapsed when scaled by the layer thickness (which increases like the square root of time) and the velocity deficit (which decreases like the square root of time). The forced case underwent a shorter period of more approximate self-similarity. The unforced wake spreads more slowly than experimental wakes, but the forced

case spreads much more rapidly. This increased spreading rate is associated with a corresponding difference in flow structure. Whereas the unforced wake appears as a somewhat homogeneous slab of vortical fluid, the forced wake exhibits a more organized large-scale structure that is suggestive of a Karman vortex street (see figure). The Reynolds stress levels also increase when forcing is used, but normalizing them by the wake growth rate improves the agreement between the two cases and experiments. The simulations require up to $600 \times 260 \times 160$ modes. The two simulations required a total of about 750 Cray C-90 hours, 10 megawords of core memory, and up to 170 megawords of solid state device space.

Significance

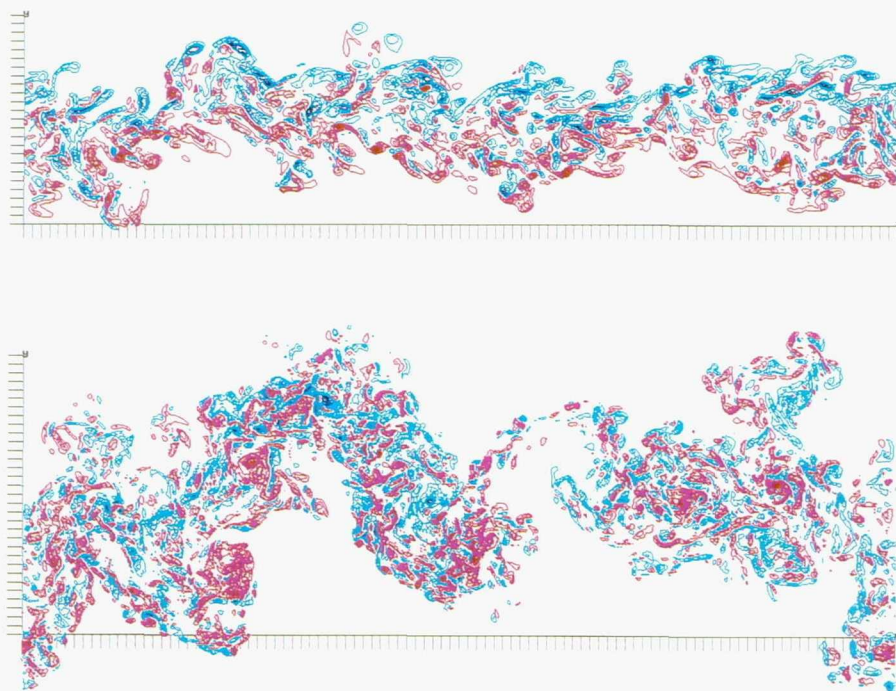
These simulations are the first turbulent wake direct numerical simulations to achieve self-similarity. The strong effect of forcing on the wake growth rate and structure helps explain discrepancies in experimental observations by different investigators.

Future Plans

To numerically simulate turbulent plane wakes subjected to mean strain in order to provide data that will assist in the development of models for high-lift airfoils.

Keywords

Direct numerical simulation, Free-shear flows



Spanwise vorticity contours (red = positive, blue = negative) in the self-similar period for the unforced wake (top) and strongly forced wake (bottom). Views are at typical spanwise locations, with a horizontal streamwise direction.

Origins of Near-Wall Turbulence

Bart A. Singer, Principal Investigator

Co-investigator: Ronald D. Joslin

High Technology Corporation/NASA Langley Research Center



Research Objective

To identify and understand the mechanisms involved in the formation and growth of boundary layer turbulence.

Approach

Spatial direct numerical simulations (DNS) of the incompressible Navier–Stokes equations were used to generate the data for this study. Data visualization was performed using the flow analysis software tool.

Accomplishment Description

In the past, hairpin vortices were generated by a variety of localized wall disturbances. In one case, the hairpin vortex grew, elongated, and spawned a secondary vortex head upstream of the primary, and a subsidiary vortex developed underneath the hairpin vortex legs. This study continued the DNS into the early stages of turbulence. The resolution requirements for the calculation required over 20 million grid points and the memory requirement was approximately 440 megawords. Approximately 1,000 Cray C-90 hours were used in the computation. Although the mean flow did not develop a log-layer profile, many features characteristic of fully turbulent flow were observed. Multiple additional vortices developed in the flow, which generated newer vortices in the near-wall region. The regeneration of new vortical structures is a poorly understood feature of turbulent flows. In the calculations, one particularly common sequence for vortex regeneration was illustrated. The figure shows activity on a cross-sectional plane that cuts through the middle of a large quasi-streamwise vortical structure. One long spiraling line on the right

indicates the circulating flow associated with the leg of the large vortex. This vortex induces a flow of near-wall fluid to the left. Two streamlines show flow from right to left near the wall. The fluid cannot continue into the region of higher pressure near the wall and must separate from the wall. A single streamline restricted to the plane is shown going from left to right. Where it meets the streamlines that go from right to left, all of them lift away from the wall and concentrate in a relatively narrow band. The rising fluid creates a new vortex to the left of the ejection zone.

Significance

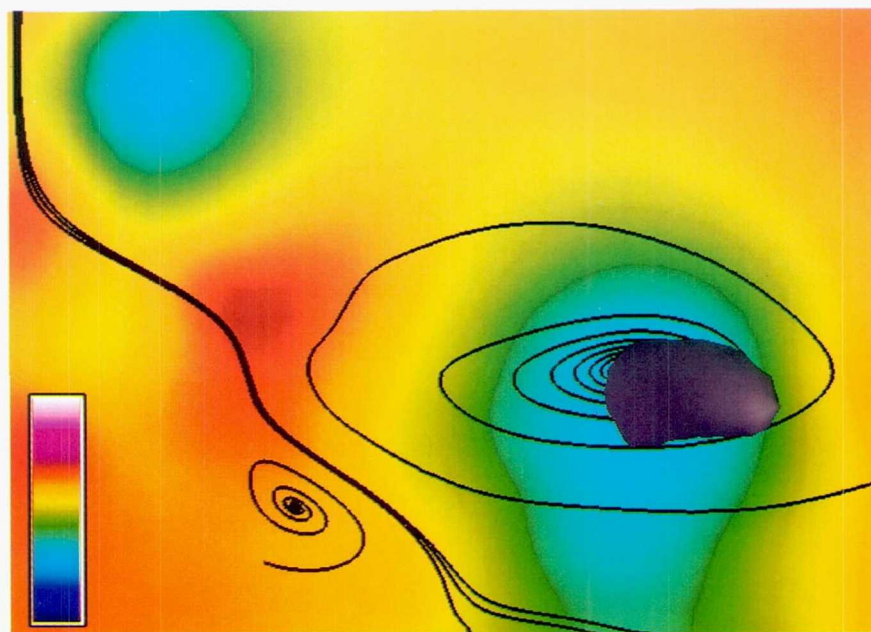
This work provides a better understanding of the way in which coherent flow structures evolve from a single localized disturbance into a group of structures that form the early stages of turbulence. It provides clues as to what kinds of structures dominate the flow and how these structures interact and regenerate, making the flow more turbulent. These insights will lead to more realistic models for predicting turbulent and transitional flows.

Future Plans

The calculation will be continued until a fully developed turbulent boundary layer is obtained. Data will be analyzed to understand how the various types of vortices form, interact, and regenerate. The role that vortices play in engulfing new fluid into the turbulent region will be studied.

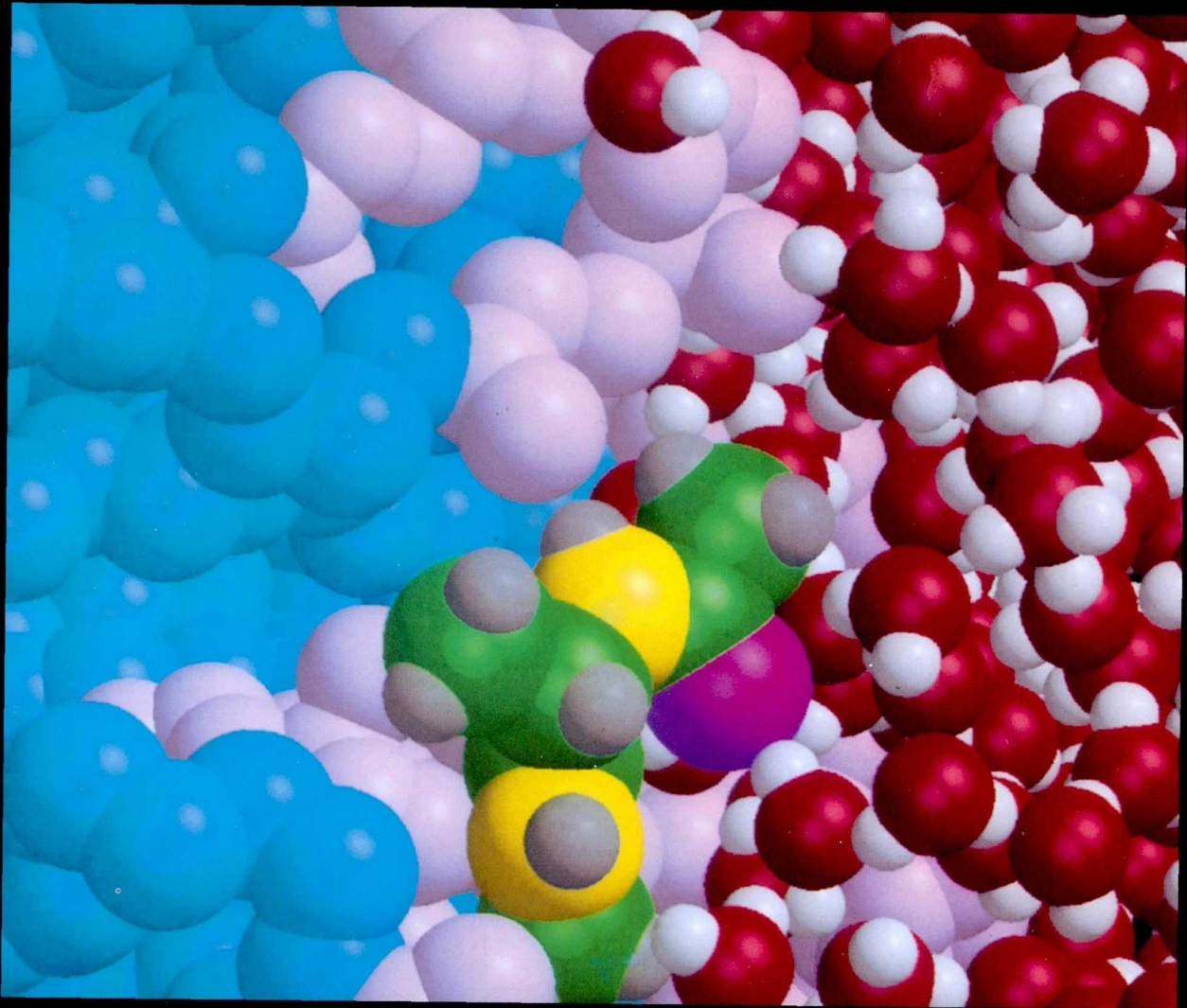
Keywords

Turbulence, Transition, Vortices, Turbulent spot



Cross-sectional plane at $x = 98.7$ and $t = 97.2$. Insert at left indicates pressure levels; high pressure is near top and low pressure is near bottom. The black surface on right is a portion of large vortex that protrudes upstream of the plane. The black lines are streamlines restricted to plane.

General



Aeroacoustics
Astronautics
Astronomy
Atmospheric Science
Chemistry
Computer Science

Electromagnetics
Fluid Mechanics
Life Science
Magnetospheric Physics
Reactive Flow
Space Science

Page intentionally left blank

Hybrid Massively Parallel Aeroacoustics Scheme

Lyle N. Long, Principal Investigator
Pennsylvania State University



Research Objective

To analyze sound propagation and radiation in high-bypass-ratio ducted fans. This research is focused on sound propagation in nonuniform engine inlets and radiation of that sound to free space.

Approach

A hybrid scheme that solves the three-dimensional Navier–Stokes equations in the near field and then uses a moving Kirchhoff surface to predict the far field is implemented. The equations are solved in a time-accurate manner using a finite-difference scheme and Runge–Kutta time marching. This code is fourth-order accurate in space and time. The solution from the code is passed to the Kirchhoff surface routine and works well. Nonreflecting boundary conditions are important in computational aeroacoustics and also work well. Preliminary results show that the schemes are effective on the massively parallel computers.

Accomplishment Description

This scheme was validated by comparing steady-state and unsteady predictions to analytical and experimental data. The scheme predicted the transonic flow over a transonic airfoil, a moving and pulsating sphere, and the flow field of a high-bypass-ratio engine inlet. The code requires more than 1 gigabyte of memory for each simulation.

Significance

Future commercial aircraft engines will have very high bypass ratios. The noise from these engines will be difficult to predict because of the very short ducts. In addition, fan noise will become a significant noise source. The hybrid scheme in this research addresses these noise issues.

Future Plans

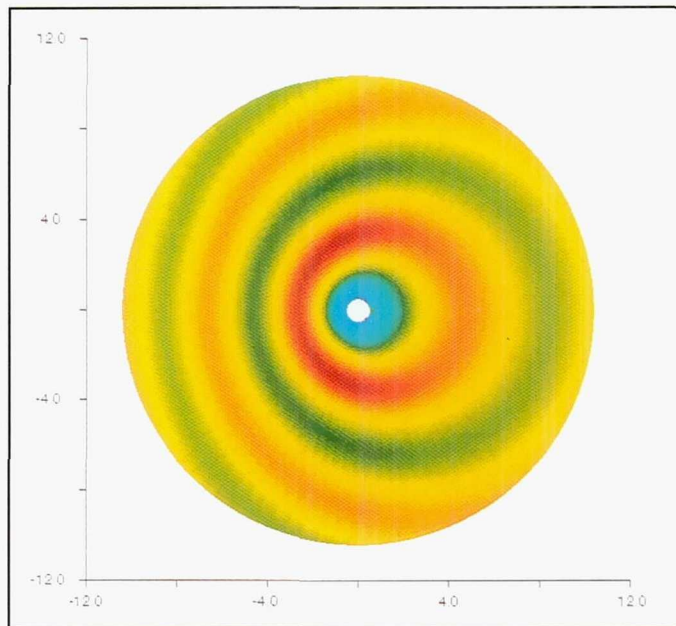
Turbulence and engine liner models will be incorporated in the scheme.

Keywords

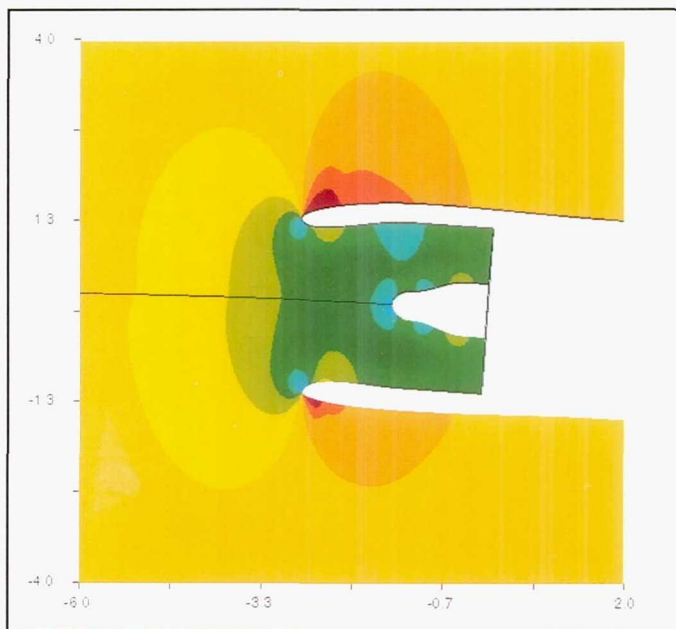
Computational fluid dynamics, Navier–Stokes, Noise

Publications

1. Chyczewski, T. S.; and Long, L. N.: An Efficient Higher Order Accurate Parallel Algorithm for Aeroacoustics Applications. AIAA Paper 94-2265, June 1994.
2. Ozyoruk, Y.; and Long, L. N.: A Navier–Stokes/Kirchhoff Method for Noise Radiation from Ducted Fans. AIAA Paper 94-0462, Jan. 1994.
3. Weinberg, Z.; and Long, L. N.: A Massively Parallel Solution of the Three-Dimensional Navier–Stokes Equations on Unstructured, Adaptive Grids. AIAA Paper 94-0760, Jan. 1994.



Euler solution of a pulsating sphere moving at Mach 0.3.



Navier–Stokes solution of flow field over a General Electric engine at Mach 0.82.

Evolution of Planetary Rings

Creon Levit, Principal Investigator
NASA Ames Research Center



Research Objective

To gain insight into the dynamics of the f-ring region of Saturn. The techniques can be applied to the study of other planetary ring systems, and asteroidal, cometary, and planetary systems stability.

Approach

A celestial mechanics algorithm was implemented that integrates the trajectories of a small number of mutually interacting massive perturbers with a large number of massless test particles in orbit around a large central body. The algorithm is based on a technique that assumes near-Keplerian orbits for all of the bodies. Collision detection, a nonspherical central force field, and smooth initiation of tidal acceleration are interesting features of the code.

Accomplishment Description

The code was implemented, calibrated, and put into production. Several simulations of the evolution of Saturn's f-ring region were run with different initial conditions for the test particles beyond a million orbits. Complete data for all bodies were saved every 500 orbits and analyzed graphically. Approximately 200 CM-5 hours were used for the simulations.

Significance

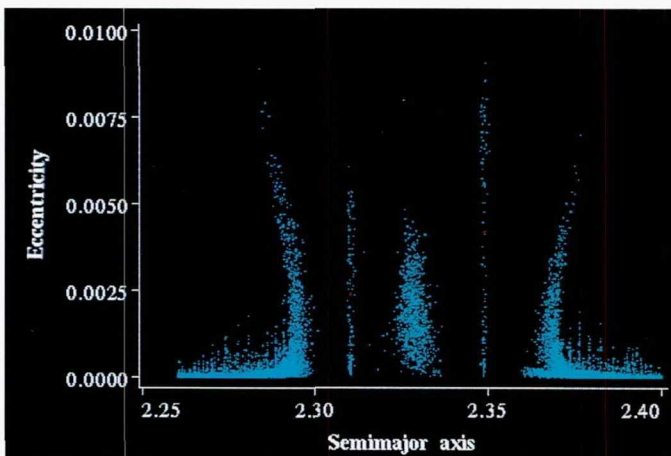
The detailed structure of Saturn's rings still contains many structures whose origins are a mystery. The pattern of ringlets in Saturn's f-ring or the overall structure of the b-ring can be simulated and analyzed with the code, as can Neptune's arc-like rings. The code is also being used to simulate the orbital stability of planets around binary stars.

Future Plans

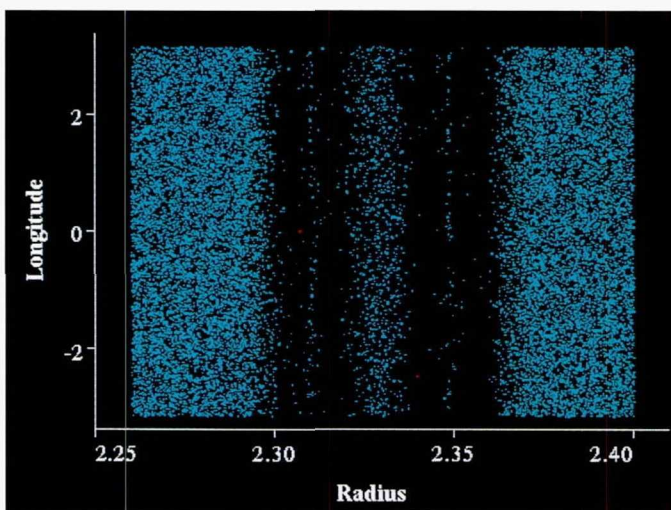
Dynamics of the f-ring region will be simulated in more detail by including additional perturbers, a wider variety of initial conditions, and dissipative forces on the test particles. The dynamics of the b-ring region will be simulated. Stability of planetary orbits in hypothetical solar systems will be tested.

Keywords

Gravitation, Dynamics, Solar system



(a)



(b)

Distribution of bodies in Saturn's f-ring region ($0.10755E + 07$ orbits). Surviving test particles are cyan, and Saturnian moons Prometheus and Pandora are red. (a) Eccentricity distribution (note the resonance at the far right and far left). (b) Physical distribution (note the lanes cleared by collisions and the thin bands of particles in horseshoe orbits).

Simulating the Cosmic X-Ray Experiment

James Caristi, Principal Investigator

Co-investigators: Brian Ramsey, Martin Weisskopf, and Jeff Youngen

Valparaiso University/NASA Marshall Space Flight Center



Research Objective

To construct an incident versus detected energy response matrix of the cosmic x-ray experiment (CXE) high-energy detector 1 (HED1), and to use this response matrix to examine the spectral measurement of the cosmic x-ray background from the CXE.

Approach

A Monte Carlo simulation of the HED1 gas proportional counter was applied. Simulation programs were parallelized and used a high-quality random number generator with very large periods. The simulation code included the photon and electron interaction physics, the atomic rearrangement physics following active xenon gas ionizations, the mechanical copper collimator, and the detector housing and shielding. The photons were isotropically incident on the top of the collimator. The CXE detector consisted of two layers of two alternating detection cell types that were below two different mechanically collimated fields of view (FOV). Taking the difference between signals removes many inherent detector backgrounds.

Accomplishment Description

Over 40 billion photons have been simulated in runs of mono-energetic incident photons from 5 to 85 keV (in 5 keV steps). The simulations indicate that effects typical at energies above 25 keV may not have been fully accounted for in the original analysis.

Significance

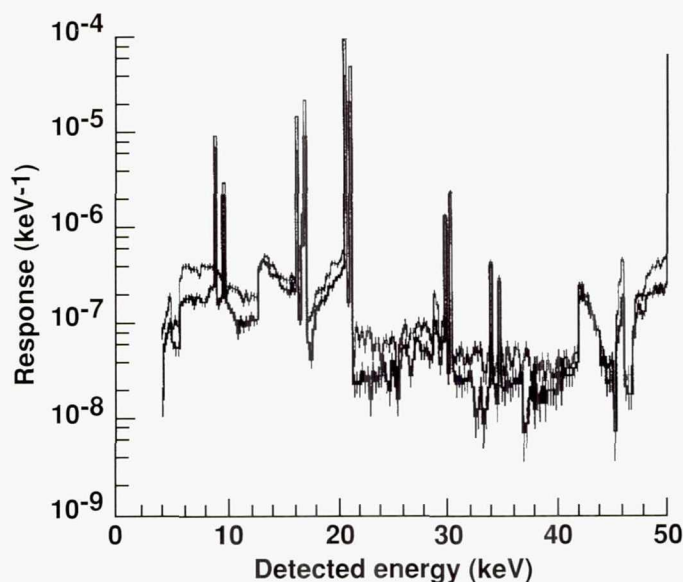
The CXE is the only experiment that has measured the spectrum of the cosmic x-ray background. A response matrix different from that used in the original analysis will change the measured spectrum, which will have a profound effect on the cosmological models currently employed to produce the spectrum of the x-ray background.

Future Plans

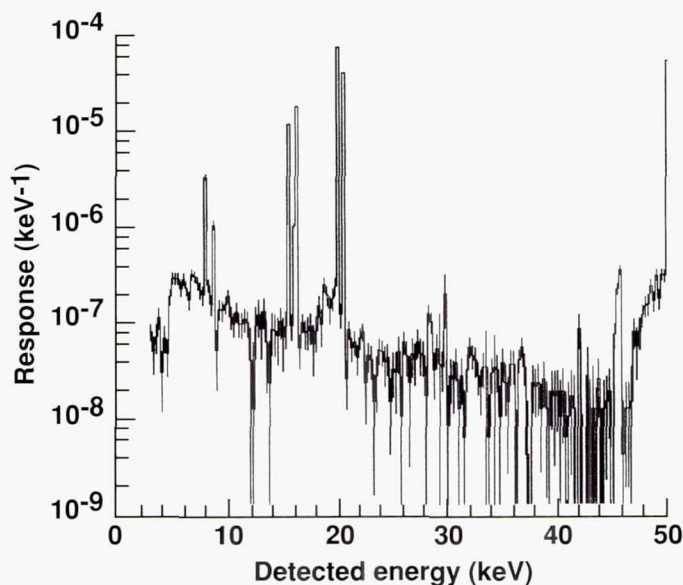
Higher fidelity simulations in excess of 100 billion photons will be run with a continuous incident spectrum from 3 to 100 keV. The high-fidelity simulations will be used to construct a new detailed response matrix for the CXE HED1 detector.

Keywords

Proportional counters, Instrumental response function



Detector response for 50 keV incident photons for the large (thin line) and small (thick line) FOV detection cells in the first layer of HED1.



Response difference between the large (thin line) and small (thick line) FOV detection cells in the first layer of HED1.

Studies of Galaxy Formation and Evolution

Bruce F. Smith, Principal Investigator

Co-investigators: Richard A. Gerber, Richard H. Miller, and Thomas Y. Steiman-Cameron

NASA Ames Research Center/University of Chicago



Research Objective

To use numerical experiments to understand the important physical processes at work in the formation and evolution of galaxies.

Approach

The development of particle and gas dynamics codes was exploited to investigate the dynamics of galaxy models and interactions of galaxies in clusters of galaxies. The codes allow the investigator to follow the time development of fully self-consistent, three-dimensional galaxy representations. The codes follow up to 10^7 particles representing both stars and the gas in the interstellar medium. Forces and potentials are computed on a 256^3 grid.

Accomplishment Description

The particle codes were used to extend earlier experiments that indicated that galaxies are not in a steady state. Global and local modes of oscillations in galaxy centers were identified. These results led to the consideration of the long-term behavior of galaxy oscillations. The long-term survival of multiple galactic nuclei was investigated using the Cray C-90. Galaxy interactions were studied to understand the stellar and gaseous responses in a

collision. These experiments used a disk galaxy model composed of stars and gas embedded in a dark matter halo.

Significance

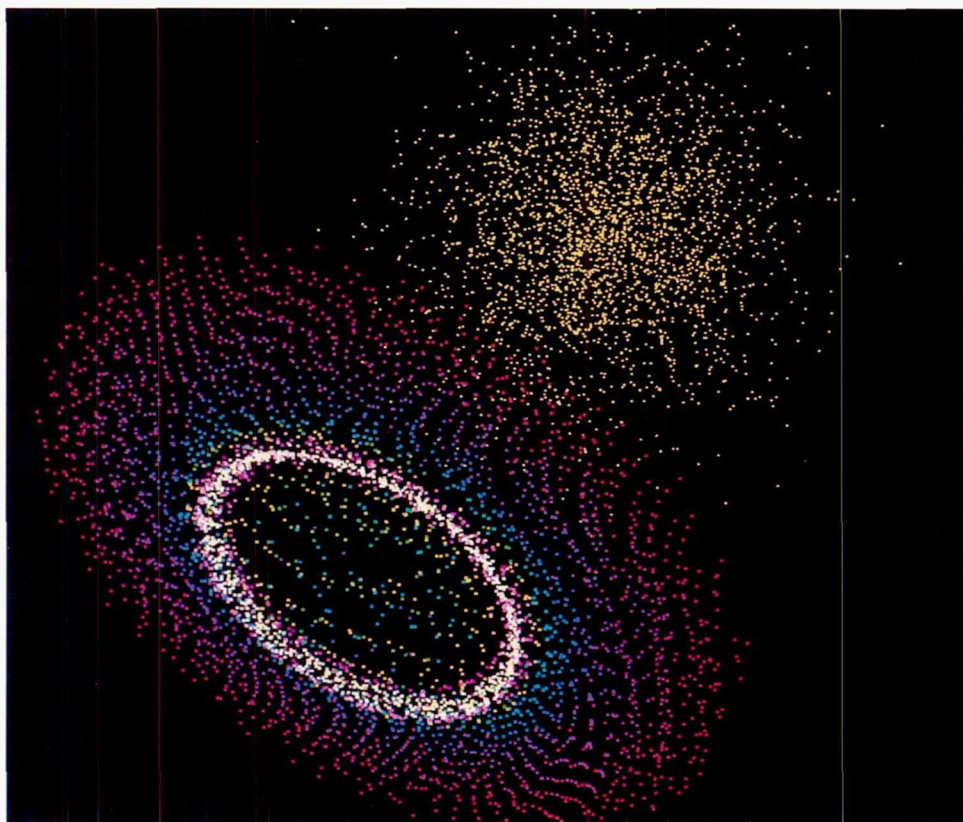
Observations of galaxies provide improved higher spatial and spectral resolution. The experiments, significantly improved, are needed to understand observations from the Hubble Space Telescope and other observational instruments. Recent observations indicate complex galaxy nuclei that are also indicated in the numerical experiments. The experiments on the collision of a disk galaxy with another galaxy will help in understanding the star formation processes in starburst galaxies.

Future Plans

The star formation process in interacting galaxies and galaxies in general will be investigated. This requires a more sophisticated treatment of the interstellar medium in a galaxy. The dynamic evolution of disk galaxies composed of both stars and galaxies will also be investigated.

Keywords

Dynamics, Stellar systems



The development of a ring structure (bottom left) in a disk galaxy after a collision with an elliptical galaxy (top right).

Intraseasonal Atmospheric Oscillations

Christian L. Keppenne, Principal Investigator
Jet Propulsion Laboratory



Research Objective

To use a global multilevel atmospheric model to investigate intraseasonal atmospheric oscillations in the Northern Hemisphere.

Approach

A global multilevel spectral-transform model of Earth's atmosphere was run for 18 years at a resolution equivalent to a grid point model on a 2° longitude \times 2° latitude grid. The data corresponding to the last 15 years of the run history were analyzed using a variant of empirical orthogonal function analysis in time and space. The results were compared with results from observational studies.

Accomplishment Description

The intraseasonal variability of the model is dominated by 3 oscillations with average periods near 70, 40, and 25 days. These periods are also present in a data set of observed atmospheric angular momentum (AAM). The spatial variability associated with the three oscillations is examined by compositing the stream function-anomaly fields of the model. As was found in observational studies, the resulting composites show that the 40-day oscillation is dominated by a standing zonal wave-number-two pattern over the Northern Hemisphere topography. Substantial mass transfer occurs between this midlatitude, wave-number-two component of the 40-day oscillation and a zonally symmetric, tropical component. The 70-day oscillation is associated with mixed wave-number-one to -three patterns and—even though a similar oscillation is present in a single-layer version of the model—has a pronounced vertical shear at all latitudes. The 25-day oscillation is reminiscent (in some aspects) of the westward-traveling wave studied by Branstator and Kushnir. It also exhibits noticeable shear in the tropics and is absent from the single-layer model. Phase relationships between adaptively filtered time series of the AAM for both layers over the cycle of each oscillation are examined as well.

Significance

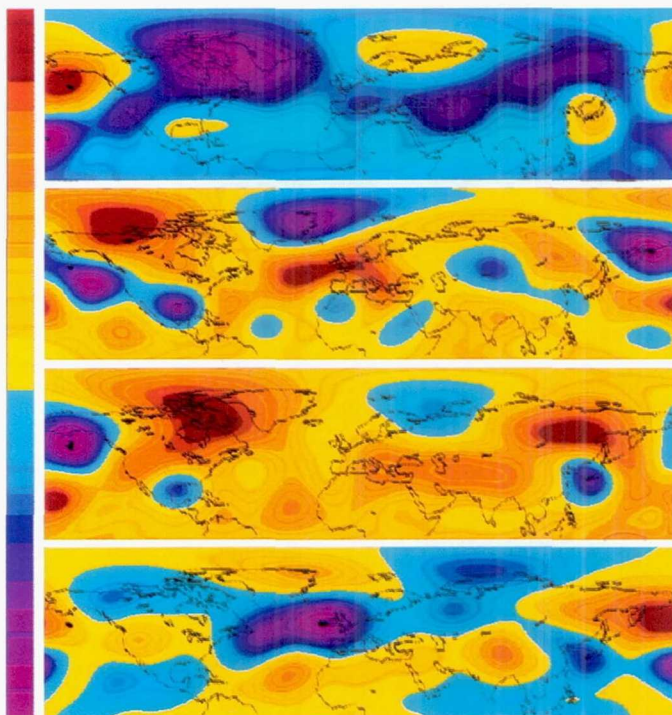
Our findings suggest that the 70-, 40-, and 25-day intraseasonal oscillations detected in observational studies are associated with non-zonal instabilities of the Northern Hemisphere jet caused by its interaction with the mountain field.

Future Plans

The bifurcation structure of the model will be analyzed in detail to identify the mechanisms that lead to non-zonal instabilities.

Keywords

Climate, Subannual variability



Model composite maps of the stream function-anomaly field at the 500 millibar level showing four stages of the dominant 40-day Northern Hemisphere oscillation. From top to bottom: phases associated with high, decreasing, low, and increasing levels of AAM.

Dynamics of the Martian Atmosphere

James B. Pollack, Principal Investigator

Co-investigator: Robert Haberle

NASA Ames Research Center



Research Objective

To simulate the present and past climate regimes on Mars. The primary tool used is a general circulation model (GCM) of the Martian atmosphere that predicts the time-evolving three-dimensional wind and temperature fields, the surface pressure, temperature, and carbon dioxide (CO_2) ice abundance fields, and atmospheric water vapor and dust abundance fields.

Approach

The Mars GCM is based upon the primitive equations of meteorology. Physics unique to Mars, including condensation and sublimation of the CO_2 (the main atmospheric constituent) are included. The Mars GCM is interfaced with an aerosol physics model to study dust transport and the impact of the absorption of sunlight by dust on temperatures and winds. Water vapor transport and its sublimation and condensation are also included in the model.

Accomplishment Description

A complete year (669 Martian days) was simulated. This simulation allowed investigation of the radiative properties (albedo, emissivity) of the CO_2 ice in the polar regions and their effects upon the annual atmospheric mass (CO_2) cycle. Calculated surface pressures at model grid points closely corresponding

to the Viking lander locations favorably compared with the observed pressures (see figure). A complete simulation required 12 Cray C-90 hours, 3 megawords of memory, and generated 12 gigabytes of output for analysis.

Significance

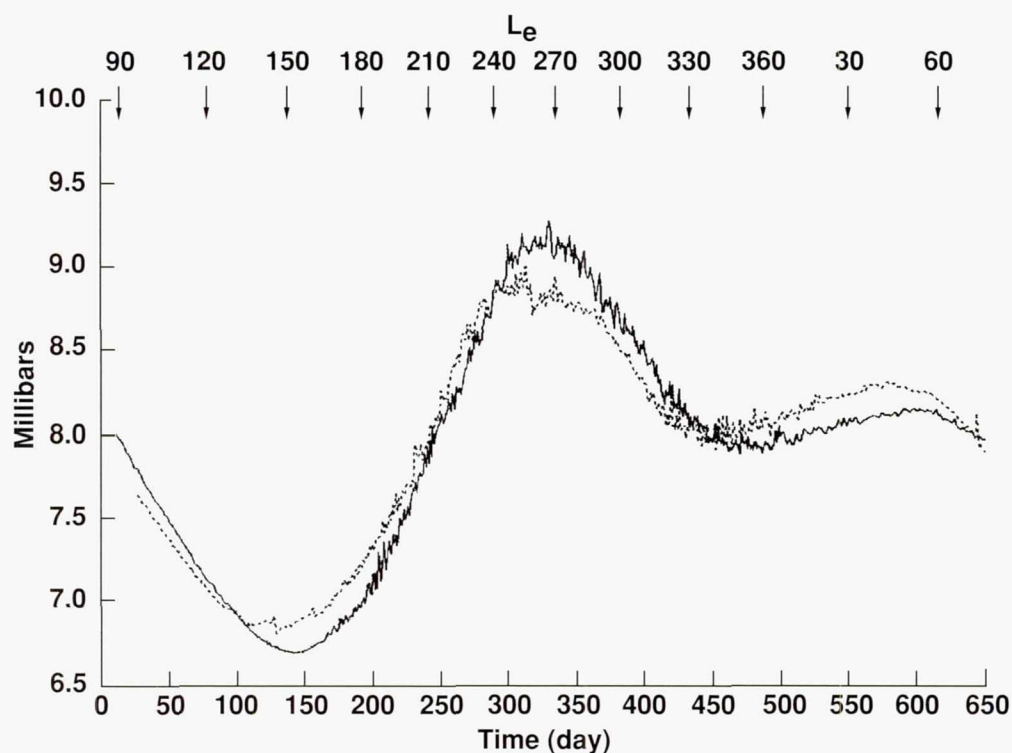
The Martian atmosphere is the best solar system analogue for the terrestrial atmosphere. Application of similar models to both atmospheres and analyses of their results illustrate similarities and differences between the two environments. On Earth, condensation and sublimation of water are the important energy sources and sinks of heat to the atmosphere. On Mars, which is much more arid, the absorption and emission of radiant energy by dust is the important source of atmospheric heating.

Future Plans

The ability to accurately simulate the Martian atmospheric circulation will be improved to come closer to the ultimate goal of having a single model to study the interactive nature of the circulation and the annual and multi-annual cycles of Mars' geophysically important CO_2 , dust, and water cycles.

Keywords

General circulation model, Martian atmosphere



Daily averaged surface pressure (millibars) measured at the Viking lander 1 site (dashed line) and calculated at the model equivalent location (solid line) from an annual simulation representative of the first Viking year. L_e is a seasonal indicator, with $L_e = 90$ at northern summer solstice, $L_e = 180$ at northern autumn equinox, $L_e = 270$ at northern winter solstice, and $L_e = 360$ at northern spring equinox.

Simulation of Volcanic Aerosol Clouds

Richard E. Young, Principal Investigator
Co-investigators: O. B. Toon and H. Houben
NASA Ames Research Center



Research Objective

To numerically simulate the behavior of the El Chichon and Mt. Pinatubo volcanic aerosol clouds in the stratosphere to better understand stratospheric transport and aerosol microphysical processes. An associated goal is to assess the climatic impact of such large volcanic eruptions on stratospheric wind and temperature fields.

Approach

A three-dimensional (3-D), spectral, primitive-equation model is used to compute wind and temperature fields in the stratosphere. This model is coupled with a 3-D aerosol transport and microphysical model that computes the dispersion of the volcanic aerosol cloud using the computed winds from the circulation model. The model accounts for sedimentation and coagulation of the aerosol particles.

Accomplishment Description

Work concentrated on simulating the behavior of the El Chichon volcanic cloud and comparing it to the behavior of the Mt. Pinatubo cloud. Prior to the Mt. Pinatubo eruption in June 1991, El Chichon represented the largest volcanic eruption this century (April 1982). In terms of dispersion in the stratosphere, the two volcanic clouds behaved quite differently. A series of 2–3 month simulations indicate that most of the difference in behavior between the volcanic clouds is due to interannual variability in stratospheric wind fields. The difference in cloud absorption of radiative energy from the troposphere also contributes to the difference. A 3-month simulation requires about 4.5 Cray C-90 hours and 18 megawords of memory. Simulation results are generally in good agreement with the extensive

data sets that exist for both aerosol clouds. The figure compares the dispersion of both clouds 21 days after each volcano erupted.

Significance

The principal goal of several major NASA programs is the study of the stratospheric climatology. Further, the High-Speed Research Program is sponsoring research to assess the climatic impact of high-speed aircraft operating in the lower stratosphere. Unique opportunities to better understand stratospheric transport and aerosol microphysical processes occurred when the El Chichon and Mt. Pinatubo volcanoes erupted. By simulating the behavior of the volcanic clouds theoretical understanding of transport and aerosol processes in the stratosphere can be assessed and improved.

Future Plans

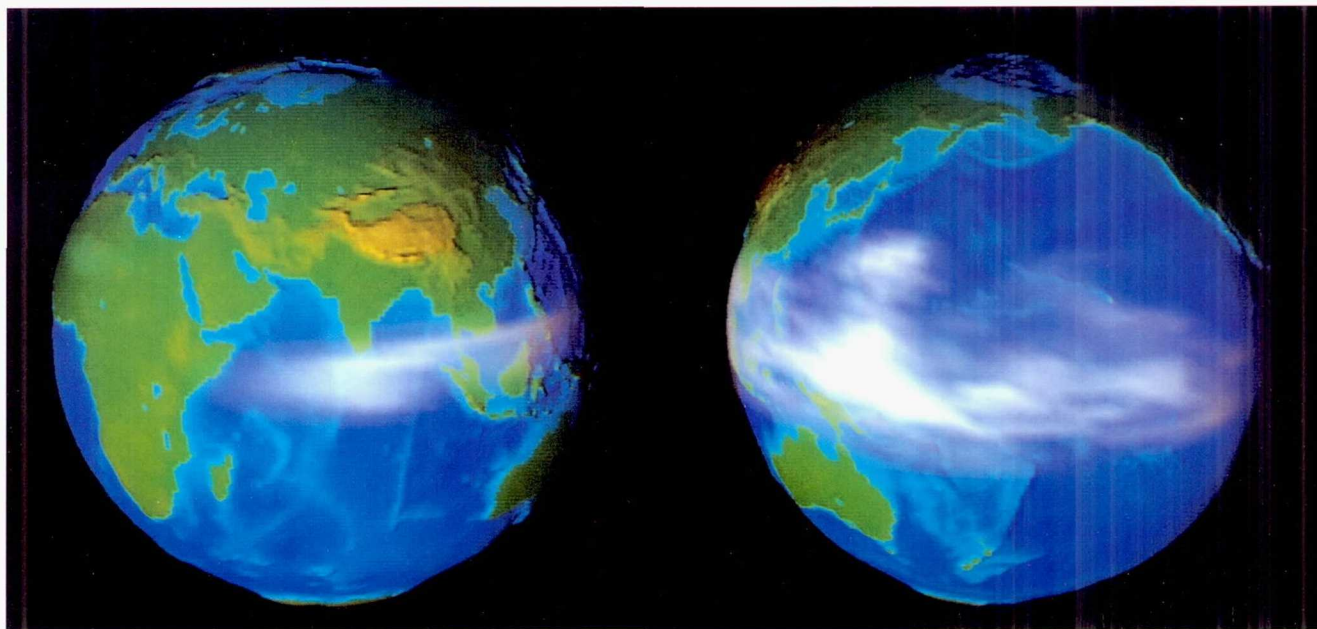
Multi-year simulations of the Mt. Pinatubo and El Chichon volcanic aerosol clouds will be conducted using passive tracer and interactive modes. Climatic feedback about the stratosphere will be assessed.

Keywords

Stratospheric transport, Climate

Publication

Young, R. E.; Houben, H.; and Toon, O. B.: Radiatively Forced Dispersion of the Mt. Pinatubo Volcanic Cloud and Induced Temperature Perturbations in the Stratosphere During the First Few Months Following the Eruption. *Geophys. Res. Lett.*, vol. 21, 1994, p. 369.



Comparison of simulated El Chichon (left) and Mt. Pinatubo (right) volcanic clouds 21 days after each volcano erupted.

Chemically Reacting Compressible Shear Layer

Sang-Wook Kim, Principal Investigator
University of Toledo



Research Objective

To develop a numerical analysis and simulation method that can resolve advanced combustion physics such as the ignition delay, flame extinction, and combustion instability occurring in aeropropulsion systems.

Approach

The Favre-averaged compressible flow equations and the convection-diffusion equations for the chemical species are solved by a finite volume method that incorporates an incremental pressure equation for the conservation of mass. The chemical reactions are described by 9 chemical species and 24 pairs of reaction steps. The turbulence field is described by multiple-time-scale turbulence equations (M-S equations). The capability of the integrated analysis method to resolve ignition delay and flame thickness is validated by solving hydrogen stream and vitiated supersonic airstream mixing with and without chemical reactions.

Accomplishment Description

The contour plot of the combustion trace species shows that combustion is initiated approximately 18.5 cm downstream of the inlet boundary; the data measured using ultraviolet radiation show that combustion is initiated 18.0 cm downstream. The excellent agreement between the measured and the calculated flame locations indicates that the M-S equations can correctly resolve the ignition delay. The ignition delay is caused by the time required for the hydrogen species to be heated until it attains the activation energy. The good agreement indicates that the present analysis method accurately describes the molecular and turbulent heat transfer occurring between the cold hydrogen stream and the vitiated airstream. The calculated species concentrations obtained using the M-S equations are in closer agreement with the measured data than those obtained using a probability

density function method and k - ϵ turbulence models. Also, the M-S equations successfully predict the increased shear layer thickness caused by the chemical reaction-turbulence interaction. Calculation of the reacting flow case using 145×140 mesh requires 1.5 Cray C-90 hours and 2.9 megawords of memory.

Significance

The present method can resolve such combustion physics as ignition delay and flame thickness. The accomplishment is an important step toward the development of a numerical method that can correctly resolve local flame extinction in unsteady turbulent flows and combustion instability for theoretical analysis of advanced aeropropulsion systems.

Future Plans

The analysis method for reacting flows near flame extinction conditions, simulations of unsteady, chemically reacting turbulent flows, and applications of the instability analysis method will be validated.

Keywords

Navier-Stokes, Combustion, Turbulence, Ignition delay, Diffusion flame

Publications

1. Kim, S-W.: Numerical Investigation of the Influence of Chemical Reaction on Turbulence Fields. AIAA Paper 94-0650, 1994.
2. Kim, S-W.; and Benson, T. J.: Fluid Flow of a Row of Jets in Crossflow—A Numerical Study. AIAA J., vol. 31, no. 5, 1993, pp. 806–811.
3. Kim, S-W.; and Benson, T. J.: Calculation of a Circular Jet in Crossflow with a Multiple-Time-Scale Turbulence Model. Int. J. Heat, vol. 35, no. 10, 1992, pp. 2,357–2,365.



Contour plot of hydroxyl combustion trace species for reacting case.

Automated Instrumentation and Monitoring System

Jerry Yan, Principal Investigator

Co-investigators: Pankaj Mehra, Sekhar Sarukkai, Cathy Schulbach, Melisa Schmidt, and Brian Vanvoorst
Recom Technologies/NASA Ames Research Center



Research Objective

To develop scalable and portable performance evaluation tools for parallel applications.

Approach

High-Performance Computing and Communication Program/Computational Aerosciences grand challenge applications are some of the most complex parallel programs ever developed. Program developers and users need to know what computations or communications are the dominant contributors to completion time. The Automated Instrumentation and Monitoring System (AIMS) measures and analyzes parallel program performance. AIMS instruments and monitors message passing programs, animates execution traces, produces execution-time profiles, and discovers and characterizes performance bottlenecks. The execution traces created by AIMS can be easily converted to formats used by other analysis or visualization tools.

Accomplishment Description

The AIMS 3.0 instrumentor is more robust than previous versions. The newly designed monitor provides two levels of tracing depending on the users need for detail and storage availability. Communication costs for various data arrays are measured automatically. Prototypes of the AIMS index kernel and statistics kernel rapidly characterize program performance.

Significance

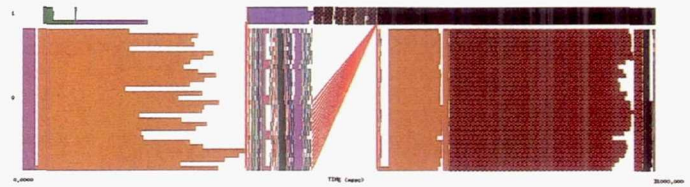
AIMS is used for tuning parallel and distributed message passing programs.

Future Plans

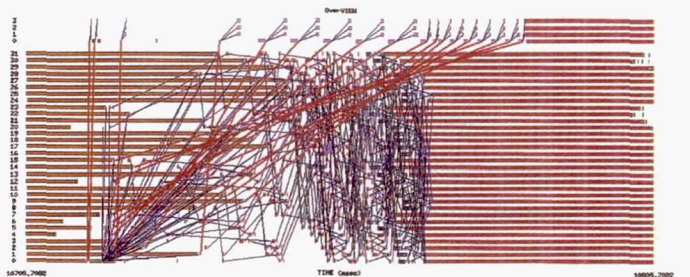
Scalable methodologies for data collection and analysis are being developed. AIMS soon will be ported to the IBM SP-2 environment.

Keywords

Performance evaluation, Parallel processing, Instrumentation, Performance monitoring and visualization

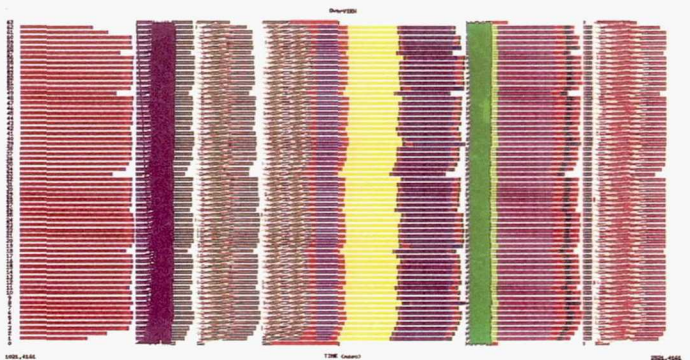


(a)

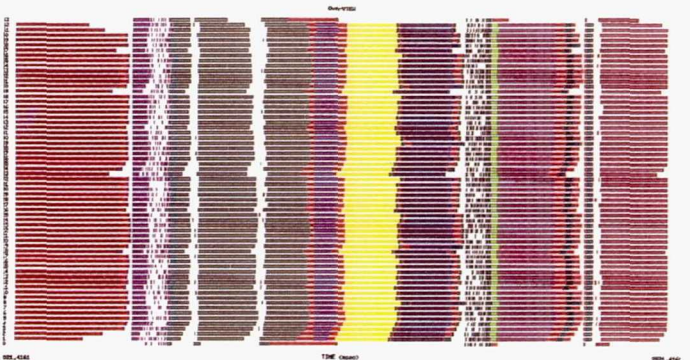


(b)

Traces gathered from an interdisciplinary application.



(c)



(d)

Implementation of NAS Parallel Benchmark SP.

Computational Fluid Dynamics Solution for Maxwell's Equations

Ramesh K. Agarwal, Principal Investigator
Co-investigators: Dau-Sing Wang and Mark R. Axe
McDonnell Douglas Corporation



Research Objective

To develop computational codes capable of predicting the electromagnetic signature of an aerospace vehicle. Such codes would be of great value in the design and development of fighter aircraft and missiles because a greater number of candidate configurations could be considered and their performance evaluated, thus reducing the cost and time required in the design cycle.

Approach

The approach taken is to solve the three-dimensional (3-D) Maxwell's equations. A central-differencing, finite-volume, time domain/frequency domain, multizone method is used to compute the electromagnetic (EM) field about scattering bodies. A hybrid approach that combines a method of moments code (CARLOS-3D) with the computational fluid dynamics-based EM code is also developed to enhance the EM modeling capability.

Accomplishment Description

The EM code (CFDMAXES) was extended to calculate the scattering from geometrically and electrically complex 3-D bodies, in both the time and the frequency domains. Accomplishments include the calculation of the radar cross section of aircraft inlets, nozzles and radomes, and radar range pylons. Modifications to the CFDMAXES code enabled efficient coupling with the CARLOS-3D code for the frequency domain scattering calculation.

Significance

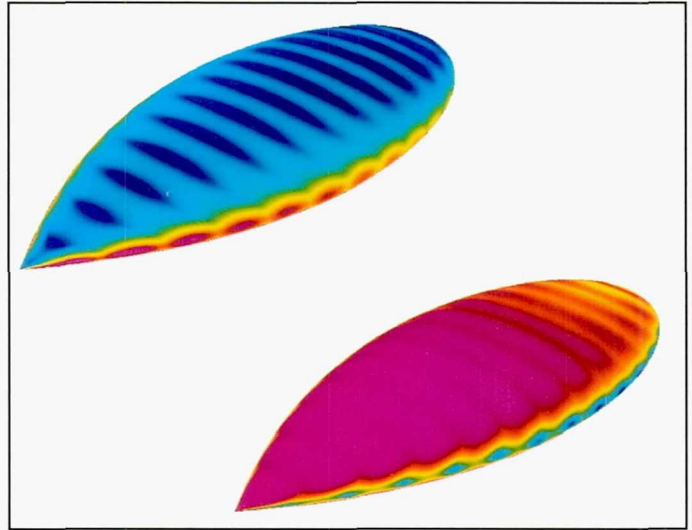
The project represents the development of a leading-edge technology in computational electromagnetics and it will have substantial impact on the development of both fighter aircraft and missile programs.

Future Plans

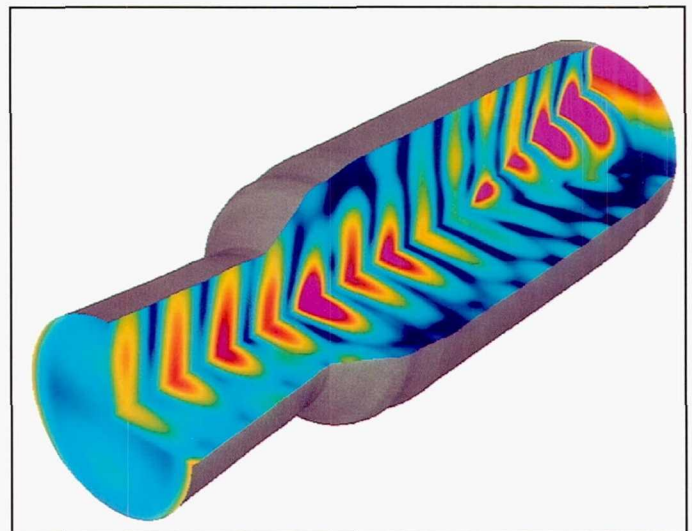
Planned extensions include implementing convergence enhancing techniques for the frequency domain formulation and applying broadband calculations for the time domain formulation.

Keywords

Computational fluid dynamics, Electromagnetic signature



Color contour plots of the magnetic current magnitude on the surface of the one meter NASA almond at 2 GHz. Plots are for axial incidence with vertical and horizontal polarization. Red = high magnitude and blue = low magnitude.



Color contour plot of the magnetic current magnitude caused by an axially incident electromagnetic field of frequency 1 GHz within an untreated aircraft exhaust system. Red = high magnitude and blue = low magnitude.

Computational Fluid Dynamics Approach to Computational Electromagnetics

Vijaya Shankar, Principal Investigator

Co-investigators: William Hall, Chris Rowell, and Alireza Mohammadian

Rockwell International Science Center



Research Objective

To extend algorithmic advances in computational fluid dynamics to the time-domain Maxwell's equations to study electromagnetic problems of interest for defense and commercial applications.

Approach

The time-domain Maxwell's equations were written in differential conservation form (for structured grid arrangement) or in integral conservation form (for unstructured grid arrangement). An appropriate upwind, finite-volume time/space discretization was employed using Riemann solvers for interface flux evaluation to update the electric and magnetic fields at each time step. The electromagnetic incident wave can be either a continuous wave (single frequency) or a pulse (broadband frequency).

Accomplishment Description

Both the structured grid (RCS3D) and the unstructured grid (RCSUN) versions of the computational electromagnetics (CEM) code run efficiently on the Cray C-90. Depending on the problem size, the RCS3D code runs at 500–700 MFLOPS per processor

and the RCSUN code runs at 200+ MFLOPS. An MPP version of the RCS3D code is also running on the Intel Paragon. The structured/unstructured CEM capability was demonstrated on a variety of electromagnetic problems including the prediction of the radar cross section (RCS) of a complete fighter requiring 10 million grid points.

Significance

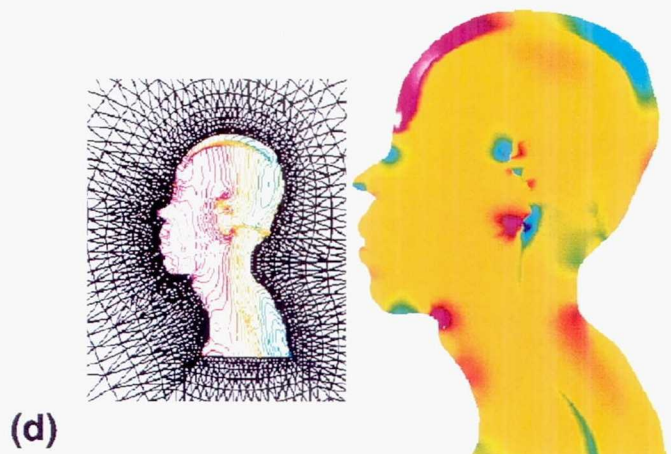
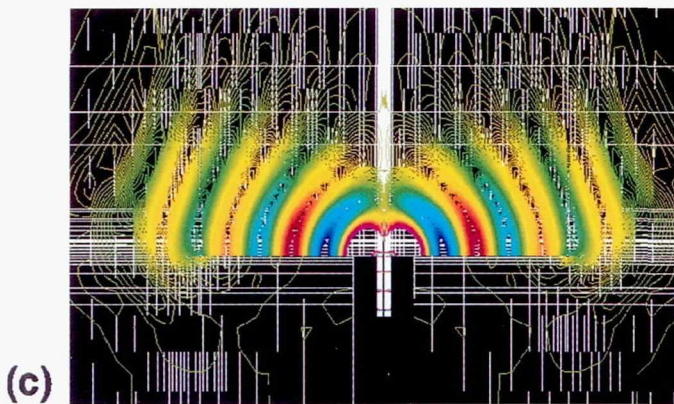
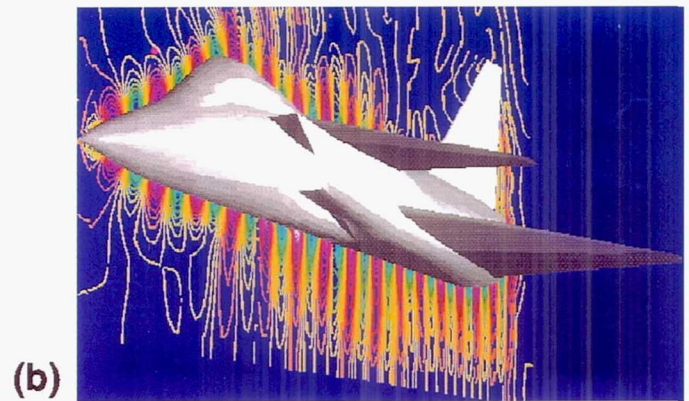
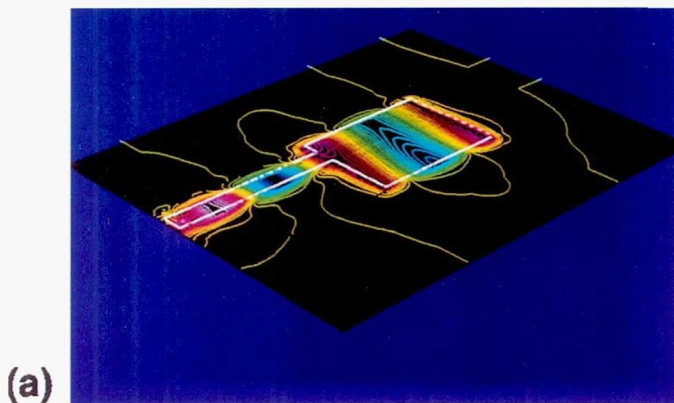
This CEM development represents the state of the art in large-scale simulation and is a critical technology for design of low observable platforms.

Future Plans

The CEM capability for RCS problems involving 100+ million cells will be demonstrated using the Intel Paragon or the Cray T3D.

Keywords

Radar cross section, Maxwell's equations



CEM applications for defense and commercial use; (a) microstrip patch antenna, (b) low observables, (c) monopole antenna, and (d) bioelectromagnetics.

Electromagnetic Scattering by Airborne Structures

John L. Volakis, Principal Investigator
Co-investigator: Arindam Chatterjee
University of Michigan



Research Objective

To develop numerical methods and associated computer codes for the analysis of electromagnetic scattering by airborne composite targets. Typically, a target is illuminated by a continuous wave radar signal; however, this study focuses on the electromagnetic energy reflected from the target.

Approach

To model arbitrary composite targets and reduce memory requirements, the finite element method (FEM) was used for electromagnetic field simulations. Even though FEM is used extensively in fluid mechanics and electrostatics, its implementation in electromagnetics is fundamentally different and is complicated by the need to model unbounded domain problems. Thus it has only recently been considered for high-frequency electromagnetic scattering computations.

Accomplishment Description

A three-dimensional (3-D) finite element code (FEMATS) for electromagnetic scattering was developed. The code employs edge-based elements for better simulation of electromagnetic field characteristics and new absorbing boundary conditions (ABCs) for more efficient truncation of the finite element mesh. The mesh truncation is based on vector absorbing boundary conditions and can be applied to a boundary conformal to the scatterer or antenna system. More than 10 Electromagnetic Code Consortium benchmark geometries were modeled and analyzed, including metallic and dielectric plates, cavities, jet engine inlets, and nonhomogeneous dielectrics. The largest problem simulated scattering by a foam cylinder with collinear and off-axis wires. The problem needed only 12.5 Cray C-90 minutes for each observation angle to converge to the desired solution.

Significance

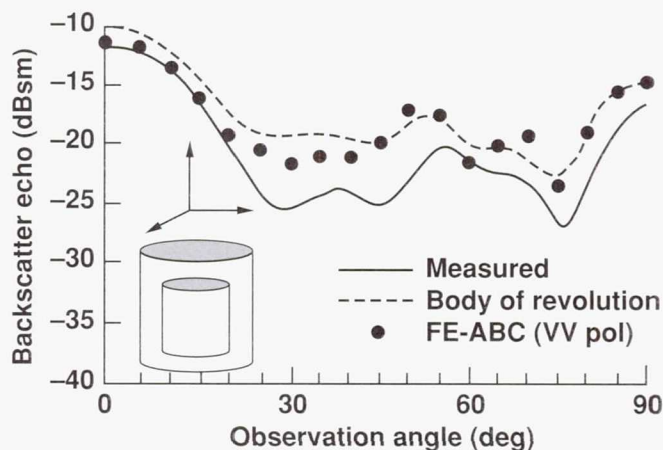
The development and validation of conformal ABCs leads to substantial reduction in the degrees of freedom required to model targets. An 11 cubic wavelength dielectric scatterer was modeled and larger problems can be modeled.

Future Plans

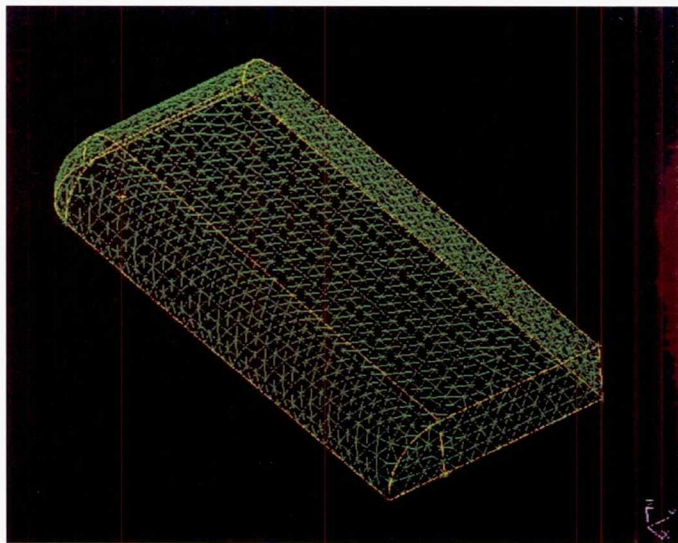
Further improvements on the ABCs and mesh refinement strategies will lead to a substantial reduction in memory and processing time. Numerical ABCs with iterative refinement and adaptive finite elements for simulating large, complex 3-D structures with minimal computational resources will be investigated.

Keywords

Three-dimensional finite elements, Absorbing boundary conditions, Parallelization



Backscatter radar cross section of a metallic cylindrical inlet (1.25λ diameter; 1.875λ height).



Mixed mesh termination scheme employing flat, cylindrical, and spherical sections.

Computational Radar Cross Sections

Alex C. Woo, Principal Investigator

Co-investigators: Michael Simon and Michael Schuh

NASA Ames Research Center/Sterling Software Systems



Research Objective

To enhance the radar cross section (RCS) prediction of bodies with metallic and treated surfaces.

Approach

A finite-volume time-domain program, RCS3D, was used to propagate electromagnetic waves through a variety of structured, body-fitted grids. Both time-harmonic and broadband-incident fields were tested. Computed and experimentally measured RCS data were compared to assess the effects of various developments on the accuracy of the solution.

Accomplishment Description

A method was developed for terminating broadband (pulse mode) calculations based on the energy of the electromagnetic field. The energy is computed at successive instants of time. The calculation ends when the energy has fallen to a specified fraction of the peak energy. A calculation for a square aperture cavity required 18 megawords of memory and 7 CPU hours on the Cray C-90. When using the pulse termination technique, the calculation had no effect on the required memory, but did reduce the CPU time to less than 6 hours. The use of energy dissipation as an automatic termination criterion is a valuable enhancement to the code's usability. A second enhancement was to develop a technique for generating bistatic inverse synthetic aperture radar (ISAR) images. This technique uses the radar return for a range of frequencies and bistatic look angles to determine where the areas of intense scattering are located. The figure shows ISAR images for a trapezoidal plate with the incident field coming from the right side. The image for horizontal polarization shows that the near edge has high return (dark grey), but for vertical polarization the far edge has high return. The returns appearing before the plate are wraparound ghost images from the ISAR algorithm.

Significance

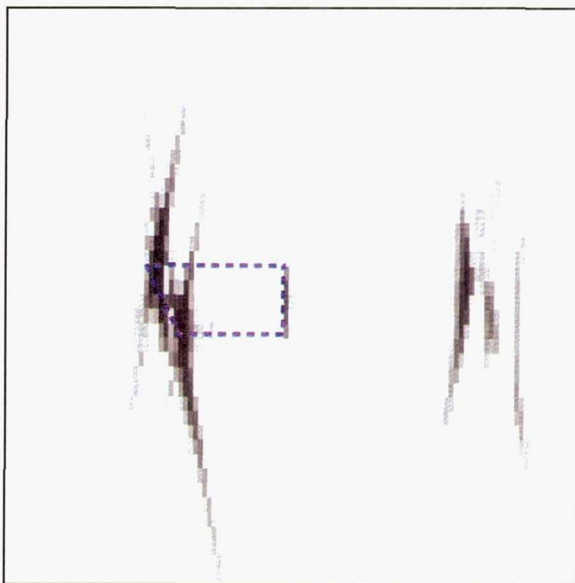
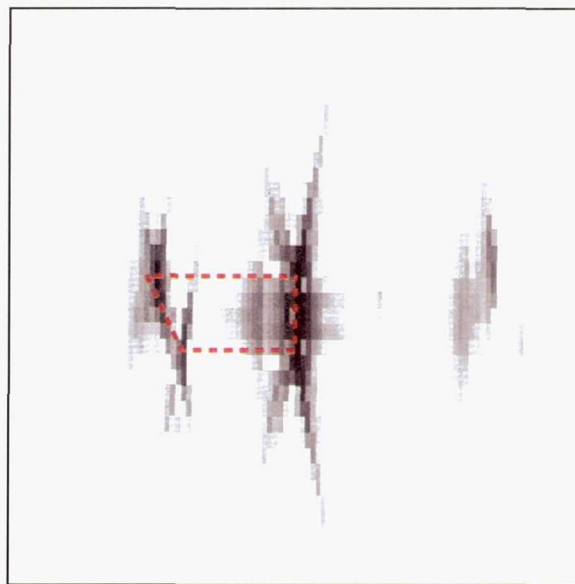
A physical basis was implemented to automatically determine the number of time steps required for a pulse mode calculation to yield accurate RCS predictions. This criterion eliminates a degree of uncertainty in the results and reduces the computational time. Also, a tool is now available to produce bistatic ISAR images of radar targets and to diagnose geometry and grid problems.

Future Plans

RCS3D will be validated on a radar test fixture with a variety of detail attachments.

Keywords

Finite volume, Time domain, Bistatic inverse synthetic aperture radar



Bistatic ISAR images from a single pulse calculation of RCS3D. The incoming wave strikes the target (dashed lines) from the right. Polarization is seen when the electric field is horizontal (top) and vertical (bottom).

Arbitrary Lagrangian–Eulerian Three-Dimensional Simulations

Joseph D. Baum, Principal Investigator

Co-investigator: Rainald Lohner

Science Applications International Corporation/George Mason University



Research Objective

To investigate shock diffraction about moving and stationary complex-geometry, three-dimensional (3-D) bodies.

Approach

A new 3-D arbitrary Lagrangian-Eulerian (ALE) hydro-solver based on the finite-element method flux-corrected transport (FEM-FCT) concept, FEFLO96, was used. The preferred approach for grid adaptation is H-refinement. The high-order scheme used was the consistent-mass Taylor–Galerkin algorithm. Combined with a modified second-order Lapidus artificial viscosity scheme, the resulting scheme is second-order accurate in space and fourth-order accurate in phase. The spatio-temporal adaptation was based on local H-refinement, where the refinement/deletion criterion is a modified H2-seminorm, and density is used as the critical parameter. Over the past year, the element-based data structure was converted to an edge-based structure, thereby significantly reducing indirect addressing, floating point operations, and memory overhead.

Accomplishment Description

The new 3-D, adaptive, finite-element, edge-based methodology was applied to two simulations. The first simulation was a blast diffraction within the passenger compartment of a civilian wide-body jetliner (a Boeing 747). This study simultaneously evaluated the ability of a wide-body jetliner to survive a terrorist attack and the feasibility of applying an adaptive grid methodology to the simulation of shock-wave diffraction about hundreds of complex-geometry structures. A large number of shock waves were produced because of shock diffraction about the seats, bulkheads, and luggage compartments. Excellent shock adaptation and resolution were obtained. The second simulation modeled pilot/seat ejection from an F-16 fighter at supersonic speed. The results demonstrate the ability of the numerical methodology to accurately predict both the steady flow around the plane and within the cockpit after canopy ejection and the transient forces acting on the pilot during ejection. The simulations identify a mechanism that may be responsible for the neck injury experienced by many ejecting pilots. The results also demonstrate that, although the ejection velocity is relatively low, the computational results are significantly different from those obtained for a captive solution under identical conditions.

Significance

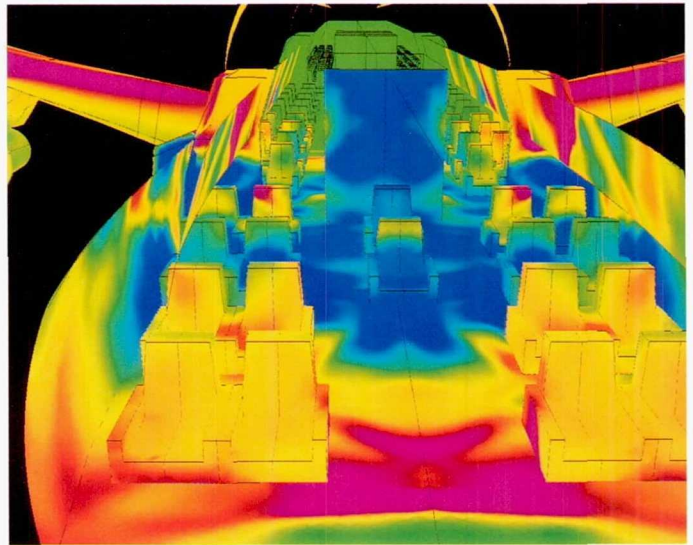
The results demonstrate the feasibility of applying 3-D, adaptive, finite-element, edge-based schemes on unstructured grids to simulate shock-wave diffraction about multiple complex-geometry moving or stationary structures.

Future Plans

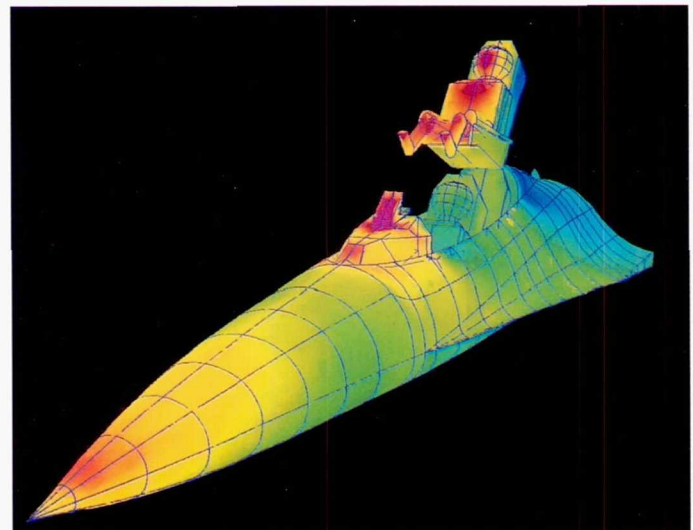
The range of applications will be extended to model the structural response to shock loading by incorporating state-of-the-art computational structural dynamics in the methodology.

Keywords

Shock-wave diffraction, Arbitrary Lagrangian–Eulerian methodology, Shock-capturing schemes, Unstructured grids



Blast diffraction in a Boeing 747. Internal pressure contours and external Mach number contours at time = 14 milliseconds.



Pressure contours about the F-16 and the ejecting pilot at initiation of ejection (time = 0 milliseconds) and during ejection (time = 27 milliseconds).

Unsteady Viscous Marine Propulsor Hydrodynamics

Fred Stern, Principal Investigator

Co-investigators: E. Paterson and B. Chen

University of Iowa



Research Objective

To develop computational fluid dynamics (CFD) simulation methods applicable to naval hydrodynamics (marine propulsors), which are unlike related applications because marine propulsors are embedded in the thick stern boundary layer and wake and are susceptible to cavitation.

Approach

The research is based on further developments and extensions of current Reynolds-averaged Navier–Stokes (RANS) methods and a new CFD capability for highly efficient unsteady RANS calculations, which also can be extended for large-eddy simulations (LES) or direct numerical simulations (DNS). The current method uses finite-analytic spatial discretization, pressure-implicit split-operator, marker and cell (MAC), and semi-implicit pressure-linked equation pressure-velocity coupling algorithms, Chimera domain decomposition, and a hierarchy of turbulence models including Baldwin–Lomax, k - ϵ with either wall functions or a one-equation model for the near-wall flow, and non-isotropic models such as the nonlinear k - ϵ and algebraic Reynolds-stress models. The new method uses high-order finite differences, fractional-step/MAC pressure-velocity coupling, fourth-order artificial dissipation, and multigrid acceleration of the pressure equation.

Accomplishment Description

Steady RANS solutions and validation were accomplished for marine propulsors P4119 and P4842 for design and off-design conditions (1 Cray C-90 hour and 24 megawords of memory). Zonal methods and advanced turbulence modeling for foils and marine propulsor P4119 were completed. Unsteady-flow calculations and validation studies were done for comparison to the Massachusetts Institute of Technology flapping-foil experiment (3 Cray C-90 hours and 6 megawords of memory). Investigations into interactions between natural and forced unsteady flows for fixed and moving boundaries using Chimera domain decomposition were completed (20 Cray C-90 hours and 8 megawords of memory). Finally, unsteady RANS solutions were extended for marine propulsors P4119 and P4132 with temporally and spatially varying inflows (28 Cray C-90 hours and 32 megawords of memory).

Significance

This research supports the Office of Naval Research basic and applied research programs focusing on the fundamental importance in the fluid mechanics of moving boundary problems and interactions between natural and forced unsteady separated flows. The research is also of strategic importance to the design of marine propulsor–body configurations—especially signature identification and reduction.

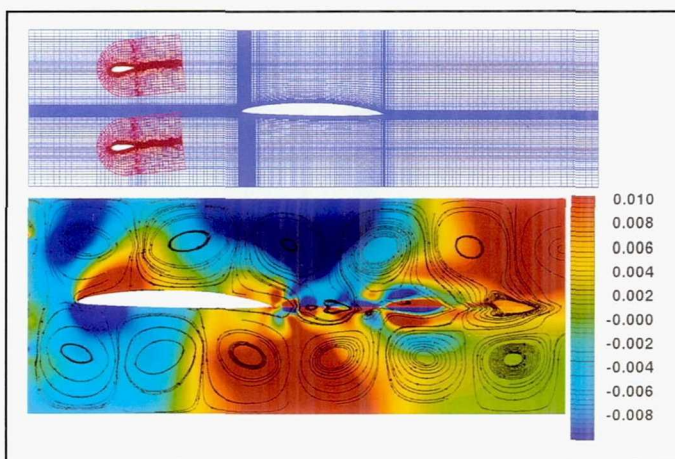
Future Plans

Development will continue on numerical methods with application to unsteady propulsor-blade flow and complete configurations. Also, traveling-wave external flows over simplified blade geometries will be studied using LES and DNS to

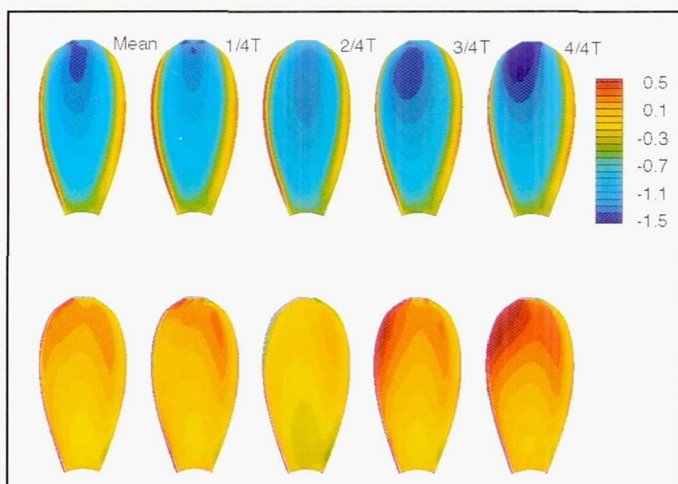
support the development of appropriate turbulence models for unsteady propeller-blade boundary layers and wakes.

Keywords

Chimera, Propeller



Flapping-foil experiment overlaid grid system (top) and perturbation pressure contours (bottom) with instantaneous perturbation velocity particle traces.



Surface pressure contours at different time periods (T) for marine propulsor P4132 with sixth-harmonic screen–wake inflow for the suction side (top) and pressure side (bottom).

Free-Surface Effects on Boundary Layers and Wakes

Fred Stern, Principal Investigator

Co-investigators: Y. Tahara and J. Choi

University of Iowa



Research Objective

To develop computational methods for the solution of the unsteady, three-dimensional Navier–Stokes equations for surface-piercing bodies with free-surface gravity waves.

Approach

The approach is based upon further developments and extensions of current Reynolds-averaged Navier–Stokes (RANS) methods and a new computational fluid dynamics capability for highly efficient unsteady calculations that can be extended for large-eddy (LES) or direct-numerical (DNS) simulations. The current method uses finite-analytic spatial discretization, marker and cell and semi-implicit pressure-linked equation pressure-velocity coupling algorithms, and a hierarchy of both isotropic and non-isotropic turbulence models. The new method uses high-order finite differences, fractional-step/MAC pressure-velocity coupling, fourth-order artificial dissipation, and multigrid acceleration of the pressure equation. Both small-domain viscous-inviscid interactive and viscous large-domain approaches are under development with special emphasis on treatment of the free-surface boundary conditions, turbulence modeling, and extensions for unsteady flow. The computational studies are guided and supported by a concurrent program of towing-tank experiments.

Accomplishment Description

A detailed study of the Navier–Stokes-wave/flat-plate flow geometry was completed (0.5 Cray C-90 hours and 10 megawords of memory). Also completed was an analysis of wake bias through Navier–Stokes, boundary-layer, and perturbation expansion equation solutions for a flat-plate boundary layer and wake in

temporal, spatial, and traveling horizontal-wave external flows (0.25 Cray C-90 hours and 6 megawords of memory). The interaction approach for the Series 60 $C_B = 0.6$ ship model was validated (0.5 Cray C-90 hours and 10 megawords of memory). Development of the large-domain approach was continued (1 Cray C-90 hour and 10 megawords of memory), and development of LES/DNS simulation methods for the Navier–Stokes wave/flat-plate flow geometry was initiated (25 Cray C-90 hours and 50 megawords of memory).

Significance

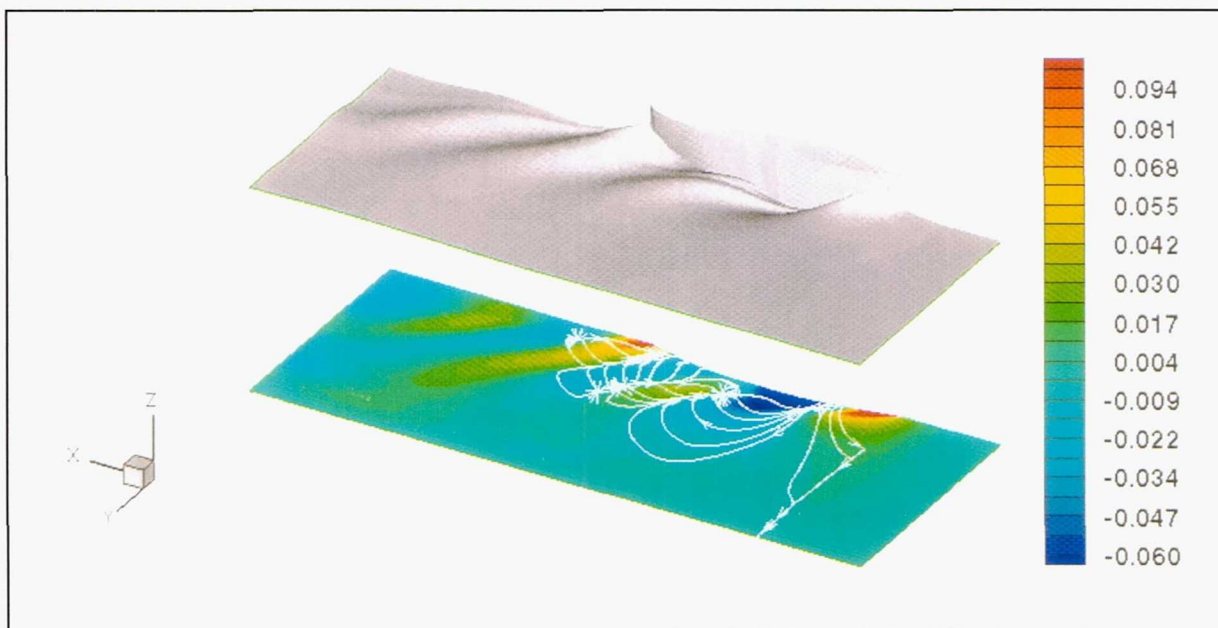
This research is sponsored by the Office of Naval Research in support of its basic research program focusing on the fundamental importance in the fluid mechanics of nonlinear free-surface problems and the physics of the solid–fluid juncture boundary layer and wake with waves. This research is of strategic importance for the identification and reduction of surface wake signatures.

Future Plans

Development of the numerical method with application to unsteady free-surface flows and free-surface/propulsor interaction will continue. Investigations concerning the physics of turbulence and turbulence modeling for the solid–fluid juncture boundary layer and wake, and studies of wave-induced separation for ships at yaw will be completed.

Keyword

Ship hydrodynamics



Large-domain solution for a Series 60 $C_B = 0.6$ ship model and Froude number = 0.316. The wave pattern (top), pressure contours (bottom), and free-surface perturbation vectors (top and bottom) are shown.

Impeller Computational Fluid Dynamics Modeling

Matthew E. Thomas, Principal Investigator

Co-investigators: Mahesh M. Athavale and Mark L. Ratcliff

CFD Research Corporation



Research Objective

To develop, demonstrate, and validate an efficient and accurate computational fluid dynamics (CFD) analysis procedure for the complex turbulent flows in liquid rocket propulsion impellers.

Approach

CFD modeling of liquid rocket propulsion components requires a combination of advanced geometric modeling procedures, boundary condition implementation, robust CFD solution techniques, and highly interactive postprocessing capabilities. Two geometric modeling packages, PATRAN and ICEM-CFD, were examined. The CFD results were validated with benchmark quality laser Doppler velocimeter (LDV) impeller data.

Accomplishment Description

Geometric data used in this effort included initial graphics exchange standard files associated with two distinct geometry classes (a Rocketdyne test inducer and the Space Shuttle main engine (SSME) high-pressure fuel turbopump (HPFTP) impeller). Each package was examined in detail for user efficiency and geometric modeling accuracy. The open-ended architecture of PATRAN has the potential for mature interaction between CFD and structural/thermal analysis packages. The structured grid modeling procedures implemented in ICEM-CFD were suitable for complex impeller geometries. Flow computations were done using REFLEQS-3D, an advanced finite-volume Navier-Stokes code with capabilities that include high-order differencing schemes, different turbulence models, a range of boundary condition types, and treatment of rotating coordinate frames. Flow calculations for the inducer were done on coarse and fine grids (41,000 and 100,000 cells) built with PATRAN. The SSME HPFTP impeller grid, with partial and full blades, was generated using ICEM-CFD. Two grids (56,000 and 130,000 cells) were used on the impeller solutions because they were more sensitive to the grid size. The figures show the surface pressure plots for the two components. The computed velocities and flow angles were compared with LDV data. Detailed comparisons on the impeller and limited comparisons on the inducer data showed very good agreement with experimental measurements. This study demonstrates that CFD technology has sufficient efficiency and accuracy for implementation into the impeller design process.

Significance

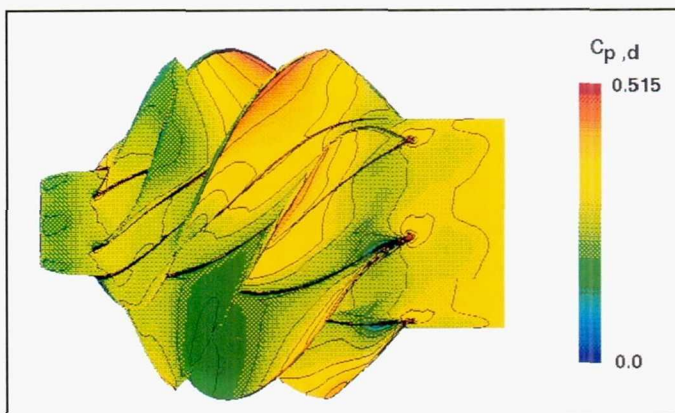
An efficient and accurate CFD analysis procedure that is applicable within the preliminary and detailed design procedures of liquid rocket propulsion turbomachinery components was demonstrated.

Future Plans

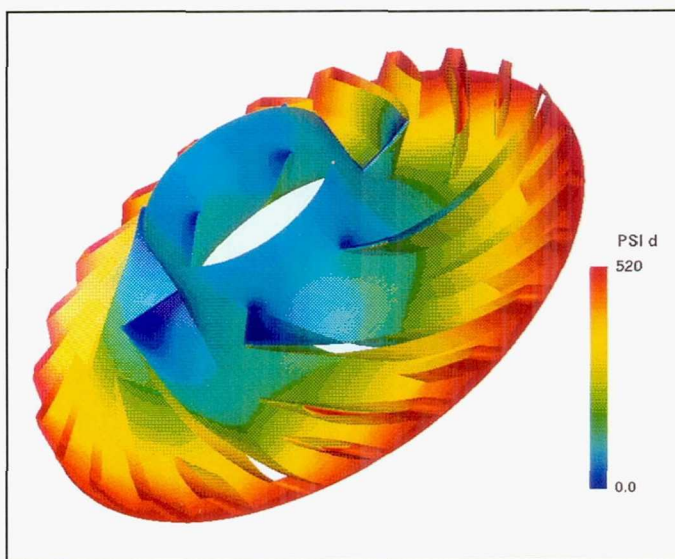
The CFD analysis methodology is being extended to include computations of cavitating flows. Attributes of PATRAN, ICEM-CFD, and REFLEQS-3D identified during this effort are being implemented to link the computer assisted design, structural, thermal, hydrodynamic, and results analysis (analytical and test) disciplines. The package will be extended to other rotating machines including turbines, fans, and propellers.

Keywords

Impeller, Turbomachinery, Computational fluid dynamics



Pressure coefficient distribution on a Rocketdyne test inducer.



SSME high-pressure fuel turbopump impeller pressure loading.

Modeling of Pulmonary Fluid Dynamics

Jeffrey R. Hammersley, Principal Investigator

Co-investigators: Rama Reddy, Dan E. Olson, Boyd Gatlin, and Joe F. Thompson

University of Arkansas/Medical College of Ohio/Mississippi State University



Research Objective

To study the complex fluid interactions within inaccessible small respiratory airways and vessels. To determine the effects that normal anatomic variations cause within airways and vessels, the complexity of flow within confined bifurcating tubes will be examined.

Approach

Multiblocked two-dimensional (2-D) and three-dimensional (3-D) structured grids were constructed to mimic the anatomic features of small airway and vascular bifurcation using the EAGLE grid code. These computational bifurcations were studied over a biologically realistic range of Reynolds numbers (50–1,400) through the use of a Taylor–Whitfield ABRAINS flow solver modified to accommodate flow reversal. Evaluation of the computed flow results was performed using FAST, PLOT3D, and secondary programs for boundary layer and shear force calculations.

Accomplishment Description

Three-dimensional flow solutions in single bifurcation have been produced along with multibranched symmetrical and asymmetrical 2-D solutions. These provide velocity, pressure, wall shear, and particle trajectory information for a wide range of realistic biologic flows. Work has been extended from steady flow to the pulsatile and oscillatory flow within the 2-D geometric grids; 3-D multibranched grids and dynamic solutions are still under development.

Significance

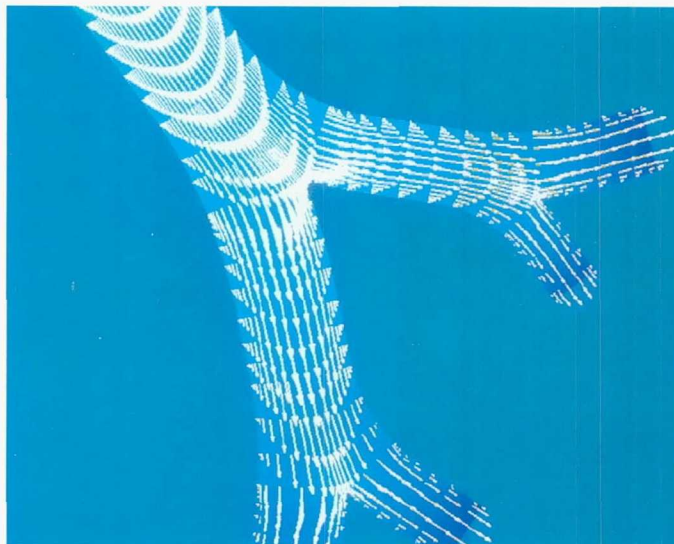
These data allow medical scientists to predict delivery of aerosolized medications, quantify particulate deposition during environmental exposures, and link changes in airway geometry to the disability seen in asthma and emphysema. This work continues a collaborative effort to provide realistic biologic flow simulations of fluidic mixing, particle transport, and shear forces on airway and vascular walls. It will be extended to pulsatile and oscillatory conditions. When completed in 3-D, flow simulation through biologic structures should produce a better understanding of the physical forces that limit transport in airways and blood vessels.

Future Plans

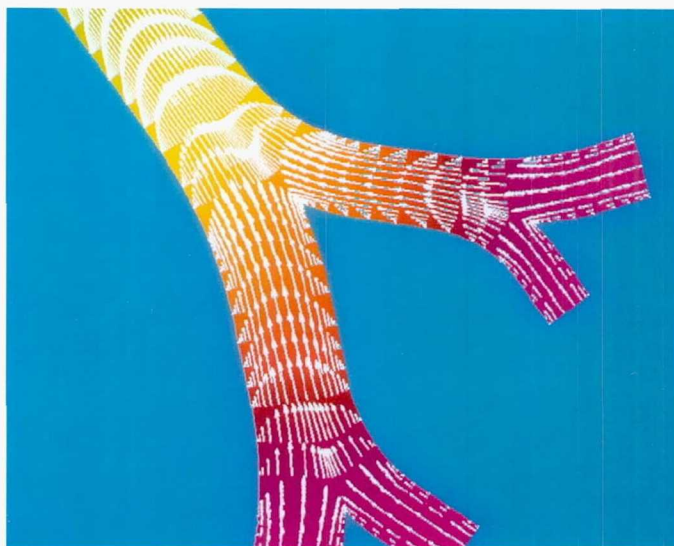
The investigation of symmetrical and asymmetrical bifurcating flows will be extended to dynamic flows in serially branching 3-D cascades. These efforts set the stage for future incorporation of wall elasticity and particle-flow interactions.

Keywords

Lung, Incompressible flow, Oscillatory, Pulsatile



Inspiratory flow in a 2-D asymmetric network under oscillatory conditions.



Expiratory phase flow in a 2-D asymmetric network.

Structure and Functions of Membranes

Andrew Pohorille, Principal Investigator

Co-investigator: Michael A. Wilson

University of California, San Francisco



Research Objective

To explain how interfaces between protocellular membranes and water could have promoted catalysis of the chemical reactions needed for cellular functions in the absence of the complex enzymes of contemporary cells.

Approach

The water–membrane system consists of a solute molecule and 72 membrane-forming molecules arranged in a bilayer between two water lamellae of 1,200 molecules each. The behavior of this system is simulated using the molecular dynamics method. The results are the statistical and dynamic properties of the system (which can be directly compared with experimental results) and a detailed microscopic description of the system.

Accomplishment Description

Alanine dipeptide, a simple model for peptides, was studied at the water–membrane interface and in other typical protobiological environments—water, oil, and at the water–oil interface. It was shown that the dipeptide’s ability to form ordered structures (*conformations*) strongly depends on the environment. It was further demonstrated that this molecule tends to accumulate at the water–membrane and water–oil interfaces. By binding the sub-

strate and lowering the activation energy the interface acts as a catalyst to the isomerization reaction. The time required for a single calculation varies from 60 Cray C-90 hours for the water–membrane system to 5 hours for bulk water and oil solvents. Central memory requirements vary from 10 to 50 megawords, depending on the data analysis performed.

Significance

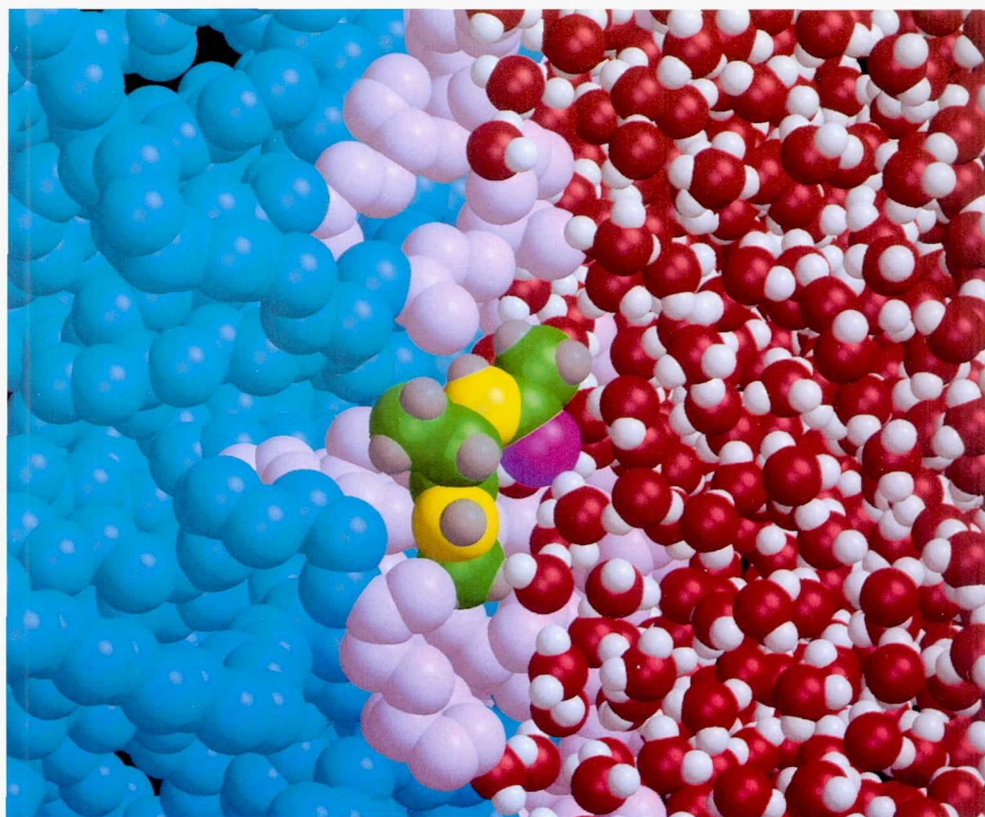
The ability of simple peptides to form ordered structures and adopt preferred orientations is unique to interfacial systems. Thus, membrane surfaces of protocells may have provided an environment for primitive catalysis even before the development of the complex enzymes of contemporary cells.

Future Plans

Studies of the transfer of small molecules across membranes and the development of a general, molecular model of the transport of nutrients and waste products through walls of protocells will continue. Also, proton transport across protocellular walls as an essential mechanism of primitive bioenergetics will be studied.

Keywords

Origin of life, Protocells, Protein–membrane interactions



Alanine dipeptide at the interface between membrane and water. The oxygen and hydrogen atoms of water are red and white, respectively; the lipid tail-group atoms are blue and the head-group atoms are pink. In the alanine dipeptide molecule, the carbon atoms are green, the nitrogen atoms are yellow, the oxygen atoms are magenta, and the hydrogen atoms are gray.

Finite Volume Neuronal Modeling

Muriel D. Ross, Principal Investigator

Co-investigators: David G. Doshay, Samuel W. Linton, and Timothy J. Barth

NASA Ames Research Center/Sterling Software Systems



Research Objective

To investigate whether application of modern computational fluid dynamics (CFD) tools can improve the accuracy of simulations used to determine the influence of ultrastructural detail on neural functioning. The one-dimensional (1-D) compartmental models used in computational neuroscience were expanded to a model based on finite volume analysis to determine whether this augmentation would produce more biologically relevant computer models when communications between complex neurons were simulated.

Approach

The morphology of the neurons was obtained from computer assisted three-dimensional (3-D) reconstructions of neurons from a vestibular gravity sensor (macula) sectioned serially and photographed in a transmission electron microscope. An unstructured mesh describes neuronal surfaces in the reconstructions. The neural structure used in the test is the calyx, a complex neuronal ending that has inner and outer membranes separated by cytoplasm as well as twig-like extensions (processes) that often have the geometric shape of frustums. The finite volume solver uses the generalized minimum residual method to solve for voltage changes in frustums (quasi-1-D) and triangular prisms (quasi-2-D) of the calyx mesh. The connectivity scheme allows for an unlimited number of quasi-1-D processes and for their arbitrary branching.

Accomplishment Description

Results show excellent agreement with available analytic solutions (see figures). The effect produced on a calyx by activation of a synapse on a process was measured over a range of cell membrane and cytoplasm resistances and synapse conductances. Each parameter sweep required 50 simulations over a single calyx, took about 3 Cray hours, and used less than 1 megaword of memory.

Significance

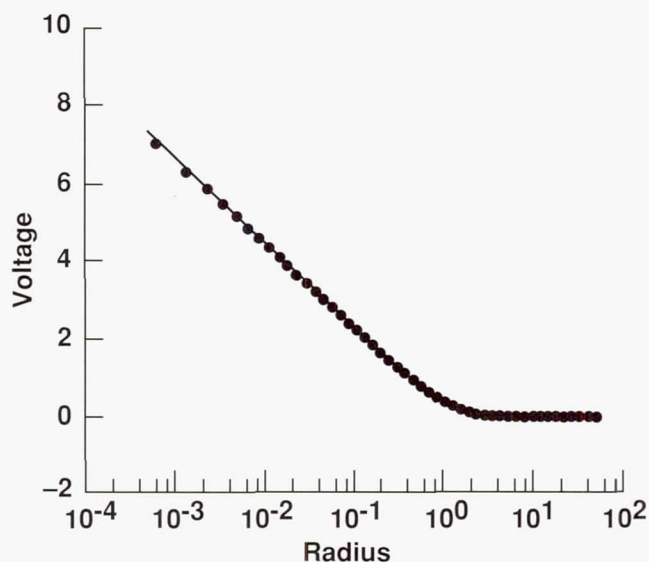
The excellent agreement with analytic solutions obtained by the solver gives credibility to the predictions it makes for more complex geometries. The parameter sweeps demonstrate the potential of the solver to provide information quickly when biologically realistic geometries are simulated. The speed of the Cray and minimal memory requirements of the solver prove the feasibility of accurate and biologically relevant simulations of neuron networks.

Future Plans

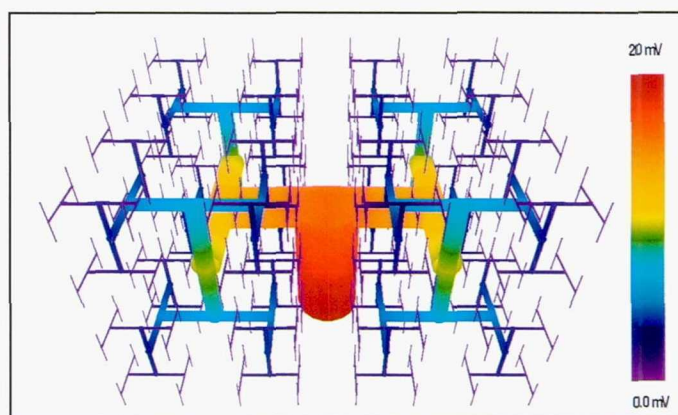
Further simulations are required to quantify the effect of morphology on electrophysiological behavior. Complex simulations involving interconnected calyces on single neurons and networks of neurons are the next step. These simulations will begin with quasi-2-D meshes, but will advance to fully 3-D meshes.

Keywords

Computational fluid dynamics, Neurons



There is excellent agreement between analytic (solid line) and computed (dots) solutions for a circular flat plate with a constant voltage at the origin.



Voltage distribution 0.025 msec after application of 20 mV to the base of an abstract neural structure that has an analytic solution.

Solar Wind Interaction with Mars

Stephen H. Brecht, Principal Investigator
Co-investigator: John R. Ferrante
Berkeley Research Associates



Research Objective

To study the kinetic interaction of the solar wind plasma with Mars and Venus using state-of-the-art three-dimensional (3-D) plasma kinetic simulations. Of principal interest is the process of shock formation where the effective viscous length is a significant fraction of the planet radii. In addition, the kinetic processes that lead to the plasma distribution functions measured by various orbiting spacecraft are studied.

Approach

The study of the solar wind interaction with Mars and Venus is performed with a 3-D hybrid particle code. A hybrid particle code treats the ions as individual particles (kinetic) and the electrons as a neutralizing massless fluid. The code can treat an unlimited number of ion species. The simulations study the effect of mass introduction via charge exchange and photoionization of the planets' atmospheres.

Accomplishment Description

The simulations show that the mass loading of the solar wind with ionospheric oxygen affect the flow characteristics around Mars. Under many circumstances the planet does not possess a "traditional" bow shock. In addition, the interaction between the solar wind and the planet changes in a nonhydrodynamic way. Strong solar wind pressure variations produce almost no effect on the subsolar shock location, but make significant differences in the flare angle and tail. The simulations were extended to include the tail region of the planet. The results were compared to the data returned to Earth from the Russian Phobos-2 spacecraft. Data from both the elliptic and circular orbits (see the figure) were tested against the simulation results by "flying" the Russian spacecraft through the simulation data. The consistency of our results with the actual data provides evidence that the solar wind interaction with Mars does not produce a classic shock, although the Alfvén Mach number is approximately 13. Comparison with the data taken in the tail of the planet demonstrates that Mars need not have an intrinsic magnetic field to explain the data taken by Phobos-2.

Significance

These results are gradually changing the view held by many scientists concerning the solar wind interaction with Mars. They clearly demonstrate that the interaction cannot be viewed in a magnetohydrodynamic or gas-dynamic sense without missing significant features of the interaction. The data as reported and interpreted by some scientists do not provide evidence of the presence of an intrinsic magnetic field within Mars.

Future Plans

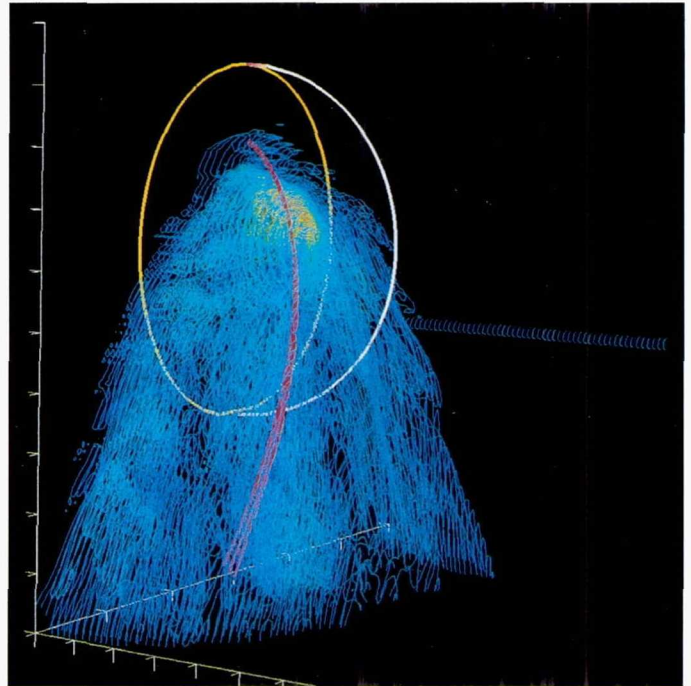
The conditions under which Mars may have a shock structure protecting it from the solar wind will be investigated. The role of the planetary ionospheres will be investigated with the time-dependent chemistry models developed for the HALFSHEL code.

Keywords

Shock formation, Mars, Solar wind

Publications

1. Brecht, S. H.; and Ferrante, J. R.: Examination of Mass Loading Effects on the Martian Magnetosphere. EOS, Trans. Am. Geophys. Union Fall Meeting, 1993, vol. 74, p. 538.
2. Brecht, S. H.; and Ferrante, J. R.: Hybrid Simulation of the Martian Boundary Layer. EOS, Trans. Am. Geophys. Union Spring Meeting, 1994, vol. 75, p. 284.



The magnetic field structure developing around Mars and the actual Phobos-2 orbits through the system.

Burner-Stabilized Flames in Microgravity

K. Kailasanath, Principal Investigator

Co-investigator: G. Patnaik

Naval Research Laboratory/Berkeley Research Associates



Research Objective

To develop a better understanding of the effects of gravity and heat loss on the structure and stability of premixed flames.

Approach

A detailed time-dependent, multidimensional, multispecies, numerical model is used as a tool to simulate flames stabilized on a burner on Earth and in zero gravity. The model includes finite-rate, detailed chemical kinetics coupled to algorithms for convection, thermal conduction, viscosity, molecular diffusion, and external forces such as gravity.

Accomplishment Description

Cellular structures are observed for the hydrogen–air flames in both zero and Earth gravity. As the inflow velocity is reduced, the flames move closer to the burner and the heat loss to the burner increases. At low inflow velocities, the cellular structures are suppressed in both cases, suggesting that increased heat loss to the

burner is the primary mechanism stabilizing these flames. As shown in the figure, Earth-gravity flames are smoother than the zero-gravity flames, indicating that gravity still plays a small part in further stabilizing the flames. A typical calculation takes 25 Cray C-90 hours.

Significance

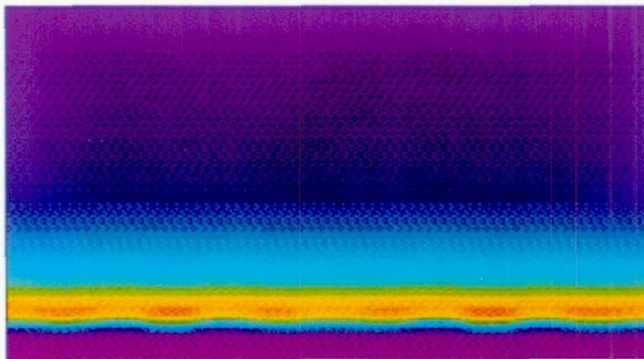
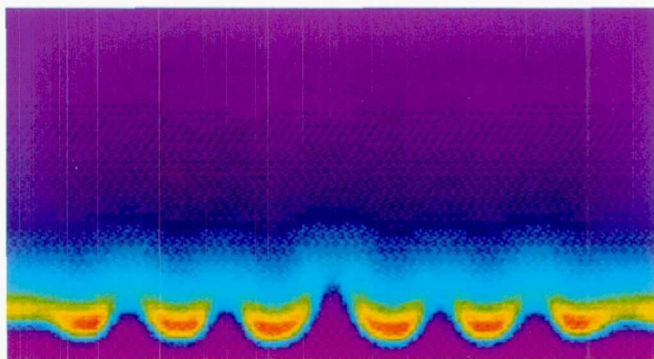
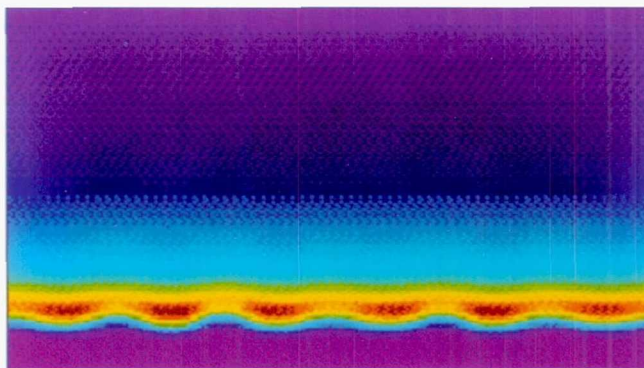
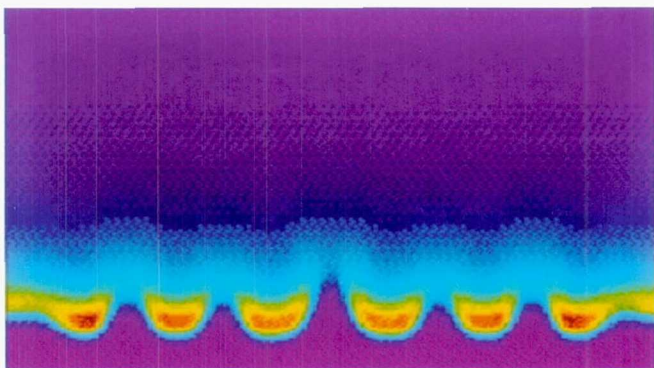
These simulations clarify the relative importance of gravity and heat loss to the burner on the structure and stability of lean hydrogen–air flames.

Future Plans

The code will now be used to simulate and understand a number of other interesting flame phenomena observed on Earth and in microgravity.

Keywords

Premixed flames, Buoyancy, Heat losses



The effect of zero gravity (top) and Earth gravity (bottom) on a hydrogen–air flame stabilized on an isothermal burner at 10 cm/sec inflow velocity (left) and 7 cm/sec inflow velocity (right).

Protoplanetary Nebula Particle-Gas Dynamics

Jeffrey N. Cuzzi, Principal Investigator

Co-investigators: Anthony R. Dobrovolskis, Robert C. Hogan, Joelle M. Champney, and Jennifer M. Dacles-Mariani

NASA Ames Research Center/University of California, Santa Cruz/Synernet, Inc.



Research Objective

To study conditions prevailing in the nebula from which the solar system formed at a time when the growing particles were small enough to have important dynamic interactions with the predominant gas, and to relate these studies to evidence seen in primitive meteorites.

Approach

Direct numerical simulations of three-dimensional turbulence were used to trace the evolution of large numbers of test particles of varying stopping time in the gas. Particles of stopping time comparable to the turn-over time of the smallest eddy are preferentially concentrated into clumps that are at least an order of magnitude more dense than average clumps. Turbulence particle damping may also be incorporated.

Accomplishment Description

Calculations were extended to higher Taylor microscale Reynolds numbers (80 completed, 150 running) and several aspects of the resulting particle density distribution were studied. Several physically based relationships were developed to allow scaling the results to the much larger Reynolds numbers of the nebula. The scaling relations are being validated with the calculations now running. The fluid regimes that are depleted or populated by par-

ticles and the relative velocities of the particles to the gas and to each other are described.

Significance

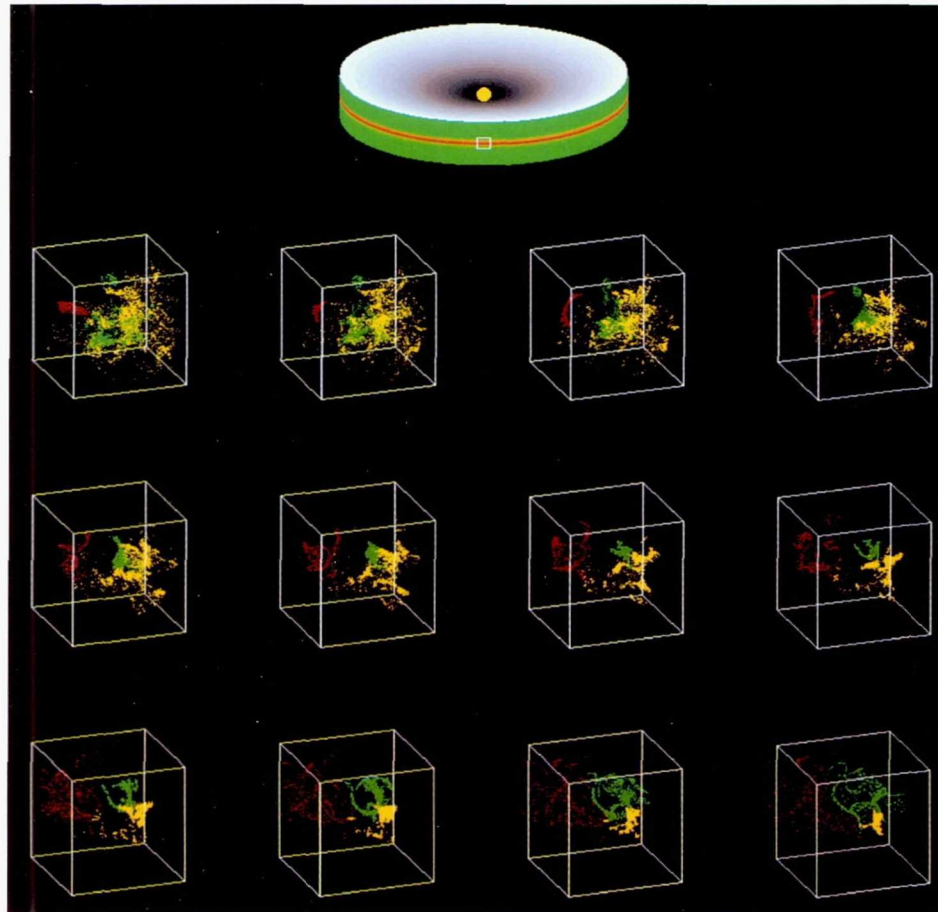
The study implies that dense concentrations of particles appear on spatial scales comparable to the Kolmogorov scale, and that particles of millimeter and submillimeter diameter will be preferentially concentrated by a factor between 10^2 and 10^5 in nebula turbulence. These sizes are in excellent agreement with the sizes of chondrules and other meteorite fragments that are dominant components of primitive meteorites. Previously, there was no explanation for the makeup or production of chondritic meteorites; this concentration process may be the cause of the sorting, and thus a critical step in the accumulation of the earliest comet- and asteroid-sized planetesimals.

Future Plans

More accurate calibration of the concentration dependence and preferred size on Reynolds number must be obtained. The effect of particle mass loading on turbulence damping at high concentrations will be studied.

Keywords

Planet formation, Turbulence, Two-phase flow



The schematic of the disk-shaped protoplanetary nebula is composed of a gas-particle mix with local vertical thickness about one-tenth the local radius. The computational grid is envisaged as a tiny representative volume in the overall nebula. The boxes represent the computational grid in a sequence of time steps showing the evolution of several different sets of particles, which come together as clumps at different times.

Page intentionally left blank

Index

Page intentionally left blank

Index by Research Sites

	Page
Adaptive Research Corporation	
Robert R. Chamberlain Jet Interaction Effects on Aerodynamic Control of Missiles	25
Allison Engine Company	
Edward J. Hall Advanced Ducted Propfan Analysis Code Certification	53
Edward J. Hall Fan Rotor/Endwall Treatment Interaction	54
Edward J. Hall Transonic Core Compressor Rotor/Stator Interaction	52
Applied Research Associates, Inc.	
Robert H. Sues Parallel Multidisciplinary Stochastic Optimization	63
AS&M, Inc.	
Michael C. Fischer Supersonic Laminar Flow Control Experiment	32
	(with NASA Lewis Research Center)
Berkeley Research Associates	
Stephen H. Brecht Solar Wind Interaction with Mars	113
K. Kailasanath Burner-Stabilized Flames in Microgravity	114
	(with Naval Research Laboratory)
Boeing Commercial Airplane Group	
David E. Ashpis Transition in a Highly Disturbed Environment	75
	(with NASA Lewis Research Center)
N. J. Yu Evaluation of Navier–Stokes Codes for Transport Configuration Analysis	31
Boeing Company, The	
Forrester T. Johnson Multipoint Aerodynamic Design	10
Brown University	
George E. Karniadakis Direct and Large-Eddy Simulation of Wake Flows	78
George E. Karniadakis Simulation of Complex-Geometry Wall-Bounded Flows	79
Cambridge Hydrodynamics, Inc.	
Steven A. Orszag Unsteady Turbulence Model Simulations	86

Carnegie Mellon University

Wei J. Chyu	Airframe/Inlet Aerodynamics (with NASA Ames Research Center)	47
Tom I-P. Shih	Flow in Turbine-Blade Cooling Passages (with NASA Lewis Research Center)	60

CFD Research Corporation

Clifford E. Smith	Jets-in-Cross-Flow Mixing (with NASA Lewis Research Center)	62
Matthew E. Thomas	Impeller Computational Fluid Dynamics Modeling	109

European Space Agency

John Rakiewicz	Titan Entry Flow Field of the Cassini-Huygens Probe (with Jet Propulsion Laboratory and McDonnell Douglas Aerospace)	27
----------------	---	----

General Motors Corporation, Allison Gas Turbine Division

Kurt F. Weber	Chimera Domain Decomposition Applied to Turbomachinery Flow	67
---------------	---	----

George Mason University

Joseph D. Baum	Arbitrary Lagrangian-Eulerian Three-Dimensional Simulations (with Science Applications International Corporation)	106
----------------	--	-----

George Washington University

Jassim A. Al-Saadi	Transonic Flows Around Complex Geometries (with NASA Langley Research Center)	35
--------------------	--	----

Grumman Corporate Research Center

Frank Marconi	Comparison of TLNS3D Computations with Test Data	13
---------------	--	----

High Technology Corporation

Bart A. Singer	Origins of Near-Wall Turbulence (with NASA Langley Research Center)	90
----------------	--	----

ICASE

Dimitri J. Mavriplis	Navier–Stokes Computations on Unstructured Grids	14
R. C. Swanson	Simulation of Scramjet Flow Fields (with NASA Langley Research Center)	64

ICOMP

Chunill Hah	Unsteady Three-Dimensional Flow in a Transonic Compressor (with NASA Lewis Research Center and Wright Patterson Air Force Base)	51
Shaye Yungster	National Aero-Space Plane Nozzles with External Burning (with NASA Lewis Research Center)	68

Iowa State University

Richard H. Pletcher	Three-Dimensional Liquid Sloshing Flow Simulation	87
---------------------	---	----

Jet Propulsion Laboratory

Christian L. Keppenne	Intraseasonal Atmospheric Oscillations	97
John Rakiewicz	Titan Entry Flow Field of the Cassini–Huygens Probe (with McDonnell Douglas Aerospace and European Space Agency)	27

Lockheed Aeronautical Systems Company

Pradeep Raj	CFL3D Code Evaluation	15
-------------	-----------------------------	----

Lockheed Engineering and Sciences Company

Kenneth M. Jones	Subsonic High-Lift Analysis (with NASA Langley Research Center and ViGYAN, Inc.)	29
Steve L. Karman, Jr.	Unstructured Grid/Flow Solver Calibration	33
Christopher L. Reed	High-Angle-of-Attack Aerodynamics	41
David M. Schuster	Analysis of High-Speed Civil Transport Transient Response	17

MCAT Institute

Guru P. Guruswamy	Aeroelasticity of Wing–Body–Control Configurations (with NASA Ames Research Center)	8
Guru P. Guruswamy	Wing–Body Aeroelasticity (with NASA Ames Research Center)	9
Nateri K. Madavan	Boundary-Layer Transition on a Heated Flat Plate	82
Lewis B. Schiff	Investigation of Forebody Flow Control (with NASA Ames Research Center)	30

		Page
E. Tu	Laminar Flow Supersonic Wind Tunnel (with NASA Ames Research Center)	34

McDonnell Douglas Aerospace

John Rakiewicz	Titan Entry Flow Field of the Cassini–Huygens Probe (with Jet Propulsion Laboratory and European Space Agency)	27
Arvin Shmilovich	Analysis of Nacelle/Pylon/Wing Installations	61
Arvin Shmilovich	Computational Studies of Advanced Wings at High Incidence	42
Scott Ward	Reusable Launch Vehicle Flow Simulations	66

McDonnell Douglas Corporation

Ramesh K. Agarwal	Computational Fluid Dynamics Solution for Maxwell's Equations	102
Ramesh K. Agarwal	Unstructured Grid Finite-Element Solutions (with Mississippi State University)	3
Alan B. Cain	Simulation of Supersonic Jet Screech	45
Raymond R. Cosner	F/A-18 Aerodynamic Assessment	37
Jerry E. Deese	Launch Vehicle Flow-Field Simulation	38
Linda D. Kral	Turbulence Modeling for Three-Dimensional Flow Fields	80

Medical College of Ohio

Jeffrey R. Hammersley	Modeling of Pulmonary Fluid Dynamics (with University of Arkansas and Mississippi State University)	110
-----------------------	--	-----

Mississippi State University

Ramesh K. Agarwal	Unstructured Grid Finite-Element Solutions (with McDonnell Douglas Corporation)	3
Jeffrey R. Hammersley	Modeling of Pulmonary Fluid Dynamics (with University of Arkansas and Medical College of Ohio)	110

NASA Ames Research Center

Timothy J. Barth	Parallel Implementation of an Unstructured Mesh Navier–Stokes Solver (with Sterling Software Systems)	4
Brian J. Cantwell	Incompressible Plane Wake Computation Comparisons (with Stanford University)	76
Neal M. Chaderjian	Effects of Roll Angle on Vortex Breakdown (with Naval Post Graduate School and Stanford University)	24

		Page
Haecheon Choi	Numerical Simulation of Riblets (with Stanford University)	77
Wei J. Chyu	Airframe/Inlet Aerodynamics (with Carnegie Mellon University)	47
Jeffrey N. Cuzzi	Protoplanetary Nebula Particle-Gas Dynamics (with University of California, Santa Cruz and Synernet, Inc.)	115
Karen L. Gundy-Burlet	Unsteady Turbomachinery Computations	50
Guru P. Guruswamy	Aeroelasticity of Wing-Body-Control Configurations (with MCAT Institute)	8
Guru P. Guruswamy	Wing-Body Aeroelasticity (with MCAT Institute)	9
Creon Levit	Evolution of Planetary Rings	94
Thomas S. Lund	Large-Eddy Simulation of Jet Combustors (with Stanford University)	81
W. J. McCroskey	Calculations of High Performance Rotorcraft (with U.S. Army Aeroflightdynamics Directorate, Sterling Software Systems, and University of California, Davis)	71
Parviz Moin	Large-Eddy Simulation of Complex Flows (with Stanford University)	85
Parviz Moin	Large-Eddy Simulation of Separated External Flows (with Stanford University)	84
James B. Pollack	Dynamics of the Martian Atmosphere	98
Yehia Rizk	Prediction of the Unsteady F-18 Flow Field	16
Michael M. Rogers	Self-Similar Turbulent Plane Wakes (with Stanford University and University of Wisconsin, Madison)	89
Muriel D. Ross	Finite Volume Neuronal Modeling (with Sterling Software Systems)	112
Lewis B. Schiff	Investigation of Forebody Flow Control (with MCAT Institute)	30
Bruce F. Smith	Studies of Galaxy Formation and Evolution (with University of Chicago)	96
Roger C. Strawn	Solution-Adaptive Computations of Helicopter Acoustics (with U.S. Army Aeroflightdynamics Directorate, RIACS, and Stanford University)	72
E. Tu	Laminar Flow Supersonic Wind Tunnel (with MCAT Institute)	34
Alex C. Woo	Computational Radar Cross Sections (with Sterling Software Systems)	105

		Page
Jerry Yan	Automated Instrumentation and Monitoring System (with Recom Technologies)	101
Richard E. Young	Simulation of Volcanic Aerosol Clouds	99
S. H. Konrad Zhu	Simulation of Rarefied Jet Interaction (with Rockwell International, Rocketdyne Division)	28

NASA Langley Research Center

Jassim A. Al-Saadi	Transonic Flows Around Complex Geometries (with George Washington University)	35
Farhad Ghaffari	Applied Computational Fluid Dynamics (with ViGYAN, Inc.)	5
Kenneth M. Jones	Subsonic High-Lift Analysis (with ViGYAN, Inc. and Lockheed Engineering and Sciences Company)	29
Man Mohan Rai	Direct Simulation of Turbulent/Transitional Airfoil Flow	88
Bart A. Singer	Origins of Near-Wall Turbulence (with High Technology Corporation)	90
R. C. Swanson	Simulation of Scramjet Flow Fields (with ICASE)	64
James L. Thomas	Complete F-18 Hybrid Solution	18

NASA Lewis Research Center

David E. Ashpis	Transition in a Highly Disturbed Environment (with Boeing Commercial Airplane Group)	75
Rodrick V. Chima	Multiblock Solver for Turbomachinery Flows	46
Michael C. Fischer	Supersonic Laminar Flow Control Experiment (with AS&M, Inc.)	32
Chunill Hah	Unsteady Three-Dimensional Flow in a Transonic Compressor (with ICOMP and Wright Patterson Air Force Base)	51
Tom I-P. Shih	Flow in Turbine-Blade Cooling Passages (with Carnegie Mellon University)	60
Clifford E. Smith	Jets-in-Cross-Flow Mixing (with CFD Research Corporation)	62
Shaye Yungster	National Aero-Space Plane Nozzles with External Burning (with ICOMP)	68

NASA Marshall Space Flight Center

James Caristi	Simulating the Cosmic X-Ray Experiment (with Valparaiso University)	95
---------------	--	----

Edward J. Reske	Complex Three-Dimensional Flows in the Advanced Solid Rocket Motor	57
-----------------	--	----

Naval Air Warfare Center

Steven B. Kern	Vortex-Flow Control	11
----------------	---------------------------	----

Naval Post Graduate School

Neal M. Chaderjian	Effects of Roll Angle on Vortex Breakdown	24
	(with NASA Ames Research Center and Stanford University)	

Naval Research Laboratory

Fernando F. Grinstein	Simulation of Spatially Evolving Jets	7
-----------------------	---	---

K. Kailasanath	Burner-Stabilized Flames in Microgravity (with Berkeley Research Associates)	114
----------------	--	-----

North Carolina State University

Hassan A. Hassan	Transition Model for High-Speed Flow	26
------------------	--	----

Overset Methods, Inc.

Christopher A. Atwood	Simulation of Coupled Fluid and Flightdynamic Systems	36
-----------------------	---	----

Pennsylvania State University

Budugur Lakshminarayana	Three-Dimensional Steady and Unsteady Turbulent Flows in Turbomachines	55
-------------------------	--	----

Lyle N. Long	Hybrid Massively Parallel Aeroacoustics Scheme	93
--------------	--	----

C. L. Merkle	Computational Propulsion Applications	56
--------------	---	----

Recom Technologies

Jerry Yan	Automated Instrumentation and Monitoring System	101
	(with NASA Ames Research Center)	

RIACS

Roger C. Strawn	Solution-Adaptive Computations of Helicopter Acoustics	72
	(with U.S. Army Aeroflightdynamics Directorate, NASA Ames Research Center, and Stanford University)	

Rockwell International Science Center

W. W. Follett	Vortex Induced Mixing Behind Ramp Injectors	49
	(with Rockwell International, Rocketdyne Division)	
Vijaya Shankar	Computational Fluid Dynamics Approach to Computational Electromagnetics	103

Rockwell International, North American Aircraft Division

Philip B. Gingrich	Design-by-Optimization Method	6
Jong H. Wang	Hydrocarbon Scramjet Combustor	65
Chung-Jin Woan	Flow Simulation about Attack Aircraft	19
David T. Yeh	Multiple-Body Aerodynamics	20

Rockwell International, Rocketdyne Division

W. W. Follett	Vortex Induced Mixing Behind Ramp Injectors	49
	(with Rockwell International Science Center)	
S. H. Konrad Zhu	Simulation of Rarefied Jet Interaction	28
	(with NASA Ames Research Center)	

Rockwell International, Space Systems Division

Daniel F. Dominik	Space Shuttle Flow Fields with Plume Simulation	39
-------------------	---	----

Rose Engineering and Research, Inc.

William C. Rose	High-Speed Inlet Design and Analysis	58
-----------------	--	----

Science Applications International Corporation

Joseph D. Baum	Arbitrary Lagrangian-Eulerian Three-Dimensional Simulations	106
	(with George Mason University)	

Scientific Research Associates, Inc.

Frederik J. de Jong	Turbine Blade Tip Clearance Flows	48
---------------------	---	----

Stanford University

Andrew Anagnost	Time-Accurate Simulation of Hypervelocity Wakes	23
Brian J. Cantwell	Incompressible Plane Wake Computation Comparisons	76
	(with NASA Ames Research Center)	
Neal M. Chaderjian	Effects of Roll Angle on Vortex Breakdown	24
	(with NASA Ames Research Center and Naval Post Graduate School)	

		Page
Haecheon Choi	Numerical Simulation of Riblets (with NASA Ames Research Center)	77
Sanjiva K. Lele	Skewed Compressible Mixing Layers	12
Thomas S. Lund	Large-Eddy Simulation of Jet Combustors (with NASA Ames Research Center)	81
Parviz Moin	Direct Numerical Simulation of Shock/Turbulence Interaction	83
Parviz Moin	Large-Eddy Simulation of Complex Flows (with NASA Ames Research Center)	85
Parviz Moin	Large-Eddy Simulation of Separated External Flows (with NASA Ames Research Center)	84
Michael M. Rogers	Self-Similar Turbulent Plane Wakes (with NASA Ames Research Center and University of Wisconsin, Madison)	89
Roger C. Strawn	Solution-Adaptive Computations of Helicopter Acoustics (with U.S. Army Aeroflightdynamics Directorate, NASA Ames Research Center, and RIACS)	72

Sterling Software Systems

Timothy J. Barth	Parallel Implementation of an Unstructured Mesh Navier–Stokes Solver (with NASA Ames Research Center)	4
W. J. McCroskey	Calculations of High Performance Rotorcraft (with NASA Ames Research Center, U.S. Army Aeroflightdynamics Directorate, and University of California, Davis)	71
Muriel D. Ross	Finite Volume Neuronal Modeling (with NASA Ames Research Center)	112
Alex C. Woo	Computational Radar Cross Sections (with NASA Ames Research Center)	105

Synernet, Inc.

Jeffrey N. Cuzzi	Protoplanetary Nebula Particle-Gas Dynamics (with NASA Ames Research Center and University of California, Santa Cruz)	115
------------------	--	-----

University of Arkansas

Jeffrey R. Hammersley	Modeling of Pulmonary Fluid Dynamics (with Medical College of Ohio and Mississippi State University)	110
-----------------------	---	-----

University of California, Davis

W. J. McCroskey	Calculations of High Performance Rotorcraft (with NASA Ames Research Center, U.S. Army Aeroflightdynamics Directorate, and Sterling Software Systems)	71
-----------------	---	----

University of California, San Francisco

Andrew Pohorille	Structure and Functions of Membranes	111
------------------	--	-----

University of California, Santa Cruz

Jeffrey N. Cuzzi	Protoplanetary Nebula Particle-Gas Dynamics	115
	(with NASA Ames Research Center and Synernet, Inc.)	

University of Chicago

Bruce F. Smith	Studies of Galaxy Formation and Evolution	96
	(with NASA Ames Research Center)	

University of Iowa

Fred Stern	Free-Surface Effects on Boundary Layers and Wakes	108
Fred Stern	Unsteady Viscous Marine Propulsor Hydrodynamics	107

University of Michigan

John L. Volakis	Electromagnetic Scattering by Airborne Structures	104
-----------------	---	-----

University of Toledo

Sang-Wook Kim	Chemically Reacting Compressible Shear Layer	100
---------------	--	-----

University of Wisconsin, Madison

Michael M. Rogers	Self-Similar Turbulent Plane Wakes	89
	(with NASA Ames Research Center and Stanford University)	

U.S. Army Aeroflightdynamics Directorate

W. J. McCroskey	Calculations of High Performance Rotorcraft	71
	(with NASA Ames Research Center, Sterling Software Systems, and University of California, Davis)	
Roger C. Strawn	Solution-Adaptive Computations of Helicopter Acoustics	72
	(with NASA Ames Research Center, RIACS, and Stanford University)	

Valparaiso University

James Caristi	Simulating the Cosmic X-Ray Experiment	95
	(with NASA Marshall Space Flight Center)	

ViGYAN, Inc.

Farhad Ghaffari	Applied Computational Fluid Dynamics	5
	(with NASA Langley Research Center)	
Kenneth M. Jones	Subsonic High-Lift Analysis	29
	(with NASA Langley Research Center and Lockheed Engineering and Sciences Company)	
W. Kelly Londenberg	Reynolds Number Effects on a Delta Wing	40

Wright Patterson Air Force Base

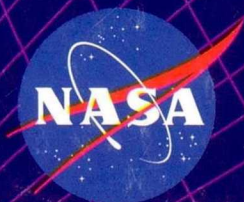
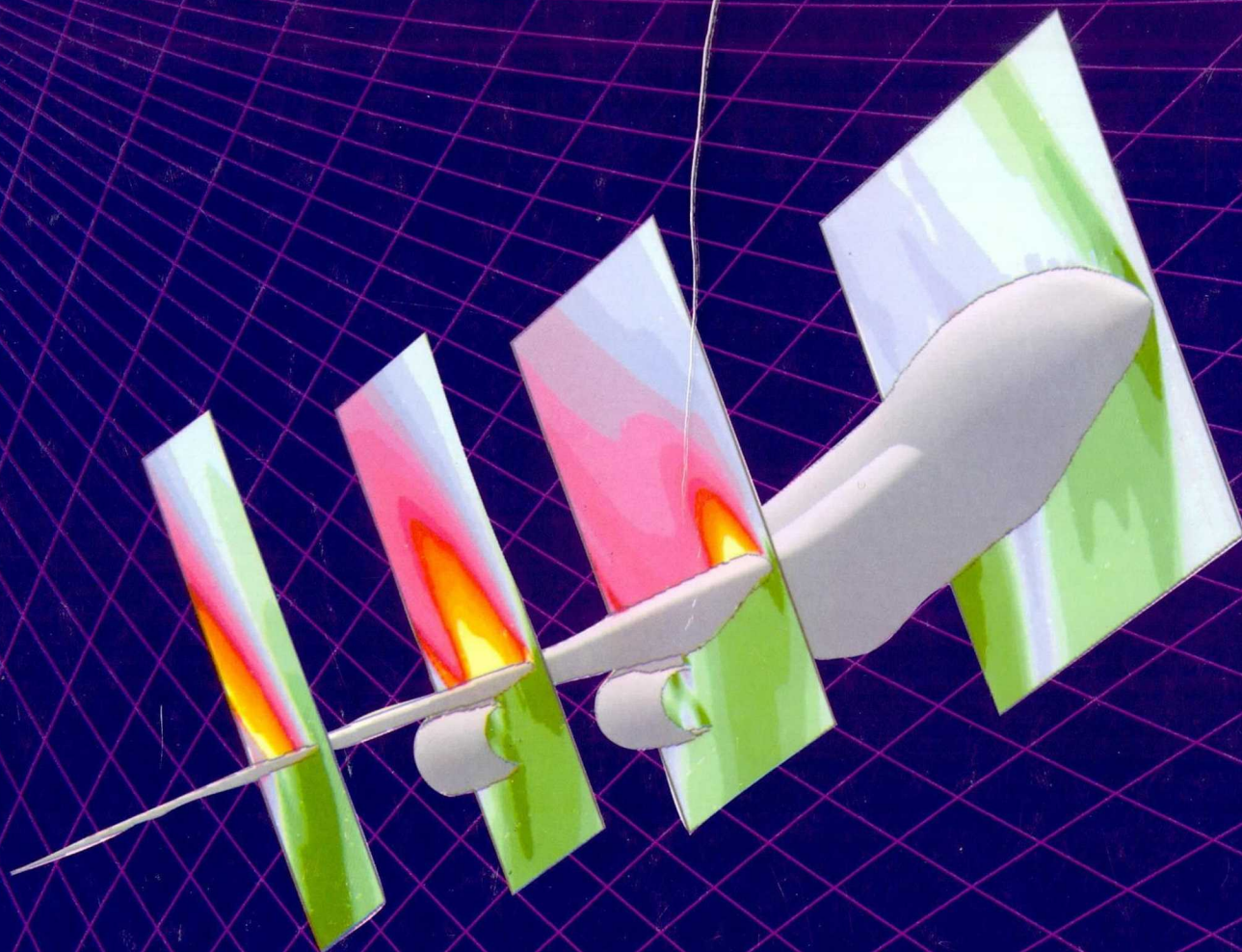
Chunill Hah	Unsteady Three-Dimensional Flow in a Transonic Compressor	51
	(with NASA Lewis Research Center and ICOMP)	
Balu Sekar	Three-Dimensional Mixing Flows in High-Speed Combustors	59

REPORT DOCUMENTATION PAGE

Form Approved
OMB No. 0704-0188

Public reporting burden for this collection of information is estimated to average 1 hour per response, including the time for reviewing instructions, searching existing data sources, gathering and maintaining the data needed, and completing and reviewing the collection of information. Send comments regarding this burden estimate or any other aspect of this collection of information, including suggestions for reducing this burden, to Washington Headquarters Services, Directorate for Information Operations and Reports, 1215 Jefferson Davis Highway, Suite 1204, Arlington, VA 22202-4302, and to the Office of Management and Budget, Paperwork Reduction Project (0704-0188), Washington, DC 20503.

1. AGENCY USE ONLY (Leave blank)		2. REPORT DATE January 1995	3. REPORT TYPE AND DATES COVERED Reference Publication	
4. TITLE AND SUBTITLE NAS Technical Summaries, March 1993–February 1994			5. FUNDING NUMBERS 536-01-11	
6. AUTHOR(S) Numerical Aerodynamic Simulation Program				
7. PERFORMING ORGANIZATION NAME(S) AND ADDRESS(ES) Ames Research Center Moffett Field, CA 94035-1000			8. PERFORMING ORGANIZATION REPORT NUMBER A-94140	
9. SPONSORING/MONITORING AGENCY NAME(S) AND ADDRESS(ES) National Aeronautics and Space Administration Washington, DC 20546-0001			10. SPONSORING/MONITORING AGENCY REPORT NUMBER NASA RP-1355	
11. SUPPLEMENTARY NOTES Point of Contact: Pat Elson, Ames Research Center, MS 258-5, Moffett Field, CA 94035-1000; (415) 604-4463				
12a. DISTRIBUTION/AVAILABILITY STATEMENT Unclassified — Unlimited Subject Category 99 Available from the NASA Center for AeroSpace Information, 800 Elkridge Landing Road, Linthicum Heights, MD 21090; (301) 621-0390.			12b. DISTRIBUTION CODE	
13. ABSTRACT (Maximum 200 words) NASA created the Numerical Aerodynamic Simulation (NAS) Program in 1987 to focus resources on solving critical problems in aeroscience and related disciplines by utilizing the power of the most advanced supercomputers available. The NAS Program provides scientists with the necessary computing power to solve today's most demanding computational fluid dynamics problems and serves as a pathfinder in integrating leading-edge supercomputing technologies, thus benefitting other supercomputer centers in government and industry. The 1993–94 operational year concluded with 448 high-speed processor projects and 95 parallel projects representing NASA, the Department of Defense, other government agencies, private industry, and universities. This document provides a glimpse at some of the significant scientific results for the year.				
14. SUBJECT TERMS Computational fluid dynamics, Supercomputing technology, Cray-2, Cray Y-MP, High-speed processing, Parallel processing			15. NUMBER OF PAGES 144	
			16. PRICE CODE A07	
17. SECURITY CLASSIFICATION OF REPORT Unclassified	18. SECURITY CLASSIFICATION OF THIS PAGE Unclassified	19. SECURITY CLASSIFICATION OF ABSTRACT	20. LIMITATION OF ABSTRACT	



National Aeronautics and
Space Administration

Ames Research Center